

**Safety Analysis Report,  
Y-12 National Security Complex,  
Model ES-3100 Package  
with Bulk HEU Contents**

**Y-12  
NATIONAL  
SECURITY  
COMPLEX**

**Volume 2  
Sections 3-8**

BWXT Y-12, L.L.C.

November 15, 2006

MANAGED BY  
BWXT Y-12, L.L.C.  
FOR THE UNITED STATES  
DEPARTMENT OF ENERGY

UCN-13672 (10-00)



**SAFETY ANALYSIS REPORT,  
Y-12 NATIONAL SECURITY COMPLEX,  
MODEL ES-3100 PACKAGE WITH BULK HEU CONTENTS**

Prepared by the  
Oak Ridge Y-12 National Security Complex  
Oak Ridge, Tennessee 37831  
Managed by  
BWXT Y-12, L.L.C.  
for the  
U. S. Department of Energy  
under contract DE-AC05-84OR21400

**October 10, 2007**





## CONTENTS

LIST OF FIGURES .....	xi
LIST OF TABLES .....	xiii
ACRONYMS AND ABBREVIATIONS .....	xvii
REVISION LOG .....	xix
1. GENERAL INFORMATION .....	1-1
1.1 INTRODUCTION .....	1-1
1.2 PACKAGE DESCRIPTION .....	1-1
1.2.1 Packaging .....	1-4
1.2.2 Containment System .....	1-7
1.2.3 Contents .....	1-9
1.2.4 Operational Features .....	1-19
1.3 GENERAL REQUIREMENTS FOR ALL PACKAGES .....	1-19
1.3.1 Minimum package size .....	1-19
1.3.2 Tamper-indicating feature .....	1-20
1.4 APPENDICES .....	1-21
1.4.1 CERTIFICATION DRAWING .....	1-23
1.4.2 EQUIPMENT SPECIFICATION JS-YMN3-801580-A002, <i>ES-3100 DRUM ASSEMBLY</i> .....	1-37
1.4.3 EQUIPMENT SPECIFICATION JS-YMN3-801580-A001, <i>ES-3100 CONTAINMENT VESSEL</i> .....	1-47
1.4.4 EQUIPMENT SPECIFICATION, JS-YMN3-801580-A003, <i>MANUFACTURING PROCESS SPECIFICATION FOR CASTING                 KAOLITE 1600™ INTO THE ES-3100 SHIPPING PACKAGE</i> .....	1-61
1.4.5 EQUIPMENT SPECIFICATION, JS-YMN3-801580-A005, <i>CASTING                 CATALOG NO. 277-4 NEUTRON ABSORBER FOR THE ES-3100                 SHIPPING PACKAGE</i> .....	1-81
1.4.6 PACKAGE CATEGORY DETERMINATION .....	1-121
1.4.7 HEU OXIDE MATERIAL SPECIFICATION AS PROVIDED BY Y-12 HIGHLY ENRICHED URANIUM DISPOSITION PROGRAM OFFICE .....	1-125
1.4.8 DETAILED ENGINEERING DRAWINGS .....	1-129
1.4.9 DESIGN ANALYSES AND CALCULATIONS, DAC-PKG-801624-A001, <i>MIXING WEIGHTS AND ELEMENTAL COMPOSITION OF 277-4                 NEUTRON POISON USED IN THE ES-3100</i> .....	1-171
1.4.10 PYROPHORICITY OF URANIUM METAL .....	1-199
SECTION 1 REFERENCES .....	1-217

## CONTENTS continued

2. STRUCTURAL EVALUATION .....	2-1
2.1 DESCRIPTION OF STRUCTURAL DESIGN .....	2-2
2.1.1 Discussion .....	2-2
2.1.2 Design Criteria .....	2-4
2.1.3 Weights and Centers of Gravity .....	2-14
2.1.4 Identification of Codes and Standards for Package Design .....	2-14
2.2 MATERIALS .....	2-18
2.2.1 Material Properties and Specifications .....	2-18
2.2.2 Chemical, Galvanic, or Other Reactions .....	2-18
2.2.3 Effects of Radiation on Materials .....	2-26
2.3 FABRICATION AND EXAMINATION .....	2-26
2.3.1 Fabrication .....	2-26
2.3.2 Examination .....	2-28
2.4 LIFTING AND TIE-DOWN STANDARDS FOR ALL PACKAGES .....	2-31
2.4.1 Lifting Devices .....	2-31
2.4.2 Tie-Down Devices .....	2-31
2.5 GENERAL CONSIDERATIONS .....	2-32
2.5.1 Evaluation by Test .....	2-32
2.5.2 Evaluation by Analysis .....	2-35
2.6 NORMAL CONDITIONS OF TRANSPORT .....	2-35
2.6.1 Heat .....	2-37
2.6.2 Cold .....	2-39
2.6.3 Reduced External Pressure .....	2-40
2.6.4 Increased External Pressure .....	2-40
2.6.5 Vibration .....	2-44
2.6.6 Water Spray .....	2-46
2.6.7 Free Drop .....	2-47
2.6.8 Corner Drop .....	2-47
2.6.9 Compression .....	2-48
2.6.10 Penetration .....	2-50
2.7 HYPOTHETICAL ACCIDENT CONDITIONS .....	2-51
2.7.1 Free Drop .....	2-53
2.7.2 Crush .....	2-64
2.7.3 Puncture .....	2-70
2.7.4 Thermal .....	2-71
2.7.5 Immersion—Fissile Material .....	2-79
2.7.6 Immersion—All Packages .....	2-81
2.7.7 Deep Water Immersion Test (for Type B Packages Containing More than $10^5$ A <sub>2</sub> ) .....	2-81
2.7.8 Summary of Damage .....	2-81
2.8 ACCIDENT CONDITIONS FOR AIR TRANSPORT OF PLUTONIUM .....	2-95

## CONTENTS continued

2.9	ACCIDENT CONDITIONS FOR FISSILE MATERIAL PACKAGES FOR AIR TRANSPORT .....	2-95
2.9a	SPECIAL FORM .....	2-95
2.9b	FUEL RODS .....	2-95
2.10	APPENDICES .....	2-97
2.10.1	ES-3100 CONTAINMENT VESSEL ASME CODE EVALUATION (DAC-EA-900000-A006 and DAC-EA-900000-A007) .....	2-99
2.10.2	IMPACT ANALYSES OF ES-3100 DESIGN CONCEPTS USING BOROBOND AND CAT 277-4 NEUTRON ABSORBERS .....	2-157
2.10.3	KAOLITE PROPERTIES .....	2-463
2.10.4	CATALOG 277-4 PROPERTIES .....	2-535
2.10.5	BOROBOND4 PROPERTIES .....	2-643
2.10.6	RECOMMENDED RANDOM VIBRATION AND SHOCK TEST SPECIFICATIONS FOR CARGO TRANSPORTED ON SST AND SGT TRAILERS .....	2-657
2.10.7	TEST REPORT OF THE ES-3100 PACKAGE, VOLUME 1 - MAIN REPORT, ORNL/NTRC-013/V1, REV. 0, SEPTEMBER 10, 2004 .....	2-675
2.10.8	TEST REPORT OF THE ES-3100, VOLUME 3 - APPENDIX K, TU - DATA SHEETS .....	2-807
2.10.9	<b>PACKAGING MATERIALS OUTGASSING STUDY FINAL REPORT</b> .....	2-851
	SECTION 2 REFERENCES .....	2-891
3.	THERMAL EVALUATION .....	3-1
3.1	DISCUSSION .....	3-1
3.1.1	Design Features .....	3-3
3.1.2	Content's Decay Heat .....	3-4
3.1.3	Summary Tables of Temperatures .....	3-4
3.1.4	Summary Tables of Maximum Pressures .....	3-11
3.2	SUMMARY OF THERMAL PROPERTIES OF MATERIALS .....	3-16
3.2.1	Material properties .....	3-16
3.2.2	Component Specifications .....	3-16
3.3	GENERAL CONSIDERATIONS .....	3-16
3.3.1	Evaluation by Analysis .....	3-16
3.3.2	Evaluation by Test .....	3-18
3.3.3	Margins of Safety .....	3-23
3.4	THERMAL EVALUATION UNDER NORMAL CONDITIONS OF TRANSPORT ....	3-27
3.4.1	Heat and Cold .....	3-27
3.4.2	Maximum Normal Operating Pressure .....	3-29
3.4.3	Maximum Thermal Stresses .....	3-29

## CONTENTS continued

3.5	HYPOTHETICAL ACCIDENT THERMAL EVALUATION .....	3-31
3.5.1	Initial Conditions .....	3-31
3.5.2	Fire Test conditions .....	3-31
3.5.3	Maximum Temperatures and Pressure .....	3-33
3.5.4	Accident Conditions for Fissile Material Packages for Air Transport .....	3-38
3.6	APPENDICES .....	3-39
3.6.1	THERMAL EVALUATION OF THE ES-3100 SHIPPING CONTAINER FOR NCT AND HAC (CONCEPTUAL DESIGN WITH BOROBOND4 NEUTRON ABSORBER) .....	3-41
3.6.2	THERMAL EVALUATION OF THE ES-3100 SHIPPING CONTAINER FOR NCT AND HAC (FINAL DESIGN WITH CATALOG 277-4 NEUTRON ABSORBER) .....	3-81
3.6.3	THERMAL STRESS EVALUATION OF THE ES-3100 SHIPPING CONTAINER DRUM BODY ASSEMBLY FOR NCT (FINAL DESIGN WITH CATALOG 277-4 NEUTRON ABSORBER) .....	3-121
3.6.4	CONTAINMENT VESSEL PRESSURE DUE TO NORMAL CONDITIONS OF TRANSPORT FOR THE PROPOSED CONTENTS .....	3-145
3.6.5	CONTAINMENT VESSEL PRESSURE DUE TO HYPOTHETICAL ACCIDENT CONDITIONS FOR THE PROPOSED CONTENTS .....	3-153
3.6.6	SILICONE RUBBER THERMAL PROPERTIES FROM THERM 1.2 DATABASE .....	3-159
	SECTION 3 REFERENCES .....	3-161
4.	CONTAINMENT .....	4-1
4.1	DESCRIPTION OF THE CONTAINMENT BOUNDARY .....	4-2
4.1.1	Containment Boundary .....	4-2
4.1.2	Special Requirements for Plutonium .....	4-4
4.2	GENERAL CONSIDERATIONS .....	4-4
4.2.1	Type A Fissile Packages .....	4-4
4.2.2	Type B Packages .....	4-4
4.3	CONTAINMENT UNDER NORMAL CONDITIONS OF TRANSPORT (TYPE B PACKAGES) .....	4-6
4.4	CONTAINMENT UNDER HYPOTHETICAL ACCIDENT CONDITIONS (TYPE B PACKAGES) .....	4-8
4.5	LEAKAGE RATE TESTS FOR TYPE B PACKAGES .....	4-10
4.6	APPENDICES .....	4-11
4.6.1	DETERMINATION OF $A_2$ FOR THE ES-3100 PACKAGE WITH HEU CONTENTS .....	4-13
4.6.2	CALCULATION OF THE ES-3100 CONTAINMENT VESSEL'S REGULATORY REFERENCE AIR LEAKAGE RATES .....	4-23
	SECTION 4 REFERENCES .....	4-35

## CONTENTS continued

5.	SHIELDING EVALUATION .....	5-1
5.1	DESCRIPTION OF SHIELDING DESIGN .....	5-1
5.1.1	Design Features .....	5-1
5.1.2	Summary Table of Maximum Radiation Levels .....	5-1
5.2	SOURCE SPECIFICATION .....	5-1
5.3	DOSE RATE ANALYSIS MODELS .....	5-3
5.3.1	Packaging Model Conservative Features .....	5-7
5.3.2	Photon model for 36-kg HEU metal content .....	5-9
5.3.3	Neutron model for 36-kg HEU metal content .....	5-11
5.3.4	Photon model for 24-kg HEU oxide content .....	5-11
5.3.5	Neutron model for 24-kg HEU oxide content .....	5-11
5.4	SHIELDING EVALUATION .....	5-11
5.5	APPENDICES .....	5-15
5.5.1	ORIGEN INPUT DATA FROM TABLE 5.3 .....	5-17
5.5.2	CSASN AND ICE INPUT FROM TABLE 5.8 .....	5-19
5.5.3	MORSE ROUTINES AND INPUT DATA .....	5-21
	SECTION 5 REFERENCES .....	5-39
6.	CRITICALITY EVALUATION .....	6-1
6.1	DESCRIPTION OF THE CRITICALITY DESIGN .....	6-1
6.1.1	Design Features .....	6-1
6.1.2	Summary of the Criticality Evaluation .....	6-2
6.1.3	Criticality Safety Index .....	6-4
6.2	PACKAGE CONTENTS .....	6-30
6.2.1	Fissile Material Contents .....	6-30
6.2.2	Convenience Cans, Teflon and Polyethylene Bottles, and 277-4 Canned Spacers .....	6-31
6.2.3	Packing Materials .....	6-31
6.2.4	Package Content Loading Restrictions .....	6-32
6.3	GENERAL CONSIDERATIONS .....	6-33
6.3.1	Model Configuration .....	6-34
6.3.2	Material Properties .....	6-50
6.3.3	Computer Codes and Cross-Section Libraries .....	6-61
6.3.4	Demonstration of Maximum Reactivity .....	6-63
6.4	SINGLE PACKAGE EVALUATION .....	6-64
6.4.1	Solid HEU Metal of Specified Geometric Shapes .....	6-65
6.4.2	HEU Solid Metal of Unspecified Geometric Shapes or HEU Broken Metal .....	6-68
6.4.3	HEU Oxide .....	6-68
6.4.4	UNH Crystals .....	6-70

## CONTENTS continued

6.5	EVALUATION OF PACKAGE ARRAYS UNDER NORMAL CONDITIONS OF TRANSPORT .....	6-71
6.5.1	Solid HEU Metal of Specified Geometric Shapes .....	6-71
6.5.2	HEU Solid Metal of Unspecified Geometric Shapes or HEU Broken Metal .....	6-74
6.5.3	HEU Oxide .....	6-75
6.5.4	UNH Crystals .....	6-75
6.6	EVALUATION OF PACKAGE ARRAYS UNDER HYPOTHETICAL ACCIDENT CONDITIONS .....	6-76
6.6.1	Solid HEU Metal of Specified Geometric Shapes .....	6-76
6.6.2	HEU Solid Metal of Unspecified Geometric Shapes or HEU Broken Metal .....	6-77
6.6.3	HEU Oxide .....	6-78
6.6.4	UNH Crystals .....	6-78
6.7	FISSILE MATERIAL PACKAGES FOR AIR TRANSPORT .....	6-79
6.7.1	Results for Solid HEU, One Piece per Convenience Can .....	6-79
6.7.2	Results for TRIGA Fuel Elements, Three Pieces per Convenience Can .....	6-83
6.7.3	Results for HEU Broken Metal, More Than One Piece per Convenience Can ...	6-85
6.7.4	Conclusions .....	6-87
6.8	BENCHMARK EXPERIMENTS .....	6-87
6.8.1	Applicability of Benchmark Experiments .....	6-87
6.8.2	Details of Benchmark Calculations .....	6-87
6.8.3	Bias Determination .....	6-88
6.9	APPENDICES .....	6-89
6.9.1	FISSILE CONTENT MODELS .....	6-91
6.9.2	HAC PACKAGE MODEL .....	6-97
6.9.3	PACKAGE MATERIAL COMPOSITIONS .....	6-109
6.9.4	QUALIFICATION OF A NEUTRON ABSORBER MATERIAL FOR THE ES-3100 .....	6-139
6.9.5	MISCELLANEOUS INFORMATION AND DATA .....	6-151
6.9.6	ABRIDGED SUMMARY TABLES OF CRITICALITY CALCULATION RESULTS .....	6-155
6.9.7	INPUT LISTINGS OF ES-3100 CALCULATION MODELS FOR SELECT CASES IDENTIFIED IN TABLES 6.1a-e .....	6-269
SECTION 6 REFERENCES .....		6-445
7.	PACKAGE OPERATIONS .....	7-1
7.1	PACKAGE LOADING .....	7-1
7.1.1	Preparation for Loading .....	7-1
7.1.2	Loading of Contents .....	7-3
7.1.3	Preparation for Transport .....	7-7
7.2	PACKAGE UNLOADING .....	7-9
7.2.1	Receipt of Package from Carrier .....	7-9
7.2.2	Removal of Contents .....	7-11

## CONTENTS continued

7.3	PREPARATION OF EMPTY PACKAGE FOR TRANSPORT .....	7-11
7.4	OTHER OPERATIONS .....	7-12
SECTION 7 REFERENCES .....		7-13
8.	ACCEPTANCE TESTS AND MAINTENANCE PROGRAM .....	8-1
8.1	ACCEPTANCE TESTS .....	8-1
8.1.1	Visual Inspections and Measurements .....	8-3
8.1.2	Weld Examinations .....	8-4
8.1.3	Structural and Pressure Tests .....	8-5
8.1.4	Leakage Tests .....	8-5
8.1.5	Component and Material Tests .....	8-6
8.1.6	Shielding Tests .....	8-6
8.1.7	Thermal Tests .....	8-6
8.1.8	Miscellaneous Tests .....	8-7
8.2	MAINTENANCE PROGRAM .....	8-7
8.2.1	Structural and Pressure Tests .....	8-7
8.2.2	Leakage Tests .....	8-7
8.2.3	Component and Material Tests .....	8-8
8.2.4	Thermal Tests .....	8-9
8.2.5	Miscellaneous Tests .....	8-9
SECTION 8 REFERENCES .....		8-11
DISTRIBUTION .....		8-13





## LIST OF FIGURES

1.1	Schematic of the ES-3100 shipping package .....	1-2
1.2	Exploded view of the ES-3100 package with bulk HEU contents .....	1-3
1.3	Containment boundary of the ES-3100 shipping package .....	1-8
1.4	Typical shipping configurations inside the ES-3100 containment vessel .....	1-16
1.5	TRIGA fuel element .....	1-20
2.1	Containment vessel calculated stress locations .....	2-11
2.2	ES-3100 shipping package center of gravity locations .....	2-15
2.3	ES-3100 vibration testing arrangement .....	2-44
2.4	Water spray test arrangement for Test Unit-4 .....	2-45
2.5	NCT free drop test on Test Unit-4 .....	2-47
2.6	Compression test on Test Unit-4 .....	2-48
2.7	Penetration test damage on Test Unit-4 .....	2-49
2.8	9-m drop test arrangement for all test units .....	2-53
2.9	9-m drop test damage on Test Unit-4 .....	2-55
2.10	Cumulative damage from 9-m drop and crush testing on Test Unit-2 .....	2-57
2.11	Test Unit-3 damage from 1.2 and 9-m drop tests .....	2-58
2.12	1.2 and 9-m drop test damage on Test Unit-1 .....	2-60
2.13	1.2 and 9-m drop test damage to Test Unit-5 .....	2-62
2.14	Cumulative damage following 9-m crush on Test Unit-1 .....	2-64
2.15	Cumulative damage following 9-m crush test on Test Unit-3 .....	2-66
2.16	Cumulative damage from 9-m drop and crush testing on Test Unit-4 .....	2-67
2.17	Cumulative damage from 9-m drop and crush testing on Test Unit-5 .....	2-69
2.18	28° oblique and horizontal puncture tests on Test Unit-1 .....	2-71
2.19	40° oblique puncture test on Test Unit-1 .....	2-71
2.20	Horizontal puncture test over Test Unit-1's containment vessel flange .....	2-72
2.21	Horizontal CG puncture test on Test Unit-2 .....	2-72
2.22	24.6° oblique puncture test on Test Unit-3 .....	2-73
2.23	Vertical puncture test on Test Unit-4 .....	2-73
2.24	Horizontal puncture test over Test Unit-5's containment vessel flange .....	2-74
2.25	Visual comparison of the cumulative damage on the crush side surface after the three drop tests (from top to bottom: Test Unit-1, analytical results with BoroBond, analytical results with Cat 277-4) .....	2-83
2.26	Visual comparison of the cumulative damage on the rigid surface side after the four drop tests (from left to right: Test Unit-2, analytical results with BoroBond, analytical results with Cat 277-4) .....	2-86
2.27	Visual comparison of the cumulative damage on the crush plate side after the three drop tests (from left to right: Test Unit-2, analytical results with BoroBond, analytical results with Cat 277-4) .....	2-86
2.28	Visual comparison of the cumulative bottom damage after the three drop tests (from left to right: Test Unit-3, analytical results with BoroBond, analytical results with Cat 277-4) .....	2-88
2.29	Visual comparison of the cumulative lid damage after the three drop tests (from top to bottom: Test Unit-3, analytical results with BoroBond, analytical results with Cat 277-4) .....	2-89
2.30	Visual comparison of the cumulative damage after the three drop tests (from left to right: Test Unit-4, analytical results with BoroBond, analytical results with Cat 277-4) .....	2-91
2.31	Containment vessel markings at assembly (swivel hoist ring removed prior to testing) .....	2-93
2.32	Containment vessel marking after compliance testing .....	2-94
3.1	MSC.Patran axisymmetric finite element model of the ES-3100 shipping container with BoroBond4—nodal locations of interest (elements representing air not shown for clarity). .....	3-6

## LIST OF FIGURES continued

3.2	Test unit preheat arrangement. ....	3-24
3.3	Test unit insertion into furnace. ....	3-24
3.4	Test unit removal from furnace. ....	3-25
3.5	Test unit cool down and monitoring arrangement. ....	3-25
5.1	Cylindrical calculational model of the ES-3100 shipping package for NCT ....	5-6
5.2	ES-3100 HEU metal content radial (top view) geometric models ....	5-10
6.1.	R/Z section view of ES-3100 single-unit packaging model ....	6-35
6.2.	R/Z section view at bottom of ES-3100 single-unit packaging showing KENO V.a geometry units 1001-1003, and 1006 (partial) ....	6-36
6.3.	R/Z section view at center of the ES-3100 single-unit packaging showing KENO V.a geometry units 1006 (partial) ....	6-37
6.4.	R/Z section view of near top of the ES-3100 single-unit packaging showing KENO V.a geometry units 1008 (partial) and 1010-1016 ....	6-38
6.5.	R/Z section view at the top of the ES-3100 single-unit packaging showing KENO V.a geometry units 1016-1019 ....	6-39
6.6.	R/Z section view of ES-3100 array packaging model ....	6-41
6.7.	R/Z section view at the bottom of the ES-3100 array packaging showing KENO V.a geometry units 1001-1003, and 1006 (partial) ....	6-42
6.8.	R/Z section view at the center of the ES-3100 array packaging showing KENO V.a geometry units 1006 (partial), 1007, and 1008 (partial) ....	6-43
6.9.	R/Z section view of near top of the ES-3100 array packaging showing KENO V.a geometry units 1008 (partial) and 1010-1016 ....	6-44
6.10.	R/Z section view at the top of the ES-3100 array packaging showing KENO V.a geometry units 1016-1019 ....	6-45
6.11.	Model 1. ....	6-49
6.12.	Model 2. ....	6-49
6.13.	Model 3. ....	6-49
6.14.	Model 4. ....	6-50
6.15.	Model 5. ....	6-50
6.16.	Model 6. ....	6-50
6.16a.	$K_{eff} + 2\sigma$ versus pitch for triangular arrangement of content in CV. ....	6-66a
6.16b.	$K_{eff} + 2\sigma$ versus triangular pitch over range of CV moderation. ....	6-66a
6.16c.	$K_{eff} + 2\sigma$ versus as a function of uranium weight fraction and moderation.. ....	6-66b
6.17.	$K_{eff}$ vs. enrichment (wt % $^{235}\text{U}$ ) for HEU ranging from 7 to 10 kg ....	6-81
6.18.	$K_{eff}$ vs. stainless steel shell radius (cm) for 7 kg HEU with enrichments ranging from 19 to 100 wt % $^{235}\text{U}$ ....	6-81
6.19.	$K_{eff}$ vs. Kaolite shell radius (cm) for 7 kg HEU with enrichments ranging from 19 to 100 wt % $^{235}\text{U}$ ....	6-82
6.20.	$K_{eff}$ vs. shell radius (cm) for dry and water-saturated Kaolite for 7 kg HEU at 100% enrichment ....	6-82
6.21.	$K_{eff}$ vs. shell radius (cm) for 10.4 kg core of $\text{UZrH}_x$ with stainless steel or Kaolite shell ....	6-83
6.22.	$K_{eff}$ vs. core radius (cm) for homogenized core of $\text{UZrH}_x$ , 500 g polyethylene, and Kaolite where the Kaolite water content ranges from the dry to the water-saturated condition ....	6-84
6.23.	$K_{eff}$ vs. excess water from Kaolite for fissile core blanketed with a variable thickness Kaolite shell ....	6-85
6.24.	$K_{eff}$ vs. excess water from Kaolite for core of 1-7 kg enriched HEU broken metal at 100% enrichment, core blanketed with a variable thickness Kaolite shell ....	6-86
6.25.	$K_{eff}$ vs. excess water from Kaolite for core 20% enriched HEU broken metal (0.6-7 kg $^{235}\text{U}$ ), core blanketed with a variable thickness Kaolite shell ....	6-86

## LIST OF TABLES

1.1	Uranium concentration limits .....	1-10
1.2	Bounding uranium isotopic concentrations in oxide .....	1-10
1.3	Authorized content and fissile mass loading limits for ground transport .....	1-14
1.4	TRIGA Fuel Specifications .....	1-20a
2.1	Proposed HEU contents for shipment in the ES-3100 .....	2-1
2.2	Category designations for Type B packages .....	2-7
2.3	Summary of load combinations for normal and hypothetical accident conditions of transport .....	2-9
2.4	Containment vessel allowable stress .....	2-10
2.5	Allowable stress intensity ( $S_m$ ) for the containment boundary construction materials of construction .....	2-10
2.6	ES-3100 containment boundary design evaluation allowable stress comparisons .....	2-12
2.7	ES-3100 packaging material specifications .....	2-13
2.8	Packaging weights for various ES-3100 shipping package arrangements .....	2-16
2.9	Compliance test unit weights .....	2-17
2.10	Calculated center of gravity for the various ES-3100 shipping arrangements .....	2-18
2.11	Applicable codes and standards for Category I packaging .....	2-20
2.12	Mechanical properties of the metallic components of the drum assembly .....	2-21
2.13	Mechanical properties of the lid fastening components for the drum assembly .....	2-22
2.14	Mechanical properties of the cast refractory insulation .....	2-23
2.15	Mechanical properties of containment vessel O-rings .....	2-23
2.16	Mechanical properties of the metallic components of the containment boundary .....	2-24
2.17	Mechanical properties of the cast neutron absorber .....	2-25
2.18	Summary of NCT – 10CFR71.71 tests for ES-3100 package .....	2-33
2.19	Summary of HAC – 10CFR71.73 tests for ES-3100 package .....	2-33
2.20	Summary of temperatures and pressures for NCT .....	2-36
2.21	ES-3100 containment boundary evaluation for both hot and cold conditions .....	2-41
2.22	NCT ES-3100 containment boundary stress compared to the allowable stress at reduced and increased external pressures .....	2-42
2.23	Test and analysis summary for the ES-3100 package .....	2-51
2.24	Recorded height damage to Test Unit-4 from 1.2-m and 9-m drop testing .....	2-54
2.25	Recorded diametrical damage to Test Unit-4 from 1.2-m and 9-m drop tests .....	2-54
2.26	Recorded diametrical damage to Test Unit-2 from NCT and HAC drop testing .....	2-56
2.27	Recorded flat contour damage to Test Unit-2 from NCT and HAC drop testing .....	2-56
2.28	Recorded height damage to Test Unit-2 from NCT and HAC drop testing .....	2-56
2.29	Recorded height damage to Test Unit-3 from 1.2-m and 9-m drop testing .....	2-58
2.30	Recorded diametrical damage to Test Unit-3 from 1.2-m and 9-m drop testing .....	2-58
2.31	Recorded height damage to Test Unit-1 from 1.2-m and 9-m drop testing .....	2-59
2.32	Recorded diametrical damage to Test Unit-1 from 1.2-m and 9-m HAC drop testing .....	2-59
2.33	Recorded flat contour damage to Test Unit-1 from 1.2-m and 9-m drop testing .....	2-60
2.34	Recorded height damage to Test Unit-5 from 1.2-m and 9-m drop testing .....	2-61
2.35	Recorded diametrical damage to Test Unit-5 from 1.2-m and 9-m HAC drop testing .....	2-61
2.36	Recorded flat contour damage to Test Unit-5 from 1.2-m and 9-m drop testing .....	2-62
2.37	Recorded height damage to Test Unit-1 from the 9-m crush test .....	2-63
2.38	Recorded diametrical damage to Test Unit-1 from the 9-m crush test .....	2-63
2.39	Recorded flat contour damage to Test Unit-1 from the 9-m crush test .....	2-64
2.40	Recorded height damage to Test Unit-3 from the 9-m crush test .....	2-65
2.41	Recorded flat contour damage to Test Unit-3 from the 9-m crush test .....	2-65
2.42	Recorded diametrical damage to Test Unit-3 from the 9-m crush test .....	2-65

## LIST OF TABLES continued

2.43	Recorded height damage to Test Unit-4 from the 9-m crush test .....	2-66
2.44	Recorded diametrical damage to Test Unit-4 from the 9-m crush test .....	2-67
2.45	Recorded height damage to Test Unit-5 from the 9-m crush test .....	2-68
2.46	Recorded diametrical damage to Test Unit-5 from the 9-m crush tests .....	2-68
2.47	Recorded flat contour damage to Test Unit-5 from the 9-m crush test .....	2-68
2.48	1-m (40-in.) puncture drop test description and results .....	2-70
2.49	Thermax temperature indicating patches for test units .....	2-74
2.50	Maximum HAC temperatures recorded on the test packages' interior surfaces .....	2-77
2.51	HAC ES-3100 containment boundary stress compared to the allowable stress .....	2-79
2.52	Diametrical damage comparison of Test Unit-1 with analytical predictions .....	2-82
2.53	Flat contour damage comparison of Test Unit-1 with analytical results .....	2-82
2.54	Cumulative analytical 12° slapdown drop tests maximum effective plastic strain results ....	2-84
2.55	Diametrical damage comparison of Test Unit-2 with analytical predictions .....	2-85
2.56	Flat contour damage comparison of Test Unit-2 with analytical predictions .....	2-85
2.57	Cumulative analytical side drop test maximum effective plastic strain results .....	2-87
2.58	Diametrical damage comparison of Test Unit-3 with analytical predictions .....	2-88
2.59	Cumulative analytical corner drop test maximum effective plastic strain results .....	2-90
2.60	Diametrical damage comparison of Test Unit-4 with analytical predictions .....	2-91
2.61	Cumulative analytical top drop test maximum effective plastic strain results .....	2-92
2.62	ES-3100 test package weights before and after 10 CFR 71.73(c)(4) HAC thermal testing ....	2-92
3.1	Isotopic mass and weight percent for the HEU contents .....	3-4
3.2	Decay heat for 35.2 kg of HEU content (watts) .....	3-5
3.3	Maximum "quasi steady-state" temperatures during NCT for the ES-3100 shipping container with various content heat loads—Kaolite density of 19.4 lb/ft <sup>3</sup> and Borobond4 .....	3-7
3.4	Maximum "quasi steady-state" temperatures during NCT for the ES-3100 shipping container with various content heat loads—Kaolite density of 30 lb/ft <sup>3</sup> and Borobond4 .....	3-8
3.5	ES-3100 shipping container maximum steady-state temperatures with Cat 277-4 (100°F ambient temperature, no insolation) .....	3-9
3.6	ES-3100 shipping container maximum "quasi steady-state" temperatures during NCT with various content heat loads and Cat 277-4 (100°F ambient temperature, with insolation) .....	3-10
3.7	ES-3100 shipping container HAC maximum temperatures (Kaolite 1600 density of 19.4 lb/ft <sup>3</sup> and Cat 277-4 density of 100 lb/ft <sup>3</sup> ) .....	3-12
3.8	ES-3100 shipping container HAC maximum temperatures (Kaolite 1600 density of 30 lb/ft <sup>3</sup> and Cat 277-4 density of 110 lb/ft <sup>3</sup> ) .....	3-13
3.9	Maximum HAC temperatures recorded on the test packages' interior surfaces .....	3-14
3.10	Total pressure inside the containment vessel at 87.81°C (190.06°F) .....	3-15
3.11	Total pressure inside the containment vessel at 123.85°C (254.93°F) .....	3-16
3.12	Thermal properties of the materials used in the thermal analysis .....	3-17
3.13	Mechanical properties of the materials used in the static stress analyses .....	3-19
3.14	Packaging material technical specifications .....	3-20
3.15	Component allowable service temperature and pressure .....	3-22
3.16	Summary of results of evaluation for the ES-3100 under NCT .....	3-26
3.17	Summary of results of evaluation under HAC for the ES-3100 shipping arrangement using bounding case parameters .....	3-26
3.18	ES-3100 test package weights before and after 10 CFR 71.73(c)(4) HAC thermal testing ....	3-34
3.19	Thermax temperature indicating patches for test units .....	3-34

## LIST OF TABLES continued

3.20	Predicted temperatures adjustments (°F) for containment vessel due to HAC .....	3-36
3.21	Predicted temperatures of the containment vessel due to HAC (°F) .....	3-37
4.1	Containment Requirements of Transport for Type B Packages .....	4-1
4.2	Summary of the containment vessel design and fabrication acceptance basis .....	4-1
4.3	Isotopic mass and weight percent for the HEU contents .....	4-5
4.4	Activity, $A_2$ value, and number of $A_2$ proposed for transport .....	4-5
4.5	Regulatory leakage criteria for NCT .....	4-7
4.6	Containment vessel verification tests criteria for NCT .....	4-7
4.7	Regulatory leakage criteria for HAC .....	4-9
4.8	Containment vessel design verification tests for HAC .....	4-9
5.1	Calculated external dose rates for the ES-3100 package with 36 kg of HEU metal contents (mrem/h) .....	5-2
5.2	Calculated external dose rates for the ES-3100 package with 24 kg of HEU oxide contents (mrem/h) .....	5-2
5.3	Radioisotope specification for all ES-3100 package analysis source calculations with HEU content and other nuclides per HEU unit weight .....	5-3
5.4	Photon source for one gram of HEU for all contents .....	5-4
5.5	Neutron source for one gram of HEU for all contents .....	5-4
5.6	Geometric data for the shielding analysis models of the ES-3100 shipping package as shown in Fig. 5.1 for NCT .....	5-5
5.7	Detector locations relative to the drum for NCT and to the containment vessel for HAC .....	5-7
5.8	Shielding model material specifications for the ES-3100 package with HEU content .....	5-8
5.9	ANSI standard photon flux-to-dose-rate conversion factors .....	5-12
5.10	ANSI standard neutron flux-to-dose-rate conversion factors .....	5-13
6.1a.	Summary of criticality evaluation for solid HEU metal cylinders and bars .....	6-5
6.1b.	Summary of criticality evaluation for solid HEU metal slugs .....	6-9
6.1c.	Summary of criticality evaluation for solid HEU metal of unspecified geometric shapes characterized as broken metal .....	6-12
6.1d.	Summary of criticality evaluation for HEU product and skull oxide .....	6-19
6.1e.	Summary of criticality evaluation for UNX crystals and unirradiated TRIGA reactor fuel elements .....	6-23
6.2a.	HEU fissile material mass loading limits for surface-only modes of transportation .....	6-28
6.2b.	HEU fissile material mass loading limits for air transport mode of transportation .....	6-29
6.3.	Deformation of 18.37-in.-diam ES-3100 drum projected by finite element analysis Case "3100 RUN1HL Lower Bound Kaolite May 2004" .....	6-47
6.4.	Material compositions used in the ES-3100 calculation models .....	6-53
7.1	Certified replacement parts for the ES-3100 packaging .....	7-2
8.1	Acceptance tests for the drum assembly .....	8-2
8.2	Acceptance tests for the containment vessel assembly .....	8-3



## ABBREVIATIONS AND ACRONYMS

ALARA	as low as reasonably achievable
AM	as-manufactured
ANC	Average Net Count
ANSI	American National Standards Institute
AS	allowable stress
ASME	American Society of Mechanical Engineers
ASTM	American Society for Testing and Materials
Cat 277-4	Thermo Electron Corporation <sup>1</sup> Catalog No. 277-4™ (or Cat. No. 277-4)
CD	capacity discharge
CERCA	Compagnie pour l'Étude et la Realisation de Combustibles Atomiques
CFR	Code of Federal Regulations
CMTR	certified material test report
CoC	Certificate of Compliance
CSI	criticality safety index
CV	containment vessel
CVA	containment vessel arrangement
DOE	U.S. Department of Energy
DOT	U.S. Department of Transportation
EPDM	ethylene-propylene-diene monomer
ETP	explicit triangular pack
FEA	finite element analysis
H/X ratio	hydrogen-to-fissile isotope ratio
HAC	Hypothetical Accident Conditions
HEU	highly enriched uranium
IAEA	International Atomic Energy Agency
$k_{eff}$	calculated neutron multiplication factor
LOD	loss on drying
LTL	lower tolerance limit
M.S.	margin of safety
MNOP	maximum normal operating pressure
MOCFR	moisture fraction inside the containment vessel
MOIFR	moisture fraction of the package external to the containment vessel
NCT	Normal Conditions of Transport
NLF	neutron leakage fraction
NRC	U.S. Nuclear Regulatory Commission
NTRC	National Transportation Research Center
OECD	Organization for Economic Cooperation and Development
ORNL	Oak Ridge National Laboratory
PGNAA	Prompt Gamma-ray Neutron Activation Analysis
ppb	parts per billion
ppm	parts per million
QA	quality assurance
QCPI	Quality Certification and Procurement
RCSB	Rackable Can Storage Box
SAR	safety analysis report

---

<sup>1</sup> Corporate name changed to Shieldwerx



SCALE	Standardized Computer Analysis for Licensing Evaluation
s <sub>i</sub>	standard error
SRS	Savannah River Site
SS304	type 304 stainless steel
SST/SGT	Safe-Secure Trailer/Safeguards Transporter
TGA	thermogravimetric analysis
TI	transport index
TID	tamper-indicating device
TS	test sample
UNH	uranyl nitrate hexahydrate
UNX	uranyl nitrate crystals
USL	upper subcritical limit
VF	Volume Fraction
Y-12	Y-12 National Security Complex

## REVISION LOG

Date	SAR Revision No.	Description	Affected Pages
38407	0	Original issue	All
08/15/05	0, Page Change 1	Page changes resulting from <i>Responses to Request for Additional Information #1</i> , Y/LF-747.	title page, iv, xxiii, 1-4, 1-145, 2-2, 2-3, 2-6, 2-31, 2-32, 2-33, 2-34, 2-57, 2-59, 2-61, 2-107, 2-125, 2-131, 2-171, 2-173, 2-181, 2-183, 2-185, 2-186, 2-189, 2-367, 2-458, 2-675, 8-8, 8-9, 8-31
38753	0, Page Change 2	Page changes resulting from <i>Responses to Request for Additional Information #2</i> , Y/LF-761.	All Sections
38795	0, Page Change 3	Page changes resulting from <i>Responses to Request for Additional Information #3</i> , Y/LF-764.	1.38, 1.48, Appendix 1.4.1, 2-120, Table 6.4
38844	0, Page Change 4	Added polyethylene bottles and nickel alloy cans as convenience containers for authorized HEU contents. (CoC Revision 1)	Various pages in chapters 1, 2, 3 and 4.
08/21/06	0, Page Change 5	Revised equipment specifications for Kaolite and 277-4 neutron absorber. (CoC Revision 3)	Appendices 1.4.4 and 1.4.5.
11/15/06	1	Updated definition of pyrophoric uranium. Evaluated air transport. Revised criticality safety calculations to remove bias correct factors. Added a CSI option of 3.2. Increased mass of off-gassing material allowed in containment vessel. Increased carbon concentration in HEU contents. Increased Np-237 concentration in HEU contents. Added uranium zirconium hydride and uranium carbide as contents (TRIGA fuel). Revised equipment specifications for 277-4 neutron absorber. (CoC Revision 3)	All Sections

Date	SAR Revision No.	Description	Affected Pages
3/29/07	1, Page Change 1	Updated definition of TRIGA fuel for air transport and added TRIGA-related criticality safety cases.	title pages, viii, xi, xx, 1-12, 1-13, 1-20, 6-30, 6-54, 6-64, 6-66, 6-87, 6-119, 6-240 to 6-286, 6-385 to end
5/31/07	1, Page Change 2	Revised SAR in response to RAIs dated May 9, 2007 in reference to CoC Revision 4	title pages, xiii, xx, Section 1 and Section 6
6/30/07	1, Page Change 3	Revised SAR in response to RAIs dated May 9, 2007 in reference to CoC Revision 5	title pages, table of contents, Section 1, and Section 7
7/31/07	1, Page Change 4	Removed oxidation as an option for treating pyrophoric uranium metal	title pages, xx, 1-12, 1-201, 1-203, 1-212, 2-26, 7-4
8/28/07	1, Page Change 5	Modified TRIGA fuel definition to include fuel pellets with cladding	title page, xx, 1-13, 1-17, 2-4, 6-29, 6-30a, 6-66c, 6-66d, 6-73, 6-87, 6-119a
10/10/07	1, Page Change 6	<p>Revised criticality safety calculations to remove bias correction factors.</p> <p>Added a CSI option of 3.2.</p> <p>Increased mass of off-gassing material in containment vessel to allow Teflon bottles.</p> <p>Increased carbon and moisture concentration in HEU contents.</p> <p>Increased Np-237 concentration in HEU contents.</p> <p>Revised equipment specifications for 277-4 neutron absorber.</p> <p>Details of alloys of uranium in contents definition.</p> <p>More precise specification of maximum fissile mass in calculations (changed from 36 kg to 35.2 kg).</p>	<p>Table 6.2a and supporting calculations.</p> <p>Table 6.2a and supporting calculations.</p> <p>Figure 1.4, page 1-15, and Appendices 3.6.4 and 3.6.5.</p> <p>Pages 1-10 and 1-11, Table 6.2a and pages 6-31 and 6-52.</p> <p>Pages 5-1 to 5-4, and supporting calculations.</p> <p>Pages 1-83 and 1-97.</p> <p>Page 1-12.</p> <p>Administrative change affecting many pages. Removed round-off.</p> <p>No new calculations.</p>

Note on revisions: Latest revision is shown as:

- Additions or changes are indicated by highlighted text
- Deletions are indicated by a mark in the margin

### 3. THERMAL EVALUATION

Design analysis, similarity, and full-scale testing (see Sect. 2) have demonstrated that the ES-3100 shipping package is in compliance with the applicable requirements of Title 10 Code of Federal Regulations (CFR) 71 (10 CFR 71) when used to ship highly enriched uranium (HEU) having a maximum gross weight up to ~~352 kg (776.0 lb)~~ <sup>352 kg (776.0 lb)</sup>. The ES-3100 has a nominal gross shipping weight that ranges from 146.88 kg (323.79 lb) to 187.81 kg (414.05 lb) for the empty and maximum weight containment vessel configurations shown in Table 2.8, respectively.

#### 3.1 DISCUSSION

The drum assembly of the shipping package is defined as the structure that maintains the position of and provides the impact and thermal barrier surrounding the containment boundary. Preserving the location of the containment boundary within the packaging prevents reduction of the shielding and subcriticality effectiveness. The drum assembly for the ES-3100 consists of an internally flanged Type 304L stainless-steel 30-gal modified drum with two Type 304L stainless-steel inner liners, one filled with noncombustible cast refractory insulation and impact limiter and one filled with noncombustible cast neutron poison; a stainless-steel top plug with noncombustible cast refractory insulation; silicone rubber pads; silicon bronze hex-head nuts; and a stainless-steel lid and bottom (Drawing M2E801580A031, Appendix 1.4.8). The nominal weight of these components is 131.89 kg (290.76 lb).

The drum's diameters (inner diameter of 18.25 in.) and corrugations meet the requirements of Military Standard, MS27683-7. All other dimensions are controlled by Drawing M2E801580A004 (Appendix 1.4.8). Modifications to the drum from MS27683-7 include the following: (1) the overall height was increased; (2) the drum was fabricated with two false wire open ends; and (3) a 0.27-cm (12-gauge, 0.1046-in.)-thick concave cover was welded to the bottom false wire opening (Drawing M2E801580A005, Appendix 1.4.8). Four 0.795-cm (0.313-in.)-diam equally spaced holes are drilled in the top external sidewall to prevent a pressure buildup between the drum and inner liner. The holes are filled with a plastic plug to provide a moisture barrier for the cast refractory insulation during Normal Conditions of Transport (NCT). The cavity created by the inner liners is a three-tiered volume with a 37.52-cm (14.77-in.) inside diameter 13.26 cm (5.22 in.) deep, a 21.84-cm (8.60-in.) inside diameter 5.59 cm (2.20 in.) deep, and an additional 15.85-cm (6.24-in.) inside diameter 78.31-cm (30.83 in.) deep. The volume between the drum and mid liner is filled with a lightweight noncombustible cast refractory material called Kaolite 1600 (Thermal Ceramics, Appendix 2.10.3). The material is composed of portland cement, water, and vermiculite and has an average density of 358.8 kg/m<sup>3</sup> (22.4 lb/ft<sup>3</sup>). The procedure for manufacturing and documenting the insulation, JS-YMN3-801580-A003 (Appendix 1.4.4), is referenced on Drawings M2E801580A002 and M2E801580A008 (Appendix 1.4.8) for the drum body weldment and top plug weldment, respectively. The insulation has a maximum continuous service temperature limit of 871°C (1600°F) due to the presence of the vermiculite and portland cement. The volume between the most internal liner and the mid liner is filled with a noncombustible cast neutron poison (absorber) material called Cat 277-4 from Thermo Electron Corporation. The material is composed of aluminum, magnesium, calcium, boron, carbon, silicone, sulfur, sodium, iron, and water. The final mixture will have an average density of 1681.9 kg/m<sup>3</sup> (105 lb/ft<sup>3</sup>). The procedure for manufacturing and documenting this material, JS-YMN3-801580-A005 (Appendix 1.4.5), is referenced on Drawing M2E801580A002 (Appendix 1.4.8). This neutron poison material has a maximum continuous service temperature limit of 150.0°C (302°F). At this temperature, the moisture inside the Cat 277-4 material remains an integral part of the composite material, and moisture content loss is negligible.

The top plug is fabricated in accordance with Drawing M2E801580A008 (Appendix 1.4.8), with an overall diameter of 36.50 cm (14.37 in.) and a height of 13.41 cm (5.28 in.). The plug's rim, bottom sheet, and top sheet are fabricated from 0.15-cm (16-gauge, 0.0598-in.)-thick Type 304/304L stainless-steel sheet per ASME SA240. Four lifting inserts are welded into the top sheet for loading and unloading operations. The internal volume of the top plug assembly is filled with Kaolite 1600 in accordance with JS-YMN3-801580-A003 (Appendix 1.4.4).

Three silicone rubber pads complete the drum assembly. One pad is placed on the bottom of the most inward liner to support the containment vessel during transport. Another pad is placed on the top shelf of the mid liner to support the top plug during transport. The final pad is placed over the top of the containment vessel lid and closure nut interface. The pads are molded to the shapes as defined on Drawing M2E801580A009 (Appendix 1.4.8). The material is silicone rubber with a Shore A durometer reading of  $22 \pm 5$ .

The ES-3100 package is evaluated for a maximum heat source of 0.4 W (Sect. 1.2.3.7); however, no active cooling systems or specific thermal design features are required. A lightweight cast refractory insulation between the inner liner and the drum provides thermal protection of the contents from external heat sources.

Thermal criteria are applied to the package in accordance with 10 CFR 71 for NCT and Hypothetical Accident Conditions (HAC). These requirements specify that each package design provide containment, shielding, and criticality safety at temperatures ranging from  $-40$  to  $38^{\circ}\text{C}$  ( $-40$  to  $100^{\circ}\text{F}$ ) with full insolation. Also, in accordance with *Packaging and Transportation of Radioactive Material* [10 CFR 71.43(g)], a package must be designed, constructed, and prepared for transport so that in still air at  $38^{\circ}\text{C}$  ( $100^{\circ}\text{F}$ ) and in the shade no accessible surface of a package would have a temperature exceeding  $50^{\circ}\text{C}$  ( $122^{\circ}\text{F}$ ) in a nonexclusive use shipment, or  $85^{\circ}\text{C}$  ( $185^{\circ}\text{F}$ ) in an exclusive use shipment. In addition, each package will experience no significant reduction in effectiveness as the result of being exposed to a thermal radiation environment of  $800^{\circ}\text{C}$  ( $1475^{\circ}\text{F}$ ) for 30 min with an emissivity coefficient of at least 0.9.

The maximum internal pressures and thermal stresses for both NCT and HAC are discussed and calculated (Sects. 3.4.2, 3.4.3, and 3.5.3) for use in the structural evaluation. The calculated pressures are well below the design pressures of the package components, and the effect of thermal stresses on the package is negligible (Sects. 2.6.1.2 and 2.7.4.2).

Compliance with the NCT thermal requirements is shown by analysis (Sect. 3.3.1). Since the components to be shipped have a maximum decay heat load of 0.4 W, a thermal analysis was conducted for the ES-3100 package (Appendix 3.6.2). Since the decay heat load is so meager, the maximum predicted temperature of the entire package, while stored at  $38^{\circ}\text{C}$  ( $100^{\circ}\text{F}$ ) in the shade, is  $38.52^{\circ}\text{C}$  ( $101.33^{\circ}\text{F}$ ) [Table 3.5]. The analysis shows that no accessible surface of the package would have a temperature exceeding  $50^{\circ}\text{C}$  ( $122^{\circ}\text{F}$ ). Therefore, the requirement of 10 CFR 71.43(g) would be satisfied. If the package is exposed to solar radiation at  $38^{\circ}\text{C}$  ( $100^{\circ}\text{F}$ ) in still air, the conservatively calculated temperatures at the top of the drum, center of containment vessel lid, and on the containment vessel near the O-ring sealing surfaces are  $117.72^{\circ}\text{C}$  ( $243.89^{\circ}\text{F}$ ),  $87.81^{\circ}\text{C}$  ( $190.06^{\circ}\text{F}$ ), and  $87.72^{\circ}\text{C}$  ( $189.90^{\circ}\text{F}$ ), respectively (Sect. 3.4.2 and Table 3.6). For conservatism, the O-ring sealing surface temperature will be assumed to be  $87.81^{\circ}\text{C}$  ( $190.06^{\circ}\text{F}$ ). At the low-temperature range and neglecting decay heating, the package components would stabilize at  $-40^{\circ}\text{C}$  ( $-40^{\circ}\text{F}$ ), which is within normal operating limits of the packaging materials (Sect. 2.2).

Five full-scale packages were subjected to the HAC thermal test following the drop, crush and puncture tests (Sects. 2.7.1 through 2.7.3). All of these test packages were exposed to a thermal radiation environment of  $>800^{\circ}\text{C}$  ( $>1475^{\circ}\text{F}$ ) for well over 30 min in a furnace. Other temperature conditions before

and during the thermal testing are given in *Test Report of the ES-3100 Package* for the furnace, test packages, and package supports. The maximum temperature recorded during the tests on the external surface of any of the containment vessels was 127.2°C (261°F). This containment vessel maximum temperature reading is the highest value shown in Table 3.9. This temperature was recorded on Test Units-4 and -5 on the containment vessel sealing lid. The maximum internal temperature adjacent to the O-rings was 116°C (241°F). Temperature adjustments are then added to the containment vessel's maximum recorded temperature to correct for measuring accuracy, internal decay heating, insulation heating during cool down, location of crush plate damage, neutron poison substitution, thermal capacitance difference between mockups and actual contents, and material density variations. Detailed discussion of each temperature adjustment is provided in Sect. 3.5.3. Since Test Unit-5 was tested with a mock-up that represented the lightest proposed content, no temperature correction was needed for mass differences. The containment vessel's recorded temperature values were lower on all other test units, which consisted of much heavier mock-up contents.

### 3.1.1 Design Features

The drum assembly for the ES-3100 consists of an internally flanged Type 304L stainless-steel 30-gal modified drum with two Type 304L stainless-steel inner liners, one filled with noncombustible cast refractory insulation and impact limiter and one filled with noncombustible cast neutron poison; a stainless-steel top plug with noncombustible cast refractory insulation, silicone rubber pads, silicon bronze hex-head nuts, and a stainless-steel lid and bottom (Drawing M2E801580A031, Appendix 1.4.8). The drum's diameter (inner diameter of 18.25 in.) and corrugations meet the requirements of Military Standard, MS27683-7. All other dimensions are controlled by Drawing M2E801580A004 (Appendix 1.4.8). Modifications to the drum from MS27683-7 include the following: (1) the overall height was increased; (2) the drum was fabricated with two false wire open ends; and (3) a 0.27-cm (12-gauge, 0.1046-in.)-thick concave cover was welded to the bottom false wire opening (Drawing M2E801580A005, Appendix 1.4.8). Four 0.795-cm (0.313-in.)-diam equally spaced holes are drilled in the top external sidewall to prevent a pressure buildup between the drum and inner liner. The cavity created by the inner liners is a three-tiered volume with a 37.52-cm (14.77-in.) inside diameter 13.26 cm (5.22 in.) deep, a 21.84-cm (8.60-in.) inside diameter 5.59 cm (2.20 in.) deep, and an additional 15.85-cm (6.24-in.) inside diameter 78.31 cm (30.83 in.) deep. Drum and inner liner wall thickness is 0.15 cm (16 gauge, 0.0598 in.).

The volume between the drum and mid liner is filled with a lightweight noncombustible cast refractory material called Kaolite 1600 (Thermal Ceramics, Appendix 2.10.3). The material is composed of portland cement, water, and vermiculite and has an average density of 358.8 kg/m<sup>3</sup> (22.4 lb/ft<sup>3</sup>). The procedure for manufacturing and documenting the insulation, JS-YMN3-801580-A003 (Appendix 1.4.4), is referenced on Drawings M2E801580A002 and M2E801580A008 (Appendix 1.4.8) for the drum body weldment and top plug weldment, respectively.

The volume between the most internal liner and the mid liner is filled with a noncombustible cast neutron poison material from Thermo Electron Corporation (Cat 277-4). The material is composed of aluminum, magnesium, calcium, boron, carbon, silicone, sulfur, sodium, iron, and water. This mixture will have an average density of 1681.9 kg/m<sup>3</sup> (105 lb/ft<sup>3</sup>). The procedure for manufacturing and documenting this material, JS-YMN3-801580-A005 (Appendix 1.4.5), is referenced on Drawing M2E801580A002 (Appendix 1.4.8).

Three silicone rubber pads complete the drum assembly. One pad is placed on the bottom of the most inward liner to support the containment vessel during transport. Another pad is placed on the top shelf of the mid liner to support the top plug during transport. The final plug is placed over the top of the containment vessel lid and closure nut assembly. Pads are molded to the shapes as defined on Drawing M2E801580A009 (Appendix 1.4.8) using silicone rubber with a Shore A durometer reading of 22 ± 5.

### 3.1.2 Content's Decay Heat

The maximum decay heat and radioactivity of the contents (Sect. 4) are based on a maximum of 35.2 kg of HEU in the isotopic and mass distribution at fabrication as shown in Table 3.1.

Table 3.1. Isotopic mass and weight percent for the HEU contents <sup>a</sup>

Nuclide	Weight percent	Mass (g)
<sup>232</sup> U	0.000004	<u>0.001408</u>
<sup>233</sup> U	0.600000	<u>211.200000</u>
<sup>234</sup> U	2.000000	<u>704.000000</u>
<sup>235</sup> U	<u>54.895996</u>	<u>19323.390592</u>
<sup>236</sup> U	40.000000	<u>14080.000000</u>
<sup>238</sup> U	0.000000	<u>0.000000</u>
Transuranic	0.004000	<u>1.408000</u>
<sup>237</sup> Np	<u>2.500000</u>	<u>880.000000</u>
Total	100.000000	<u>35200.000000</u>

<sup>a</sup> Weight percent values of individual isotopes are those that generate the largest activity within the allowable ranges presented in Sect. 1.2.3.

Using the ORIGEN-S program for determining decay heat values and predicting the isotopic decay patterns from 0 to 70 years from original fabrication, the following decay heat loads are predicted and shown in Table 3.2. Isotopic mass distribution has been calculated in Sect. 4 and shown in Table 2 of Appendix 4.6.1. The maximum decay heat load is rounded up from 0.3954 to 0.4 W, and 0.4 W is used in subsequent analyses for temperature predictions. Contributions from the transuranics and <sup>237</sup>Np at the bottom of Table 3.2 remain constant for the time period evaluated. The decay heat per gram value used for the transuranic isotopes was an average of the decay heat values for <sup>238</sup>Pu, <sup>239</sup>Pu, <sup>240</sup>Pu, <sup>241</sup>Pu, <sup>242</sup>Pu and <sup>241</sup>Am.

### 3.1.3 Summary Tables of Temperatures

#### 3.1.3.1 NCT Summary Tables

The ES-3100 shipping container has been conservatively evaluated empty of all containment vessel internal components for NCT. Prior to the change of neutron absorber from BoroBond4 to Cat 277-4, parameters, such as Kaolite 1600 density, BoroBond4 thermal conductivity, and decay heat loads, were varied to encompass the range of potential variations in material properties. The available thermal conductivity information on BoroBond4 was limited to moderate temperatures in the range of -3.89°C (25°F) to 40°C (104°F) [Eagle-Picher presentation excerpts sent to Gerry Byington via e-mail from Jim Hall on March 12, 2004]. Using the available thermal conductivity data for BoroBond4, thermal analyses for NCT and HAC have been performed and are documented in DAC-PKG-801699-A001 (summarized in Appendix 3.6.1). Nodal locations for temperatures presented are shown in Fig. 3.1. Based on the results reported in the above document and shown in Tables 3.3 and 3.4, it was determined that the higher temperatures occurred when the lowest density of the Kaolite 1600 was used. Therefore, subsequent analysis using the proposed Cat 277-4 neutron absorber during NCT uses a Kaolite 1600 density of 19.4 lb/ft<sup>3</sup>. The results for the steady state condition at 38°C (100°F) in the shade, and the transient condition of applying solar insolation are shown in Tables 3.5 and 3.6 for the proposed configuration (package with Cat 277-4 neutron absorber).



Table 3.2. Decay heat for 35.2 kg of HEU content (watts)

Decay Heat (Watts per gram)	Isotope	DECAY TIME								
		0 years	5 years	10 years	20 years	30 years	40 years	50 years	60 years	70 years
1.7920e-02	Pb-210	0.0000e+00	2.5380e-12	1.9556e-11	1.4835e-10	4.6789e-10	1.0156e-09	1.8547e-09	3.0280e-09	4.6284e-09
2.6280e+03	Pb-212	0.0000e+00	4.7733e-05	6.3284e-05	4.9583e-05	4.4773e-05	4.0703e-05	3.6781e-05	3.3302e-05	3.0157e-05
2.8650e+02	Bi-210	0.0000e+00	2.5008e-11	1.9280e-10	1.4339e-09	4.6176e-09	1.0003e-08	1.8312e-08	2.8848e-08	4.4570e-08
2.4500e+05	Bi-212	0.0000e+00	4.2147e-04	4.6984e-04	4.3975e-04	3.9729e-04	3.5928e-04	3.2578e-04	2.9503e-04	2.6705e-04
1.4420e+02	Po-210	0.0000e+00	3.4728e-10	2.6806e-09	1.9902e-08	8.2761e-08	1.3911e-07	2.5488e-07	4.1327e-07	6.1939e-07
5.1130e+03	Rn-222	0.0000e+00	7.2356e-08	2.8942e-08	1.1666e-07	2.5980e-07	4.6077e-07	7.1895e-07	1.0331e-06	1.4075e-06
1.8230e+03	Ra-223	0.0000e+00	1.1907e-06	4.5091e-06	1.6416e-07	3.3642e-07	5.4802e-07	7.8557e-07	1.0403e-06	1.3210e-06
5.4700e+03	Ra-224	0.0000e+00	8.6280e-04	9.6272e-04	9.0111e-04	8.1839e-04	7.3783e-04	6.6748e-04	6.0459e-04	5.4760e-04
2.8380e+01	Ra-225	0.0000e+00	5.9942e-07	1.2947e-06	2.6895e-06	3.8842e-06	5.1730e-06	6.4737e-06	7.7325e-06	9.0512e-06
2.8600e-02	Ra-226	0.0000e+00	6.3026e-09	2.5170e-08	1.0088e-07	2.2653e-07	4.0071e-07	6.2624e-07	9.0009e-07	1.2243e-06
1.5200e-02	Ra-228	0.0000e+00	3.1241e-15	1.0485e-14	3.1241e-14	5.4992e-14	7.9599e-14	1.0442e-13	1.2946e-13	1.5449e-13
2.0290e+03	Ac-225	0.0000e+00	3.4282e-06	8.2644e-06	1.2613e-04	1.8789e-04	2.4883e-04	3.1239e-04	3.7453e-04	4.3709e-04
3.5000e-02	Ac-227	0.0000e+00	1.8186e-10	8.1483e-10	2.2253e-09	4.5658e-09	7.4402e-09	1.0887e-08	1.4204e-08	1.7924e-08
1.7460e+04	Ac-228	0.0000e+00	4.3780e-13	1.4701e-12	4.3780e-12	7.6949e-12	1.1161e-11	1.4652e-11	1.8143e-11	2.1659e-11
1.1250e+03	Th-227	0.0000e+00	1.2085e-08	4.5889e-08	1.8630e-07	3.4130e-07	5.5434e-07	7.9781e-07	1.0609e-06	1.3413e-06
2.6850e+01	Th-228	0.0000e+00	8.2427e-04	9.1879e-04	8.6830e-04	7.7886e-04	7.0327e-04	6.3900e-04	5.7850e-04	5.2178e-04
6.0870e-03	Th-229	0.0000e+00	3.8588e-05	5.5025e-05	1.0892e-04	1.6458e-04	2.1984e-04	2.7384e-04	3.2912e-04	3.8440e-04
5.8220e-04	Th-230	0.0000e+00	5.6970e-06	1.1363e-05	2.2747e-05	3.4100e-05	4.6494e-05	5.8970e-05	6.8037e-05	7.9513e-05
5.7940e+02	Th-231	0.0000e+00	4.5588e-05	4.5588e-05	4.5588e-05	4.5588e-05	4.5588e-05	4.5588e-05	4.5588e-05	4.5588e-05
2.6590e-09	Th-232	0.0000e+00	5.4281e-12	1.0884e-11	2.1787e-11	3.2681e-11	4.3425e-11	5.4281e-11	6.5512e-11	7.6368e-11
9.5900e+00	Th-234	0.0000e+00	0.0000e+00	0.0000e+00	0.0000e+00	0.0000e+00	0.0000e+00	0.0000e+00	0.0000e+00	0.0000e+00
1.4390e-03	Pa-231	0.0000e+00	1.3457e-07	2.8942e-07	5.3940e-07	8.0910e-07	1.0780e-06	1.3457e-06	1.6154e-06	1.8823e-06
5.2710e+01	Pa-233	0.0000e+00	0.0000e+00	0.0000e+00	0.0000e+00	0.0000e+00	0.0000e+00	0.0000e+00	0.0000e+00	0.0000e+00
7.0800e-01	U-232	9.9888e-04	9.4702e-04	9.0216e-04	8.1743e-04	7.3987e-04	6.6989e-04	6.0709e-04	5.4927e-04	4.9744e-04
2.8070e-04	U-233	5.9280e-02	5.9278e-02	5.9278e-02	5.9275e-02	5.9273e-02	5.9270e-02	5.9268e-02	5.9265e-02	5.9263e-02
1.7910e-04	U-234	1.2609e-01	1.2609e-01	1.2609e-01	1.2609e-01	1.2608e-01	1.2608e-01	1.2608e-01	1.2607e-01	1.2607e-01
6.0000e-08	U-235	1.1594e-03	1.1594e-03	1.1594e-03	1.1594e-03	1.1594e-03	1.1594e-03	1.1594e-03	1.1594e-03	1.1594e-03
2.0000e-06	U-236	2.4656e-02	2.4656e-02	2.4656e-02	2.4656e-02	2.4656e-02	2.4656e-02	2.4656e-02	2.4656e-02	2.4656e-02
8.5111e-09	U-238	0.0000e+00	0.0000e+00	0.0000e+00	0.0000e+00	0.0000e+00	0.0000e+00	0.0000e+00	0.0000e+00	0.0000e+00
1.1580e-01	transuranic	1.6306e-01	1.6306e-01	1.6306e-01	1.6306e-01	1.6306e-01	1.6306e-01	1.6306e-01	1.6306e-01	1.6306e-01
2.0100e-05	Np-237	1.7688e-02	1.7688e-02	1.7688e-02	1.7688e-02	1.7688e-02	1.7688e-02	1.7688e-02	1.7688e-02	1.7688e-02
Total watts		3.9293e-01	3.9517e-01	3.9542e-01	3.9530e-01	3.9514e-01	3.9500e-01	3.9489e-01	3.9480e-01	3.9473e-01

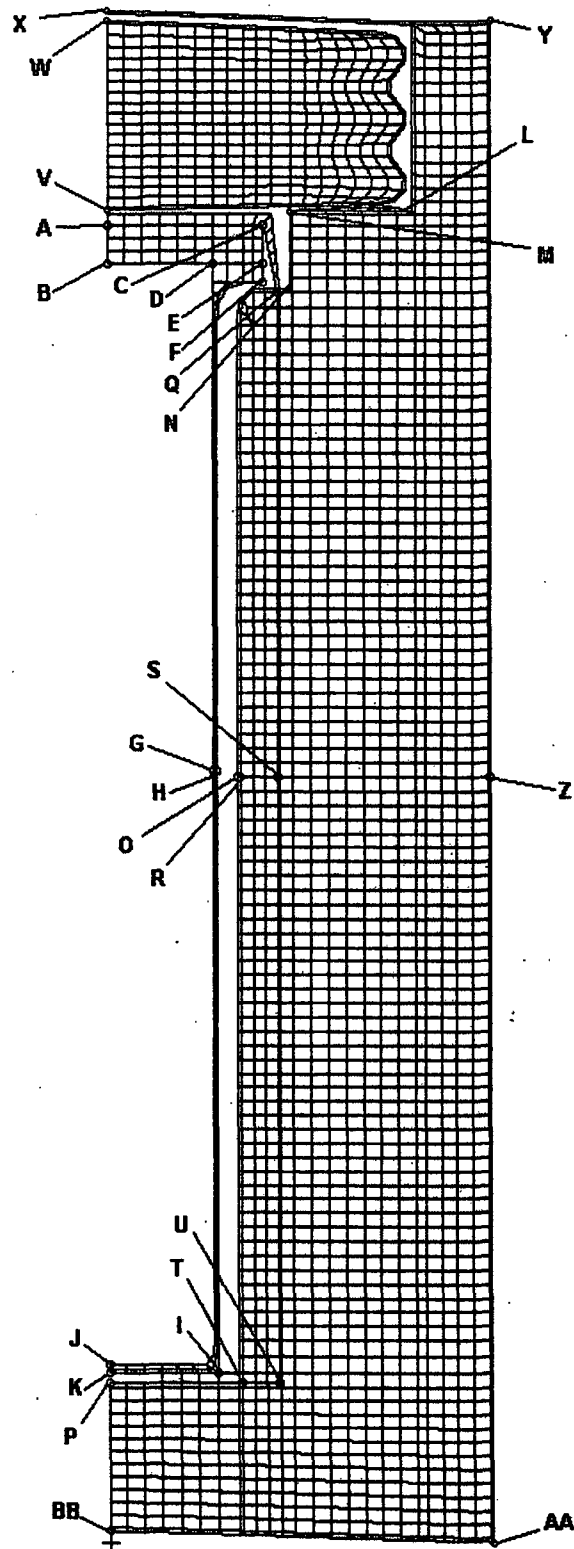


**Fig. 3.1. MSC.Patran axisymmetric finite element model of the ES-3100 shipping container with BoroBond 4—nodal locations of interest (elements representing air not shown for clarity).**

**Table 3.3. Maximum "quasi steady-state" temperatures during NCT for the ES-3100 shipping container with various content heat loads—Kaolite density of 19.4 lb/ft<sup>3</sup> and BoroBond4**

Node <sup>a</sup>	Location	Maximum "quasi steady-state" temperature, °C (°F)			
		0 W	0.4 W	20 W	30 W
A	CV lid, top, center	88.30 (190.95)	88.62 (191.52)	103.84 (218.91)	111.35 (232.42)
B	CV lid, bottom, center	88.28 (190.90)	88.60 (191.48)	103.90 (219.03)	111.45 (232.62)
C	CV lid, top, outer	88.32 (190.97)	88.63 (191.54)	103.61 (218.50)	111.00 (231.80)
D	CV flange at interface, inner <sup>b</sup>	88.24 (190.83)	88.56 (191.41)	103.87 (218.96)	111.42 (232.55)
E	CV flange at interface, outer <sup>b</sup>	88.25 (190.84)	88.56 (191.41)	103.77 (218.78)	111.27 (232.28)
F	CV flange, bottom, outer	88.24 (190.82)	88.55 (191.39)	103.75 (218.75)	111.25 (232.24)
G	CV shell, mid-height, inner	83.04 (181.47)	83.61 (182.50)	110.50 (230.89)	123.46 (254.23)
H	CV shell, mid-height, outer	83.04 (181.47)	83.61 (182.50)	110.49 (230.88)	123.45 (254.21)
I	CV bottom, outer	83.36 (182.04)	83.75 (182.74)	102.58 (216.64)	111.99 (233.59)
J	CV bottom, center, inner	88.37 (182.07)	83.76 (182.77)	102.70 (216.86)	112.17 (233.91)
K	CV bottom, center, outer	88.37 (181.07)	83.76 (182.77)	102.69 (216.84)	112.15 (233.87)
L	Drum liner, plug cavity, outer	98.72 (209.70)	98.80 (209.85)	102.63 (216.73)	104.58 (220.24)
M	Drum liner, plug cavity, inner	94.43 (201.97)	94.58 (202.24)	101.92 (215.46)	105.65 (222.16)
N	Drum liner, CV flange cavity, outer	89.43 (192.97)	89.63 (193.34)	99.83 (211.70)	105.01 (221.02)
O	Drum liner, CV cavity, mid-height, inner	83.12 (181.62)	83.43 (182.18)	98.63 (209.54)	106.40 (223.52)
P	Drum liner, CV cavity, bottom, inner	83.62 (182.52)	83.96 (183.13)	100.36 (212.65)	108.60 (227.48)
Q	Borobond4, top, outer	88.82 (191.88)	89.04 (192.27)	99.65 (211.38)	105.04 (221.07)
R	Borobond4, mid-height, inner	83.12 (181.62)	83.43 (182.18)	98.63 (209.53)	106.39 (223.51)
S	Borobond4, mid-height, outer	83.03 (181.46)	83.33 (182.00)	97.91 (208.23)	105.36 (221.65)
T	Borobond4, bottom, inner	83.55 (182.39)	83.85 (182.93)	98.58 (209.45)	106.03 (222.86)
U	Borobond4, bottom, outer	83.51 (182.31)	83.80 (182.83)	97.82 (208.07)	104.90 (238.82)
V	Drum plug liner, bottom, center	112.01 (233.62)	112.05 (233.69)	113.95 (237.11)	114.90 (238.82)
W	Drum plug liner, top, center	92.09 (197.77)	92.31 (198.16)	102.93 (217.27)	108.26 (226.87)
X	Drum lid, top, center	118.01 (244.42)	118.03 (244.45)	118.77 (245.79)	119.15 (246.47)
Y	Drum lid, top, outer	107.33 (225.19)	107.34 (225.22)	108.22 (226.80)	108.67 (227.60)
Z	Drum, mid-height, outer	92.27 (198.08)	92.30 (198.14)	93.81 (200.86)	94.58 (202.24)
AA	Drum bottom, outer	91.70 (197.06)	91.74 (197.13)	93.61 (200.49)	94.54 (202.18)
BB	Drum bottom, center	88.82 (191.88)	88.93 (192.07)	93.84 (200.91)	96.30 (205.35)

<sup>a</sup> See Fig. 3.1.

<sup>b</sup> Approximate location of the CV O-rings.

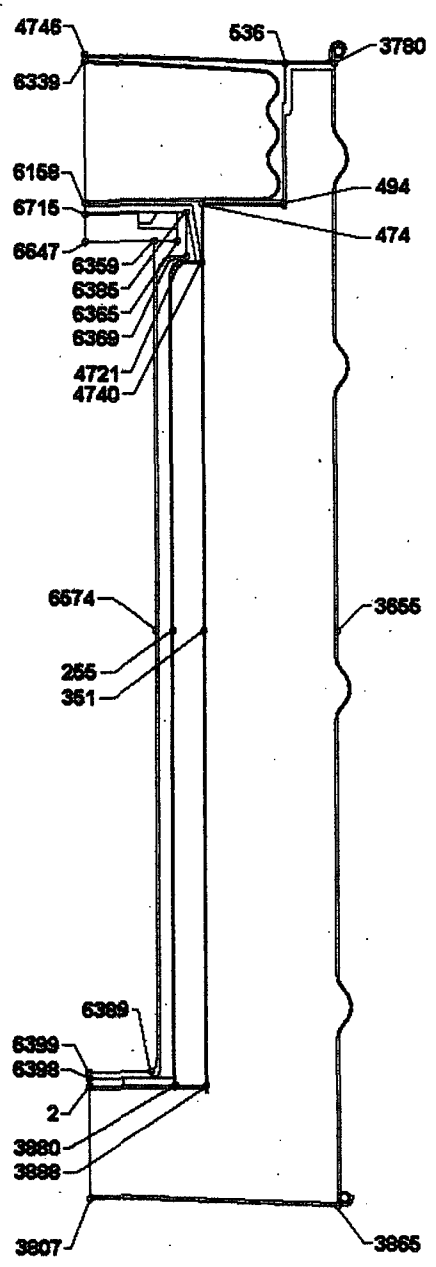
**Table 3.4. Maximum "quasi steady-state" temperatures during NCT for the ES-3100 shipping container with various content heat loads—Kaolite density of 30 lb/ft<sup>3</sup> and BoroBond4**

Node <sup>a</sup>	Location	Maximum "quasi steady-state" temperature, °C (°F)			
		0 W	0.4 W	20 W	30 W
A	CV lid, top, center	86.56 (187.81)	86.88 (188.38)	102.98 (215.74)	109.59 (229.26)
B	CV lid, bottom, center	86.56 (187.80)	86.88 (188.38)	102.16 (215.90)	109.71 (229.47)
C	CV lid, top, outer	86.54 (187.78)	86.86 (188.34)	101.89 (215.41)	109.31 (228.75)
D	CV flange at interface, inner <sup>b</sup>	86.47 (187.64)	86.79 (188.21)	102.09 (215.77)	109.67 (229.40)
E	CV flange at interface, outer <sup>b</sup>	86.44 (187.59)	86.76 (188.16)	102.00 (215.61)	109.53 (229.15)
F	CV flange, bottom, outer	86.42 (187.56)	86.74 (188.13)	101.99 (215.58)	109.51 (229.12)
G	CV shell, mid-height, inner	81.52 (178.74)	82.09 (179.76)	109.01 (228.21)	121.98 (251.57)
H	CV shell, mid-height, outer	81.52 (178.74)	82.09 (179.76)	109.00 (228.19)	121.97 (251.55)
I	CV bottom, outer	81.32 (178.37)	81.71 (179.08)	100.57 (213.02)	109.99 (229.99)
J	CV bottom, center, inner	81.37 (178.47)	81.77 (179.18)	100.73 (213.31)	110.21 (230.38)
K	CV bottom, center, outer	81.37 (178.47)	81.77 (179.18)	100.72 (213.29)	110.19 (230.34)
L	Drum liner, plug cavity, outer	97.74 (207.93)	97.82 (208.07)	101.65 (214.96)	103.59 (218.47)
M	Drum liner, plug cavity, inner	92.91 (199.23)	93.06 (199.50)	100.40 (212.72)	104.13 (219.43)
N	Drum liner, CV flange cavity, outer	87.69 (189.84)	87.90 (190.21)	98.09 (208.57)	103.27 (217.43)
O	Drum liner, CV cavity, mid-height, inner	81.30 (178.35)	81.61 (178.90)	96.82 (206.27)	104.13 (219.43)
P	Drum liner, CV cavity, bottom, inner	81.52 (178.74)	81.86 (179.35)	98.30 (208.94)	106.56 (223.80)
Q	Borobond4, top, outer	87.36 (189.25)	87.58 (189.64)	98.19 (208.74)	103.57 (218.43)
R	Borobond4, mid-height, inner	81.30 (178.35)	81.61 (178.90)	98.81 (206.26)	104.58 (220.24)
S	Borobond4, mid-height, outer	81.37 (178.46)	81.66 (178.99)	96.24 (205.23)	103.69 (218.64)
T	Borobond4, bottom, inner	81.67 (179.01)	81.98 (179.56)	96.73 (206.12)	104.19 (219.55)
U	Borobond4, bottom, outer	81.78 (179.21)	82.07 (179.72)	96.11 (205.00)	103.23 (217.81)
V	Drum plug liner, bottom, center	111.30 (232.35)	111.34 (232.42)	113.25 (235.85)	114.21 (237.57)
W	Drum plug liner, top, center	90.70 (195.26)	90.92 (195.66)	101.53 (214.76)	106.87 (224.36)
X	Drum lid, top, center	117.74 (243.93)	117.75 (243.96)	118.50 (245.30)	118.88 (245.98)
Y	Drum lid, top, outer	107.04 (224.68)	107.06 (224.71)	107.94 (226.29)	108.39 (227.10)
Z	Drum, mid-height, outer	91.86 (197.36)	91.90 (197.41)	93.42 (200.15)	94.18 (201.53)
AA	Drum bottom, outer	91.00 (195.79)	91.04 (195.86)	92.92 (199.26)	93.87 (200.96)
BB	Drum bottom, center	87.21 (188.97)	87.31 (189.15)	92.26 (198.07)	94.74 (202.54)

<sup>a</sup> See Fig. 3.1.

<sup>b</sup> Approximate location of the CV O-rings.

**Table 3.5. ES-3100 shipping container maximum steady-state temperatures with Cat 277-4 (100°F ambient temperature, no insolation)**

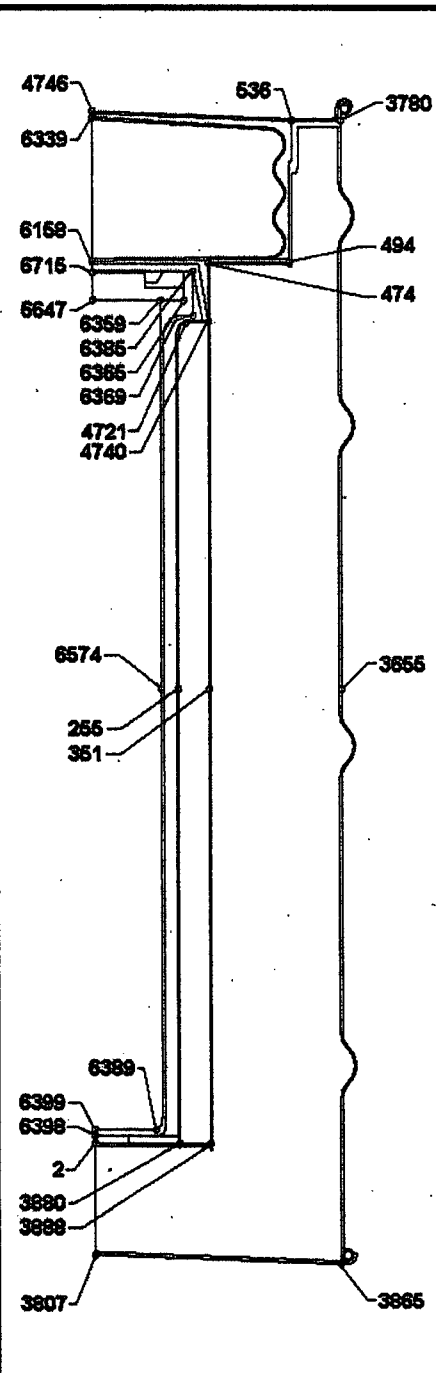
Node map <sup>a</sup>	Node coordinates (in.)			Maximum "quasi steady-state" temperature (°F)		
	No.	r	z	0.4 W	20° W	30° W
	2	0.000	4.505	100.83	134.54	150.15
	255	3.180	21.528	100.75	131.57	146.21
	351	4.300	21.528	100.71	129.45	142.87
	474	4.300	37.535	100.46	117.90	125.67
	494	7.325	37.525	100.32	110.87	115.19
	536	7.385	42.755	100.21	105.50	107.19
	3655°	9.185	21.528	100.28	107.58	109.92
	3780°	9.185	42.755	100.21	105.29	106.89
	3807°	0.000	0.320	100.43	114.39	120.08
	3865°	9.185	0.008	100.32	108.97	111.97
	3880	3.178	4.505	100.74	130.48	144.23
	3888	4.300	4.505	100.71	128.60	141.42
	4721	3.500	35.275	100.59	124.08	134.90
	4740	4.300	35.275	100.57	122.92	133.15
	4746°	0.000	43.065	100.20	104.99	106.43
	6158	0.000	37.579	100.57	123.14	133.42
	6339	0.000	42.859	100.25	107.42	110.04
	6359 <sup>b</sup>	2.530	36.075	100.80	133.51	148.56
	6365 <sup>b</sup>	3.425	36.075	100.79	133.33	148.28
	6369	3.750	35.525	100.79	133.27	148.20
	6385	3.750	37.175	100.78	132.85	147.58
	6389	2.310	5.025	100.97	141.27	160.06
	6398	0.000	4.775	100.96	140.91	159.55
	6399	0.000	5.025	100.96	140.94	159.60
	6574	2.530	21.528	101.33	157.70	183.56
	6647	0.000	36.075	100.80	133.56	148.63
	6715	0.000	37.135	100.79	133.40	148.40

<sup>a</sup> See Figs. 8 through 11 in Appendix 3.6.2 for details of node locations.

<sup>b</sup> Approximate location of the CV O-ring.

<sup>c</sup> These nodes are at the accessible surfaces of the package (i.e., the drum, drum lid, and drum bottom plate).

**Table 3.6. ES-3100 shipping container maximum "quasi steady-state" temperatures during NCT with various content heat loads and Cat 277-4 (100°F ambient temperature, with insolation)**

Node map <sup>a</sup>	Node coordinates (in.)			Maximum "quasi steady-state" temperature (°F)			
	No.	r	z	0 W	0.4 W	20 W	30 W
	2	0.000	4.505	180.59	181.23	210.15	224.69
	255	3.180	21.528	179.33	179.93	207.32	221.43
	351	4.300	21.53	179.59	180.14	204.73	217.27
	474	4.300	37.54	198.88	199.20	212.72	219.58
	494	7.325	37.53	207.40	207.56	214.4	217.87
	536	7.385	42.76	226.44	226.49	228.31	229.24
	3655	9.185	21.528	198.09	198.15	200.81	202.16
	3780	9.185	42.755	223.47	223.51	225.13	225.95
	3807	0.000	0.320	190.48	190.70	199.84	204.43
	3865	9.185	0.008	195.87	195.97	199.91	201.90
	3880	3.178	4.505	180.72	181.28	206.65	219.52
	3888	4.300	4.505	181.03	181.55	205.08	217.01
	4721	3.500	35.275	189.45	189.90	209.53	219.47
	4740	4.300	35.275	190.56	190.98	209.37	218.68
	4746	0.000	43.065	243.86	243.89	245.32	246.03
	6158	0.000	37.579	198.42	198.84	217.12	226.32
	6339	0.000	42.859	233.98	234.06	237.32	238.95
	6359 <sup>b</sup>	2.530	36.075	189.28	189.90	217.07	230.51
	6365 <sup>b</sup>	3.425	36.075	189.27	189.88	216.88	230.23
	6369	3.750	35.525	189.23	189.85	216.79	230.12
	6385	3.750	37.175	189.39	190.00	216.57	229.72
	6389	2.310	5.025	179.94	180.70	215.75	233.27
	6398	0.000	4.775	179.99	180.76	215.52	232.92
	6399	0.000	5.025	179.99	180.76	215.55	232.96
	6574	2.530	21.528	179.27	180.35	229.19	252.87
	6647	0.000	36.075	189.40	190.02	217.24	230.72
	6715	0.000	37.14	189.44	190.06	217.14	230.54

<sup>a</sup> See Figs. 8 through 11 in Appendix 3.6.2 for details of node locations.

<sup>b</sup> Approximate location of the CV O-ring.

### 3.1.3.2 HAC Temperature Summary Tables

In order to predict the maximum temperature for the packaging components during HAC, a transient thermal analyses was performed on the finite element model of the ES-3100 shipping container (undamaged configuration) to simulate HAC as prescribed by 10 CFR 71.73(c)(4). A 30-min fire of 800°C (1475°F) was simulated by applying natural convection and radiant exchange boundary conditions to all external surfaces of the drum (assuming the drum is in a horizontal orientation) with content heat loads of 0, 0.4, 20, and 30 W. There are no heat flux boundary conditions simulating insolation applied to the model before and during the 30-minute fire. The initial temperature distribution within the package having content heat loads of 0.4, 20, and 30 W is obtained from their respective steady-state analyses (Table 3.5). The initial temperature distribution within the package having no content heat load (0 W) is assumed to be at a uniform temperature equal to the ambient temperature of 38°C (100°F). The content heat load is simulated by applying a uniform heat flux to the internal surfaces of the elements representing the containment vessel.

Following the 30-min fire transient analyses, 48-h cool-down transient thermal analyses are performed using the temperature distribution at the end of the fire as the initial temperature distribution. During post-fire cool-down, natural convection and radiant exchange boundary conditions are applied to all external surfaces of the drum (assuming the drum is in a horizontal orientation). Additionally, cases are analyzed in which insolation is included during the post-fire cool-down. For the cases in which insolation is applied to the model during cool-down, insolation is applied during the first 12-h period following the 30-min fire, and then alternated (off, then on) as was done for NCT.

Based on the previous analysis of the ES-3100 package using BoroBond4 (Appendix 3.6.1), it was noted that using the low-end density of Kaolite 1600 results in higher containment vessel temperatures than using the high-end density of Kaolite 1600. For this reason, the NCT and HAC thermal analyses were run using a density of 19.4 lb/ft<sup>3</sup>. Similarly, the low-end density of the Cat 277-4 material (100 lb/ft<sup>3</sup>) was also used in these analyses. However, while using these low-end densities will result in higher temperatures to the containment vessel, using the high-end densities for these two materials will result in higher temperature differences from the baseline case. Thus, HAC runs are also made for heat loads of 0, 0.4, 20, and 30 W using a Kaolite 1600 density of 30 lb/ft<sup>3</sup> and a Cat 277-4 density of 110 lb/ft<sup>3</sup>.

The maximum temperatures calculated for the ES-3100 shipping container for HAC are summarized in Table 3.7 for the analyses using a Kaolite 1600 density of 19.4 lb/ft<sup>3</sup> and a Cat 277-4 density of 100 lb/ft<sup>3</sup>. The maximum temperatures calculated for the ES-3100 shipping container for HAC are summarized in Table 3.8 for the analyses using a Kaolite 1600 density of 30 lb/ft<sup>3</sup> and a Cat 277-4 density of 110 lb/ft<sup>3</sup>. The thermal analyses that use the low-end density values for Kaolite 1600 and Cat 277-4 achieve the higher package temperatures (see Table 3.7).

### 3.1.4 Summary Tables of Maximum Pressures

#### 3.1.4.1 Maximum NCT Pressures

Table 3.10 summarizes the results from Appendix 3.6.4 in which the pressure of the containment vessel when subjected to the tests and conditions of NCT per 10 CFR 71.71 has been determined for the most restrictive containment vessel arrangements (CVAs) shipped in the ES-3100. The most restrictive CVAs are those in which the void volume inside the containment vessel is minimized based on content volumes and those CVAs that carry the largest mass of items that off-gas at the predicted temperatures during NCT. Several convenience container heights are proposed for shipment (Fig. 1.4). Shipping configurations will use these containers in any configuration as long as it does not exceed the HEU weight limit and form and does not exceed the height constraint of the containment vessel. However, in order to determine the worst-case

**Table 3.7. ES-3100 shipping container HAC maximum temperatures (Kaolite 1600 density of 19.4 lb/ft<sup>3</sup> and Cat 277-4 density of 100 lb/ft<sup>3</sup>)**

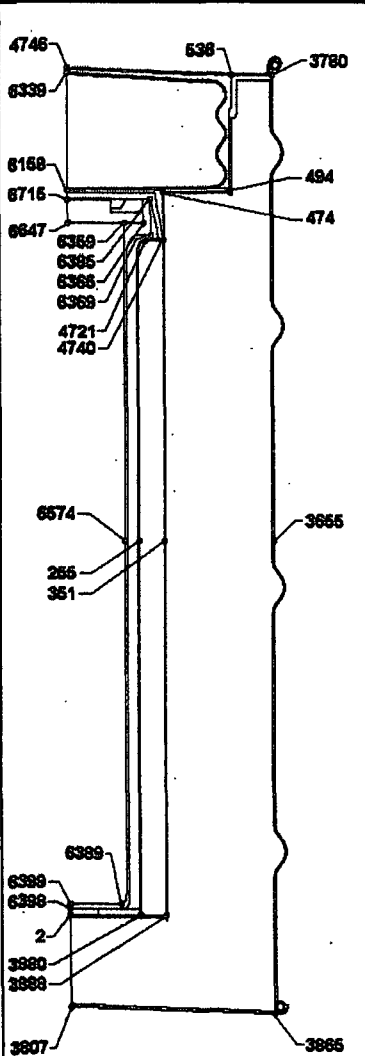
Node map	Node coordinates (in.)			HAC maximum temperature (°F)							
	No.	r	z	0 W		0.4 W		20 W		30 W	
				Insolation during cool-down?		Insolation during cool-down?		Insolation during cool-down?		Insolation during cool-down?	
				No <sup>b</sup>	Yes	No	Yes	No	Yes	No	Yes
	2	0.000	4.505	225.5	232.1	226.2	232.8	255.5	261.7	269.5	275.7
	255	3.180	21.528	194.5	212.5	195.2	213.2	223.8	241.3	237.8	255.3
	351	4.300	21.528	195.8	211.9	196.4	212.5	222.3	237.8	234.8	250.3
	474	4.300	37.535	392.9	395.0	393.2	395.4	407.6	409.7	414.2	416.3
	494	7.325	37.525	671.2	672.0	671.4	672.3	679.1	680.0	682.5	683.3
	536	7.385	42.755	1380.4	1380.4	1380.4	1380.4	1380.9	1380.9	1381.1	1381.1
	3655	9.185	21.528	1457.8	1457.8	1457.8	1457.8	1458.0	1458.0	1458.1	1458.1
	3780	9.185	42.755	1427.8	1427.8	1427.9	1427.9	1428.1	1428.1	1428.2	1428.2
	3807	0.000	0.320	1454.5	1454.5	1454.5	1454.5	1454.9	1454.9	1455.0	1455.0
	3865	9.185	0.008	1470.1	1470.1	1470.1	1470.1	1470.1	1470.1	1470.2	1470.2
	3880	3.178	4.505	230.6	236.4	231.2	237.0	257.1	262.5	269.4	274.8
	3888	4.300	4.505	236.9	241.7	237.5	242.3	261.5	266.1	272.9	277.5
	4721	3.500	35.275	245.7	252.8	246.2	253.3	266.8	273.8	276.6	283.6
	4740	4.300	35.275	258.4	263.5	258.8	264.0	278.1	283.1	287.1	292.1
	4746	0.000	43.065	1448.0	1448.0	1448.0	1448.0	1448.2	1448.2	1448.3	1448.3
	6158	0.000	37.579	308.7	311.6	309.1	312.0	328.3	331.2	337.3	340.2
	6339	0.000	42.859	1335.1	1335.1	1335.2	1335.2	1336.4	1336.4	1336.9	1336.9
	6359 <sup>a</sup>	2.530	36.075	236.7	247.6	237.3	248.3	266.2	276.6	279.8	289.9
	6365 <sup>a</sup>	3.425	36.075	236.6	247.6	237.3	248.3	266.0	276.4	279.5	289.7
	6369	3.750	35.525	236.5	247.6	237.2	248.2	265.8	276.2	279.3	289.5
	6385	3.750	37.175	237.3	248.2	237.9	248.8	266.1	276.4	279.4	289.5
	6389	2.310	5.025	219.0	227.4	219.9	228.2	255.3	263.1	272.2	279.9
	6398	0.000	4.775	219.7	227.9	220.5	228.7	255.6	263.3	272.5	280.0
	6399	0.000	5.025	219.7	227.9	220.5	228.7	255.6	263.3	272.5	280.0
	6574	2.530	21.528	196.1	214.9	197.3	216.0	246.7	263.8	269.9	286.5
	6647	0.000	36.075	237.2	248.0	237.9	248.6	266.8	277.0	280.4	290.4
	6715	0.000	37.135	237.4	248.1	238.0	248.8	266.8	277.0	280.4	290.4

<sup>a</sup> Approximate location of the CV O-ring.

<sup>b</sup> Baseline case for  $\Delta T$  comparisons.



**Table 3.8. ES-3100 shipping container HAC maximum temperatures (Kaolite 1600 density of 30 lb/ft<sup>3</sup> and Cat 277-4 density of 110 lb/ft<sup>3</sup>)**

Node map	Node coordinates (in.)			HAC maximum temperature (°F)							
	No.	r	z	0 W		0.4 W		20 W		30 W	
				Insolation during cool-down?		Insolation during cool-down?		Insolation during cool-down?		Insolation during cool-down?	
				No <sup>b</sup>	Yes	No	Yes	No	Yes	No	Yes
	2	0.000	4.505	209.9	218.9	210.6	219.6	240.4	248.8	254.6	262.8
	255	3.180	21.528	185.5	207.7	186.1	208.4	215.1	236.6	229.3	250.6
	351	4.300	21.528	185.6	207.4	186.2	208.0	212.3	233.3	225.0	245.9
	474	4.300	37.535	342.9	345.5	343.3	345.9	358.1	360.7	365.0	367.5
	494	7.325	37.525	596.3	597.4	596.5	597.6	604.7	605.8	608.3	609.4
	536	7.385	42.755	1366.8	1366.8	1366.8	1366.8	1367.4	1367.4	1367.6	1367.6
	3655	9.185	21.528	1452.8	1452.8	1452.8	1452.8	1453.0	1453.0	1453.1	1453.1
	3780	9.185	42.755	1420.8	1420.8	1420.8	1420.8	1421.0	1421.0	1421.2	1421.2
	3807	0.000	0.320	1449.4	1449.4	1449.4	1449.4	1449.8	1449.8	1449.9	1449.9
	3865	9.185	0.008	1467.3	1467.3	1467.3	1467.3	1467.4	1467.4	1467.4	1467.4
	3880	3.178	4.505	213.1	221.4	213.7	222.0	240.0	247.9	252.5	260.3
	3888	4.300	4.505	217.0	224.4	217.6	225.0	242.1	249.1	253.8	260.7
	4721	3.500	35.275	228.0	237.5	228.5	238.0	249.7	259.0	259.7	269.0
	4740	4.300	35.275	236.5	243.8	236.9	244.3	256.7	263.9	266.0	273.2
	4746	0.000	43.065	1441.8	1441.8	1441.8	1441.8	1442.0	1442.0	1442.1	1442.1
	6158	0.000	37.579	277.3	281.8	277.8	282.3	297.5	302.0	306.7	311.2
	6339	0.000	42.859	1299.5	1299.5	1299.6	1299.6	1301.1	1301.1	1301.7	1301.7
	6359 <sup>a</sup>	2.530	36.075	225.1	237.3	225.8	237.9	254.7	266.1	268.3	279.6
	6365 <sup>a</sup>	3.425	36.075	225.0	237.3	225.7	237.9	254.5	266.0	268.1	279.3
	6369	3.750	35.525	224.9	237.2	225.6	237.8	254.3	265.8	267.9	279.2
	6385	3.750	37.175	225.5	237.6	226.2	238.3	254.6	266.1	268.0	279.2
	6389	2.310	5.025	205.3	215.9	206.2	216.8	242.0	251.9	259.2	268.9
	6398	0.000	4.775	205.8	216.3	206.7	217.1	242.2	252.0	259.2	268.8
	6399	0.000	5.025	205.8	216.3	206.7	217.1	242.2	252.0	259.3	268.8
	6574	2.530	21.528	187.8	209.1	189.0	210.2	238.9	258.4	262.4	281.3
	6647	0.000	36.075	225.6	237.7	226.3	238.3	255.2	266.5	268.9	280.0
	6715	0.000	37.135	225.8	237.8	226.4	238.4	255.2	266.5	268.9	280.0

<sup>a</sup> Approximate location of the CV O-ring.

<sup>b</sup> Baseline case for  $\Delta T$  comparisons.

**Table 3.9. Maximum HAC temperatures recorded on the test packages' interior surfaces**

Temperature patch location <sup>a</sup>	ES-3100 Test Unit				
	1	2	3	4	5
	°C (°F)	°C (°F)	°C (°F)	°C (°F)	°C (°F)
Top plug bottom	149 (300)	163 (325)	177 (350)	177 (350)	177 (350)
Inner liner					
Flange step wall	135 (275)	163 (325)	135 (275)	135 (275)	135 (275)
BoroBond4 step	107 (225)	135 (275)	107 (225)	177 (350) <sup>b</sup>	121 (250)
Adjacent to CV body wall high	99 (210)	99 (210)	99 (210)	99 (210)	104 (219)
Adjacent to CV body wall middle	99 (210)	93 (199)	116 (241)	93 (199)	99 (210)
Bottom flat portion	104 (219)	99 (210)	99 (210)	127 (261)	110 (230)
Containment boundary					
Lid (external top)	116 (241)	110 (230)	116 (241)	127 (261)	127 (261)
Lid (internal)	104 (219)	104 (219)	110 (230)	110 (230)	116 (241)
Flange (external)	116 (241)	110 (230)	110 (230)	116 (241)	121 (250)
Flange (internal)	104 (219)	99 (210)	116 (241) <sup>b</sup>	104 (219)	116 (241)
Body wall mid height	99 (210)	88 (190)	99 (210)	82 (180)	93 (199)
Bottom end cap (center)	99 (210)	99 (210)	88 (190)	110 (230)	99 (210)
Mock-up					
Side top	82 (180)	77 (171)	77 (171)	77 (171)	99 (210)
Side middle	77 (171)	77 (171)	77 (171)	77 (171)	93 (199)
Side bottom	77 (171)	77 (171)	77 (171)	77 (171)	88 (190)

<sup>a</sup> Refer to figures for exact locations and to Tables 5.3 through 5.7 in ORNL/NTRC-013, Vol. 1 for recorded values.

<sup>b</sup> Temperature indicating patch may have been damaged due to impact with surrounding structure.

shipping configuration, the arrangements that minimize the void volume inside the containment vessel are analyzed as follows:

1. one shipment will contain six cans with external dimensions of 10.8 cm (4.25 in.) diameter by 12.38 cm (4.875 in.) high cans;
2. one shipment will contain five cans with external dimensions of 10.8 cm (4.25 in.) diameter by 12.38 cm (4.875 in.) high cans and four can spacers;
3. one shipment will contain three cans with external dimensions of 10.8 cm (4.25 in.) diameter by 22.23 cm (8.75 in.) high and three can spacers;
4. one shipment will contain three cans with external dimensions of 10.8 cm (4.25 in.) diameter by 25.4 cm (10 in.) high;
5. one shipment will contain six nickel cans with external dimensions of 7.62 cm (3.00 in.) diameter by 12.07 cm (4.75 in.) high;
6. one shipment will contain three polyethylene bottles with external dimensions of 12.54 cm (4.94 in.) diameter by 22.1 cm (8.7 in.) high; and
7. one shipment will contain three teflon bottles with external dimensions of 11.91 cm (4.69 in.) diameter by 23.88 cm (9.4 in.) high.

These arrangements are shown in Fig. 1.4. To determine the ES-3100's maximum normal operating pressure, the following assumptions have been used in the calculations:

1. The HEU contents are loaded into convenience cans, and convenience cans are placed inside the containment vessel at standard temperature ( $T_{amb}$ ) and pressure ( $P_i$ ) [25°C (77°F) and 101.35 kPa (14.7 psia)] with air at a maximum relative humidity of 100%;
2. The convenience cans and bottles are assumed to be sealed to minimize the void volume inside the containment vessel;
3. Convenience can and bottle geometry does not change during pressure increase inside containment vessel; and
4. All off-gassing material (polyethylene bagging or bottles, Teflon bottles, silicone pads) is limited to 1500 g per containment vessel shipping arrangement.

Table 3.10. Total pressure inside the containment vessel at 87.81°C (190.06°F) <sup>a</sup>

CVA	$n_a$ (lb-mole)	$n_v$ (lb-mole)	$n_{po}$ (lb-mole)	$n_{bo}$ (lb-mole)	$n_g$ (lb-mole)	$n_T$ (lb-mole)	$P_T$ (psia)
1	3.0855e-04	1.0057e-05	0.0000e+00	0.0000e+00	0.0000e+00	3.1861e-04	17.786
2	3.0826e-04	1.0047e-05	0.0000e+00	0.0000e+00	0.0000e+00	3.1831e-04	17.786
3	3.0227e-04	9.8522e-06	0.0000e+00	0.0000e+00	0.0000e+00	3.1212e-04	17.786
4	2.9252e-04	9.5344e-06	0.0000e+00	0.0000e+00	0.0000e+00	3.0205e-04	17.786
5	1.9163e-05	5.8795e-04	0.0000e+00	0.0000e+00	0.0000e+00	6.0711e-04	17.786
6	2.0206e-04	6.5858e-06	0.0000e+00	0.0000e+00	0.0000e+00	2.0865e-04	17.786
7	5.6450e-06	1.7320e-04	0.0000e+00	0.0000e+00	2.2296e-05	2.0114e-04	20.004

<sup>a</sup> This assumes that the internal convenience cans, polyethylene bottles, Teflon FEP bottles, and Cat 277-4 spacer cans are sealed.

### 3.1.4.2 Maximum HAC Pressures

Table 3.11 summarizes the results from Appendix 3.6.5 in which the pressure of the containment vessel when subjected to the tests and conditions of HAC per 10 CFR 71.73 has been determined for the most restrictive CVAs shipped in the ES-3100. The shipping configurations discussed in Sect. 3.1.4.1 are evaluated for HAC. To determine the maximum pressure generated inside the ES-3100's containment vessel due to HAC conditions, the following assumptions have been used in the calculations:

1. The initial pressure inside the containment vessel is the maximum normal operating pressure shown in Table 3.10 for each CVA at ambient temperature;
2. The convenience cans and bottles are assumed to be sealed in order to minimize the void volume inside the containment vessel;
3. Convenience can and bottle geometry does not change during pressure increase inside containment vessel or because of damage from compliance testing; and
4. All off-gassing material (polyethylene bagging or bottles, Teflon bottles, silicone pads) is limited to 1500 g per containment vessel shipping arrangement.

The above assumptions are very conservative because the convenience cans buckle and deform significantly under an external pressure differential of one atmosphere as demonstrated during the helium leak checking. When the convenience cans deform inward under external pressure, additional void volume is created, thereby reducing the overall pressure inside the containment vessel. However, quantitative data on this structural deformation of the convenience cans has not been measured, and repeatability of the deformation is not predictable. Therefore, convenience can geometry is assumed not to change for the calculation of pressure inside the containment vessel.

**Table 3.11. Total pressure inside the containment vessel at 123.85°C (254.93°F) <sup>a</sup>**

CVA	$n_{MNOP}$ (lb-mole)	$n_{po}$ (lb-mole)	$n_{bo}$ (lb-mole)	$n_{tr}$ (lb-mole)	$n_T$ (lb-mole)	$P_T$ (psia)
1	3.8549e-04	1.3458e-05	3.1529e-04	0.0000e+00	7.1424e-04	43.852
2	3.8514e-04	1.7302e-05	3.1529e-04	0.0000e+00	7.1773e-04	44.108
3	3.7765e-04	1.1535e-05	3.1529e-04	0.0000e+00	7.0448e-04	44.151
4	3.6547e-04	7.6901e-06	3.1529e-04	0.0000e+00	6.8845e-04	44.585
5	7.3457e-04	0.0000e+00	3.1529e-04	0.0000e+00	1.0499e-03	33.827
6	2.5245e-04	0.0000e+00	5.3284e-04	0.0000e+00	7.8529e-04	73.625
7	2.4337e-04	0.0000e+00	3.1529e-04	2.2296e-05	5.8096e-04	63.545

<sup>a</sup> This assumes that the internal convenience cans, polyethylene or Teflon FEP bottles, and Cat 277-4 spacer cans are sealed.

## 3.2 SUMMARY OF THERMAL PROPERTIES OF MATERIALS

### 3.2.1 Material properties

Thermal properties at various temperatures for the stainless steel used in the fabrication of the drum, noncombustible cast refractory (Kaolite 1600), noncombustible neutron poison (BoroBond 4 or Cat 277-4), silicone rubber pads, and air are listed in Table 3.12. Properties used to evaluate thermal stresses due to differences in coefficient of thermal expansion are listed in Table 3.13.

### 3.2.2 Component Specifications

Component specifications are listed in Tables 3.14 and 3.15.

## 3.3 GENERAL CONSIDERATIONS

Thermal evaluation of the package design for NCT was performed by analysis. Evaluation of the package design for HAC was performed by a combination of testing and analysis.

### 3.3.1 Evaluation by Analysis

A description of the method and calculations used to perform the thermal and thermal stress analyses of the package for NCT and HAC is presented in detail in Appendices 3.6.1, 3.6.2 and 3.6.3.

**Table 3.12. Thermal properties of the materials used in the thermal analysis**

Material	Temperature (°F)	Thermal conductivity (Btu/h-in.-°F)	Density (lbm/in. <sup>3</sup> )	Specific heat (Btu/lbm-°F)	Emissivity
Stainless steel	-279.67	0.443 <sup>a</sup>	0.285 <sup>a</sup>	0.065 <sup>a</sup>	0.22 <sup>a</sup>
	-99.67	0.607	—	0.096	—
	260.33	0.799	—	0.123	—
	620.33	0.953	—	0.133	—
	980.33	1.088	—	0.139	—
	1340.33	1.223	—	0.146	—
	1700.33	1.348	—	0.153	—
	2240.33	1.526	—	0.163	—
Kaolite 1600	68	0.0093 <sup>b</sup>	0.011 <sup>c</sup>	0.2 <sup>d</sup>	—
	212	0.0091	—	—	—
	392	0.0081	—	—	—
	572	0.0072	—	—	—
	1112	0.0082	—	—	—
Neutron poison (Cat 277-4)	-31	0.0457 <sup>e</sup>	0.0579 <sup>f</sup>	0.125 <sup>e</sup>	—
	73.4	0.0485	—	0.186	—
	140	0.04	—	0.239	—
	212	0.0295	—	0.242	—
	302	0.0305	—	0.291	—
Neutron poison (BoroBond4)	25	0.0450 <sup>g</sup>	0.0683 <sup>g</sup>	0.2160 <sup>g</sup>	—
	77	0.0576	—	—	—
	100	0.0632	—	—	—
	104	0.0642	—	—	—
Silicone rubber	—	0.0161 <sup>h</sup>	0.047 <sup>h</sup>	0.300 <sup>h</sup>	1.01
Air	-9.67	$1.074 \times 10^{-3}$ <sup>a</sup>	$4.064 \times 10^{-5}$ <sup>a,j</sup>	0.240 <sup>a</sup>	—
	80.33	$1.266 \times 10^{-3}$	—	0.241	—
	170.33	$1.445 \times 10^{-3}$	—	0.241	—
	260.33	$1.628 \times 10^{-3}$	—	0.242	—
	350.33	$1.796 \times 10^{-3}$	—	0.244	—
	440.33	$1.960 \times 10^{-3}$	—	0.246	—
	530.33	$2.114 \times 10^{-3}$	—	0.248	—
	620.33	$2.258 \times 10^{-3}$	—	0.251	—
	710.33	$2.393 \times 10^{-3}$	—	0.254	—
	800.33	$2.523 \times 10^{-3}$	—	0.257	—

**Table 3.12. Thermal properties of the materials used in the thermal analysis (cont.)**

Material	Temperature (°F)	Thermal Conductivity (Btu/h-in.-°F)	Density (lbm/in. <sup>3</sup> )	Specific Heat (Btu/lbm-°F)	Emissivity
Air (cont.)	890.33	$2.644 \times 10^{-3}$	—	0.260	—
	980.33	$2.759 \times 10^{-3}$	—	0.263	—
	1070.33	$2.870 \times 10^{-3}$	—	0.265	—
	1160.33	$2.985 \times 10^{-3}$	—	0.268	—
	1250.33	$3.096 \times 10^{-3}$	—	0.270	—
	1340.33	$3.212 \times 10^{-3}$	—	0.273	—
	1520.33	$3.443 \times 10^{-3}$	—	0.277	—

- <sup>a</sup> F. P. Incropera and D. P. DeWitt, *Fundamentals of Heat and Mass Transfer*, 2nd edition, John Wiley & Sons, New York, 1985.
- <sup>b</sup> Hsin Wang, *Thermal Conductivity Measurements of Kaolite*, ORNL/TM-2003/49 (Appendix 2.10.3).
- <sup>c</sup> Based on a baked density of 19.4 lbm/ft<sup>3</sup> (0.011 lbm/in.<sup>3</sup>). Specification JS-YMN3-801580-A003 (Appendix 1.4.4) requires a baked density of  $22.4 \pm 3$  lbm/ft<sup>3</sup>. Using a lower value for the Kaolite density results in higher temperatures on the containment vessel because the heat capacity of the Kaolite is minimized-allowing more heat to flow to the containment vessel; therefore, the thermal analyses are performed using a low-end density of 19.4 lbm/ft<sup>3</sup>. The HAC analyses also consider a high-end density of 30 lbm/ft<sup>3</sup>.
- <sup>d</sup> FAX communication from J. W. Breuer of Thermal Ceramics, Engineering Department, August 11, 1995.
- <sup>e</sup> Hsin Wang, *Thermophysical Properties of Heat Resistant Shielding Material*, ORNL/TM-2004/290 (Appendix 2.10.4). Specific heat values are presented in MJ/m<sup>3</sup>-K in ORNL/TM-2004/290-converted to mass-based units using a density of 105 lbm/ft<sup>3</sup>.
- <sup>f</sup> Based on a cured density of density of 100 lbm/ft<sup>3</sup> (0.0579 lbm/in.<sup>3</sup>). B. F. Smith and G. A. Byington, *Mechanical Properties of 277-4*, Y/DW-1987, January 19, 2005 (Appendix 2.10.4), presents a range of measured densities between approximately 100 and 110 lbm/ft<sup>3</sup> for Catalog No. 277-4. Therefore, in order to minimize the heat capacity of the material and allow more heat to be transferred to the containment vessel, the lower-bound value is used. The HAC analyses also consider a high-end density of 110 lbm/ft<sup>3</sup>.
- <sup>g</sup> E-mail communication with presentation attachment, Jim Hall (Eagle-Picher) to Jerry Byington (BWXT Y-12), 3/12/2004.
- <sup>h</sup> THERM 1.2, thermal properties database by R. A. Bailey.
- <sup>i</sup> Conservatively modeled as 1.0.
- <sup>j</sup> Constant density value evaluated at 100°F.

### 3.3.2 Evaluation by Test

Full-scale testing of five ES-3100 test units was conducted in accordance with 10 CFR 71.73 for HAC. A single full-scale ES-3100 (TU-4) was assembled and subjected to both NCT testing and the sequential tests specified in 10 CFR 71.73(c). The furnace used for thermal testing was the No. 3 furnace at Timken Steel Company in Latrobe, Penn., which is a gas-fired furnace. This furnace employs “pulsed” fire burners, in which the natural gas flow rate is varied based on furnace controller demands, but the flow of air through the burners is constant, even when no gas is flowing. This ensures a very rich furnace atmosphere capable of supporting any combustion of package materials of construction.

Table 3.13. Mechanical properties of the materials used in the static stress analyses

Material	Temperature (°F)	Modulus of Elasticity (psi)	Poisson's Ratio	Density (lbm/in. <sup>3</sup> )	Coefficient of thermal expansion (in./in./°F)
Stainless steel	-40	$28.6 \times 10^6$ <sup>a</sup>	0.29 <sup>b</sup>	0.285 <sup>d</sup>	$8.2 \times 10^{-6}$ <sup>e</sup>
	100	$28.14 \times 10^6$	—	—	$8.6 \times 10^{-6}$
	200	$27.6 \times 10^6$	—	—	$8.9 \times 10^{-6}$
	300	$27.0 \times 10^6$	—	—	$9.2 \times 10^{-6}$
Kaolite	—	29,210 <sup>c</sup>	0.01 <sup>c</sup>	0.013 <sup>f</sup>	$5.04 \times 10^{-6}$ <sup>g</sup>
Neutron absorber (Cat 277-4)	-40	$1.991 \times 10^6$ <sup>h</sup>	0.33 <sup>h</sup>	0.0608 <sup>h</sup>	$7.056 \times 10^{-6}$ <sup>i</sup>
	-4	—	—	—	$7.222 \times 10^{-6}$
	32	—	—	—	$7.222 \times 10^{-6}$
	70	$0.984 \times 10^6$	0.28	—	—
	100	$0.403 \times 10^6$	0.25	—	—
	104	—	—	—	$7.000 \times 10^{-6}$
	140	—	—	—	$6.444 \times 10^{-6}$
	176	—	—	—	$5.778 \times 10^{-6}$
	212	—	—	—	$5.389 \times 10^{-6}$
	248	—	—	—	$5.056 \times 10^{-6}$
	284	—	—	—	$4.889 \times 10^{-6}$
	302	—	—	—	$4.833 \times 10^{-6}$

<sup>a</sup> ASME Boiler and Pressure Vessel Code, Sect. II, Part D, Subpart 2, Tables TE-1, B column, and TM-1.

<sup>b</sup> R. A. Bailey, *Strain - A Material Database*, Lawrence Livermore National Laboratory, 1989.

<sup>c</sup> The Poisson's Ratio of Kaolite is assumed to be a small value of 0.01 (Appendix 2.10.2).

<sup>d</sup> F. P. Incropera and D. P. DeWitt, *Fundamentals of Heat and Mass Transfer*, 2<sup>nd</sup> edition, John Wiley & Sons, New York, 1985.

<sup>e</sup> *Metallic Materials and Elements for Aerospace Vehicle Structures*, MIL-HDBK-5H, May 1986.

<sup>f</sup> Specification JS-YMN3-801580-A003 (Appendix 1.4.4) requires a baked density of  $22.4 \pm 3$  lbm/ft<sup>3</sup>.

<sup>g</sup> E-mail communication, Ken Moody (Thermal Ceramics, Inc.) to Paul Bales (BWXT Y-12), December 9, 2004.

<sup>h</sup> B. F. Smith and G. A. Byington, *Mechanical Properties of 277-4*, Y/DW-1987, January 19, 2005 (Appendix 2.10.4).

<sup>i</sup> W. D. Porter and H. Wang, *Thermophysical Properties of Heat Resistant Shielding Material*, ORNL/TM-2004/290, Oak Ridge National Laboratory, Oak Ridge, Tenn., December 2004 (Appendix 2.10.4). Coefficient of thermal expansion at each temperature taken as the maximum of values for Runs #2, #3, and #5.

**Table 3.14. Packaging material technical specifications**

Component	Specifications
<i>Drum assembly</i>	
Drum washers	1.375 OD × 0.812 ID × 0.25-in. thick, 300 Series stainless steel
Drum threaded weld studs	5/8-11 × 7/8 long, fabricated per ASME SA-193, using Type 304/304L stainless-steel per ASME 479
Drum hex nuts	5/8-11 UNC-2B, silicon bronze C65100, ASTM F-467
Drum lid weldment	Modified 30-gal, 16-gauge (MS27683-61) lid, type 304 or 304L stainless steel; and a 11-gauge thick sheet, type 304 or 304L stainless steel, ASME SA-240
Drum weldment	Modified 30-gal, 16-gauge (MS27683-7), type 304 or 304L stainless steel, ASME SA-240, manufactured per Drawing M2E801580A004 (Appendix 1.4.8)
Drum plugs	Nylon plastic plug, Micro Plastic, Inc.
<i>Impact limiter, insulation enclosure, neutron absorber, and drum packing material</i>	
Insulation and impact limiter (not removable)	Lightweight cast refractory insulation, Kaolite 1600, 358.8 kg/m <sup>3</sup> (22.4 lb/ft <sup>3</sup> ) density, cast in stainless-steel shells in the drum and top plug
Neutron absorber	Cat 277-4, 1681.9 <del>240/80</del> kg/m <sup>3</sup> (105 <del>15/5</del> lb/ft <sup>3</sup> ) density
Top plug (removable)	Type 304 or 304L stainless steel, ASME SA-240 (body), ASME SA-79 (lifting inserts),
Inner liners	Type 304 or 304L stainless steel, ASME SA-240 (body), ASME SA-79 (modified angle)
Aluminum tape	
Silicone pads	Silicone rubber, 22 ± 5 Shore A, color black/gray
<i>Containment boundary</i>	
Containment vessel plug	Part # 04-2126, Modified VCO threaded plug, brass
Containment vessel swivel hoist ring	3052T56, Swivel hoist ring, alloy steel (not used for shipment)
Containment vessel	<p>Method 1: Type TP304L stainless steel ASME SA-312 (welded or seamless pipe body); type F304L, stainless steel, ASME SA-182 (flange, and end cap); type 304, stainless steel, ASME SA-479 (sealing lid), Nitronic 60 SST per ASME SA-479, UNS-S21800 (closure nut)</p> <p>Method 2: Type F304L stainless ASME SA-182 (body, flange, and end cap); type 304, stainless steel, ASME SA-479 (sealing lid), Nitronic 60 SST per ASME SA-479, UNS-S21800 (closure nut)</p> <p>All components per <i>ASME Boiler and Pressure Vessel Code</i>, Sect. II, Part D, Table 2A</p>



**Table 3.14. Packaging material technical specifications (cont.)**

<b>Component</b>	<b>Specifications</b>
Containment vessel O-rings	Elastomer, ethylene propylene, normal service temperature range of -40 to 150°C, Specification M 3BA712A14B13F17 in ASTM D-2000, per OO-PP-986, Rev. D
Containment vessel lid assembly retaining ring	Part # WSM-400-S02, type 302 stainless steel
Containment vessel O-ring lubricant	Clear dimethyl siloxane polymer
Containment vessel closure nut lubricant	Krytox #240AC
Containment vessel body dowel pins	0.2501/0.2503 OD × 0.50 long, 18-8 stainless steel
<i>Containment vessel packing material</i>	
Convenience cans	Stainless steel or tin plated carbon steel with stainless-steel can handles and nylon coated stainless-steel wire, or passivated nickel
Silicone rubber pads	Silicone rubber, 22 ±5 Shore A, color black/gray
Spacers	Stainless-steel can filled with Cat 277-4
Bottles	Polyethylene or <del>Teflon FEP</del>
Bagging	Polyethylene
Metal scrubbers	Stainless steel, McMaster Carr Part # 7361T13

**Table 3.15. Component allowable service temperature and pressure**

Component	Allowable service temperature range °C (°F)	Allowable pressure range kPa (psia)
<i>Drum assembly</i>		
Stainless-steel drum and lid	-40 to 871 (-40 to 1600) <sup>a</sup>	48.3 (7)
Silicon bronze nuts	-40 to 871 (-40 to 1600) <sup>a</sup>	N/A
Stainless-steel washers	-40 to 871 (-40 to 1600) <sup>a</sup>	N/A
Stainless-steel mid liner	-40 to 350 (-40 to 176.7)	N/A
Stainless-steel inner liner	-40 to 350 (-40 to 176.7)	N/A
Stainless-steel top plug weldment	-40 to 871 (-40 to 1600) <sup>a</sup>	
Kaolite 1600	-40 to 871 (-40 to 1600) <sup>a</sup>	N/A
Cat 277-4	-40 to 150 (-40 to 302) <sup>b</sup>	N/A
Silicone rubber pads	-40 to 232 (-40 to 450)	N/A
<i>Containment vessel</i>		
Stainless-steel body and sealing lid	-40 to 427 (-40 to 800) <sup>c</sup>	149.62 (21.7) external 699.82 (101.5) internal
Nitronic 60 closure nut	-40 to 427 (-40 to 800) <sup>c</sup>	149.62 (21.7) external 699.82 (101.5) internal
Stainless-steel retaining ring	-40 to 427 (-40 to 800) <sup>c</sup>	N/A
Dowel pins	-40 to 427 (-40 to 800) <sup>c</sup>	N/A
Brass VCO fitting (Viton O-rings)	-40 to 204 (-40 to 400) <sup>d</sup>	N/A
Ethylene propylene O-rings	-40 to 150 (-40 to 302) <sup>d</sup>	5.52 × 10 <sup>3</sup> (800) with no backing rings
Containment vessel silicone pads	-40 to 232 (-40 to 450)	N/A

<sup>a</sup> This limit is established by the proximity of the Kaolite 1600 material.

<sup>b</sup> This limit is established based on criticality limits of moisture loss.

<sup>c</sup> This limit is established by the *ASME Boiler and Pressure Vessel Code*.

<sup>d</sup> This limit is provided by the *Parker O-Ring Handbook* for each material's continuous service limit.

Oxygen content was not monitored in stack gases of the furnace because it was not anticipated that any of the package's materials of construction were combustible. There was some burning of the silicone pads which are placed between the inner liner and the top plug of the package.

The most significant change to the definition of the HAC thermal test in the current 10 CFR 71 is the requirement for calculation purposes to base convective heat input on "that value which may be demonstrated to exist if the package was exposed to the fire specified." This is not especially significant for this package because it was tested in the gas-fired furnace with burners placed in an attitude which produced a strong convective swirl. Careful examination of the thermal test data indicates that the total heat imparted to the packages was significantly greater than the required total heat specified in 10 CFR 71.73(c)(4).

Compliance with ASTM E-2230-02, *Standard Practice for Thermal Qualification of Type B Packages for Radioactive Materials* (ASTM E-2230-02), was accomplished by the method described in Sect. 7.3 of this standard. This standard is in general agreement with Paragraph 2.2.1 ("Steady-state Method of Compliance") of SG 140.1 entitled *Combination Test Analysis/Method Used to Demonstrate Compliance to DOE Type B Packaging Thermal Test Requirements (30 Minute Fire Test)*. The data from each of the thermal tests, as shown in the test report, show that five of the six thermocouple-instrumented exterior surfaces of each package reached temperatures well in excess of 800°C (1475°F) during the 30-min thermal testing. Similarly, all other surfaces of the furnace, including the support stand, exceeded 800°C (1475°F) during the timed portion of the thermal test. For the test specified in the regulations, regardless of the amount of heat input by convection, radiation, or conduction, the maximum temperature the skin of the package could reach would be 800°C (1475°F). That is, the source of the heat in the regulatory-specified test is at 800°C (1475°F). Heat can only be transferred from a hotter source to a colder source. Thus, regardless of the mode of heat transfer, the greatest temperature a specimen exposed to the 10 CFR 71.73(c)(4) thermal test can attain is 800°C (1475°F). The thermal performance of the packaging components as an assembled unit has been demonstrated through full-scale tests. Actual tests and procedures followed are described in Sect. 4.5 of ORNL/NTRC-013, Vol. 1. Figures 3.2 through 3.5 show the general testing arrangements.

Since full-scale testing in accordance with 10 CFR 71.73 for HAC was conducted on prototypical packages. No analyses were conducted to show compliance with the HAC thermal test. However, to determine the thermal impacts of (1) an internal heat source, (2) application of insulation during cool down, (3) thermal capacitance differences between test mock-ups and actual contents, and (4) the change in neutron absorbing material, analyses were conducted and are summarized in Appendices 3.6.1 and 3.6.2. Further discussion of these issues is found in Sect. 3.5.3.

### **3.3.3 Margins of Safety**

Tables 3.16 and 3.17 summarize the results of thermal analysis and testing in accordance with NCT and HAC regulatory requirements. Margins of safety have not been calculated. However, the calculated results are compared with the allowable limits for individual components. Based on these results, the ES-3100 components are well below the allowable limits concerning temperature, stress, and pressure during transportation.

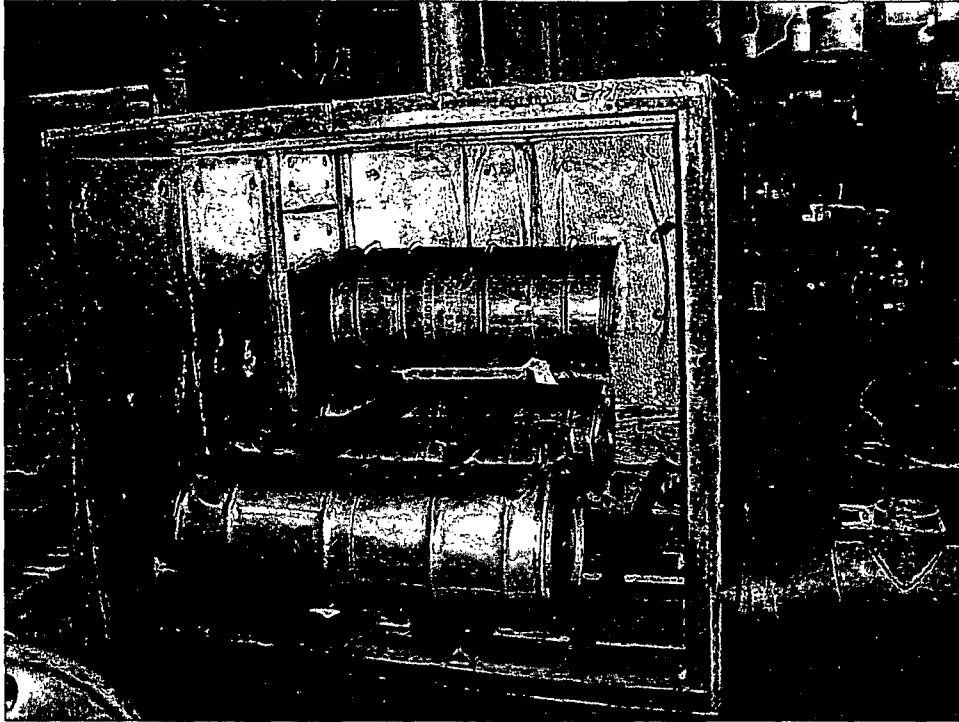


**Fig. 3.2. Test unit preheat arrangement.**



**Fig. 3.3. Test unit insertion into furnace.**

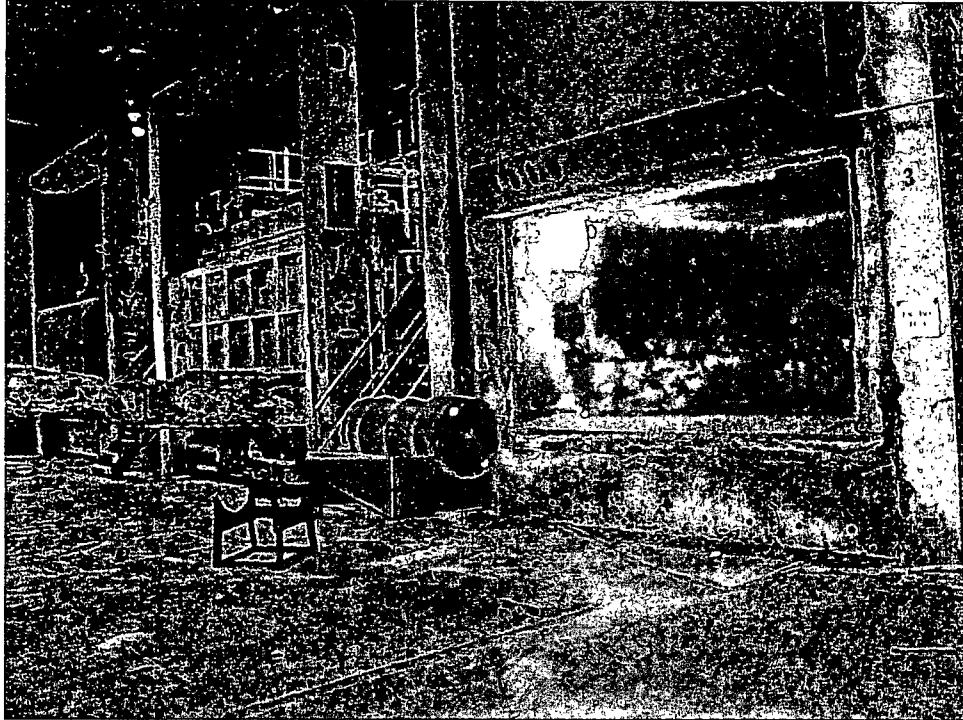


**Fig. 3.4. Test unit removal from furnace.**

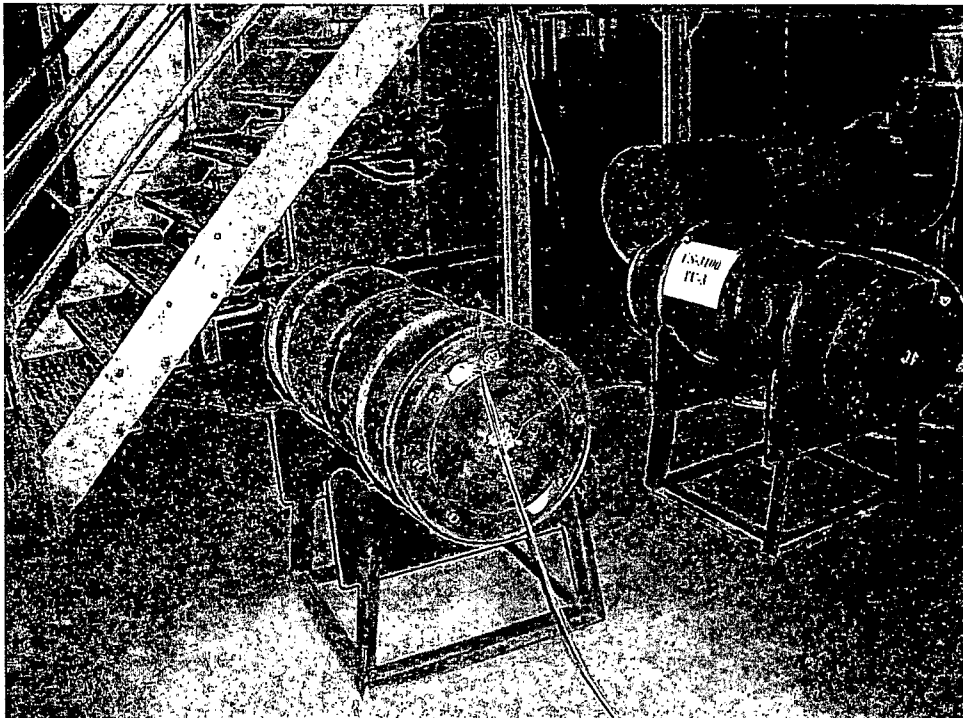


**Fig. 3.5. Test unit cool down and monitoring arrangement.**

**Table 3.16. Summary of results of evaluation for the ES-3100 under NCT**

Conditions	Calculated results	Allowable limit	SARP reference
Minimum package temperature, °C (°F)	-40 (-40)	-40 (-40)	Sect. 3.4.1
Maximum drum assembly stress due to cold conditions per 10 CFR 71.71(c)(2), kPa (psia)	61,150 (8,869)	132,379 (19,200)	Appendix 3.6.3
Minimum containment vessel pressure, kPa (psia)	76.74 (11.13)	0.0 (0.0)	Sect. 3.4.1
Maximum drum temperature with insolation, °C (°F)	117.72 (243.89) <sup>a</sup>	N/A	Appendix 3.6.2 Sect. 3.4.1
Maximum drum assembly stress due to hot conditions per 10 CFR 71.71(c)(1), kPa (psia)	66,934 (9,708)	132,379 (19,200)	Appendix 3.6.3
Containment vessel temperature with insolation, °C (°F)	87.81 (190.06) <sup>a</sup>	427 (800) <sup>b</sup>	Appendix 3.6.2 Sect. 3.4.1
Maximum O-ring temperature, °C (°F)	87.81 (190.06)	150 (302) <sup>c</sup>	Appendix 3.6.2 Sect. 3.4.1
Maximum containment vessel pressure, kPa (psia)	137.92 (20,004) <sup>d</sup>	801.2 (116.2) <sup>e</sup>	Appendix 3.6.4 Sect. 3.4.2

<sup>a</sup> Appendix 3.6.2.

<sup>b</sup> *ASME Boiler and Pressure Code*, Sect. II, Part D, maximum allowable temperature for Sect. III, Div. 1, Subsection NB vessel.

<sup>c</sup> Maximum O-ring seal life up to 150°C (302°F) for continuous service (*Parker O-ring Handbook*, Fig. 2-24).

<sup>d</sup> Appendix 3.6.4.

<sup>e</sup> Appendix 2.10.1 allowable limit.

**Table 3.17. Summary of results of evaluation under HAC for the ES-3100 shipping arrangement using bounding case parameters**

Condition	Results	Design limits	SARP references
Maximum adjusted containment vessel temperature during testing, °C (°F)	152.22 (306.00)	426.67 (800) <sup>a</sup>	Sect. 3.5.3
Maximum containment vessel pressure during testing, kPa (psia)	507.63 (73,625) <sup>b</sup>	801.2 (116.2) <sup>c</sup>	Appendix 3.6.5 Sect. 3.5.3
Maximum adjusted O-ring temperature, °C (°F)	141.22 (286.20)	150 (302) <sup>d</sup>	Sect. 3.5.3

<sup>a</sup> *ASME Boiler and Pressure Code*, Sect. II, Part D, maximum allowable temperature for Sect. III, Div. 1, Subsection NB vessel.

<sup>b</sup> Appendix 3.6.5.

<sup>c</sup> Appendix 2.10.1 at 148.89°C (300°F).

<sup>d</sup> Maximum O-ring seal life up to 150°C (302°F) for continuous service (*Parker O-ring Handbook*, Fig. 2-24).

### 3.4 THERMAL EVALUATION UNDER NORMAL CONDITIONS OF TRANSPORT

#### 3.4.1 Heat and Cold

The ambient temperature requirement for NCT is 38°C (100°F). The 35.2 kg of HEU shipped in the ES-3100 package generates a maximum bounding heat load of 0.4 W. The insolation heat flux stipulated in 10 CFR 71.71(c)(1) was used in the calculations. If the package is exposed to solar radiation at 38°C (100°F) in still air, the conservatively calculated temperatures at the top of the drum, on the top surface of the containment vessel, and on the containment vessel near the O-ring sealing surfaces, are 117.72, 87.81, and 87.72°C (243.89, 190.06, 189.90°F), respectively, for the ES-3100. Nevertheless, these temperatures are within the service limits of all packaging components, including the O-rings. The normal service temperature range of the O-rings used in the containment boundary is -40 to 150°C (-40 to 302°F), in accordance with B&PVC, Sect. III; thus, the seal will not be affected by this maximum normal operating temperature.

Using the temperatures calculated for the conditions of 10 CFR 71.71(c)(1), Appendix 3.6.4 predicts that the maximum normal operating pressure inside the containment vessel will be 137.92 kPa (20.004 psia). The design absolute pressure of the containment vessel is 801.17 kPa (116.2 psia), and the hydrostatic test pressure is 1135.57 kPa (164.7 psia). Thus, increasing the internal pressure of the containment vessel to a maximum of 137.92 kPa (20.004 psia) during NCT would have no detrimental effect. Stresses generated in the containment vessel at this pressure are insignificant compared to the materials of construction allowable stress. Table 2.20 provides a summary of the pressure and temperature for the various shipping configurations. As discussed in Sect. 2.6.1.4, the containment vessel and vessel closure nut stresses for these pressure conditions are below the allowable stress values.

Summarizing 10 CFR 71.43(f), the tests and conditions of NCT shall not substantially reduce the effectiveness of the packaging to withstand HAC sequential testing. The effectiveness of the ES-3100 to withstand HAC sequential testing is not diminished through application of the tests and conditions stipulated in 10 CFR 71.71. The justification for this statement is provided by physical testing of both the ES-2M and ES-3100 test packages. Due to the similarities in design, fabrication, and material used in construction of both the ES-2M and the ES-3100 package, the Kaolite 1600 physical characteristics will hold true for both designs. The integrity of the Kaolite 1600 is not significantly affected by the NCT vibration and 1.2-m (4-ft) drop tests.

Prior to testing the ES-2M design (a similarly constructed shipping package), each test unit was radiographed to determine the integrity of the Kaolite 1600 impact and insulation material. Following casting of the material inside the drum, some three-dimensional curving cracks were seen in some packages near the top thinner sections from the bottom of the liner to the bottom drum edge. After vibration testing, radiography of the ES-2M Test Unit-4 showed that the lower half of the impact limiter was broken into small pieces (Byington 1997). To evaluate these findings, Test Unit-4 was reassembled and subjected to HAC sequential testing (Byington 1997). After vibration and impact testing, many three-dimensional curving cracks were seen around the impact areas, and the inner liner was also visibly deformed. Nevertheless, temperatures at the containment boundary were also similar to other packages not subjected to vibration testing prior to HAC testing. No leakage of water was recorded following immersion. Also, Test Unit-4 of the ES-3100 shipping package was subjected to the full NCT test battery including vibration.

Following these tests, the containment vessel of the ES-2M Test Unit-4 was removed, and a full body helium leak check was performed. The test unit passed the leak-tight criteria in accordance with ANSIN14.5-1997. The containment vessel was then reassembled into the previously tested drum assembly and subjected to the complete HAC testing. Based on the success of this unit and the similar design of the

ES-2M, it can be concluded that vibration normally incident to transport does not reduce the effectiveness of the ES-3100 packaging during HAC testing. The ES-3100 has been tested to determine the effectiveness of the package following a sequential NCT 1.2-m (4-ft) drop test and HAC test battery. Throughout all of the vibration and structural testing, the effectiveness of the Kaolite 1600 material as an impact limiter and thermal insulation was not substantially reduced.

Since the components to be shipped have an assumed decay heat load of 0.4 W, a thermal analysis was conducted for the ES-3100 package with and without full solar insolation. The package was analyzed using the ABAQUS/Standard computer code, and the finite element geometry was constructed for each model using MSC.Patran 2004. The predicted temperature, while stored at 38°C (100°F) in the shade, for the drum lid center and the containment vessel flange near the inner O-ring, is 37.89°C (100.20°F) and 38.22°C (100.80°F), respectively. The analysis shows that no accessible surface of the package would have a temperature exceeding 50°C (122°F). Therefore, the requirement of 10 CFR 71.43(g) would be satisfied for either transportation mode (exclusive use or nonexclusive use).

Also, in accordance with 10 CFR 71.71(c)(2), the containment vessel pressure must be calculated at -40°C (-40°F). Given the initial conditions of temperature, relative humidity, no silicone rubber or polyethylene bag off-gassing, the pressure is calculated as follows:

$$P_1 @ 25^{\circ}\text{C} = P_a + P_v + P_{f_0},$$

where

$$\begin{aligned} P_a &= 98.15 \text{ kPa (14.236 psia)} && \text{(Appendix 3.6.4)} \\ P_v &= 3.20 \text{ kPa (0.464 psia)} && \text{(Appendix 3.6.4)} \\ P_{f_0} &= 0 && \text{(no off-gassing, Appendix 3.6.4)} \end{aligned}$$

At -40°C (-40°F), the partial pressure of the water vapor is conservatively assumed to be zero. Therefore, the final pressure of the mixture at -40°C (-40°F) is calculated according to the ideal gas law based solely on the partial pressure of the air.

$$\frac{P_1 V_1}{T_1} = \frac{P_2 V_2}{T_2}$$

where,

$$\begin{aligned} P_1 &= 98.15 \text{ kPa (14.236 psia)} \\ T_1 &= 25^{\circ}\text{C (298.15 K)} \\ T_2 &= -40^{\circ}\text{C (233.15 K)} \\ V_1 &= V_2 \end{aligned}$$

rearranging and solving for  $P_2$ ,

$$\begin{aligned} P_2 &= P_1 (T_2/T_1) \\ &= (98.15)(233.15/298.15) \\ P_2 &= 76.76 \text{ kPa (11.13 psia).} \end{aligned}$$

The cold condition for NCT specified in 10 CFR 71.71 is an ambient temperature in still air and shade of -40°C (-40°F). The ~~35.2 kg (77.60 lb)~~ of HEU contents in the ES-3100 package generates a maximum bounding decay heat load of 0.4 W. However, in accordance with Regulatory Guide 7.6, the thermal effects of this internal heat source are neglected during evaluation of the package performance at -40°C (-40°F). When exposed to this condition, the package component temperatures will stabilize over



time at a temperature approaching  $-40^{\circ}\text{C}$  ( $-40^{\circ}\text{F}$ ). The package has been examined for use at  $-40^{\circ}\text{C}$  ( $-40^{\circ}\text{F}$ ) (Sect. 2.6.2). No detrimental effects on the package structure or sealing capability result from this minimum temperature requirement. The normal service temperature range of the O-rings used in the containment boundary is  $-40$  to  $150^{\circ}\text{C}$  ( $-40$  to  $302^{\circ}\text{F}$ ), in accordance with the *Parker O-ring Handbook*; thus, the seal will not be affected by this minimum package temperature in accordance with 10 CFR 71.71(c)(2). Leak testing conducted on Test Unit-2 to the leak tight criteria stipulated by ANSI N14.5-1997 following compliance testing provides justification of the above statements.

### 3.4.2 Maximum Normal Operating Pressure

The stainless-steel drum and cast refractory system will not pressurize as a result of temperature increases because of four ventilation holes (0.795 cm [0.313 in.] in diameter) drilled in the drum side wall 3.81 cm (1.5 in.) from the flanged top and equally spaced around the drum. The holes are filled with nylon plugs, but they are not hermetically sealed. The inner liner encapsulating the noncombustible neutron poison (Cat 277-4) will not pressurize as a result of temperature increases because of three ventilation holes (0.635 cm [0.25 in.] in diameter) and a slot (1.63 cm [0.64 in.] in width and 4.17 cm [1.64 in.] in length) drilled into this inner liner. These features are covered during transport with aluminum tape to prevent contamination of the neutron poison. This tape does not represent a hermetic seal.

The maximum normal operating pressure is defined in 10 CFR 71.4 as the maximum gauge pressure that would develop in the containment system in a period of one year under the heat conditions specified in 10 CFR 71.71(c)(1). The internal pressure developed under these conditions in the ES-3100 containment vessel is calculated in Appendix 3.6.4 for the most restrictive containment vessel configurations. For conservatism, the decay heat of 0.4 W was used for the maximum internal heat load in evaluating the package for NCT. The maximum calculated internal absolute pressure in the containment vessel with solar insolation and the bounding case parameters is 137.92 kPa (20.004 psia). This pressure incorporated the off-gassing from the silicone rubber pads, polyethylene bottles, teflon bottles, and polyethylene bagging and assumes that the containment vessel is assembled at ambient temperature and pressure at 100% relative humidity. The heat-transfer capability of the packaging is not degraded due to gap creation caused by differences in the fabrication material's coefficient of thermal expansion. Modeling assumed nominal gaps and position based on the engineering drawings of Appendix 1.4.8.

Little or no hydrogen gas is generated inside the containment vessel due to thermal- or radiation-induced decomposition of the water vapor, polyethylene bagging and bottles, or teflon bottles.

### 3.4.3 Maximum Thermal Stresses

The temperature of the package under NCT will vary from a low of  $-40^{\circ}\text{C}$  ( $-40^{\circ}\text{F}$ ) throughout the package to a maximum of  $117.72$  and  $87.81^{\circ}\text{C}$  ( $243.89$  and  $190.06^{\circ}\text{F}$ ) (Appendix 3.6.2) on the surface of the drum and the containment vessel, respectively (Sect. 3.4.1). The slow temperature increase or decrease experienced in normal conditions between these limits will result in an essentially uniform temperature change throughout the package. All materials of construction are within this operating temperature range (Table 3.15). Thermal stresses due to differences in thermal expansion are insignificant, as discussed in Sects. 2.6.1.2 and 2.6.2.

Most of the components of the packaging are completely unrestrained. Therefore, any thermal stresses in the packaging components as the temperature varies between the extremes listed above will have no effect on the ability of the packaging to maintain containment, shielding integrity, and nuclear subcriticality. The maximum stresses due to pressure under NCT for the containment vessel are given in Tables 2.21 and 2.22. These values are significantly below the allowable stresses for the packaging

components. The Kaolite 1600 insulation and Cat 277-4 materials are poured and cast in place during the fabrication of the drum weldment (Drawing M2E801508A002, Appendix 1.4.8). This situation produces a zero gap between these materials and the bounding drum and inner liners. Due to differences in coefficients of thermal expansion, some radial and axial interference is expected due to thermal growth or contraction of the inner liners. These radial and axial interferences and induced stresses are calculated in Appendix 3.6.3. The results show that the stresses induced are minimal and do not reduce the effectiveness of the drum assembly.

The containment vessel, which is Type 304L austenitic (iron-nickel-chromium) stainless steel, is designed and fabricated in accordance with Sects. III Subsect. NB and IX of the *ASME Boiler and Pressure Vessel Code* (B&PVC Sect. III and B&PVC Sect. IX). The two sealing surfaces of each containment boundary are joined together by torquing the closure nut inside the containment vessel body to  $162.7 \pm 6.8 \text{ N}\cdot\text{m}$  ( $120 \pm 5 \text{ lbf}\cdot\text{ft}$ ). The O-ring material is ethylene-propylene elastomer.

The design temperature range of the containment vessel is  $-29$  to  $148.89^\circ\text{C}$  ( $-20$  to  $300^\circ\text{F}$ ) (Appendix 2.10.1). However, the package has been evaluated to  $-40^\circ\text{C}$  ( $-40^\circ\text{F}$ ) (Sect. 2.6.2). The thermal properties of the stainless-steel container body, lid, and closure nut are not critical at these temperatures. The O-ring seal is important for the containment properties of the containment vessel. The normal service temperature range for the elastomer O-ring is  $-40$  to  $150^\circ\text{C}$  ( $-40$  to  $302^\circ\text{F}$ ) for continuous service and up to  $165^\circ\text{C}$  ( $329^\circ\text{F}$ ) for 72 h (*Parker O-ring Handbook*). The maximum adjusted HAC temperature of the ES-3100 containment vessel was based upon the thermal testing results in the vicinity of the O-rings. The maximum temperature recorded in the vicinity of the ES-3100 O-rings ( $241^\circ\text{F}$ ) is shown in Table 3.9. As shown in Sect. 3.5.3, the maximum temperature for the containment vessel at the O-ring location was adjusted for the ES-3100 package to  $141.22^\circ\text{C}$  ( $286.20^\circ\text{F}$ ). Hence, no damage would be expected to the O-rings during HAC.

The test packages were all preheated to above  $38^\circ\text{C}$  ( $100^\circ\text{F}$ ) prior to being placed in the furnace, which was heated to over  $800^\circ\text{C}$  ( $1475^\circ\text{F}$ ). As noted in the test report (Appendix 2.10.7), the temperatures recorded on the containment vessels of all the test units were fairly uniform, both vertically and circumferentially. The maximum temperature variation on the containment vessels was  $\sim 50^\circ\text{F}$  (from the test temperatures reported in Table 3.9). No damage would be expected on the containment vessel from thermal stresses resulting from a temperature differential of this magnitude. This conclusion is based on the guidelines given in B&PVC, Sect. III. Thermal stress is defined as a self-balancing stress produced by a nonuniform distribution of temperature (Paragraph NB-3213.13 of B&PVC, Sect. III). This paragraph further states that there are two types of thermal stresses: general thermal stress and local thermal stress. An example of a general stress is that produced by an axial temperature distribution in a cylindrical shell (Paragraph NB-3213.9). This general stress is further classified (Paragraph NB-3213.9) as a secondary stress (that is, a normal stress or a shear stress developed by the constraint of adjacent materials or by self-constraint of the structure). Paragraph NB-3213.9 further states that the basic characteristic of a secondary stress is that it is self-limiting. Local yielding and minor distortions can satisfy the conditions that cause the stress to occur, and failure from a single application would not be expected. An example of a local thermal stress is a small hot spot in the wall of a pressure vessel (Paragraph NB-3213.13). Local thermal stress is associated with almost complete suppression of the differential expansion and thus produces no significant distortion. Such stresses are considered only from a fatigue standpoint. Fatigue will not result from a one-time cyclic event such as an accidental fire.

Following the thermal test, the volume between the O-rings on the five containment vessels (Sect. 2.7.4) was then leak tested and met the air leak-rate criterion of  $10^{-4} \text{ ref}\cdot\text{cm}^3/\text{s}$ . Following the O-ring leak check, the five containment vessels were drilled and tapped for full body helium leak testing. All five containment vessels passed the leak rate criteria for leaktightness per ANSI N14.5-1997. The containment

vessels were then submerged under a pressure equivalent to 0.9 m (3 ft) of water for 8 h, with no leakage noted. (Sect. 2.7.5). Visual inspection following testing and disassembly also indicated that no distortion or damage occurred in the containment vessel wall, sealing lid, closure nut, O-rings, or sealing surfaces. These tests and observations demonstrate that thermal stresses produced during testing did not affect the containment capability of the containment vessel.

### 3.5 HYPOTHETICAL ACCIDENT THERMAL EVALUATION

#### 3.5.1 Initial Conditions

Five full-scale packages were tested in the sequence shown in Table 2.19. Each ES-3100 test package was subjected to the 1.2-m (4-ft) drop test in accordance with 10 CFR 71.71(c)(5) prior to the sequential HAC tests in accordance with 10 CFR 71.73 (free drop, crush, puncture, thermal, and immersion tests). One of these units (Test Unit-4) had previously completed the tests and conditions stipulated in 10 CFR 71.71(c)(5) through (c)(10), excluding (c)(8). Two different mock-up configurations were used to represent the minimum and maximum proposed shipping weight and to simulate various center of gravity locations. The structural and thermal interface between the mock-up component and the containment vessel was designed to match that of the actual hardware proposed for transport. Based on LS-DYNA-3D drop simulations (Appendix 2.10.2) the five test units with their associated test weights represent the worst drop orientations for the ES-3100 package. Test Unit-5 used a near replicate of the lightest weight contents for its mock-up component. NCT free-drop, 9 m (30 ft) free drop, 9 m (30 ft) crush and puncture tests were made as specified in 10 CFR 71.71(c)(1), and 73(c)(1) through (c)(3) on all five full-scale test packages prior to thermal testing. The results of this testing are discussed in Sects. 2.7.1, 2.7.2, and 2.7.3. The 1.2-m (4-ft), 9-m (30-ft) drop and crush test orientations were as follows: two tests with the long axis of drum at an oblique angle of 12° to impact surface; a center of gravity over the corner of the drum lid; a drop with the long axis of drum parallel with the impact surface; and a vertical drop on to the drum's lid. The subsequent 40-in. puncture drops were made at various orientations as shown in Table 2.19.

Prior to the thermal test, each test unit was preheated to the maximum temperature extreme in accordance with 10 CFR 71.73(b)(1). Since the containment vessels were initially assembled at ~101.35 kPa (14.7 psia) at 25°C (77°F), the initial internal containment vessel pressure was ~105.70 kPa (15.33 psia) at 38°C (100°F) using the ideal gas law. In accordance with 10 CFR 71.73(b)(1), the internal pressure should be that calculated for the maximum normal operating pressure or 137.92 kPa (20.004 psia). This slight pressure differential has little or no effect on the thermal test results. The maximum decay heat load of the contents is calculated to be 0.4 W based on 352 kg of HEU. Analysis of the ES-3100 package after thermal HAC tests both with and without the decay heat load has been performed. The maximum projected temperature differential between the two packages following furnace exposure, as calculated in Appendix 3.6.2, would be 0.4°C (0.7°F) at the top center of the containment vessel lid, 0.4°C (0.7°F) at the containment vessel flange near the O-rings, 0.45°C (0.8°F) at the containment vessel bottom center, and 0.6°C (1.1°F) at the containment vessel mid body. These temperature differentials are representative for both the Kaolite 1600 densities evaluated.

#### 3.5.2 Fire Test Conditions

Full-scale testing in accordance with 10 CFR 71.73 for HAC was conducted on prototypical packages. Therefore, no analyses were conducted to show compliance with the HAC thermal test. However, analyses were conducted and are discussed in Sect. 3.5.3 to determine the thermal impacts of an internal heat source, application of insulation during cool down, location of crush plate impact on test unit, and thermal capacitance differences between test hardware and proposed shipping hardware.

Full-scale testing of five ES-3100 test units was conducted in accordance with 10 CFR 71.73(c)(4) for HAC. A single full-scale ES-3100 test unit (TU-4) was assembled and subjected to both NCT and to the sequential tests specified in 10 CFR 71.73(c). The furnace used for thermal testing was the No. 3 Furnace at Timken Steel Company in Latrobe, Penn., which is a gas-fired furnace. Oxygen content in stack gases from the furnace were not monitored because it was not anticipated that any of the package's materials of construction were combustible. There was some burning of the silicone pads which are placed between the inner liners and the top plugs of the packages. However, it should be noted that this furnace employs "pulsed" fire burners. This type of burner is unique in that the natural gas flow rate is varied based on furnace controller demands, but the flow of air through the burners is constant, even when no gas is flowing, thereby ensuring a very rich furnace atmosphere capable of supporting any combustion of package materials of construction.

The most significant change to the definition of the HAC thermal test in the current 10 CFR 71 is the requirement for calculation purposes to base convective heat input on "that value which may be demonstrated to exist if the package was exposed to the fire specified." This is not especially significant for this package because it was tested in the gas-fired furnace with burners placed in an attitude which produced a strong convective swirl. Careful examination of the thermal test data indicates that the total heat imparted to the packages was significantly greater than the required total heat specified in 10 CFR 71.73(c)(4). Compliance with ASTM E-2230-02, *Standard Practice for Thermal Qualification of Type B Packages for Radioactive Materials*, was accomplished by the method described in Sect. 7.3 of this standard. This standard is in general agreement with Paragraph 2.2.1 ("Steady-state Method of Compliance") of SG 140.1 entitled *Combination Test Analysis/ Method Used to Demonstrate Compliance to DOE Type B Packaging Thermal Test Requirements (30 Minute Fire Test)*.

Prior to the beginning of the thermal test, the furnace was characterized for temperature and heat recovery times. The support stand was welded to a large steel plate which had been placed on the floor of the furnace prior to heating. This steel plate acted as the radiating surface at the bottom of the furnace, as well as providing the ability to hold the test stand rigidly in place. Before heating the furnace, workers practiced loading and unloading test packages from the cold furnace to ensure that the furnace door would not remain open >90 s during each loading. In fact, the maximum time the door was open during any loading was 64 s. As discussed in *Test Report of the ES-3100 Package* (Appendix 2.10.7), six thermocouples were affixed to the drum assembly's exterior surface. Metal retainer clips were welded to the exterior surface to hold the thermocouples in place. The thermocouple tips were inserted underneath the metal clips, and the wire was wrapped around the metal clip. To eliminate any radiant heat exchange between the thermocouples and the furnace walls, the tips and metal clips were covered with a ceramic coating. Three thermocouples were mounted on each of the walls of the furnace, as well as on the furnace floor, on the furnace door, and three thermocouples were mounted on the test stand.

A minimum of 24 h prior to the beginning of all testing, the furnace was turned on with a set-point temperature of 871°C (1600°F). Following each test, the furnace set point was adjusted to 871°C (1600°F) for at least 45 min prior to the beginning of the next test. The furnace control data recorder ran continuously for the entire duration of the preheat cycle test. Each test unit was preheated to over 38°C (100°F) by placing the packages in an environmental chamber. The environmental chamber was heated by a torpedo-type kerosene space heater controlled by a mechanical bulb thermostat with a control range of 38 to 93°C (100 to 200°F). The environmental chamber is a welded steel frame with fiberglass insulation panels. It was heated from the bottom with four floor register vents located around the perimeter and a 20.32-cm (8-in.)-diam manual dampened center venting stove pipe.

The set point temperature of the environmental chamber was monitored and adjusted for the duration of the preheat cycle. Initially, the thermostat was set to 66°C (150°F) for ~23 h. The thermostat set point

was then reduced to 43°C (110°F) for the remainder of the preheat cycle (24 h). All packages were preheated for at least 47 h. No test package was loaded into the furnace until 15 of the 18 thermocouples monitoring the furnace had a reading of 800°C (1475°F) or higher. All packages were placed in the preheated furnace on the support stand with the long axis positioned horizontally, and the package lid facing toward a furnace side wall. During the testing of each package, the thermocouple temperature data recorder was set to record every 15 s.

These packages were exposed to the radiation environment for a minimum of 30 min after all functioning furnace thermocouples and at least five of the six test package exterior surface thermocouples reached a temperature of 800°C (1475°F). During the testing, the package thermocouple temperature data were recorded every 15 s.

After each test, the furnace was allowed to reheat for a minimum of 45 min after obtaining the set point temperature before testing the next unit. The furnace control temperature data recorder ran continuously for the duration of the preheat. No test package was loaded into the furnace until all functioning thermocouples on the furnace walls and support stand had again reached a temperature of 800°C (1475°F) or higher.

All units were tested in a horizontal attitude with the top end of the package facing to the right side wall of the furnace and the 0° mark on the drum facing the floor of the furnace. The data from each of the thermal tests, as shown in the test report, show that at least four of the six external drum thermocouples reached temperatures well in excess of 800°C (1475°F) and remained above 800°C (1475°F) during the 30-min thermal testing. Similarly, all other surfaces of the furnace, including the support stand, exceeded 800°C (1475°F) during the timed portion of the thermal test. For the test specified in the regulations, regardless of the amount of heat input by convection, radiation, or conduction, the maximum temperature the skin of the package could reach would be 800°C (1475°F). That is, the source of the heat in the regulatory specified test is at 800°C (1475°F). Heat can only be transferred from a hotter source to a colder source. Thus, regardless of the mode of heat transfer, the greatest temperature a specimen exposed to the 10 CFR 71.73(c)(4) thermal test can attain is 800°C (1475°F). Therefore, the fact that these test packages attained temperatures well in excess of 800°C (1475°F) is an excellent indication that the thermal tests performed not only met the requirements of 10 CFR 71.73(c)(4) but actually exceeded them markedly. The results of these tests are provided in the test report (Appendix 2.10.7).

Each test package was removed from the furnace and placed in an area where it was not exposed to artificial cooling. As the furnace door was opened for each test unit, flaming or smoking was visible at the tamper indicating device (TID) holes in the drum/lid interface. Flaming continued on some of the packages for a short duration; the longest flame duration was 22 min after removal from the furnace. Smoke was also visible from each of the packages and continued after flames were no longer visible. The packages continued to smoke between 12 and 60 min after removal from the furnace. All the packages were allowed to cool naturally to room temperature. The post-thermal testing weights of each unit are summarized in Table 3.18. The drums were disassembled, and the damage was photographed. Each package was visually inspected, and the condition of the package and any observations were recorded.

### **3.5.3 Maximum Temperatures and Pressure**

The five test unit's previously subjected to both NCT and HAC drop testing were thermal tested in accordance with 10 CFR 71.73(c)(4). To determine the maximum temperatures reached during thermal testing, temperature indicating patches were placed at various locations throughout the test package at assembly. The temperature range for each patch used is identified in Table 3.19. When the temperature of

**Table 3.18. ES-3100 test package weights before and after 10 CFR 71.73(c)(4) HAC thermal testing**

Test Unit	Pre-test <sup>a</sup> weight kg (lb)	Post-test <sup>a</sup> weight kg (lb)	Thermal test weight loss kg (lb)	BoroBond4 original weight <sup>b</sup> kg (lb)	Water weight in BoroBond4 <sup>c</sup> kg (lb)	Water loss percent <sup>d</sup> (%)
1	202.3 (446)	202.3 (446)	0.0 (0)	20.7 (45.64)	4.91 (10.82)	0.00
2	202.8 (447)	202.8 (447)	0.0 (0)	20.5 (45.19)	4.86 (10.72)	0.00
3	203.7 (449)	203.2 (448)	0.45 (1)	20.5 (45.19)	4.87 (10.74)	9.31
4	201.8 (445)	201.4 (444)	0.45 (1)	20.4 (44.97)	4.84 (10.66)	9.38
5	157.4 (347)	156.9 (346)	0.45 (1)	20.6 (45.42)	4.89 (10.77)	9.29

<sup>a</sup> Data from ORNL/NTRC-013.

<sup>b</sup> Weight of BoroBond4 and water obtained from casting data. (ES-3100 Weldments 2004)

<sup>c</sup> This weight is based on TGA measurements and calculation showing that the minimum water percent is 23.71%.

<sup>d</sup> All weight loss attributed to loss of water in BoroBond4.

an indicator was reached, the color would change to black (i.e., blackout temperature). The range of possible blackout temperatures of the patches was from 51.67 to 260°C (125 to 500°F). For Test Units-1 through -5, Table 3.19 defines the number and location of the temperature indicating patches.

Since the structural and thermal interface between the various mock-ups and containment vessels is the same as the actual hardware, the use of steel mock-ups to simulate the contents is not expected to affect the results of the thermal test significantly. The total maximum weight of the test packages ranged from 157.4 kg (347 lb) to 203.7 kg (449 lb). The ES-3100 package has a nominal gross shipping weight that ranges from 146.88 kg (323.79 lb) to ~~187.81 kg (414.05 lb)~~ for the minimum and maximum weight containment vessel configurations shown in Table 2.8, respectively. However, the effect on temperature is evaluated in the following paragraphs due to thermal capacitance differences between the mock-up and the actual contents.

**Table 3.19. Thermax temperature indicating patches for test units**

Patch Location	Internal surface	External surface	Temperature range °C (°F)	Test report figure <sup>a</sup>
Inner liner of drum assembly		17 (Full Range)	52–260 (125–500)	5.30
Top plug weldment		4 (Full Range)	52–260 (125–500)	5.31
Containment vessel body flange	8 (4B & 4C)	8 (4B & 4C)	"B" 77–127 (171–261) "C" 132–182 (270–360)	5.28
Containment vessel body (end cap and cylinder)		5 (B)	"B" 77–127 (171–261)	5.28
Containment vessel sealing lid	4 (B)	4 (B)	"B" 77–127 (171–261)	5.29
Test mock-up components		6 (B)	"B" 77–127 (171–261)	5.26 & 5.27

<sup>a</sup> ORNL/NTRC-013, Volume 1.

As previously stated, temperature indicators (patches) were placed on the surface of each containment vessel, inner liner, and mock-up component. The blackout temperatures that occurred during thermal testing are recorded for each test unit; the maximum blackout temperatures are listed in Table 3.9. A maximum blackout temperature of 116°C (241°F) was recorded in the vicinity of the O-rings on the containment vessel of Test Unit-5. As discussed below, this temperature will be conservatively adjusted to correlate the test conditions to shipping conditions with decay heat and solar insolation. The blackout temperatures are increased to account for (1) the temperature interval between blackout dots; (2) the ambient temperature of the package prior to insertion into the furnace; (3) the temperature increase due to the effects of applying solar insolation during post-HAC thermal test cool down; (4) the temperature increase due to the decay heat load of the actual contents being shipped; (5) effects of crushing at different locations along the body of the shipping package; (6) thermal capacitance difference in the proposed contents and hardware used during testing; (7) temperature difference occurring when using BoroBond4 and Cat 277-4; and (8) temperature difference resulting from variations in Kaolite 1600 and Cat 277-4 material densities.

The initial adjustment for the blackout reading is an increase of 6.11°C (11.0°F) from the patch that blacked out. The highest blackout reading indicates that the actual temperature is somewhere between the highest temperature indicated and the next higher temperature.

The second adjustment compensates for thermal testing at package soak temperatures less than the maximum temperature of 38°C (100°F). In the case of the ES-3100 package, each test unit was thermally soaked to over 38°C (100°F) prior to insertion into the furnace. Therefore, there is no temperature adjustment required.

The third adjustment is a temperature increase to represent the effect of insolation heat flux on the package immediately following the conclusion of the thermal HAC test. Analyses of the ES-3100 package after thermal HAC tests both with and without insolation have been performed. Results from these analyses indicate an increase of ~5.94°C (10.7°F) at the containment vessel top (node 6715), ~6.06°C (10.9°F) at the containment vessel O-ring (node 6359), ~10.44°C (18.8°F) at the containment vessel mid body (Node 6574), and ~4.56°C (8.2°F) at the containment vessel bottom (node 6399), as a result of applying insolation following HAC thermal testing. These increases are extracted from Tables 3.7 and 3.8. The most pronounced effect of applying the insolation heat flux was that it increased the time required to cool the package to NCT type conditions. Nevertheless, the influence of insolation is included in the adjustments to the blackout temperatures.

The fourth temperature adjustment considered is the temperature increase due to the decay heat load of the actual contents being shipped. A maximum decay heat load of 0.4 W is calculated as the bounding case for ~~35.2~~ kg of HEU. HAC analysis of the ES-3100 package both with and without the decay heat load has been performed, with the results shown in Tables 3.7 and 3.8. The maximum projected temperature increase during HAC due to a 0.4-W heat source, as calculated in Appendix 3.6.2, would be ~0.39°C (0.7°F) at the containment vessel's top (node 6715), ~0.39°C (0.7°F) at the containment vessel's O-ring (node 6359), ~0.6°C (1.1°F) at the containment vessel's mid body (node 6574), and ~0.45°C (0.8°F) at the containment vessel bottom (node 6399).

The fifth temperature adjustment considered is the temperature increase to the containment vessel based on the location of impact from the 500 kg (1100 lb) crush plate. Based on the differences in location of the crush plate between Test Units-1 and -2, crushing the shipping package with the center of gravity of the plate directly above the containment vessel flange increases the containment vessel temperature on average ~6.11°C (11°F).

The sixth adjustment compensates for the shipment of only 3 kg of HEU rather than the steel mock-ups. The higher content weight was used for testing to cover the possibility of shipping larger components without retesting. The larger content weight gave conservative structural deformation test results to the drum assembly than would the actual shipping weight. One effect, however, of using the larger test mass could be to reduce the containment vessel's temperature rise during the thermal test because the mock-up acts like a heat sink. In order to eliminate this temperature adjustment, a mock-up of the lightest proposed shipment was used in Test Unit-5. The structural and thermal interface between the mock-up components and the containment vessel was designed to match that of the actual shipping hardware, thereby providing the same conductive heat path for thermal testing. As shown by the test results, both the containment vessel and mock-up components of Test Unit-5 recorded higher temperatures than the other test units. This supports the theory that the heavier mock-ups act as heat sinks for the containment vessel. Therefore, by testing the 3.6-kg (8-lb) mock-up representing the lightest assembly to be shipped, a more accurate prediction of actual temperatures reached during thermal testing was achieved. No further temperature adjustments due to differences in mock-up weight are needed.

The seventh temperature adjustment compensates for conducting the HAC compliance tests with BoroBond4 and substituting Cat 277-4 for the production shipping containers. This adjustment is determined by using an undamaged package and subjecting it to a thermal environment representative of that required by 10 CFR 71.73(c)(4). Based on the analytical results shown in Appendix 3.6.2, the containment vessel in a package using Cat 277-4 would be from 2.5°F to 8.°F cooler than a package with BoroBond4. Conservatively, the temperatures will not be adjusted due to the neutron poison change.

The eighth and final temperature adjustment compensates for material density variation in the Kaolite 1600 and Cat 277-4 material during HAC compliance tests. Again, this temperature adjustment was predicted for an undamaged package using the finite element method. Based on the analytical results shown in Appendix 3.6.2 (Tables 3.7 and 3.8), the containment vessel temperature was predicted to be ~6.4°C (11.6°F) higher at the containment vessel's top (node 6715), ~6.4°C (11.6°F) higher at the containment vessel's O-ring (node 6359), ~4.6°C (8.3°F) higher at the containment vessel's mid body, and ~7.72°C (13.9°F) at the containment vessel's bottom (node 6399) when the lower density values for Kaolite 1600 and the neutron poison were used. Since actual compliance testing was conducted with these densities on the high side, the above adjustments must be added to the containment vessel temperatures.

Table 3.20 summarizes the numerous temperature adjustments needed for the containment vessel.

**Table 3.20. Predicted temperature adjustments (°F) for containment vessel due to HAC**

Node <sup>a</sup>	Analytical Temperature Adjustments								Total Temp Adjustment
	1	2	3	4	5	6	7	8	
6715	11.00	0.00	10.70	0.70	11.00	0.00	0.00	11.60	45.00
6359	11.00	0.00	10.90	0.70	11.00	0.00	0.00	11.60	45.20
6574	11.00	0.00	18.80	1.10	11.00	0.00	0.00	8.30	50.20
6399	11.00	0.00	8.20	0.80	11.00	0.00	0.00	13.90	44.90

<sup>a</sup> See Figs. 8 through 11 in Appendix 3.6.2 for details of node locations.



Table 3.21 shows the results of adding the eight temperature adjustments previously discussed to the black-out temperatures for the containment vessel with the 3.6-kg (8-lb) mock-up (Test Unit-5). These adjusted temperatures would not adversely affect the stainless-steel components or the O-ring materials of the containment vessel.

**Table 3.21. Predicted temperatures of the containment vessel due to HAC (°F)**

Node <sup>a</sup>	Analytical temperature adjustments (°F)	Maximum blackout temperature on Test Unit-5 (°F)	Final predicted CV temperature (°F)
6715	45.00	261	306.00
6359	45.20	241	286.20
6574	50.20	199	249.20
6399	44.90	210	254.90

<sup>a</sup> See Figs. 8 through 11 in Appendix 3.6.2 for details of node locations.

To determine the maximum pressure inside the containment vessel as a result of thermal testing, the average adjusted gas temperature must be calculated based on the above results. The approach used is to divide the containment vessel volume into three distinct equal regions and then average the three together. The first volume is represented by the gas adjacent to the containment vessel lid and flange region and the top convenience can. Based on the temperature recorded near the O-rings [116.11°C (241°F)] and the temperature recorded on the external surface of the convenience can [98.89°C (210°F)], the average temperature of the gas in this region is 107.50°C (225.50°F). Using the temperature adjustment of 25.11°C (45.20°F) for this region, the adjusted average temperature in the first region is 132.61°C (270.70°F). The second volume is represented by the gas adjacent to the second convenience can from the top. Based on the temperature recorded on the containment vessel wall and convenience can [92.78°C (199°F)], the average temperature of gas in this region is 92.78°C (199°F). Using the temperature adjustment of 27.89°C (50.20°F) for this region, the adjusted average temperature in the second region is 120.67°C (249.20°F). The third and final volume is represented by the gas adjacent to the bottom convenience can. Again based on the convenience can temperature [87.78°C (190°F)] and the containment vessel end cap temperature [98.89°C (210°F)], the average temperature of gas in this region is 93.33°C (200°F). Using the temperature adjustment of 24.94°C (44.90°F) for this region, the adjusted average temperature in the third region is 118.28°C (244.90°F). Averaging these three temperatures, an average adjusted gas temperature of 123.85°C (254.93°F) is determined for the containment vessel.

As shown in Appendix 3.6.5, the maximum adjusted average gas temperature and pressure in the containment vessel during accident conditions was calculated to be 123.85°C (254.93°F), and 507.63 kPa (73.625 psia), respectively.

The maximum adjusted temperature on the surface of the containment vessel, adjacent to the O-rings, was 141.22°C (286.20°F). This is well within the design range for the packaging. The full body helium leak test on all test units following thermal testing meets the "leaktight" criteria in accordance with ANSIN14.5-1997. Visual inspection following testing and unloading indicated that no distortion or damage occurred in the containment vessel wall, sealing lid, closure nut, O-rings, or sealing surfaces. No water was

visible inside the containment vessel following the 0.9-m (3-ft) water immersion test or the 15-m (50-ft) water immersion test on Test Unit-6.

The ES-3100 package satisfies the requirements of 10 CFR 71.73 for transport of the ~~352-kg~~ ~~(17.60-lb)~~ arrangements shown in Table 2.8. Section 2.7 has additional details to support this conclusion.

#### **3.5.4 Accident Conditions for Fissile Material Packages for Air Transport**

~~The expanded fire test conditions specified in 10 CFR 71.55(f)(1)(iv) for fissile material package designs for air transportation was not conducted. The issue of subcriticality is addressed in Section 6 with content mass limits as addressed in Section 1 for air transport.~~

### 3.6 APPENDICES

Appendix	Description
3.6.1	THERMAL EVALUATION OF THE ES-3100 SHIPPING CONTAINER FOR NCT AND HAC (CONCEPTUAL DESIGN WITH BOROBOND4 NEUTRON ABSORBER)
3.6.2	THERMAL EVALUATION OF THE ES-3100 SHIPPING CONTAINER FOR NCT AND HAC (FINAL DESIGN WITH CATALOG 277-4 NEUTRON ABSORBER)
3.6.3	THERMAL STRESS EVALUATION OF THE ES-3100 SHIPPING CONTAINER DRUM BODY ASSEMBLY FOR NCT (FINAL DESIGN WITH CATALOG 277-4 NEUTRON ABSORBER)
3.6.4	CONTAINMENT VESSEL PRESSURE DUE TO NORMAL CONDITIONS OF TRANSPORT FOR THE PROPOSED CONTENTS
3.6.5	CONTAINMENT VESSEL PRESSURE DUE TO HYPOTHETICAL ACCIDENT CONDITIONS FOR THE PROPOSED CONTENTS
3.6.6	SILICONE RUBBER THERMAL PROPERTIES FROM THERM 1.2 DATABASE



## **APPENDIX 3.6.1**

### **THERMAL EVALUATION OF THE ES-3100 SHIPPING CONTAINER FOR NCT AND HAC (CONCEPTUAL DESIGN WITH BOROBOND4 NEUTRON ABSORBER)**



## APPENDIX 3.6.1

### THERMAL EVALUATION OF THE ES-3100 SHIPPING CONTAINER FOR NCT AND HAC (CONCEPTUAL DESIGN WITH BORBOND4 NEUTRON ABSORBER)

#### INTRODUCTION

Thermal analyses of the ES-3100 shipping container are performed to determine the temperature distribution within the packaging during Normal Conditions of Transport (NCT) as specified in 10 CFR 71.71(c)(1).<sup>[1]</sup> Transient thermal analyses are performed by treating the problem as a cyclic transient with the incident heat flux due to solar radiation applied and not applied in alternating 12-hour periods.

Additionally, thermal analyses of the ES-3100 shipping container are performed to determine the thermal response of the packaging to Hypothetical Accident Conditions (HAC) as specified in 10 CFR 71.73(c)(4).<sup>[1]</sup> Since physical testing of the ES-3100 shipping container will be conducted with no internal heat source or insolation during cool-down, temperature increases due to internal heat loads of 0.4, 20, and 30 W as well as temperature increases due to the application of insolation during cool-down following the HAC fire are calculated. Although earlier revisions of 10 CFR 71 specifically state that insolation does not need to be evaluated before, during, or after HAC, the current version of 10 CFR 71 and associated guidance are unclear regarding the need for consideration following HAC testing. Since the Nuclear Regulatory Commission (NRC) has taken the position that insolation must be considered and evaluated following fire testing, analyses are conducted to determine the effect of insolation following the HAC fire on the ES-3100 shipping container. The predicted temperature increases may be used to adjust physical test data for those loads not included in the tests.

#### FINITE ELEMENT MODEL DESCRIPTION

A two-dimensional axisymmetric (r-z) finite element model of the ES-3100 shipping container is constructed using MSC.Patran (2004, Version 12.0.044)<sup>[2]</sup> for evaluation for NCT. The actual contents of the ES-3100 shipping container are not specifically modeled—instead, the content source heat load (if desired) is modeled by applying a uniform heat flux to the inner surfaces of the containment vessel. This is a conservative approach in that package temperatures will not be reduced in a transient analysis by the heat capacity of the contents. A schematic of the finite element model is presented in Figure 1. The model consists of five materials: stainless steel (drum, liners, and containment vessel), Kaolite, Borobond4, silicone rubber, and air in the gaps between the drum liner and containment vessel and between the drum liner and top plug. Thermal properties of the materials used in the analysis are presented in Table 1.

Heat is transferred to the model from the contents (i.e., decay heat of the contents) via heat flux boundary conditions applied to the inner surface of the elements representing the containment vessel. Additionally, solar heat fluxes are applied to the model during NCT and HAC post-fire cool-down via heat flux boundary conditions. The heat applied to the model via the boundary conditions is transferred through the model via conduction and thermal radiation. Heat is rejected from the external surfaces of the model via natural convection and thermal radiation boundary conditions.

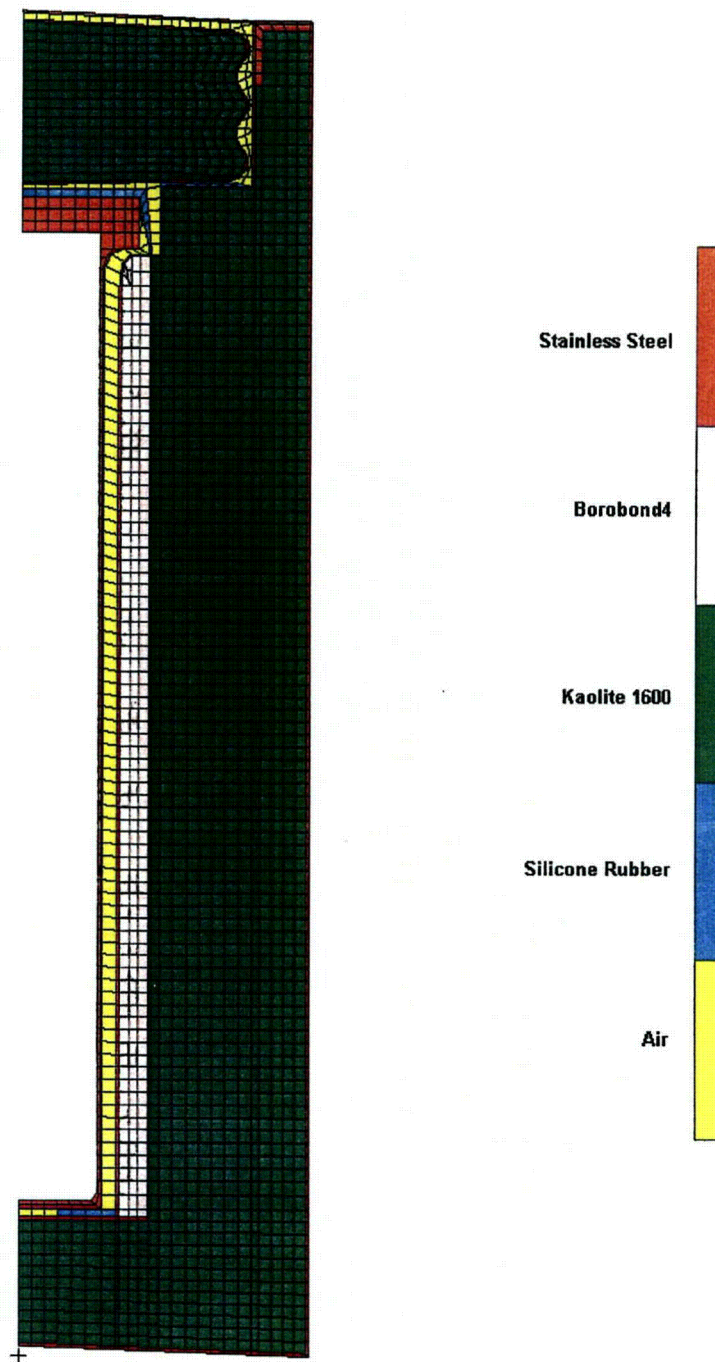


Figure 1. MSC.Patran axisymmetric finite element model of the ES-3100 shipping container.



**Table 1. Thermal properties of the materials used in the thermal analysis.**

Material	Temperature (°F)	Thermal conductivity (Btu/h-in.-°F)	Density (lbm/in. <sup>3</sup> )	Specific heat (Btu/lbm-°F)	Emissivity
Stainless steel	-279.67	0.443 <sup>(a)</sup>	0.285 <sup>(a)</sup>	0.065 <sup>(a)</sup>	0.22 <sup>(a)</sup>
	-99.67	0.607	—	0.096	—
	260.33	0.799	—	0.123	—
	620.33	0.953	—	0.133	—
	980.33	1.088	—	0.139	—
	1340.33	1.223	—	0.146	—
	1700.33	1.348	—	0.153	—
	2240.33	1.526	—	0.163	—
Kaolite 1600	68	0.0093 <sup>(b)</sup>	0.011 <sup>(c)</sup>	0.2 <sup>(d)</sup>	—
	212	0.0091	—	—	—
	392	0.0081	—	—	—
	572	0.0072	—	—	—
	1112	0.0082	—	—	—
Borobond4	25	0.0450 <sup>(f)</sup>	0.0683 <sup>(f)</sup>	0.2160 <sup>(f)</sup>	—
	77	0.0576	—	—	—
	100	0.0632	—	—	—
	104	0.0642	—	—	—
Silicone rubber	—	0.0161 <sup>(g)</sup>	0.047 <sup>(g)</sup>	0.300 <sup>(g)</sup>	1.0 <sup>(h)</sup>
Air	-9.67	1.074×10 <sup>-3(a)</sup>	4.064×10 <sup>-5(a),(i)</sup>	0.240 <sup>(a)</sup>	—
	80.33	1.266×10 <sup>-3</sup>	—	0.241	—
	170.33	1.445×10 <sup>-3</sup>	—	0.241	—
	260.33	1.628×10 <sup>-3</sup>	—	0.242	—
	350.33	1.796×10 <sup>-3</sup>	—	0.244	—
	440.33	1.960×10 <sup>-3</sup>	—	0.246	—
	530.33	2.114×10 <sup>-3</sup>	—	0.248	—
	620.33	2.258×10 <sup>-3</sup>	—	0.251	—
	710.33	2.393×10 <sup>-3</sup>	—	0.254	—
	800.33	2.523×10 <sup>-3</sup>	—	0.257	—
	890.33	2.644×10 <sup>-3</sup>	—	0.260	—
	980.33	2.759×10 <sup>-3</sup>	—	0.263	—
	1070.33	2.870×10 <sup>-3</sup>	—	0.265	—
	1160.33	2.985×10 <sup>-3</sup>	—	0.268	—
	1250.33	3.096×10 <sup>-3</sup>	—	0.270	—
	1340.33	3.212×10 <sup>-3</sup>	—	0.273	—
	1520.33	3.443×10 <sup>-3</sup>	—	0.277	—

- Notes:
- (a) F. P. Incropera and D. P. DeWitt, *Fundamentals of Heat and Mass Transfer*, 2nd edition, John Wiley & Sons, New York, 1985.
  - (b) Hsin Wang, *Thermal Conductivity Measurements of Kaolite*, ORNL/TM-2003/49.
  - (c) Based on a baked density of 19.4 lbm/ft<sup>3</sup> (0.011 lbm/in.<sup>3</sup>). Specification JS-YMN3-801580-A003 requires a baked density of 22.4 ± 3 lbm/ft<sup>3</sup>. Using a lower value for the Kaolite density results in higher temperatures on the containment vessel because the heat capacity of the Kaolite is minimized—allowing more heat to flow to the containment vessel; therefore, the thermal analyses are performed using a low-end density of 19.4 lbm/ft<sup>3</sup>. The HAC analyses also consider a high-end density of 30 lbm/ft<sup>3</sup>.
  - (d) FAX communication from J. W. Breuer of Thermal Ceramics, Engineering Department, August 11, 1995.
  - (e) W. D. Porter and H. Wang, *Thermophysical Properties of Heat Resistant Shielding Material*, ORNL/TM-2004/290, ORNL, Dec. 2004. Specific heat values are presented in MJ/m<sup>3</sup>-K in ORNL/TM-2004/290—converted to mass-based units using a density of 105 lbm/ft<sup>3</sup>.
  - (f) Data via email from Jim Hall (Eagle-Picher) to Jerry Byington (BWXT Y-12), March 12, 2004.
  - (g) THERM 1.2, thermal properties database by R. A. Bailey.
  - (h) Conservatively modeled as 1.0.
  - (i) Constant density value evaluated at 100°F.

## MODELED HEAT TRANSFER MECHANISMS

The heat transfer mechanisms included in the thermal model such as thermal radiation, natural convection, and insolation (solar heat flux) are described in detail in the following sections.

### Heat Transfer Between Package Exterior and Ambient

The heat transfer between the exterior of the package and the ambient (or fire) is modeled as a combination of radiant heat transfer and natural convection. The heat transfer due to radiant exchange with the environment is calculated as:<sup>[3]</sup>

$$q''_{\text{rad}} = \sigma F_e (T_s^4 - T_a^4), \quad (1)$$

where  $\sigma$  = Stefan-Boltzmann constant,  
 $F_e$  = overall exchange factor,  
 $T_s$  = container outer surface temperature (absolute), and  
 $T_a$  = ambient or fire temperature (absolute).

The overall interchange factor is calculated as:<sup>[3]</sup>

$$F_e = \left[ \frac{1}{\frac{1}{\epsilon_p} + \frac{A_p}{A_s} \left( \frac{1}{\epsilon_s} - 1 \right)} \right], \quad (2)$$

where  $\epsilon_p$  = emissivity of package surface,  
 $A_p$  = surface area of the package,  
 $A_s$  = surface area of the surroundings, and  
 $\epsilon_s$  = emissivity of surroundings.

For NCT and the cool-down period following the HAC fire, the area of the surroundings is assumed to be much larger than the surface area of the package; therefore, Eq. 2 reduces to:

$$F_e \approx \epsilon_p. \quad (3)$$

An emissivity value of 0.22,<sup>[4]</sup> which is typical of clean stainless steel, is assumed for the outer surfaces of the drum during NCT and during the cool-down period following the HAC fire. In reality, the outer surfaces of the drum will have a much higher emissivity following the HAC fire; therefore, this assumption is conservative.

During the HAC fire, the area of the surroundings is assumed to be approximately equal to the surface area of the drum; therefore, Eq. 2 reduces to:

$$F_e = \left[ \frac{1}{\frac{1}{\epsilon_p} + \frac{1}{\epsilon_s} - 1} \right] \quad (4)$$

During the HAC 30-minute fire, an emissivity of 0.8 is assumed for the drum, and an emissivity of 0.9 is assumed for the fire per the guidance of 10 CFR 71.74(c)(4).<sup>[1]</sup> This results in an overall exchange factor of 0.7347 during the HAC fire using Eq. 4.

The natural convection heat transfer from the package surface to the ambient air is calculated as:

$$q''_{\text{convection}} = h(T_s - T_a) \quad (5)$$

where,  $h$  = natural convection heat transfer coefficient,  
 $T_s$  = container outer surface temperature, and  
 $T_a$  = ambient or fire temperature.

During the NCT transient thermal analyses and the steady-state thermal analyses (used to obtain the starting temperature distribution in the package for NCT and HAC when a content heat load is present), the shipping container is assumed to be in an upright (vertical) orientation. The top of the drum is modeled as a heated horizontal flat plate facing up using the following correlation:<sup>[5]</sup>

$$h = \left( \frac{k}{L} \right) C_1 Ra^{C_2} \quad (6)$$

where,  $k$  = thermal conductivity of air,  
 $L$  = characteristic length (= D/4 per Ref. 5),  
 $D$  = diameter of the package,  
 $Ra$  = Rayleigh number,  
 $C_1$  = constant (see Table 2), and  
 $C_2$  = constant (see Table 2).

The Rayleigh number in Eq. 6 is defined as:

$$Ra = \frac{g\beta\Delta TL^3}{\nu\alpha} \quad (7)$$

where,  $g$  = acceleration of gravity,  
 $\beta$  = coefficient of thermal expansion,  
 $\Delta T$  = temperature difference,  
 $\nu$  = kinematic viscosity [ $\mu/\rho$ ],  
 $\mu$  = absolute viscosity,  
 $\alpha$  = thermal diffusivity [ $k/(\rho C_p)$ ],  
 $\rho$  = density of air, and  
 $C_p$  = specific heat of air.

The properties of air used in the natural convection calculations are presented in Table 3.

**Table 2. Coefficients for natural convection correlations.**

Coefficient	Rayleigh Number Range	Value
$C_1$	$2.6 \times 10^4 < Ra < 1.0 \times 10^7$	0.54
	$1.0 \times 10^7 < Ra < 3.0 \times 10^{10}$	0.15
$C_2$	$2.6 \times 10^4 < Ra < 1.0 \times 10^7$	0.25
	$1.0 \times 10^7 < Ra < 3.0 \times 10^{10}$	1/3
$C_3$	$Ra < 1.0 \times 10^9$	0.680
	$Ra > 1.0 \times 10^9$	0.825
$C_4$	$Ra < 1.0 \times 10^9$	0.670
	$Ra > 1.0 \times 10^9$	0.387
$C_5$	$Ra < 1.0 \times 10^9$	0.25
	$Ra > 1.0 \times 10^9$	1/6
$C_6$	$Ra < 1.0 \times 10^9$	4/9
	$Ra > 1.0 \times 10^9$	8/27
$C_7$	$Ra < 1.0 \times 10^9$	1
	$Ra > 1.0 \times 10^9$	2
$C_8$	$1.0 \times 10^4 < Ra < 1.0 \times 10^9$	0.53
	$1.0 \times 10^9 < Ra < 1.0 \times 10^{12}$	0.13
$C_9$	$1.0 \times 10^4 < Ra < 1.0 \times 10^9$	0.25
	$1.0 \times 10^9 < Ra < 1.0 \times 10^{12}$	1/3

Source: *MSC.Patran Thermal User's Guide, Volume 1: Thermal/Hydraulic Analysis*, MSC.Software Corporation, Santa Ana, CA 92702, 2003.

**Table 3. Properties of air used in natural convection calculations.**

Temperature (K)	Thermal Conductivity (W/m-K)	Density (kg/m <sup>3</sup> )	Specific heat (J/kg-K)	Absolute viscosity (N-s/m <sup>2</sup> )	Coefficient of thermal expansion (K <sup>-1</sup> )
250	$22.3 \times 10^{-3}$	1.3947	1006	$159.6 \times 10^{-7}$	$4.00 \times 10^{-3}$
300	$26.3 \times 10^{-3}$	1.1614	1007	$184.6 \times 10^{-7}$	$3.33 \times 10^{-3}$
350	$30.0 \times 10^{-3}$	0.9950	1009	$208.2 \times 10^{-7}$	$2.86 \times 10^{-3}$
400	$33.8 \times 10^{-3}$	0.8711	1014	$230.1 \times 10^{-7}$	$2.50 \times 10^{-3}$
450	$37.3 \times 10^{-3}$	0.7740	1021	$250.7 \times 10^{-7}$	$2.22 \times 10^{-3}$
500	$40.7 \times 10^{-3}$	0.6964	1030	$270.1 \times 10^{-7}$	$2.00 \times 10^{-3}$
550	$43.9 \times 10^{-3}$	0.6329	1040	$288.4 \times 10^{-7}$	$1.82 \times 10^{-3}$
600	$46.9 \times 10^{-3}$	0.5804	1051	$305.8 \times 10^{-7}$	$1.67 \times 10^{-3}$
650	$49.7 \times 10^{-3}$	0.5356	1063	$322.5 \times 10^{-7}$	$1.54 \times 10^{-3}$
700	$52.4 \times 10^{-3}$	0.4975	1075	$338.8 \times 10^{-7}$	$1.43 \times 10^{-3}$
750	$54.9 \times 10^{-3}$	0.4643	1087	$354.6 \times 10^{-7}$	$1.33 \times 10^{-3}$
800	$57.3 \times 10^{-3}$	0.4354	1099	$369.8 \times 10^{-7}$	$1.25 \times 10^{-3}$
850	$59.6 \times 10^{-3}$	0.4097	1110	$384.3 \times 10^{-7}$	$1.18 \times 10^{-3}$
900	$62.0 \times 10^{-3}$	0.3868	1121	$398.1 \times 10^{-7}$	$1.11 \times 10^{-3}$
950	$64.3 \times 10^{-3}$	0.3666	1131	$411.3 \times 10^{-7}$	$1.05 \times 10^{-3}$
1000	$66.7 \times 10^{-3}$	0.3482	1141	$424.4 \times 10^{-7}$	$1.00 \times 10^{-3}$
1100	$71.5 \times 10^{-3}$	0.3166	1159	$449.0 \times 10^{-7}$	$9.09 \times 10^{-4}$

Source: F. P. Incropera and D. P. DeWitt, *Fundamentals of Heat and Mass Transfer*, 2<sup>nd</sup> ed., John Wiley & Sons, New York, 1985.

During the NCT transient thermal analyses and the steady-state thermal analyses, the sides of the drum are modeled as a vertical flat plate using the following correlation:<sup>[5]</sup>

$$h = \left( \frac{k}{L} \right) \left[ C_3 + \frac{C_4 Ra^{C_5}}{\left( 1 + \left[ \frac{0.492}{Pr} \right]^{9/16} \right)^{C_6}} \right]^{C_7}, \quad (8)$$

where  $L$  = characteristic length = the drum height,  
 $C_3$  = constant (see Table 2),  
 $C_4$  = constant (see Table 2),  
 $C_5$  = constant (see Table 2),  
 $C_6$  = constant (see Table 2),  
 $C_7$  = constant (see Table 2), and  
 $Pr$  = Prandtl number  $[(C_p \times \mu)/k]$ .

The bottom of the drum is conservatively modeled as adiabatic during the NCT transient analyses and the steady-state analyses.

During the HAC 30-minute fire and the post-fire cool-down, the shipping container is assumed to be in a horizontal orientation (as it is during furnace testing). As such, the top and bottom of the drum are modeled as vertical flat plates using Eq. 8 having a characteristic length,  $L$ , equivalent to the drum diameter, and the sides of the drum are modeled as a horizontal cylinder using the following correlation:<sup>[5]</sup>

$$h = \left( \frac{k}{D} \right) C_8 Ra^{C_9}, \quad (9)$$

where  $D$  = diameter of the package,  
 $C_8$  = constant (see Table 2), and  
 $C_9$  = constant (see Table 2).

## Insolation

The following insolation (incident solar radiation) data is required for NCT per 10 CFR 71.71(c)(1):<sup>[1]</sup>

Form and location of surface	Total insolation for a 12-hour period (cal/cm <sup>2</sup> )
Flat surfaces transported horizontally	
Base	None
Other surfaces	800
Flat surfaces not transported horizontally	200
Curved surfaces	400

The total insolation values specified in the previous table are for a 12-hour period. For analytical purposes, these values are "time-averaged" over the entire 12-hour period (i.e., divided by 12).

Therefore, the incident solar heat fluxes ( $q''_{\text{solar},i}$ ) used in the analyses for NCT and cool-down following the HAC fire are as follows:

During NCT, the drum is in an upright (vertical) orientation; therefore, the following heat fluxes are applied to the external surfaces of the drum to represent insolation:

$$\text{Top} \quad q''_{\text{solar},i} = 775.3 \text{ W/m}^2, \quad (10)$$

$$\text{Sides} \quad q''_{\text{solar},i} = 387.7 \text{ W/m}^2, \quad (11)$$

$$\text{Bottom} \quad q''_{\text{solar},i} = 0. \quad (12)$$

During the cool-down period following the HAC 30-minute fire, the drum is assumed to be in a horizontal orientation; therefore, the following heat fluxes are applied to the external surfaces of the drum to represent insolation:

$$\text{Top} \quad q''_{\text{solar},i} = 193.83 \text{ W/m}^2, \quad (13)$$

$$\text{Sides} \quad q''_{\text{solar},i} = 387.7 \text{ W/m}^2, \quad (14)$$

$$\text{Bottom} \quad q''_{\text{solar},i} = 193.83 \text{ W/m}^2. \quad (15)$$

The insolation is applied as a square-wave function (i.e., alternating on and off in 12-hour periods) in the thermal analysis. The heat flux values presented in Eqs. 10–15 represent the insolation absorbed by the package surface since a drum absorptivity of 1.0 was conservatively assumed. An analytical study has been performed on a similar shipping package that investigated three methods of applying the insolation.<sup>[6]</sup> The three methods consisted of 1) performing a steady-state analysis assuming the insolation is applied continuously by distributing the heat flux evenly throughout a 24-hour period, 2) performing a transient analysis assuming the insolation is represented by a step function (i.e., applied and then not applied in 12-hour cycles, and 3) performing a transient analysis where the incident insolation is represented by a sinusoidal function that varies throughout the day. The results of the study indicate that the method used in applying the insolation has a significant effect on the temperatures of the outermost portions of the package. However, since the total insolation over any 24-hour period is the same for all cases, internal package temperatures are relatively unaffected by the way in which the insolation is applied. Since containment vessel O-ring temperatures are of primary concern in this report, the step function method for applying the insolation is suitable.

### Heat Transfer Across Gaps in the Package

Heat transfer across all gaps in the package is modeled by a combination of radiant exchange and conduction. Natural convection heat transfer is not included across the gaps in the model. Scoping studies performed for a similar shipping package indicate that the heat transfer due to natural convection in relatively small gaps is approximately a factor of 6 times less than the heat transfer due to radiant exchange.<sup>[6]</sup> These calculations assumed a temperature difference of 5°C across the gap. Based on these previous calculations, the effect of neglecting the natural convection in the gap regions is minimal. P/VIEWFACTOR<sup>[7]</sup> was used to calculate the view factors in all enclosures.

## Content Heat Load

In order to simulate the decay heat generated by the ES-3100 shipping container contents, a uniform heat flux is applied to the inner surfaces of the elements representing the containment vessel in the model. Content heat loads of 0.4, 20, and 30 W as well as no content heat load are investigated in this report. The uniform heat flux ( $q''_{\text{source}}$ ) for a given content heat load is calculated using the following equation:

$$q''_{\text{source}} = \frac{Q}{2\left(\frac{\pi D_i^2}{4}\right) + \pi(D_i)(H)}, \quad (16)$$

where  $Q$  = content heat load,  
 $D_i$  = inside diameter of the containment vessel (0.12802 m),  
 $H$  = height of the containment vessel cavity (0.78867 m).

Using Eq. 16, a content heat load of 0.4 W results in a uniform heat flux of 1.1664 W/m<sup>2</sup>, a content heat load of 20 W results in a uniform heat flux of 58.32 W/m<sup>2</sup>, and a content heat load of 30 W results in a uniform heat flux of 87.48 W/m<sup>2</sup>.

## DISCUSSION OF ANALYTICAL RESULTS

All thermal analyses discussed in this report were performed using MSC.Patran Thermal (2004 Version 12.0.044)<sup>[8]</sup> on an Intel Pentium 4-based Microsoft Windows 2000 computer. Temperatures are monitored at selected locations in the model as shown in Figure 2.

### Steady-state Conditions Analyses Results

Steady-state thermal analyses are performed on the finite element model of the ES-3100 shipping container for three cases having content heat loads of 0.4, 20, and 30 W. The temperature distribution results from these analyses are used as the starting temperature distribution within the model when performing the transient thermal analyses for NCT and the HAC 30-minute fire. The boundary conditions for these steady-state analyses include a combination of thermal radiation exchange and natural convection applied to the top and sides of the drum using an ambient temperature of 37.8°C (100°F). The bottom of the drum is modeled as an adiabatic surface (i.e., no heat transfer). Additionally, the content heat load is simulated by applying a uniform heat flux to the internal surfaces of the elements representing the containment vessel. The calculated steady-state temperature distribution with the model of the ES-3100 shipping container for content heat loads of 0.4, 20, and 30 W is presented in Table 4.

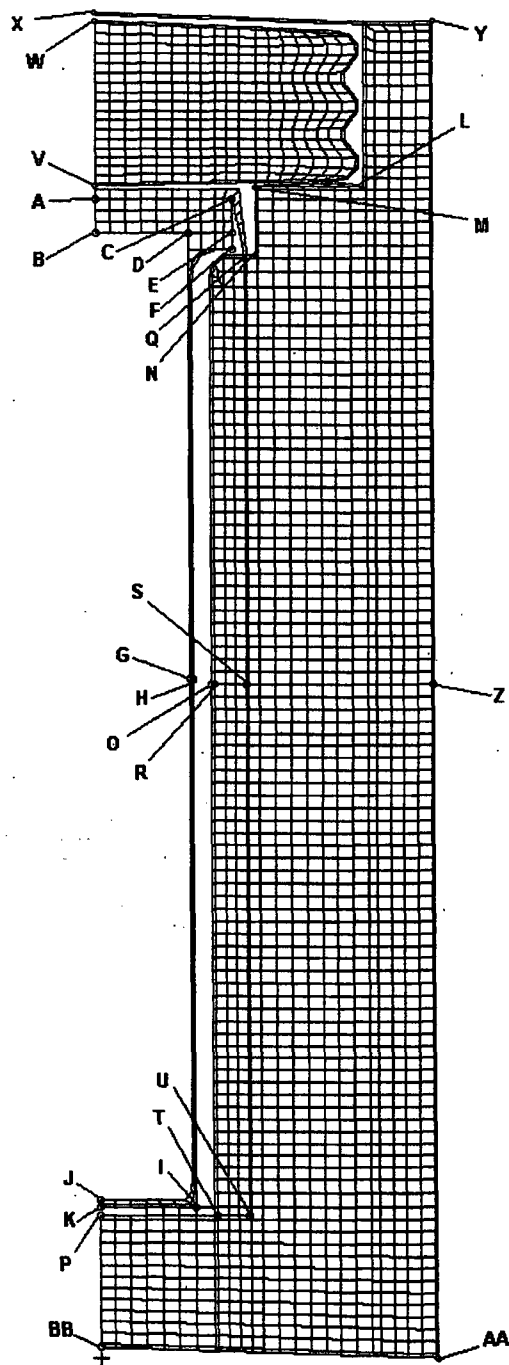


**Figure 2. MSC.Patran axisymmetric finite element model of the ES-3100 shipping container—nodal locations of interest (elements representing air not shown for clarity).**



**Table 4. ES-3100 shipping container steady-state temperatures (37.8°C ambient temperature, no insolation).**

Node <sup>(a)</sup>	Location	Steady-state temperature, °C (°F)		
		0.4 W	20 W	30 W
A	CV lid, top, center	38.09 (100.56)	56.06 (132.90)	64.65 (148.37)
B	CV lid, bottom, center	38.09 (100.56)	56.16 (133.08)	64.79 (148.63)
C	CV lid, top, outer	38.09 (100.55)	55.82 (132.47)	64.30 (147.73)
D	CV flange at interface, inner <sup>(b)</sup>	38.09 (100.57)	56.17 (133.10)	64.81 (148.66)
E	CV flange at interface, outer <sup>(b)</sup>	38.09 (100.56)	56.06 (132.90)	64.65 (148.37)
F	CV flange, bottom, outer	38.09 (100.56)	56.05 (132.88)	64.63 (148.34)
G	CV shell, mid-height, inner	38.36 (101.04)	69.36 (156.85)	83.91 (183.04)
H	CV shell, mid-height, outer	38.36 (101.04)	69.35 (156.83)	83.90 (183.01)
I	CV bottom, outer	38.18 (100.72)	59.56 (139.20)	69.97 (157.94)
J	CV bottom, center, inner	38.18 (100.72)	59.65 (139.38)	70.11 (158.20)
K	CV bottom, center, outer	38.18 (100.72)	59.64 (139.35)	70.09 (158.17)
L	Drum liner, plug cavity, outer	37.85 (100.13)	43.26 (109.87)	45.81 (114.46)
M	Drum liner, plug cavity, inner	37.91 (100.25)	46.93 (116.47)	51.29 (124.33)
N	Drum liner, CV flange cavity, outer	37.97 (100.34)	49.87 (121.77)	55.70 (132.26)
O	Drum liner, CV cavity, mid-height, inner	38.07 (100.52)	55.08 (131.15)	63.53 (146.36)
P	Drum liner, CV cavity, bottom, inner	38.12 (100.62)	56.87 (134.37)	66.02 (150.83)
Q	Borobond4, top, outer	37.97 (100.35)	50.31 (122.55)	56.35 (133.43)
R	Borobond4, mid-height, inner	38.07 (100.52)	55.08 (131.14)	63.53 (146.35)
S	Borobond4, mid-height, outer	38.12 (100.50)	54.45 (130.02)	62.59 (144.66)
T	Borobond4, bottom, inner	38.08 (100.55)	54.95 (130.91)	63.21 (145.79)
U	Borobond4, bottom, outer	38.07 (100.52)	54.16 (129.48)	62.05 (143.69)
V	Drum plug liner, bottom, center	37.82 (100.07)	41.36 (106.46)	42.96 (109.34)
W	Drum plug liner, top, center	37.98 (100.37)	50.51 (122.93)	56.59 (133.87)
X	Drum lid, top, center	37.79 (100.03)	39.82 (103.67)	40.67 (105.20)
Y	Drum lid, top, outer	37.79 (100.03)	40.08 (104.14)	41.06 (105.90)
Z	Drum, mid-height, outer	37.84 (100.11)	41.60 (106.88)	43.26 (109.86)
AA	Drum bottom, outer	37.85 (100.13)	41.94 (107.50)	43.76 (110.76)
BB	Drum bottom, center	37.91 (100.23)	45.14 (113.25)	48.51 (119.33)

Notes: (a) See Figure 2.

(b) Approximate location of the CV O-ring.

### Normal Conditions of Transport Analyses Results

Transient thermal analyses are performed on the finite element model of the ES-3100 shipping container to simulate NCT with content heat loads of 0, 0.4, 20, and 30 W. The insolation required for NCT per 10 CFR 71.71(c)(1)<sup>[1]</sup> is applied to the top and sides of the drum in alternating 12-hour periods (i.e., 12 hours on and 12 hours off) with the drum bottom remaining adiabatic during the transient thermal analysis. An ambient temperature of 37.8°C (100°F) as stipulated in 10 CFR 71 is used in the NCT analysis. The initial temperature distribution within the package for the NCT transients was determined from steady-state analyses (with radiation and natural convection boundary conditions applied to the top and sides of the drum) for each internal heat load. For the case with no internal heat source (0 W), the initial temperature distribution within the package was assumed to be at a uniform 37.8°C (100°F).

The transient thermal analyses simulate a five-day period of cyclic solar loading with 12 hours of insolation being applied at the beginning of each day (i.e., onset of sunrise) followed by 12 hours in which there is no insolation to end the day (i.e., onset of sunset). This five-day period allows for "quasi

steady-state" conditions to be reached. While the temperature of a particular node within the model changes with respect to time in the transient analyses, the maximum temperature that node reaches from day-to-day does not change once a "quasi steady-state" condition is reached. In particular, the maximum temperature of the key location on the containment vessel (i.e., at the O-ring) on day 5 is within 0.01°C of the maximum temperature of the same location on day 4.

The maximum temperatures of several locations within the model are summarized in Table 5 and Table 6 for content heat loads of 0, 0.4, 20, and 30 W and Kaolite densities of 30 (maximum density) and 19.4 lbm/ft<sup>3</sup> (minimum density), respectively. The maximum temperatures reported in Table 5 and Table 6 represent "quasi steady-state." Temperature-history plots of several locations within the model are also depicted graphically in Figure 3 through Figure 10 for various content heat loads and Kaolite density. Additionally, temperature contours of the model at sunrise (0 hours) and sunset (12 hours) for day 5 of the transient are presented in Figure 11 through Figure 18 for various content heat loads and Kaolite density. The elements representing the air between the drum liner and containment vessel and between the drum liner and top plug liner are not shown in the temperature contours presented in these figures so that the containment vessel temperature contours can be more easily viewed.

The maximum temperature in the model occurs at the top center of the drum lid. This maximum temperature is 118.01°C (244.42°F), 118.03°C (244.45°F), 118.77°C (245.79°F), and 119.15°C (246.47°F) for content heat loads of 0, 0.4, 20, and 30 W, respectively, and occurs at sunset in each case (see Table 6, Kaolite density of 19.4 lbm/ft<sup>3</sup>). The maximum temperature at the containment vessel O-ring is 88.25°C (190.84°F), 88.56°C (191.41°F), 103.87°C (218.96°F), and 111.42°C (232.55°F) for content heat loads of 0, 0.4, 20, and 30 W, respectively, and occurs at approximately 1 hour after sunset in each case (see Table 6, Kaolite density of 19.4 lbm/ft<sup>3</sup>).

**Table 5. Maximum “quasi steady-state” temperatures during NCT for the ES-3100 shipping container with various content heat loads (see Figure 2 for node locations)—Kaolite density of 30 lbm/ft<sup>3</sup>.**

Node <sup>(a)</sup>	Location	Maximum “quasi steady-state” temperature, °C (°F)			
		0 W	0.4 W	20 W	30 W
A	CV lid, top, center	86.56 (187.81)	86.88 (188.38)	102.98 (215.74)	109.59 (229.26)
B	CV lid, bottom, center	86.56 (187.80)	86.88 (188.38)	102.16 (215.90)	109.71 (229.47)
C	CV lid, top, outer	86.54 (187.78)	86.86 (188.34)	101.89 (215.41)	109.31 (228.75)
D	CV flange at interface, inner <sup>(b)</sup>	86.47 (187.64)	86.79 (188.21)	102.09 (215.77)	109.67 (229.40)
E	CV flange at interface, outer <sup>(b)</sup>	86.44 (187.59)	86.76 (188.16)	102.00 (215.61)	109.53 (229.15)
F	CV flange, bottom, outer	86.42 (187.56)	86.74 (188.13)	101.99 (215.58)	109.51 (229.12)
G	CV shell, mid-height, inner	81.52 (178.74)	82.09 (179.76)	109.01 (228.21)	121.98 (251.57)
H	CV shell, mid-height, outer	81.52 (178.74)	82.09 (179.76)	109.00 (228.19)	121.97 (251.55)
I	CV bottom, outer	81.32 (178.37)	81.71 (179.08)	100.57 (213.02)	109.99 (229.99)
J	CV bottom, center, inner	81.37 (178.47)	81.77 (179.18)	100.73 (213.31)	110.21 (230.38)
K	CV bottom, center, outer	81.37 (178.47)	81.77 (179.18)	100.72 (213.29)	110.19 (230.34)
L	Drum liner, plug cavity, outer	97.74 (207.93)	97.82 (208.07)	101.65 (214.96)	103.59 (218.47)
M	Drum liner, plug cavity, inner	92.91 (199.23)	93.06 (199.50)	100.40 (212.72)	104.13 (219.43)
N	Drum liner, CV flange cavity, outer	87.69 (189.84)	87.90 (190.21)	98.09 (208.57)	103.27 (217.43)
O	Drum liner, CV cavity, mid-height, inner	81.30 (178.35)	81.61 (178.90)	96.82 (206.27)	104.13 (219.43)
P	Drum liner, CV cavity, bottom, inner	81.52 (178.74)	81.86 (179.35)	98.30 (208.94)	106.56 (223.80)
Q	Borobond4, top, outer	87.36 (189.25)	87.58 (189.64)	98.19 (208.74)	103.57 (218.43)
R	Borobond4, mid-height, inner	81.30 (178.35)	81.61 (178.90)	98.81 (206.26)	104.58 (220.24)
S	Borobond4, mid-height, outer	81.37 (178.46)	81.66 (178.99)	96.24 (205.23)	103.69 (218.64)
T	Borobond4, bottom, inner	81.67 (179.01)	81.98 (179.56)	96.73 (206.12)	104.19 (219.55)
U	Borobond4, bottom, outer	81.78 (179.21)	82.07 (179.72)	96.11 (205.00)	103.23 (217.81)
V	Drum plug liner, bottom, center	111.30 (232.35)	111.34 (232.42)	113.25 (235.85)	114.21 (237.57)
W	Drum plug liner, top, center	90.70 (195.26)	90.92 (195.66)	101.53 (214.76)	106.87 (224.36)
X	Drum lid, top, center	117.74 (243.93)	117.75 (243.96)	118.50 (245.30)	118.88 (245.98)
Y	Drum lid, top, outer	107.04 (224.68)	107.06 (224.71)	107.94 (226.29)	108.39 (227.10)
Z	Drum, mid-height, outer	91.86 (197.36)	91.90 (197.41)	93.42 (200.15)	94.18 (201.53)
AA	Drum bottom, outer	91.00 (195.79)	91.04 (195.86)	92.92 (199.26)	93.87 (200.96)
BB	Drum bottom, center	87.21 (188.97)	87.31 (189.15)	92.26 (198.07)	94.74 (202.54)

Notes: (a) See Figure 2.  
(b) Approximate location of the CV O-ring.

**Table 6. Maximum “quasi steady-state” temperatures during NCT for the ES-3100 shipping container with various content heat loads (see Figure 2 for node locations)—Kaolite density of 19.4 lbm/ft<sup>3</sup>.**

Node <sup>(a)</sup>	Location	Maximum “quasi steady-state” temperature, °C (°F)			
		0 W	0.4 W	20 W	30 W
A	CV lid, top, center	88.30 (190.95)	88.62 (191.52)	103.84 (218.91)	111.35 (232.42)
B	CV lid, bottom, center	88.28 (190.90)	88.60 (191.48)	103.90 (219.03)	111.45 (232.62)
C	CV lid, top, outer	88.32 (190.97)	88.63 (191.54)	103.61 (218.50)	111.00 (231.80)
D	CV flange at interface, inner <sup>(b)</sup>	88.24 (190.83)	88.56 (191.41)	103.87 (218.96)	111.42 (232.55)
E	CV flange at interface, outer <sup>(b)</sup>	88.25 (190.84)	88.56 (191.41)	103.77 (218.78)	111.27 (232.28)
F	CV flange, bottom, outer	88.24 (190.82)	88.55 (191.39)	103.75 (218.75)	111.25 (232.24)
G	CV shell, mid-height, inner	83.04 (181.47)	83.61 (182.50)	110.50 (230.89)	123.46 (254.23)
H	CV shell, mid-height, outer	83.04 (181.47)	83.61 (182.50)	110.49 (230.88)	123.45 (254.21)
I	CV bottom, outer	83.36 (182.04)	83.75 (182.74)	102.58 (216.64)	111.99 (233.59)
J	CV bottom, center, inner	88.37 (182.07)	83.76 (182.77)	102.70 (216.86)	112.17 (233.91)
K	CV bottom, center, outer	88.37 (181.07)	83.76 (182.77)	102.69 (216.84)	112.15 (233.87)
L	Drum liner, plug cavity, outer	98.72 (209.70)	98.80 (209.85)	102.63 (216.73)	104.58 (220.24)
M	Drum liner, plug cavity, inner	94.43 (201.97)	94.58 (202.24)	101.92 (215.46)	105.65 (222.16)
N	Drum liner, CV flange cavity, outer	89.43 (192.97)	89.63 (193.34)	99.83 (211.70)	105.01 (221.02)
O	Drum liner, CV cavity, mid-height, inner	83.12 (181.62)	83.43 (182.18)	98.63 (209.54)	106.40 (223.52)
P	Drum liner, CV cavity, bottom, inner	83.62 (182.52)	83.96 (183.13)	100.36 (212.65)	108.60 (227.48)
Q	Borobond4, top, outer	88.82 (191.88)	89.04 (192.27)	99.65 (211.38)	105.04 (221.07)
R	Borobond4, mid-height, inner	83.12 (181.62)	83.43 (182.18)	98.63 (209.53)	106.39 (223.51)
S	Borobond4, mid-height, outer	83.03 (181.46)	83.33 (182.00)	97.91 (208.23)	105.36 (221.65)
T	Borobond4, bottom, inner	83.55 (182.39)	83.85 (182.93)	98.58 (209.45)	106.03 (222.86)
U	Borobond4, bottom, outer	83.51 (182.31)	83.80 (182.83)	97.82 (208.07)	104.90 (238.82)
V	Drum plug liner, bottom, center	112.01 (233.62)	112.05 (233.69)	113.95 (237.11)	114.90 (238.82)
W	Drum plug liner, top, center	92.09 (197.77)	92.31 (198.16)	102.93 (217.27)	108.26 (226.87)
X	Drum lid, top, center	118.01 (244.42)	118.03 (244.45)	118.77 (245.79)	119.15 (246.47)
Y	Drum lid, top, outer	107.33 (225.19)	107.34 (225.22)	108.22 (226.80)	108.67 (227.60)
Z	Drum, mid-height, outer	92.27 (198.08)	92.30 (198.14)	93.81 (200.86)	94.58 (202.24)
AA	Drum bottom, outer	91.70 (197.06)	91.74 (197.13)	93.61 (200.49)	94.54 (202.18)
BB	Drum bottom, center	88.82 (191.88)	88.93 (192.07)	93.84 (200.91)	96.30 (205.35)

Notes: (a) See Figure 2.  
(b) Approximate location of the CV O-ring.

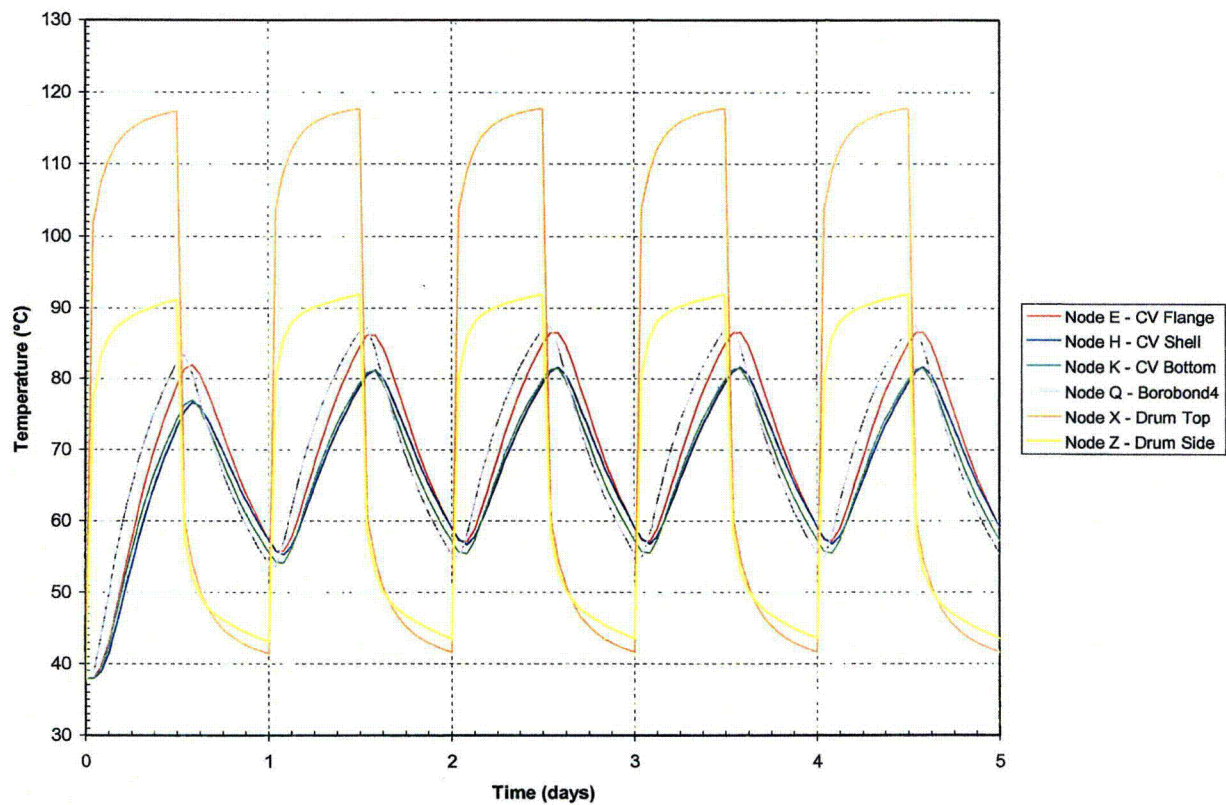


**Figure 3. Transient temperatures of the ES-3100 shipping container for NCT (no content heat load) Kaolite density of 30 lbm/ft<sup>3</sup> (see Figure 2 for node locations).**

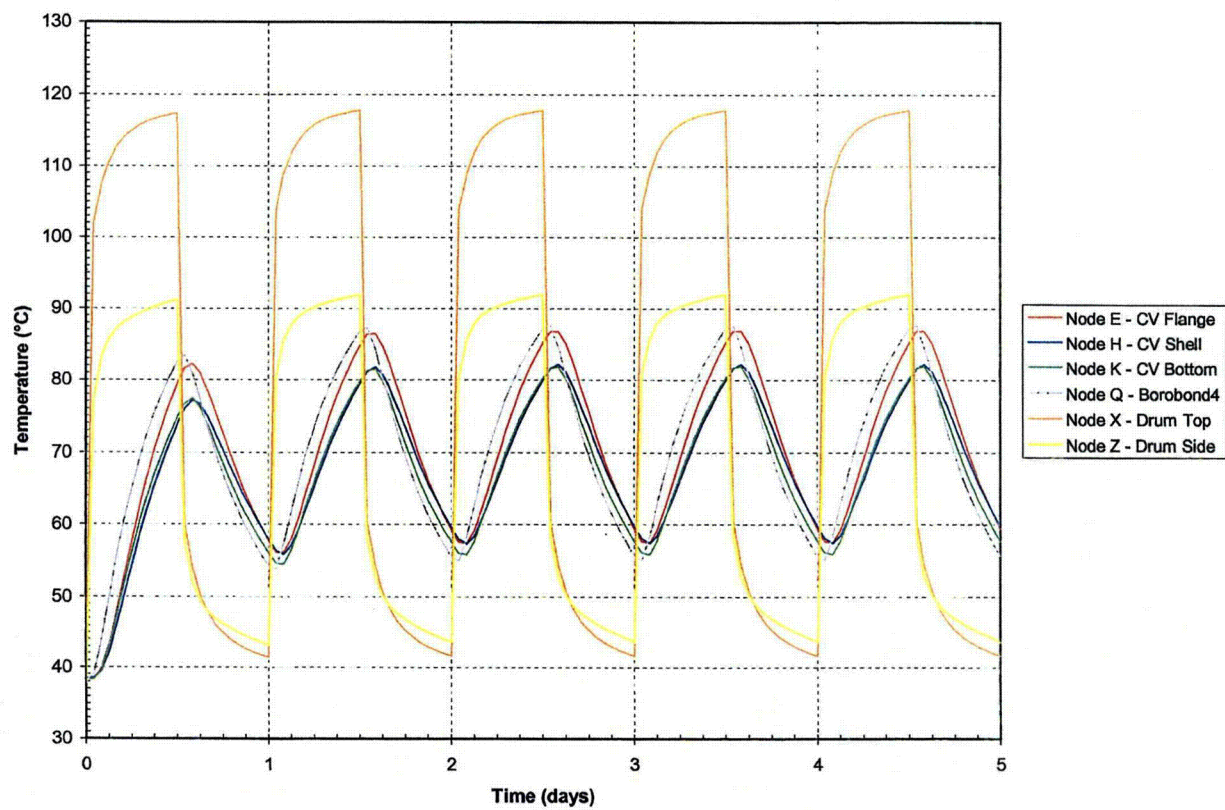


**Figure 4. Transient temperatures of the ES-3100 shipping container for NCT (0.4 W content heat load)  
Kaolite density of 30 lbm/ft<sup>3</sup> (see Figure 2 for node locations).**

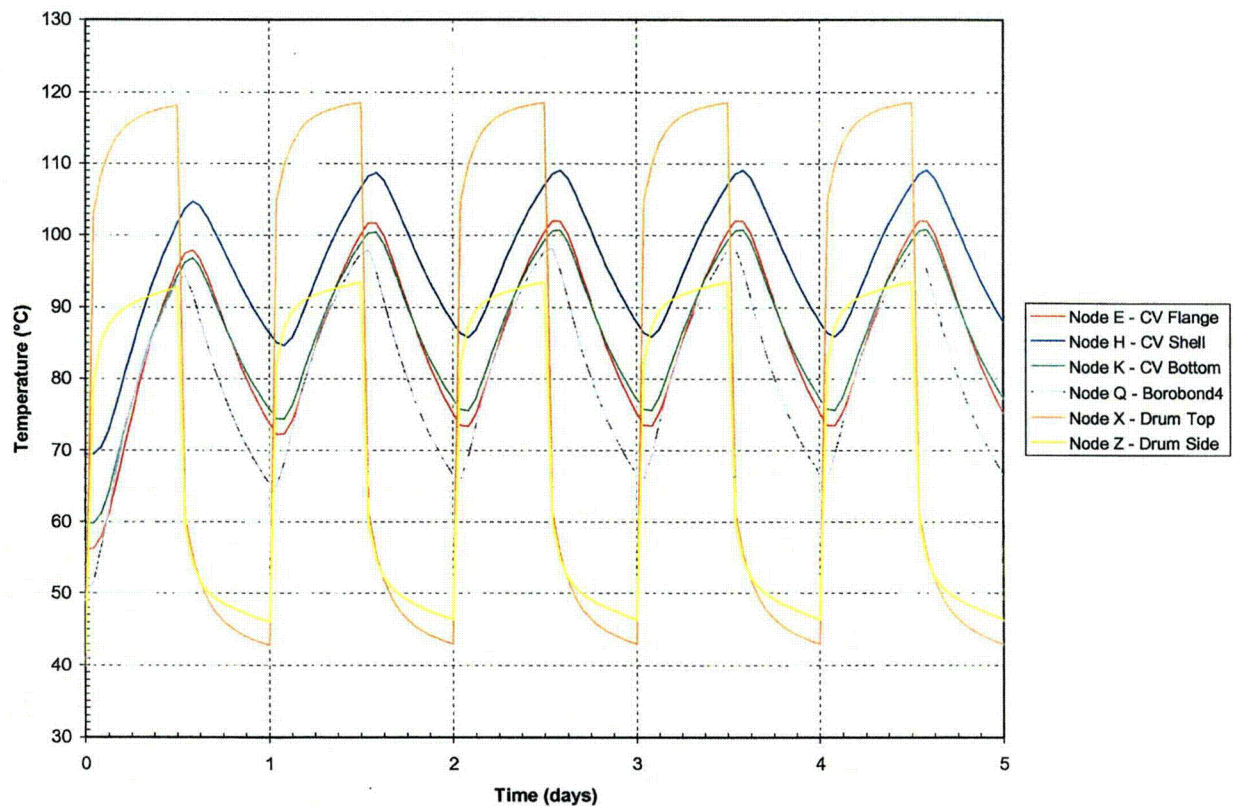


**Figure 5. Transient temperatures of the ES-3100 shipping container for NCT (20 W content heat load) Kaolite density of 30 lbm/ft<sup>3</sup> (see Figure 2 for node locations).**



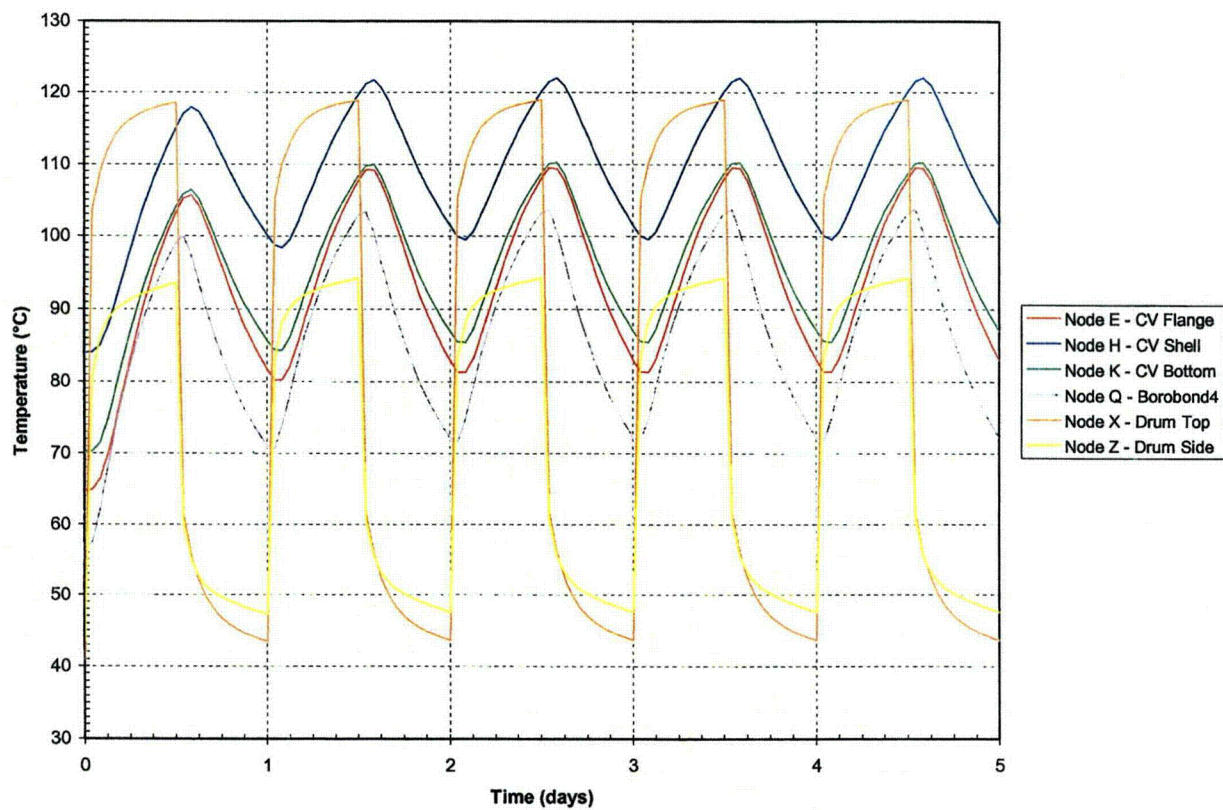


**Figure 6. Transient temperatures of the ES-3100 shipping container for NCT (30 W content heat load) Kaolite density of 30 lbm/ft<sup>3</sup> (see Figure 2 for node locations).**



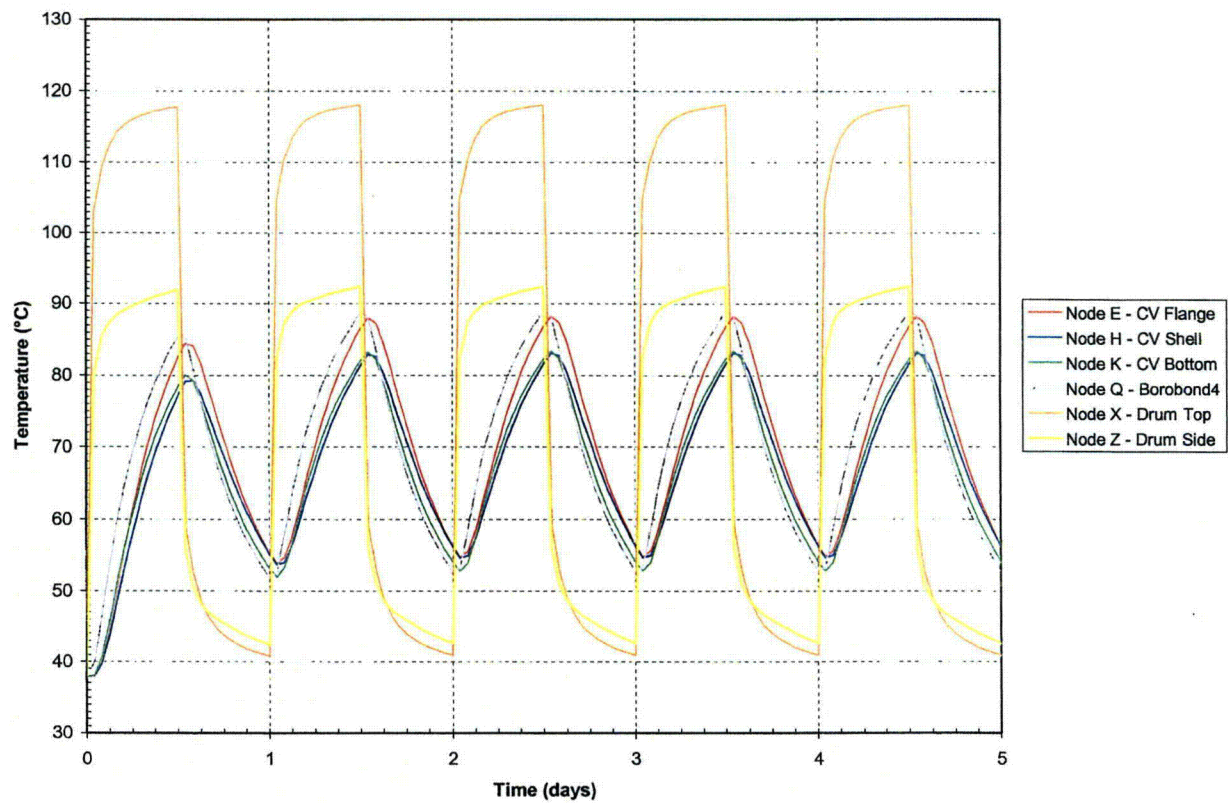


**Figure 7. Transient temperatures of the ES-3100 shipping container for NCT (no content heat load) Kaolite density of 19.4 lbm/ft<sup>3</sup> (see Figure 2 for node locations).**

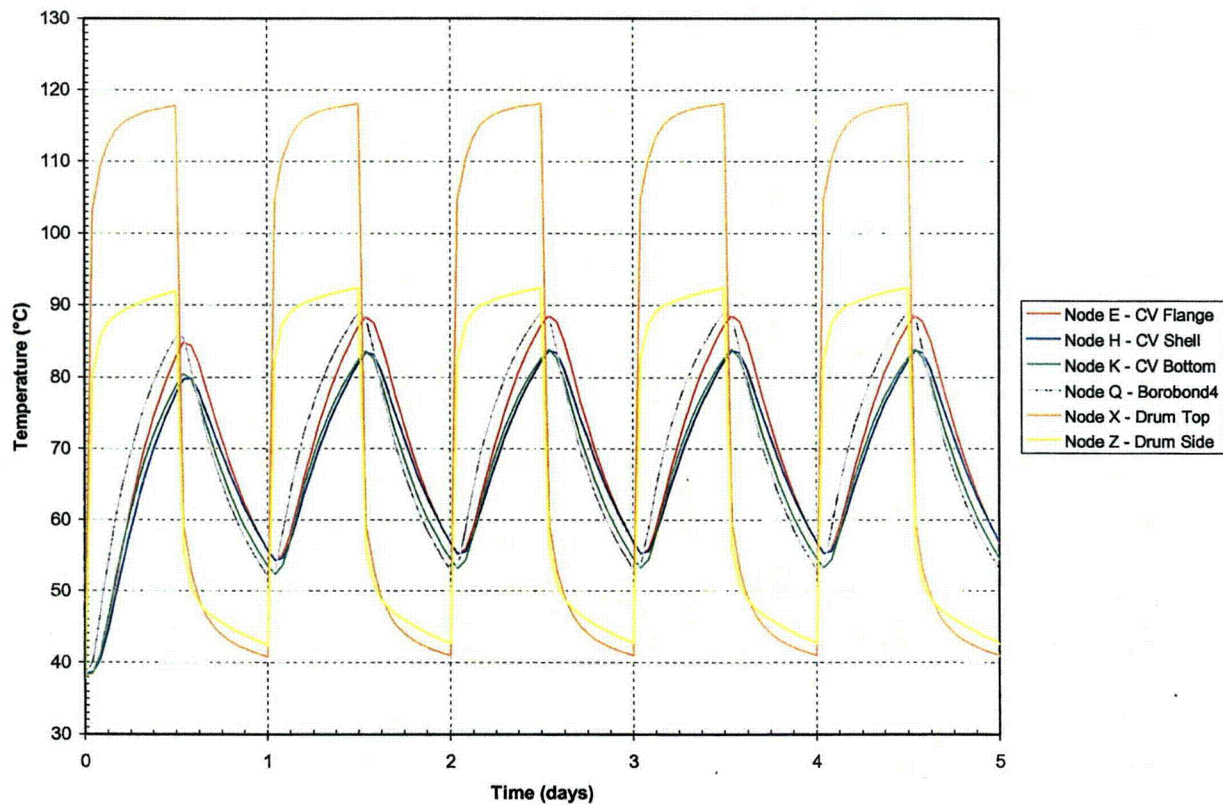


**Figure 8. Transient temperatures of the ES-3100 shipping container for NCT (0.4 W content heat load) Kaolite density of 19.4 lbm/ft<sup>3</sup> (see Figure 2 for node locations).**

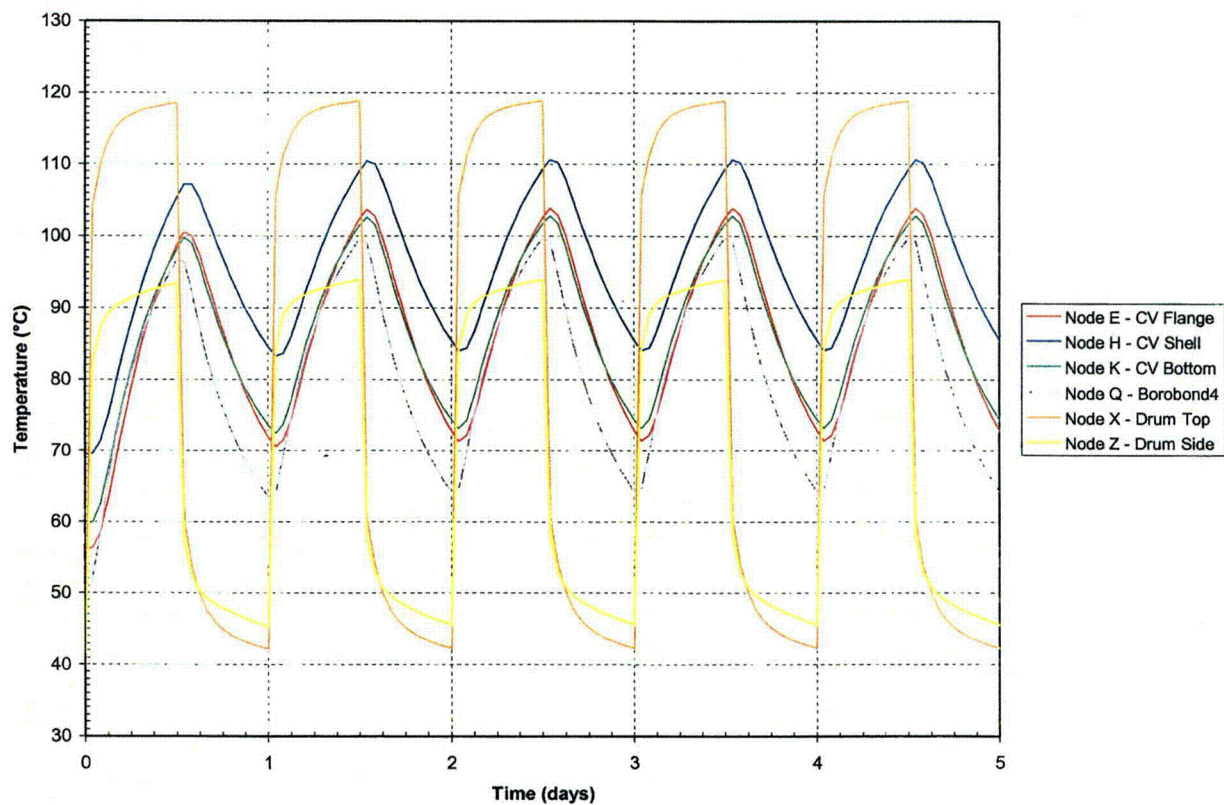


**Figure 9. Transient temperatures of the ES-3100 shipping container for NCT (20 W content heat load)  
Kaolite density of 19.4 lbm/ft<sup>3</sup> (see Figure 2 for node locations).**

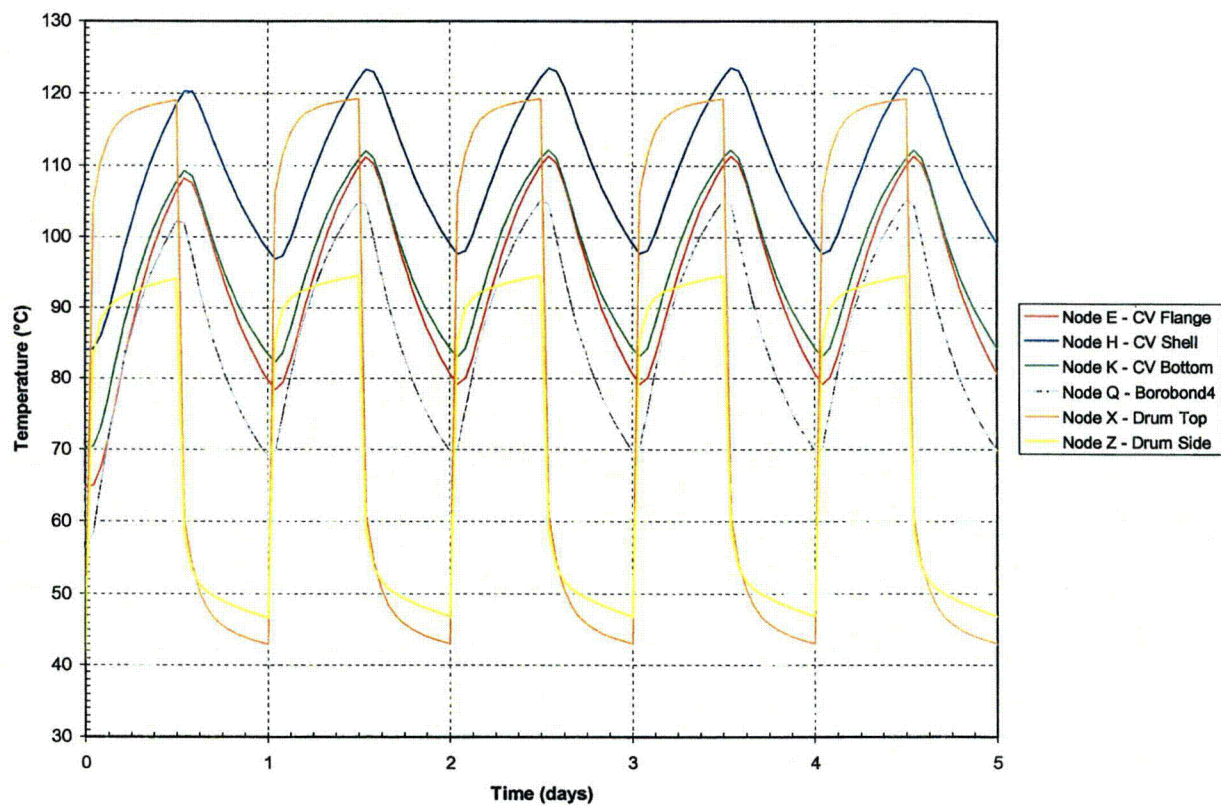


**Figure 10. Transient temperatures of the ES-3100 shipping container for NCT (30 W content heat load) Kaolite density of 19.4 lbm/ft<sup>3</sup> (see Figure 2 for node locations).**



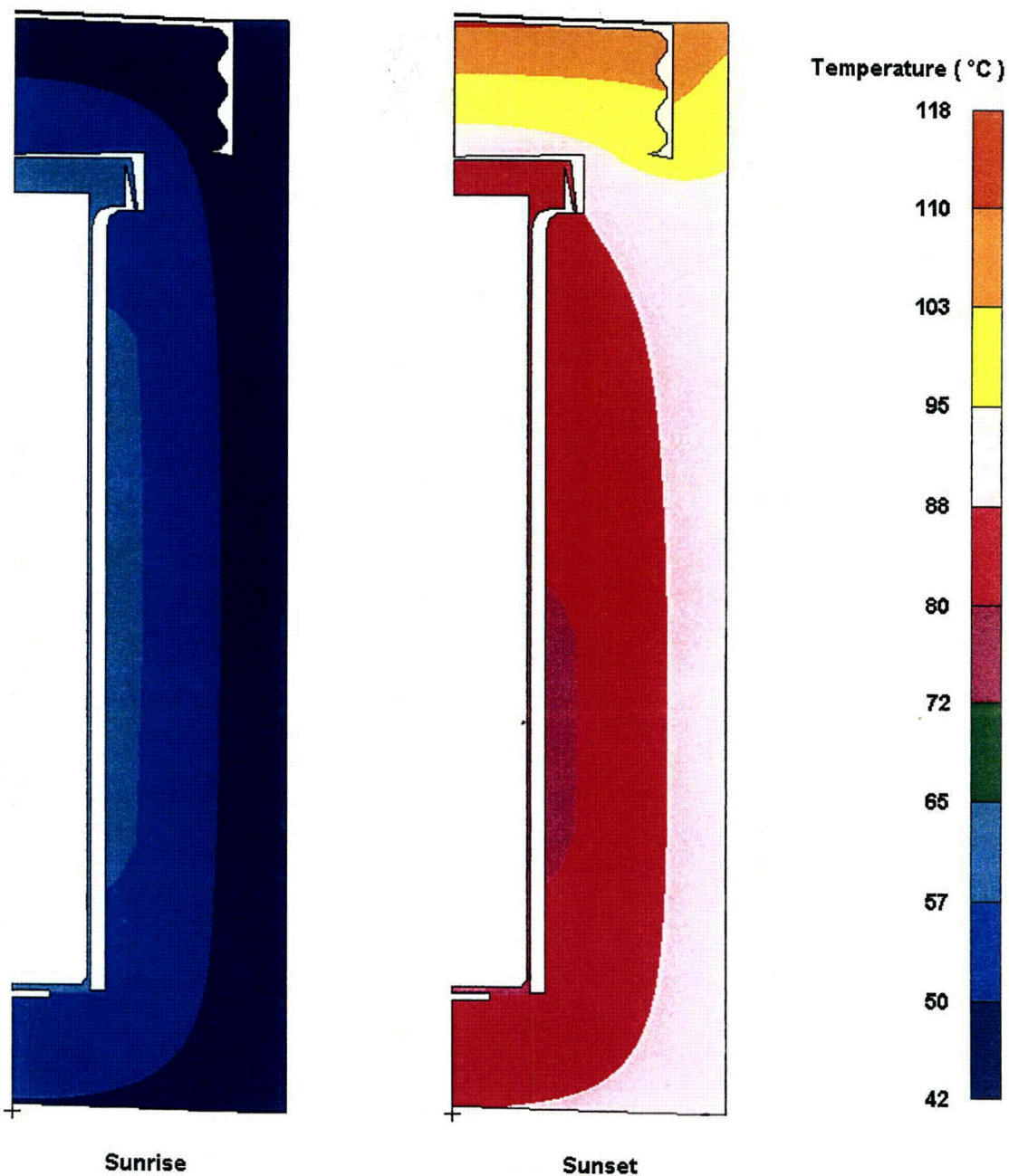


Figure 11. Temperature distribution in the ES-3100 shipping container for NCT (no content heat load)—Kaolite density of 30 lbm/ft<sup>3</sup>—day 5 of transient analysis (elements representing air not shown for clarity).

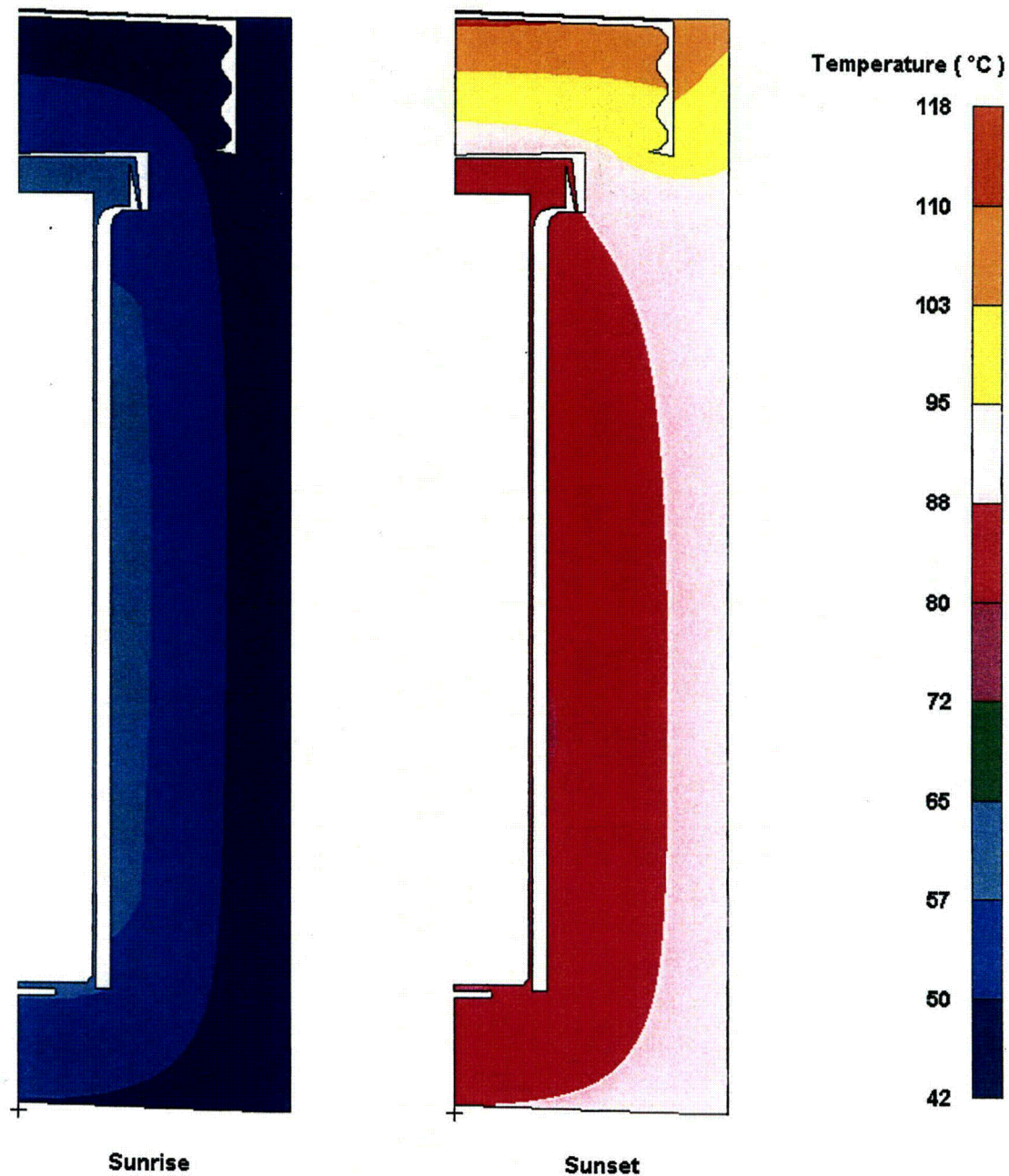


Figure 12. Temperature distribution in the ES-3100 shipping container for NCT (0.4 W content heat load)—Kaolite density of 30 lbm/ft<sup>3</sup>—day 5 of transient analysis (elements representing air not shown for clarity).



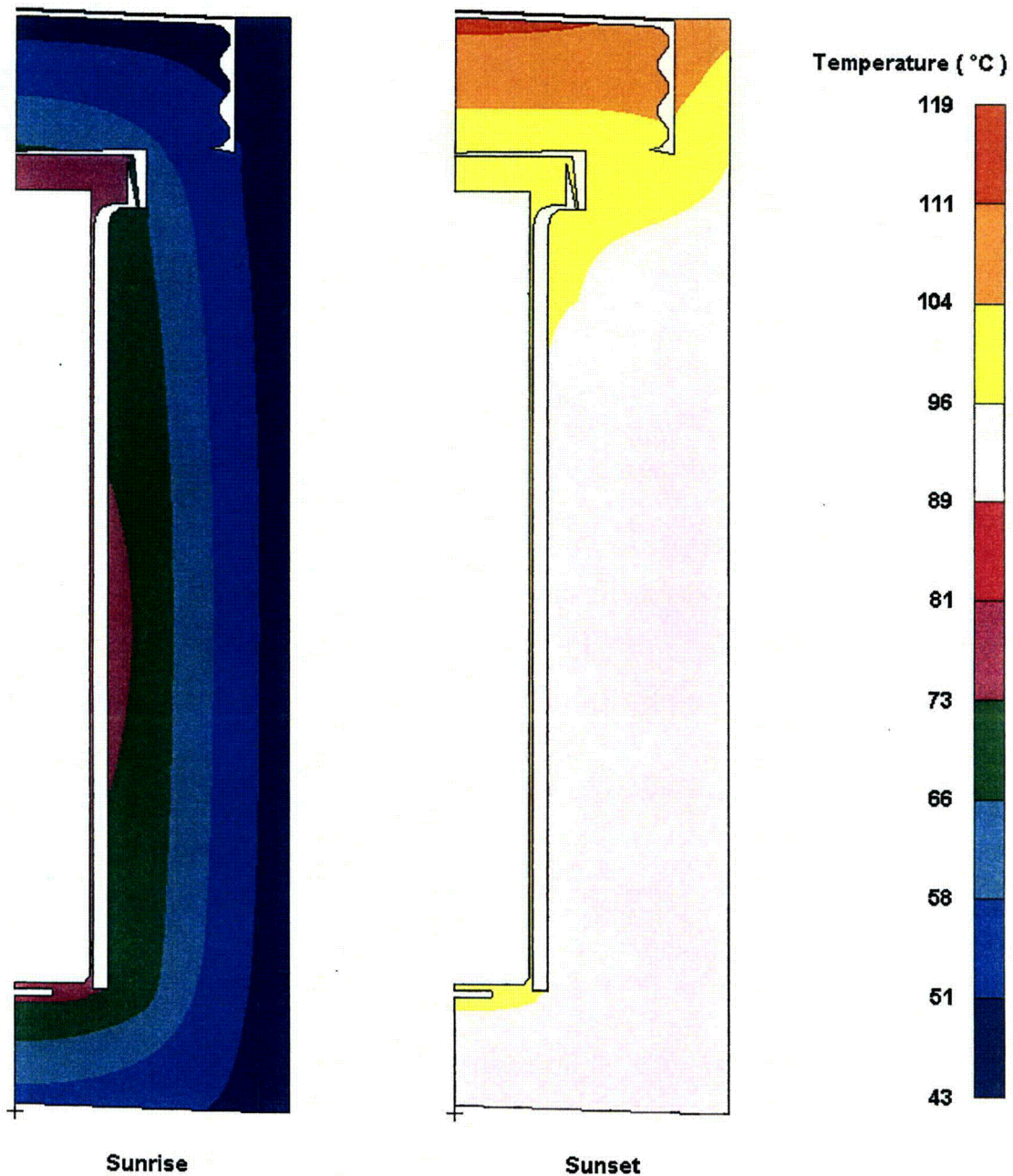
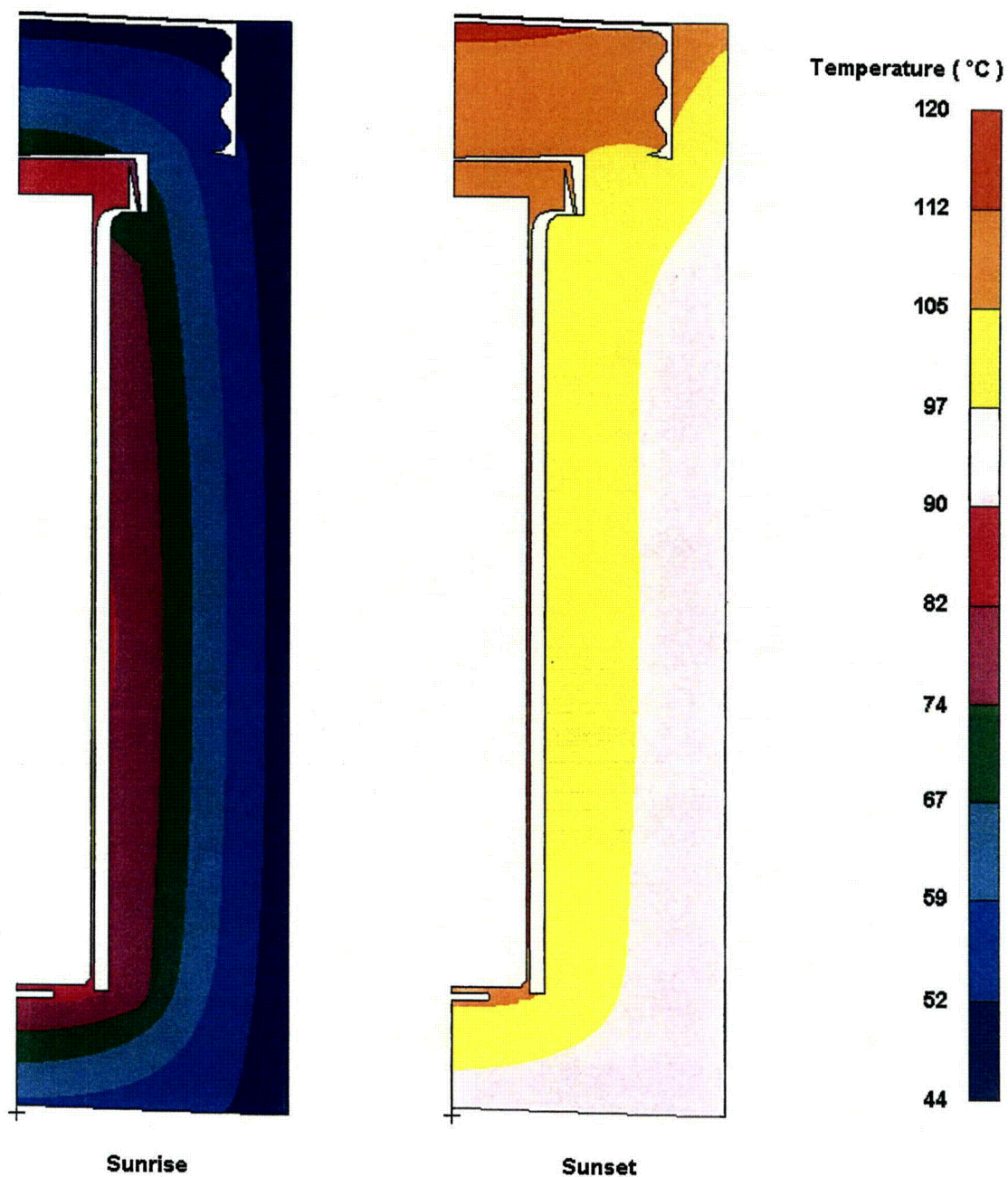


Figure 13. Temperature distribution in the ES-3100 shipping container for NCT (20 W content heat load)—Kaolite density of 30 lbm/ft<sup>3</sup>—day 5 of transient analysis (elements representing air not shown for clarity).



**Figure 14. Temperature distribution in the ES-3100 shipping container for NCT (30 W content heat load)—Kaolite density of 30 lbm/ft<sup>3</sup>—day 5 of transient analysis (elements representing air not shown for clarity).**



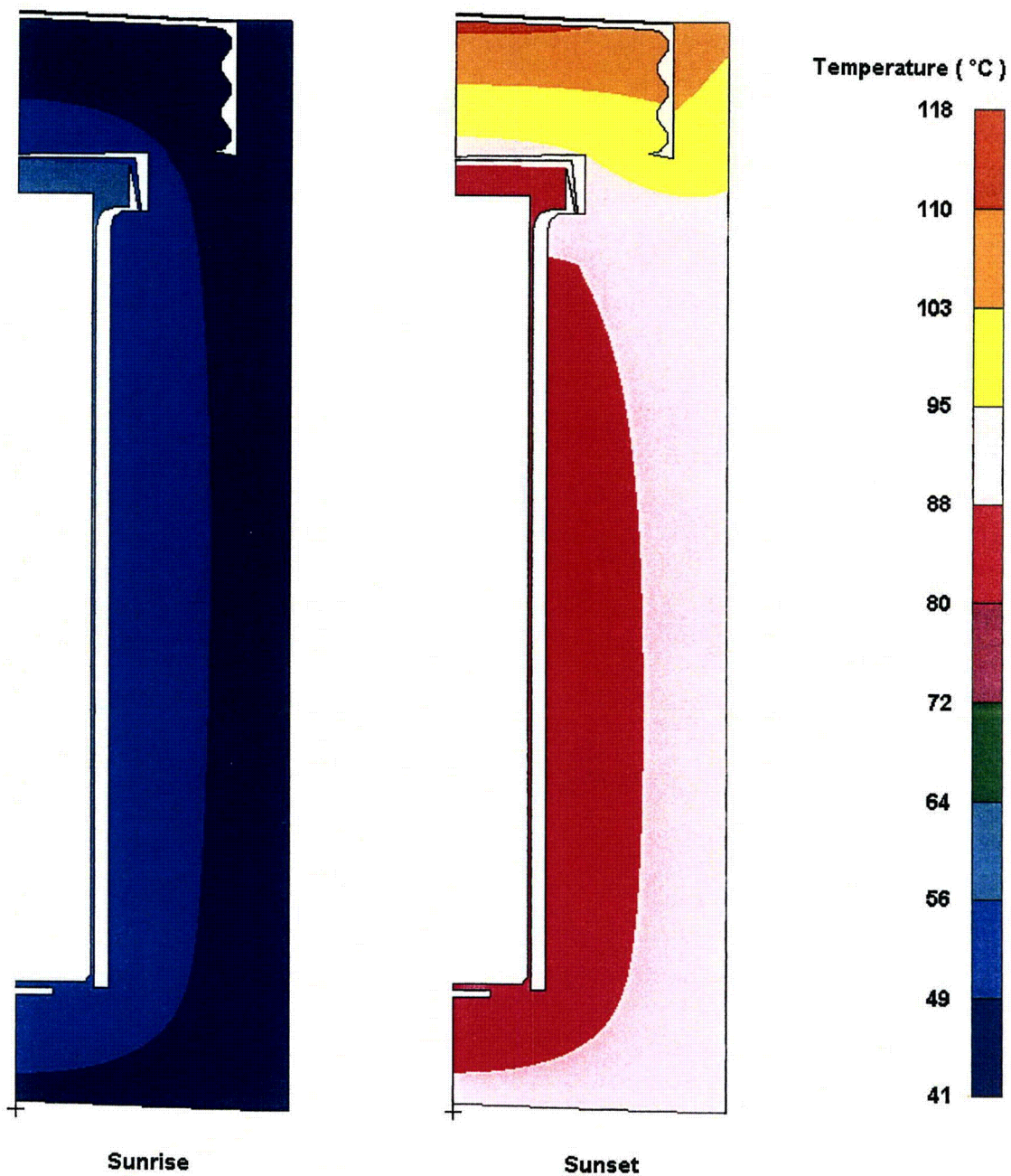


Figure 15. Temperature distribution in the ES-3100 shipping container for NCT (no content heat load)—Kaolite density of 19.4 lbm/ft<sup>3</sup>—day 5 of transient analysis (elements representing air not shown for clarity).

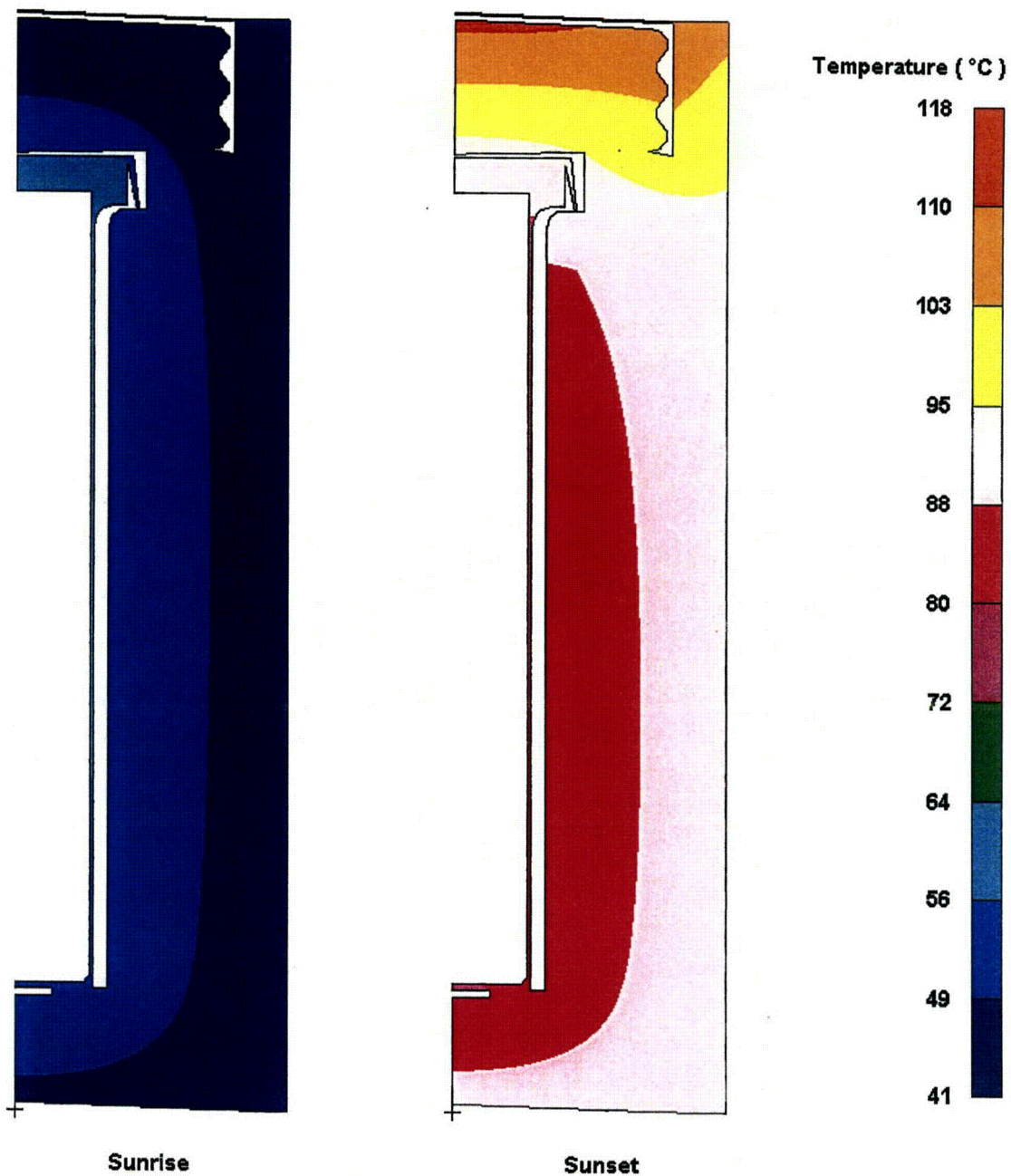


Figure 16. Temperature distribution in the ES-3100 shipping container for NCT (0.4 W content heat load)—Kaolite density of 19.4 lbm/ft<sup>3</sup>—day 5 of transient analysis (elements representing air not shown for clarity).

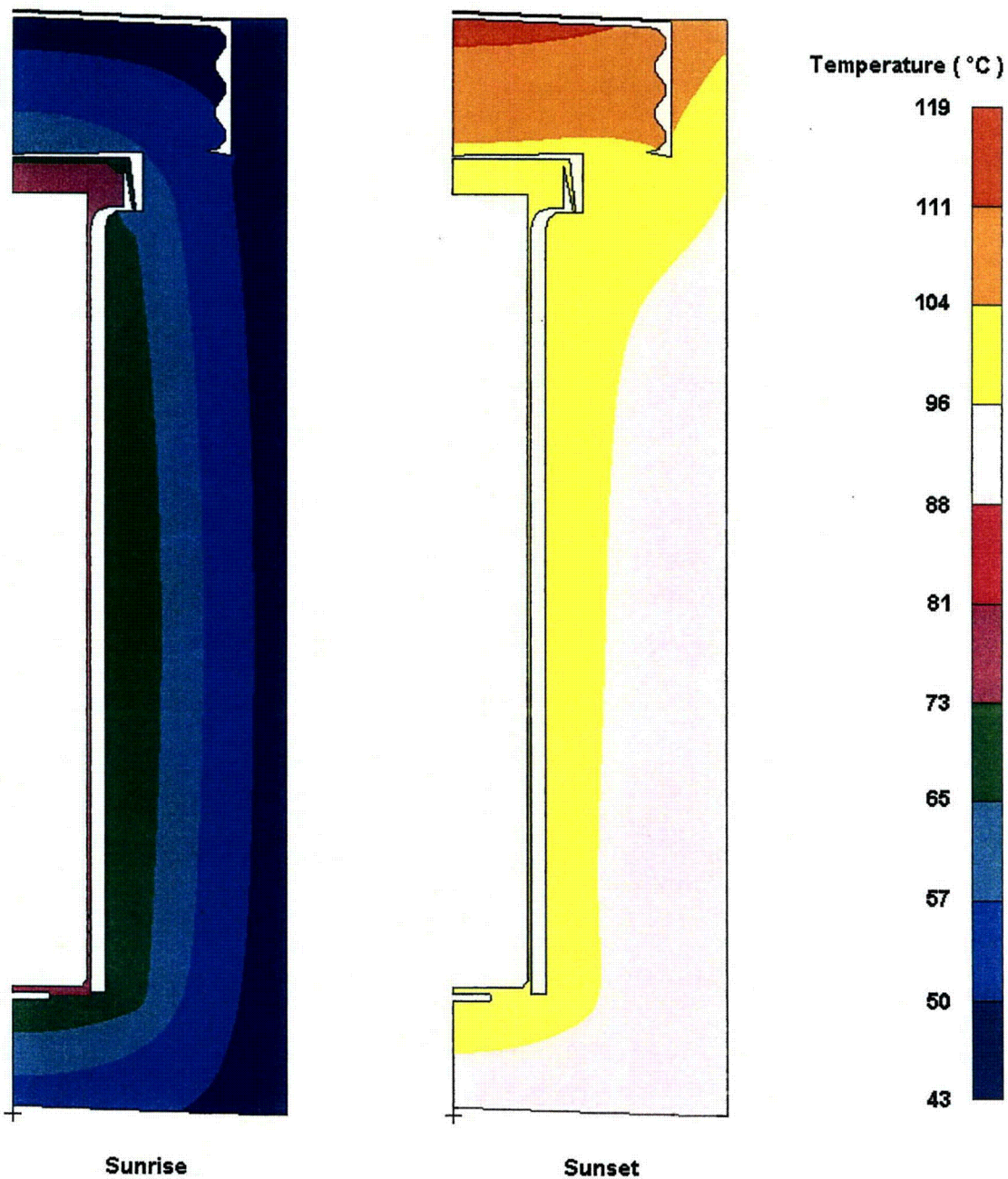


Figure 17. Temperature distribution in the ES-3100 shipping container for NCT (20 W content heat load)—Kaolite density of 19.4 lbm/ft<sup>3</sup>—day 5 of transient analysis (elements representing air not shown for clarity).



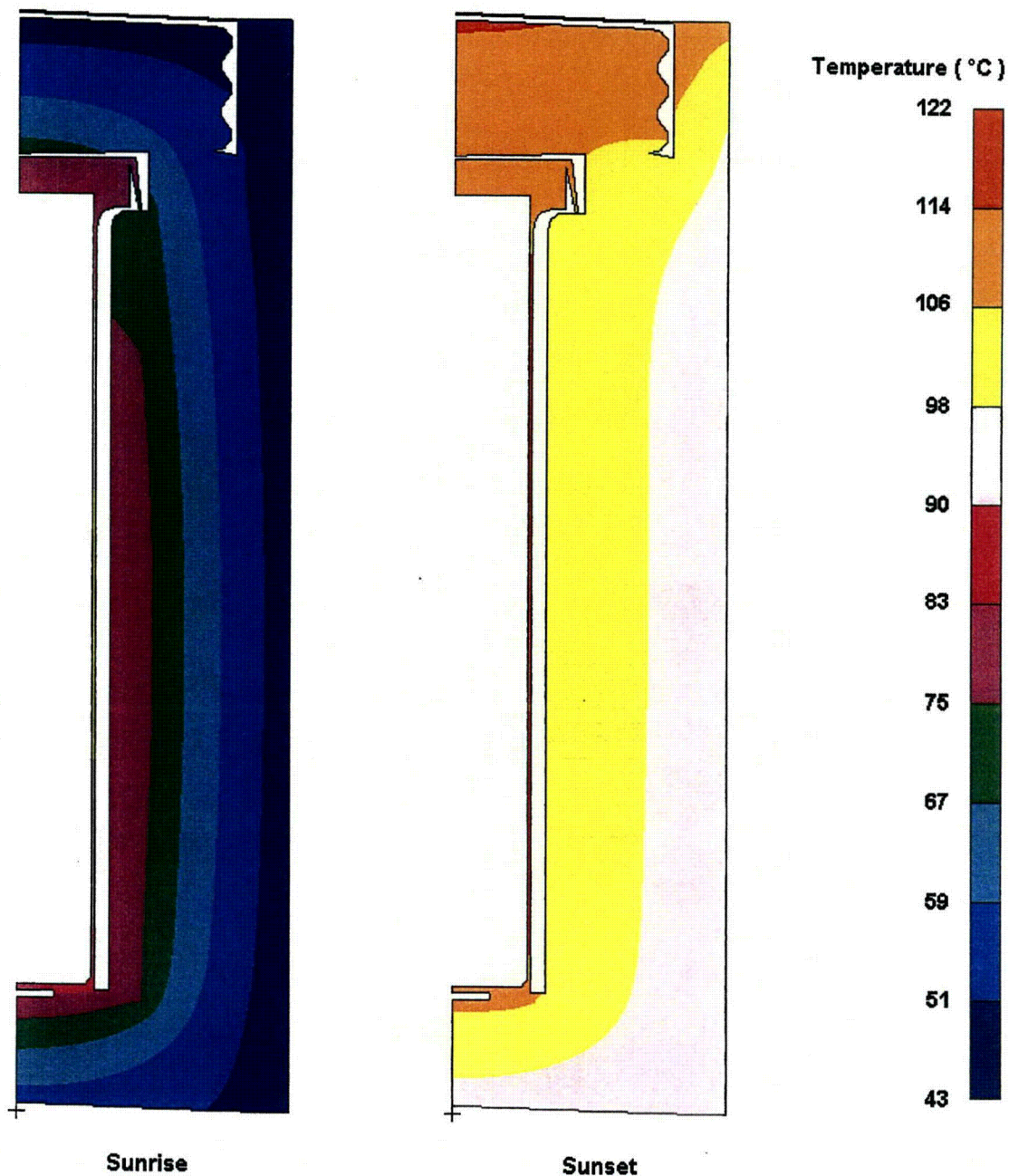


Figure 18. Temperature distribution in the ES-3100 shipping container for NCT (30 W content heat load)—Kaolite density of 19.4 lbm/ft<sup>3</sup>—day 5 of transient analysis (elements representing air not shown for clarity).

## Hypothetical Accident Conditions Analyses Results

Transient thermal analyses are performed on the finite element model of the ES-3100 shipping container (undamaged configuration) to simulate HAC as prescribed by 10 CFR 71.73(c)(4).<sup>[1]</sup> A 30-minute fire of 800°C (1472°F) is simulated by applying natural convection and radiant exchange boundary conditions to all external surfaces of the drum (assuming the drum is in a horizontal orientation) with content heat loads of 0, 0.4, 20, and 30 W and Kaolite densities of 30 (maximum density) and 19.4 lbm/ft<sup>3</sup> (minimum density). No heat flux boundary conditions simulating insolation are applied to the model during the 30-minute fire. The initial temperature distribution within the package having content heat loads of 0.4, 20, and 30 W is obtained from their respective steady-state analyses. The initial temperature distribution within the package having no content heat load (0 W) is assumed to be at a uniform temperature equal to the ambient temperature of 37.8°C (100°F).

Following the 30-minute fire transient analyses, 48-hour cool-down transient thermal analyses are performed using the temperature distribution at the end of the fire as the initial temperature distribution. During post-fire cool-down, natural convection and radiant exchange boundary conditions are applied to all external surfaces of the drum (assuming the drum is in a horizontal orientation). Additionally, cases are analyzed in which insolation is included during the post-fire cool-down. For the cases in which insolation is applied to the model during cool-down, insolation is applied during the first 12-hour period following the 30-minute fire, then alternated (off, then on) as was done for NCT.

The maximum temperatures calculated for the ES-3100 shipping container for HAC are summarized in Table 7 for the analyses using a Kaolite density of 30 lbm/ft<sup>3</sup> and Table 8 for the analyses using a Kaolite density of 19.4 lbm/ft<sup>3</sup>. Temperature-history plots of several locations within the model are also depicted graphically in Figure 19 through Figure 22 for content heat loads of 0, 0.4, 20, and 30 W and a Kaolite density of 19.4 lbm/ft<sup>3</sup> (the graphs for the cases having a Kaolite density of 30 lbm/ft<sup>3</sup> are not shown because of their similarity to the presented graphs).

**Table 7. ES-3100 shipping container HAC maximum temperatures—Kaolite density of 30 lbm/ft<sup>3</sup>.**

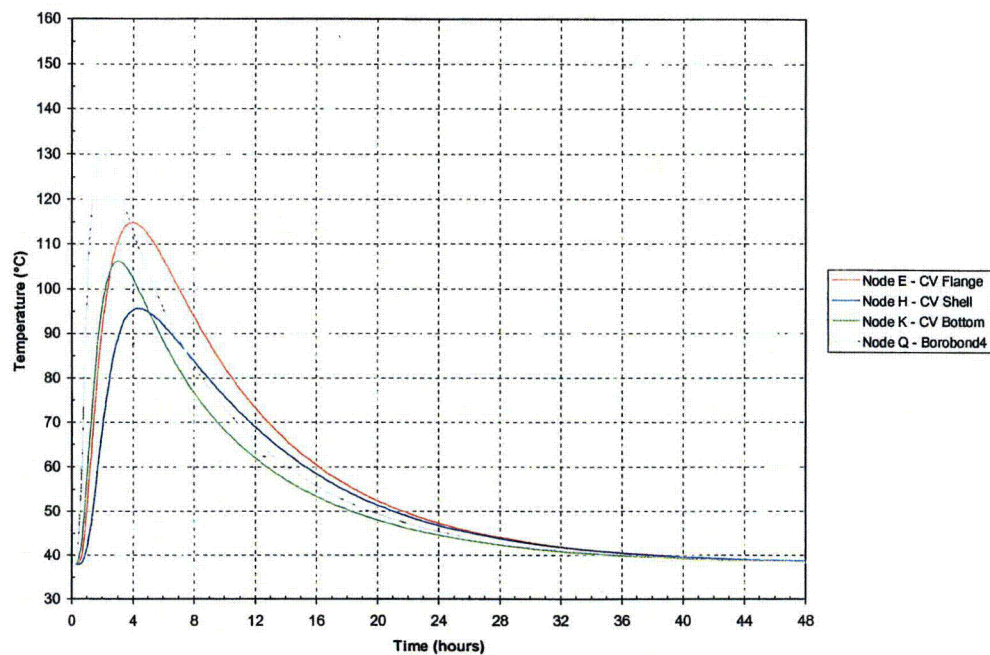
Content heat load (W)	Insolation during cool-down	Maximum temperature, °C (°F)						
		Node A <sup>(a)</sup> CV lid	Node E <sup>(a)</sup> CV flange at O-ring	Node H <sup>(a)</sup> CV shell (mid-elevation)	Node K <sup>(a)</sup> CV bottom (center)	Node Q <sup>(a)</sup> Borobond4 (top)	Node S <sup>(a)</sup> Borobond4 (mid-elevation)	Node T <sup>(a)</sup> Borobond4 (bottom)
0	No <sup>(b)</sup>	109.61 (229.29)	109.34 (228.81)	92.21 (197.98)	99.71 (211.47)	118.48 (245.26)	90.42 (194.76)	102.07 (215.73)
	Yes	116.91 (242.43)	116.74 (242.12)	104.22 (219.59)	106.13 (223.04)	122.46 (252.43)	103.28 (217.90)	107.63 (225.73)
0.4	No	109.93 (229.87)	109.66 (229.38)	92.78 (199.00)	100.11 (212.19)	118.69 (245.64)	90.73 (195.31)	102.38 (216.29)
	Yes	117.22 (243.00)	117.05 (242.68)	104.77 (220.58)	106.52 (223.74)	122.67 (252.81)	103.58 (218.45)	107.93 (226.28)
20	No	126.14 (259.05)	125.85 (258.53)	120.27 (248.48)	119.75 (247.56)	130.06 (266.11)	106.49 (223.67)	117.92 (244.25)
	Yes	133.07 (271.52)	132.85 (271.17)	131.38 (268.48)	125.90 (258.91)	134.05 (273.28)	118.96 (246.13)	123.31 (253.95)
30	No	134.00 (273.20)	133.69 (272.56)	133.41 (272.14)	129.43 (264.97)	135.69 (276.23)	114.38 (237.89)	125.62 (258.11)
	Yes	140.79 (285.42)	140.58 (285.05)	144.22 (291.59)	135.47 (275.85)	139.68 (283.42)	126.76 (260.17)	130.95 (267.71)

Notes: (a) See Figure 2 for node locations.  
(b) Baseline case for  $\Delta T$  comparisons.

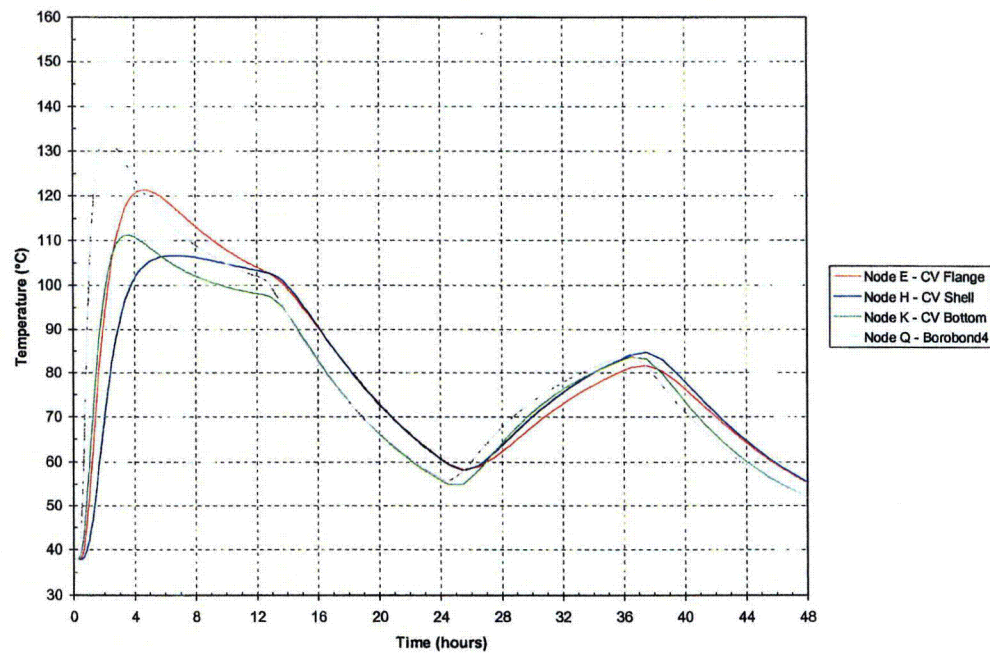
**Table 8. ES-3100 shipping container HAC maximum temperatures—Kaolite density of 19.4 lbm/ft<sup>3</sup>.**

Content heat load (W)	Insolation during cool-down	Maximum temperature, °C (°F)						
		Node A <sup>(a)</sup> CV lid	Node E <sup>(a)</sup> CV flange at O-ring	Node H <sup>(a)</sup> CV shell (mid-elevation)	Node K <sup>(a)</sup> CV bottom (center)	Node Q <sup>(a)</sup> Borobond4 (top)	Node S <sup>(a)</sup> Borobond4 (mid-elevation)	Node T <sup>(a)</sup> Borobond4 (bottom)
0	No <sup>(b)</sup>	114.95 (238.92)	114.69 (238.43)	95.48 (203.86)	105.98 (222.77)	129.89 (265.79)	93.95 (201.11)	109.65 (229.36)
	Yes	121.44 (250.60)	121.27 (250.28)	106.43 (223.58)	111.02 (231.83)	132.73 (270.92)	105.10 (221.19)	113.62 (236.51)
0.4	No	115.27 (239.49)	115.00 (239.00)	96.04 (204.87)	106.37 (223.47)	130.09 (266.17)	94.25 (201.65)	109.95 (229.91)
	Yes	121.75 (251.16)	121.58 (250.85)	106.97 (224.57)	111.41 (232.53)	132.94 (271.30)	105.41 (221.73)	113.92 (237.06)
20	No	131.51 (268.71)	131.22 (268.19)	123.43 (254.17)	126.00 (258.80)	141.29 (286.32)	109.98 (229.96)	125.44 (257.80)
	Yes	137.69 (279.84)	137.49 (279.48)	133.54 (272.37)	130.83 (267.49)	144.13 (291.44)	120.84 (249.51)	129.33 (264.79)
30	No	139.39 (282.90)	139.08 (282.25)	136.53 (277.75)	135.66 (276.19)	146.82 (296.28)	117.85 (244.14)	133.11 (271.60)
	Yes	145.45 (293.82)	145.24 (293.44)	146.35 (295.43)	140.42 (284.75)	149.67 (301.41)	128.65 (263.57)	136.97 (278.55)

Notes: (a) See Figure 2 for node locations.  
(b) Baseline case for  $\Delta T$  comparisons.



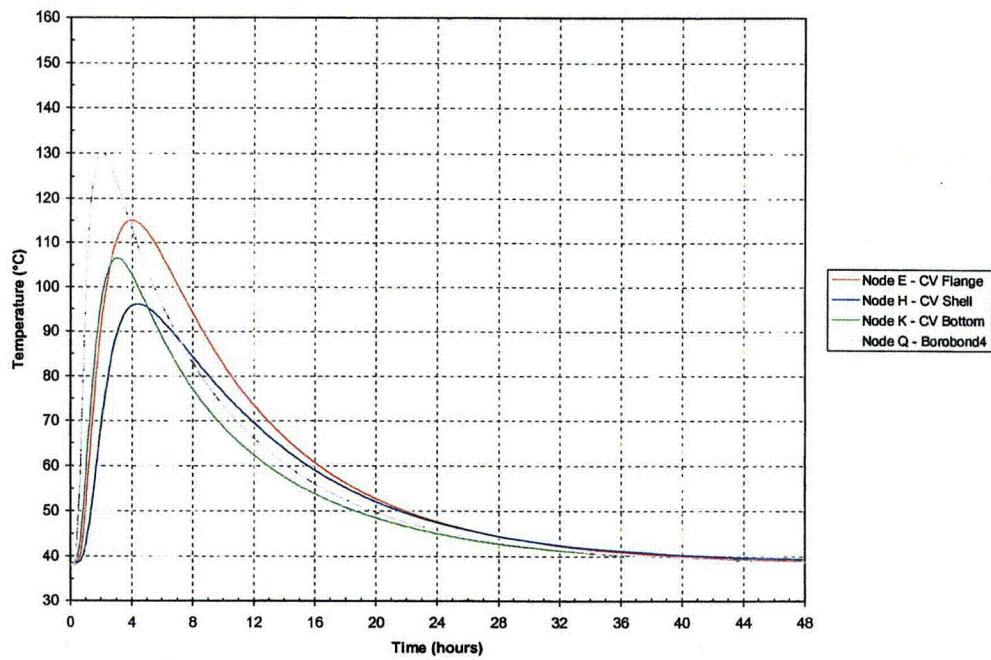
(a) No insolation during post-fire cool-down.



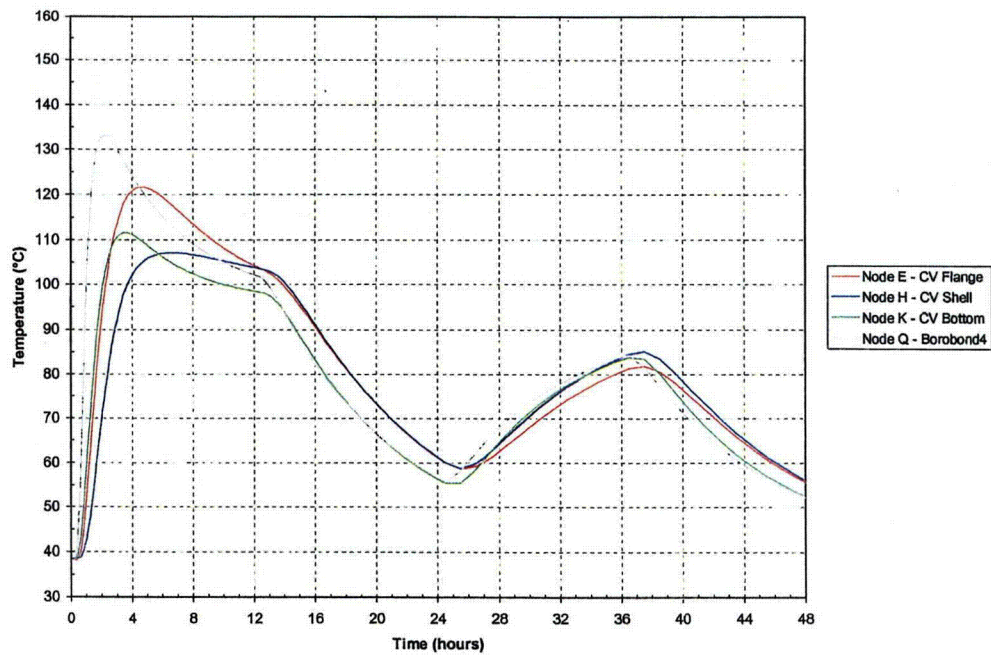
(b) Insolation during post-fire cool-down.

Figure 19. ES-3100 shipping container transient temperatures for HAC (no content heat load) Kaolite density of 19.4 lbm/ft<sup>3</sup> (see Figure 2 for node locations).





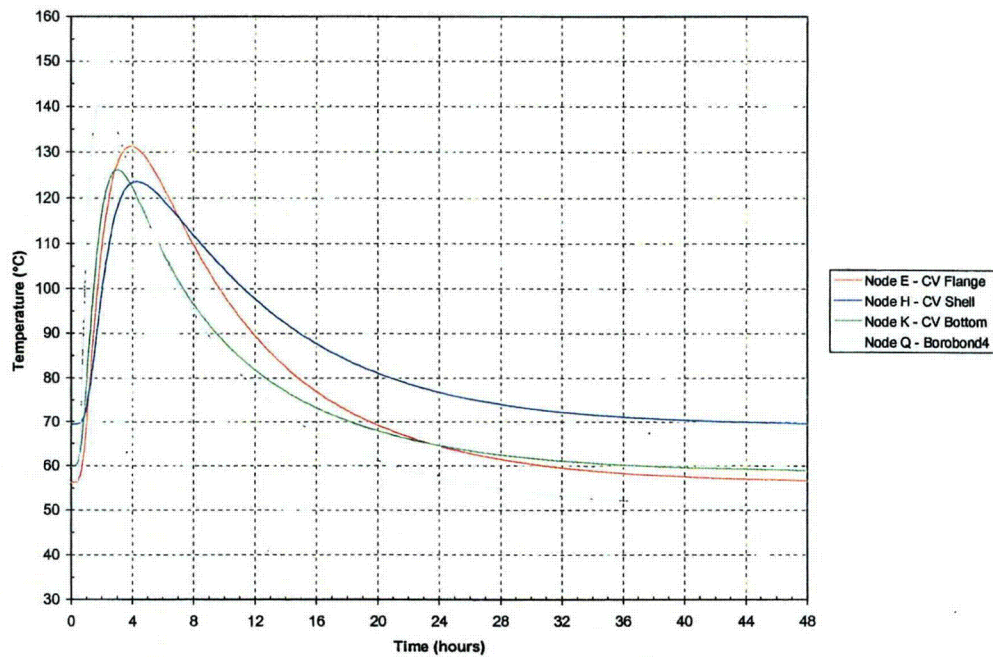
(a) No insolation during post-fire cool-down.



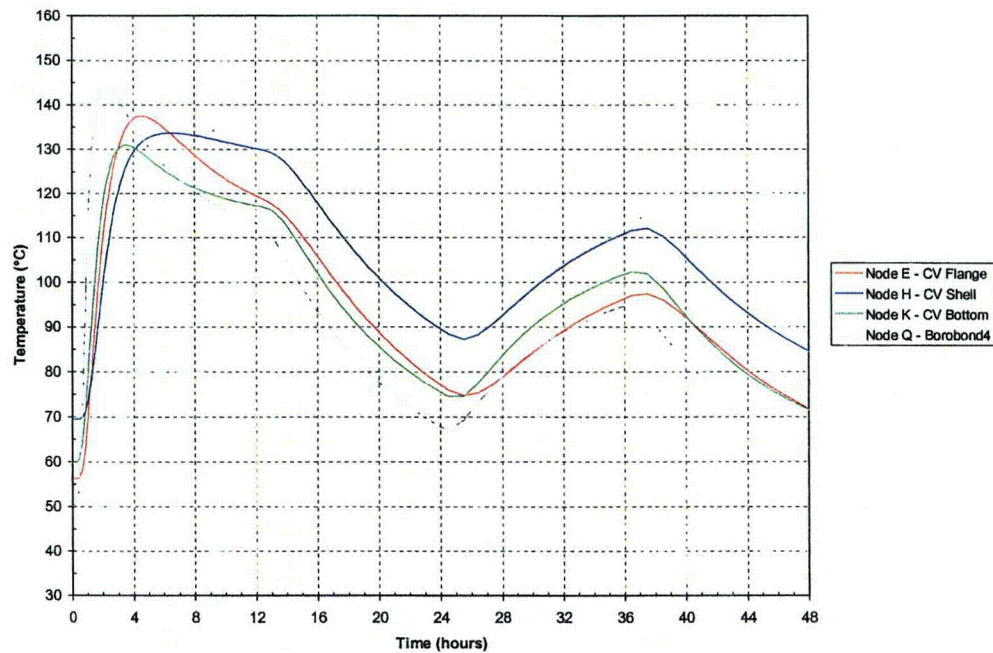
(b) Insolation during post-fire cool-down.

Figure 20. ES-3100 shipping container transient temperatures for HAC (0.4 W content heat load) Kaolite density of 19.4 lbm/ft<sup>3</sup> (see Figure 2 for node locations).



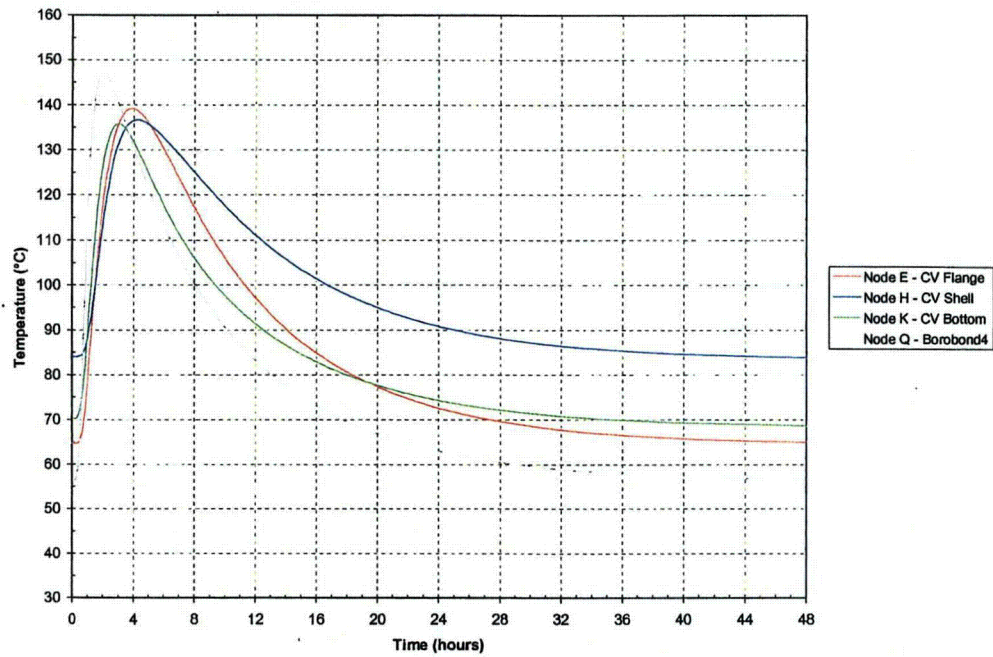


(a) No insulation during post-fire cool-down.

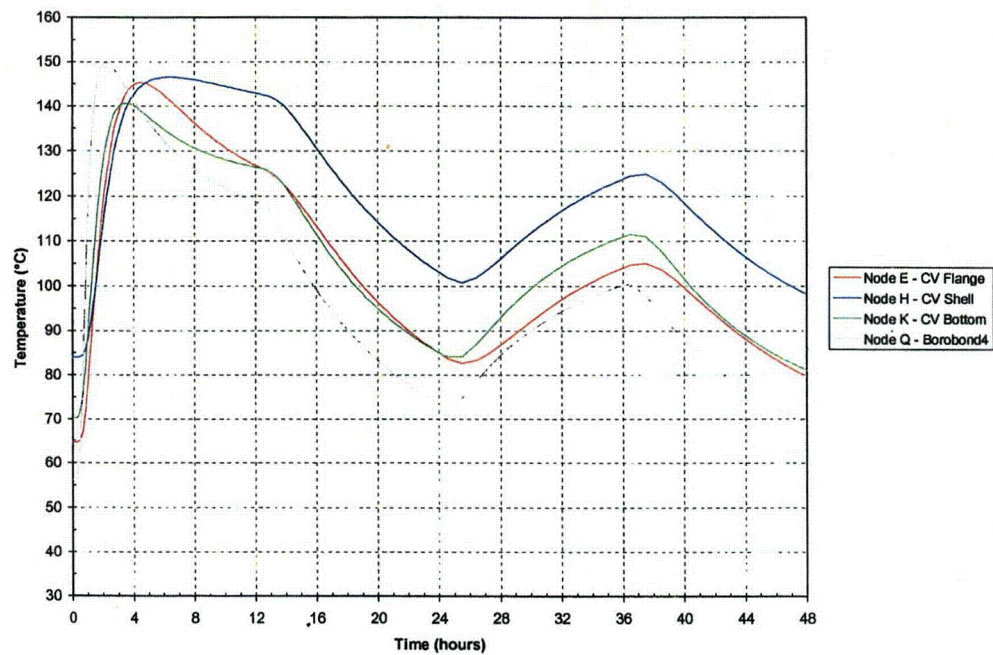


(b) Insulation during post-fire cool-down.

Figure 21. ES-3100 shipping container transient temperatures for HAC (20 W content heat load) Kaolite density of 19.4 lbm/ft<sup>3</sup> (see Figure 2 for node locations).



(a) No insolation during post-fire cool-down.



(b) Insolation during post-fire cool-down.

Figure 22. ES-3100 shipping container transient temperatures for HAC (30 W content heat load)  
Kaolite density of 19.4 lbm/ft<sup>3</sup> (see Figure 2 for node locations).

## APPENDIX 3.6.1 REFERENCES

1. *Packaging and Transportation of Radioactive Materials*, U.S. Nuclear Regulatory Commission, Code of Federal Regulations, Title 10 – Energy, Part 71, 2003.
2. MSC.Patran 2004 Version 12.0.044, MacNeal Schwendler Corporation, 2004.
3. R. Siegel and J. R. Howell, *Thermal Radiation Heat Transfer*, Second Edition, Hemisphere Publishing Corporation, 1981.
4. F. P. Incropera and D. P. DeWitt, *Fundamentals of Heat and Mass Transfer*, Second Edition, John Wiley & Sons, New York, 1985.
5. *MSC.Patran 2003, Thermal User's Guide Volume 1, Thermal/Hydraulic Analysis*, MSC.Software Corporation, Santa Ana, CA, 2003.
6. J. C. Anderson and M. R. Feldman, *Thermal Modeling of Packages for Normal Conditions of Transport with Insolation*, Proceedings of the ASME Heat Transfer Division, HTD-Vol. 317-2, 1995, International Mechanical Engineering Congress and Exposition, November 1995.
7. P/VIEWFACTOR, Version 12.0.044, MacNeal Schwendler Corporation, 2004.
8. MSC.Patran Thermal, Version 12.0.044, MacNeal Schwendler Corporation, 2004.



## **APPENDIX 3.6.2**

### **THERMAL EVALUATION OF THE ES-3100 SHIPPING CONTAINER FOR NCT AND HAC (FINAL DESIGN WITH CATALOG 277-4 NEUTRON ABSORBER)**



## APPENDIX 3.6.2

### THERMAL EVALUATION OF THE ES-3100 SHIPPING CONTAINER FOR NCT AND HAC (FINAL DESIGN WITH CATALOG 277-4 NEUTRON ABSORBER)

#### INTRODUCTION

Thermal analyses of the ES-3100 shipping container are performed to determine the temperature distribution within the packaging during Normal Conditions of Transport (NCT) as specified in 10 CFR 71.71(c)(1).<sup>[1]</sup> Transient thermal analyses are performed by treating the problem as a cyclic transient with the incident heat flux due to solar radiation applied and not applied in alternating 12-hour periods.

Additionally, thermal analyses of the ES-3100 shipping container are performed to determine the thermal response of the packaging to Hypothetical Accident Conditions (HAC) as specified in 10 CFR 71.73(c)(4).<sup>[1]</sup> Since physical testing of the ES-3100 shipping container was conducted with no internal heat source or insolation during cool-down,<sup>[2]</sup> temperature increases due to internal heat loads of 0.4, 20, and 30 W as well as temperature increases due to the application of insolation during cool-down following the HAC fire are calculated. Although earlier revisions of 10 CFR 71 specifically state that insolation does not need to be evaluated before, during, or after HAC, the current version of 10 CFR 71 and associated guidance are unclear regarding the need for consideration following HAC testing. Since the Nuclear Regulatory Commission (NRC) has taken the position that insolation must be considered and evaluated following fire testing, analyses are conducted to determine the effect of insolation following the HAC fire on the ES-3100 shipping container. The predicted temperature increases may be used to adjust physical test data for those loads not included in the physical tests.

#### FINITE ELEMENT MODEL DESCRIPTION

A two-dimensional axisymmetric finite element model of the ES-3100 shipping container is constructed using MSC.Patran<sup>[3]</sup> and imported as an orphaned mesh into ABAQUS/CAE<sup>[4]</sup> for application of boundary conditions, interactions, and loads. The model is constructed of DCAX4 (four-node linear axisymmetric heat transfer quadrilateral) and DCAX3 (3-node linear axisymmetric heat transfer triangular) elements for evaluation for NCT and HAC. The actual contents of the ES-3100 shipping container are not specifically modeled—instead, the content source heat load (if desired) is modeled by applying a uniform heat flux to the inner surfaces of the containment vessel. This is a conservative approach in that package temperatures will not be reduced in a transient analysis by the heat capacity of the contents. A schematic of the finite element model is presented in Figure 1 with details of the upper and lower portions of the model shown in Figure 2 and Figure 3, respectively. The model consists of five materials: stainless steel (drum, liners, and containment vessel), Kaolite, neutron absorber, silicone rubber, and air in the gaps between the drum liner and containment vessel and between the drum liner and top plug. Degree-of-freedom “ties” are made at the interfaces of the different material regions in order to allow the heat to flow through the model. Thermal properties of the materials used in the analysis are presented in Table 1.

Heat is transferred to the model from the contents (i.e., decay heat of the contents) via heat flux boundary conditions applied to the inner surface of the elements representing the containment vessel. Additionally, solar heat fluxes are applied to the model during NCT and HAC post-fire cool-down via heat flux boundary conditions. The heat applied to the model via the boundary conditions is transferred through the model via conduction and thermal radiation. Heat is rejected from the external surfaces of the model via natural convection and thermal radiation boundary conditions.



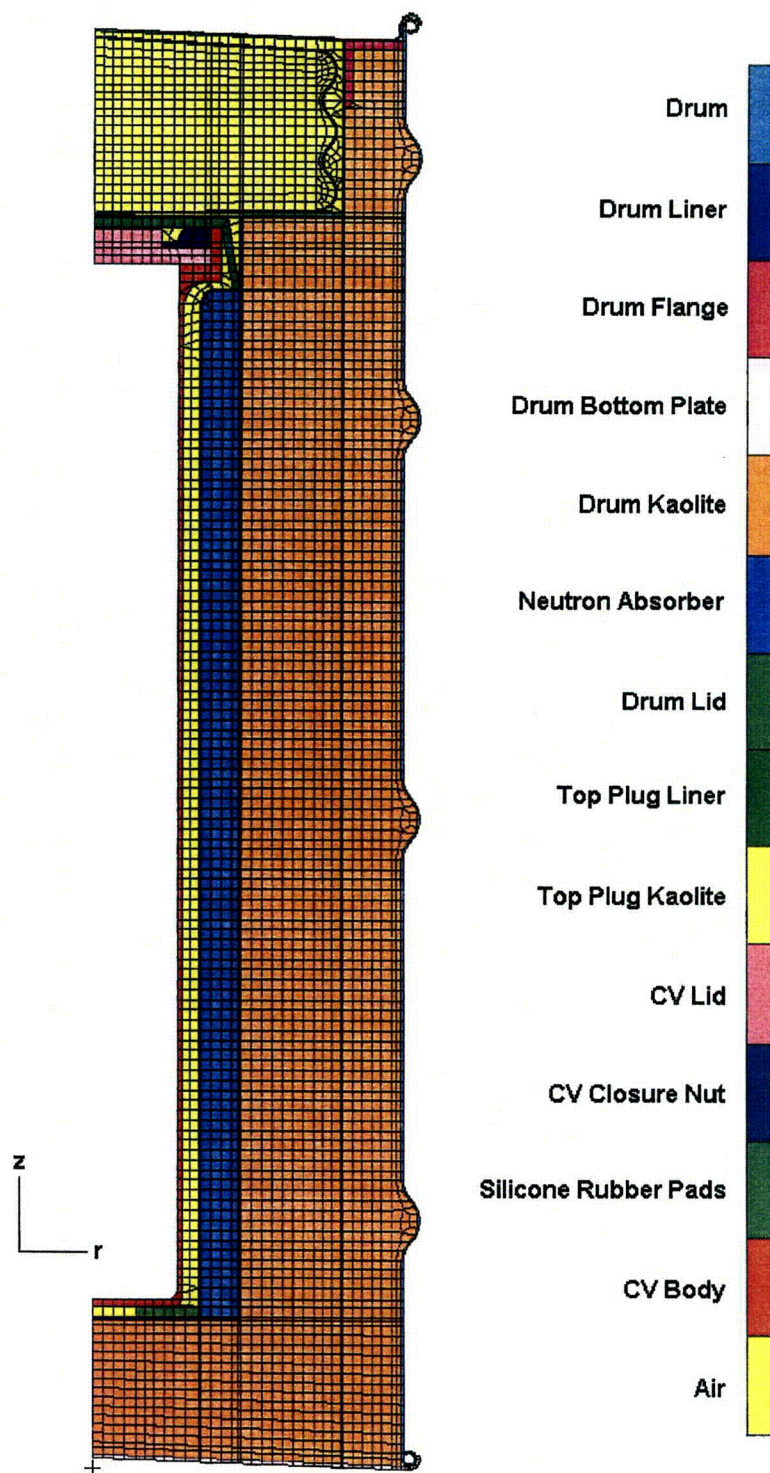


Figure 1. MSC.Patran axisymmetric finite element model of the ES-3100 shipping container.



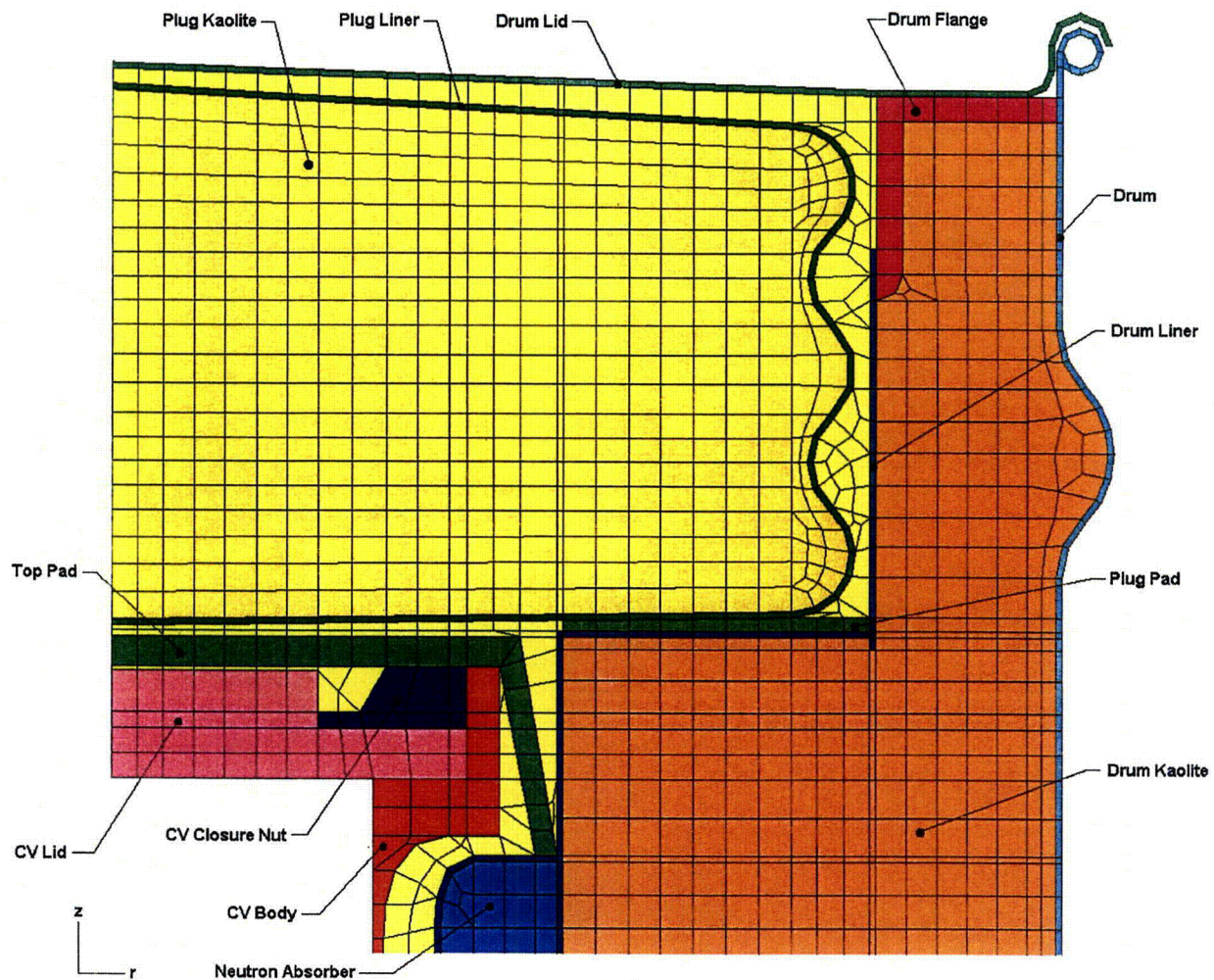
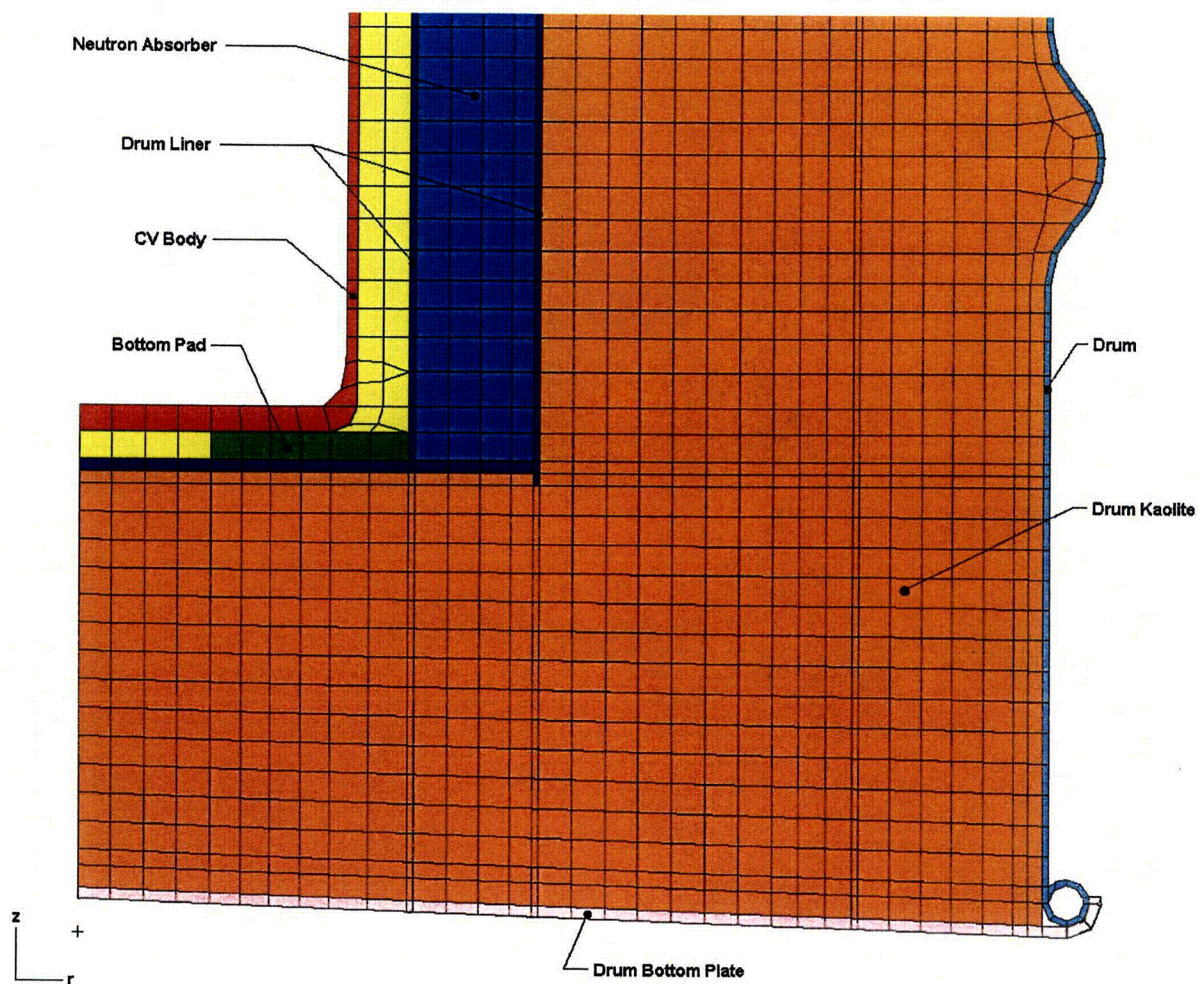


Figure 2. MSC.Patran axisymmetric finite element model of the ES-3100 shipping container (upper portion detail).



**Figure 3. MSC.Patran axisymmetric finite element model of the ES-3100 shipping container (lower portion detail).**



**Table 1. Thermal properties of the materials used in the thermal analyses.**

Material	Temperature (°F)	Thermal Conductivity (Btu/h-in.-°F)	Density (lbm/in. <sup>3</sup> )	Specific heat (Btu/lbm-°F)	Emissivity
Stainless steel	-279.67	0.443 <sup>(a)</sup>	0.285 <sup>(a)</sup>	0.065 <sup>(a)</sup>	0.22 <sup>(a)</sup>
	-99.67	0.607	—	0.096	—
	260.33	0.799	—	0.123	—
	620.33	0.953	—	0.133	—
	980.33	1.088	—	0.139	—
	1340.33	1.223	—	0.146	—
	1700.33	1.348	—	0.153	—
	2240.33	1.526	—	0.163	—
Kaolite 1600	68	0.0093 <sup>(b)</sup>	0.011 <sup>(c)</sup>	0.2 <sup>(d)</sup>	—
	212	0.0091	—	—	—
	392	0.0081	—	—	—
	572	0.0072	—	—	—
	1112	0.0082	—	—	—
Neutron absorber (Catalog No. 277-4)	-31	0.0457 <sup>(e)</sup>	0.0579 <sup>(f)</sup>	0.125 <sup>(g)</sup>	—
	73.4	0.0485	—	0.186	—
	140	0.0400	—	0.239	—
	212	0.0295	—	0.242	—
	302	0.0305	—	0.291	—
Silicone rubber	—	0.0161 <sup>(g)</sup>	0.047 <sup>(g)</sup>	0.300 <sup>(g)</sup>	1.0 <sup>(h)</sup>
Air	-9.67	1.074×10 <sup>-3(a)</sup>	4.064×10 <sup>-3(a),(i)</sup>	0.240 <sup>(a)</sup>	—
	80.33	1.266×10 <sup>-3</sup>	—	0.241	—
	170.33	1.445×10 <sup>-3</sup>	—	0.241	—
	260.33	1.628×10 <sup>-3</sup>	—	0.242	—
	350.33	1.796×10 <sup>-3</sup>	—	0.244	—
	440.33	1.960×10 <sup>-3</sup>	—	0.246	—
	530.33	2.114×10 <sup>-3</sup>	—	0.248	—
	620.33	2.258×10 <sup>-3</sup>	—	0.251	—
	710.33	2.393×10 <sup>-3</sup>	—	0.254	—
	800.33	2.523×10 <sup>-3</sup>	—	0.257	—
	890.33	2.644×10 <sup>-3</sup>	—	0.260	—
	980.33	2.759×10 <sup>-3</sup>	—	0.263	—
	1070.33	2.870×10 <sup>-3</sup>	—	0.265	—
	1160.33	2.985×10 <sup>-3</sup>	—	0.268	—
	1250.33	3.096×10 <sup>-3</sup>	—	0.270	—
	1340.33	3.212×10 <sup>-3</sup>	—	0.273	—
	1520.33	3.443×10 <sup>-3</sup>	—	0.277	—

- Notes:
- (a) F. P. Incropera and D. P. DeWitt, *Fundamentals of Heat and Mass Transfer*, 2nd edition, John Wiley & Sons, New York, 1985.
  - (b) Hsin Wang, *Thermal Conductivity Measurements of Kaolite*, ORNL/TM-2003/49.
  - (c) Based on a baked density of 19.4 lbm/ft<sup>3</sup> (0.011 lbm/in.<sup>3</sup>). Specification JS-YMN3-801580-A003 requires a baked density of 22.4 ± 3 lbm/ft<sup>3</sup>. Using a lower value for the Kaolite density results in higher temperatures on the containment vessel because the heat capacity of the Kaolite is minimized—allowing more heat to flow to the containment vessel; therefore, the thermal analyses are performed using a low-end density of 19.4 lbm/ft<sup>3</sup>. The HAC analyses also consider a high-end density of 30 lbm/ft<sup>3</sup>.
  - (d) FAX communication from J. W. Breuer of Thermal Ceramics, Engineering Department, August 11, 1995.
  - (e) W. D. Porter and H. Wang, *Thermophysical Properties of Heat Resistant Shielding Material*, ORNL/TM-2004/290, ORNL, Dec. 2004. Specific heat values are presented in MJ/m<sup>3</sup>-K in ORNL/TM-2004/290—converted to mass-based units using a density of 105 lbm/ft<sup>3</sup>.
  - (f) Based on a cured density of density of 100 lbm/ft<sup>3</sup> (0.0579 lbm/in.<sup>3</sup>). B. F. Smith and G. A. Byington, *Mechanical Properties of 277-4*, Y/DW-1987, January 19, 2005 presents a range of measured densities between approximately 100 and 110 lbm/ft<sup>3</sup> for Catalog No. 277-4. Therefore, in order to minimize the heat capacity of the material and allow more heat to be transferred to the containment vessel, the lower-bound value is used. The HAC analyses also consider a high-end density of 110 lbm/ft<sup>3</sup>.
  - (g) THERM 1.2, thermal properties database by R. A. Bailey.
  - (h) Conservatively modeled as 1.0.
  - (i) Constant density value evaluated at 100°F.

## MODELED HEAT TRANSFER MECHANISMS

The heat transfer mechanisms included in the thermal model such, as thermal radiation, natural convection, and insolation (solar heat flux) are described in detail in the following sections.

### Heat Transfer Between Package Exterior and Ambient

The heat transfer between the exterior of the package and the ambient (or fire) is modeled as a combination of radiant heat transfer and natural convection. The heat transfer due to radiant exchange with the environment is calculated as:<sup>[5]</sup>

$$q''_{\text{rad}} = \sigma F_e (T_s^4 - T_a^4), \quad (1)$$

where  $\sigma$  = Stefan-Boltzmann constant,  
 $F_e$  = overall exchange factor,  
 $T_s$  = container outer surface temperature (absolute), and  
 $T_a$  = ambient or fire temperature (absolute).

The overall interchange factor is calculated as:<sup>[5]</sup>

$$F_e = \left[ \frac{1}{\frac{1}{\epsilon_p} + \frac{A_p}{A_s} \left( \frac{1}{\epsilon_s} - 1 \right)} \right], \quad (2)$$

where  $\epsilon_p$  = emissivity of package surface,  
 $A_p$  = surface area of the package,  
 $A_s$  = surface area of the surroundings, and  
 $\epsilon_s$  = emissivity of surroundings.

For NCT and the cool-down period following the HAC fire, the area of the surroundings is assumed to be much larger than the surface area of the package; therefore, Eq. 2 reduces to:

$$F_e \approx \epsilon_p. \quad (3)$$

An emissivity value of 0.22,<sup>[6]</sup> which is typical of clean stainless steel, is assumed for the outer surfaces of the drum during NCT and during the cool-down period following the HAC fire. In reality, the outer surfaces of the drum will have a much higher emissivity following the HAC fire; therefore, this assumption is conservative.

During the HAC fire, the area of the surroundings is assumed to be approximately equal to the surface area of the drum; therefore, Eq. 2 reduces to:

$$F_e = \left[ \frac{1}{\frac{1}{\epsilon_p} + \frac{1}{\epsilon_s} - 1} \right]. \quad (4)$$

During the HAC 30-minute fire, an emissivity of 0.8 is assumed for the drum, and an emissivity of 0.9 is assumed for the fire per the guidance of 10 CFR 71.74(c)(4).<sup>[1]</sup> This results in an overall exchange factor of 0.7347 during the HAC fire using Eq. 4.

The natural convection heat transfer from the package surface to the ambient air is calculated as:

$$q''_{\text{convection}} = h(T_s - T_a). \quad (5)$$

where  $h$  = natural convection heat transfer coefficient,  
 $T_s$  = container outer surface temperature, and  
 $T_a$  = ambient or fire temperature.

During the NCT transient thermal analyses and the steady-state thermal analyses (used to obtain the starting temperature distribution in the package for NCT and HAC when a content heat load is present), the shipping container is assumed to be in an upright (vertical) orientation. The top of the drum is modeled as a heated horizontal flat plate facing up using the following correlation:<sup>[6]</sup>

$$h = \left( \frac{k}{L} \right) C_1 Ra^{C_2}, \quad (6)$$

where  $k$  = thermal conductivity of air,  
 $L$  = characteristic length (= D/4 per Ref. 6),  
 $D$  = diameter of the package,  
 $Ra$  = Rayleigh number,  
 $C_1$  = constant (see Table 2), and  
 $C_2$  = constant (see Table 2).

The Rayleigh number in Eq. 6 is defined as:

$$Ra = \frac{g \beta \Delta T L^3}{\nu \alpha}, \quad (7)$$

where  $g$  = acceleration of gravity,  
 $\beta$  = coefficient of thermal expansion,  
 $\Delta T$  = temperature difference,  
 $\nu$  = kinematic viscosity [ $\mu/\rho$ ],  
 $\mu$  = absolute viscosity,  
 $\alpha$  = thermal diffusivity [ $k/(\rho C_p)$ ],  
 $\rho$  = density of air, and  
 $C_p$  = specific heat of air.

The properties of air used in the natural convection calculations are presented in Table 3.

**Table 2. Coefficients for natural convection correlations.**

Coefficient	Rayleigh Number Range	Value
$C_1$	$10^4 < Ra < 10^7$	0.54
	$10^7 < Ra < 10^{11}$	0.15
$C_2$	$10^4 < Ra < 10^7$	0.25
	$10^7 < Ra < 10^{11}$	1/3
$C_3$	$Ra < 10^9$	0.680
	$Ra > 10^9$	0.825
$C_4$	$Ra < 10^9$	0.670
	$Ra > 10^9$	0.387
$C_5$	$Ra < 10^9$	0.25
	$Ra > 10^9$	1/6
$C_6$	$Ra < 10^9$	4/9
	$Ra > 10^9$	8/27
$C_7$	$Ra < 10^9$	1
	$Ra > 10^9$	2

Source: F. P. Incropera and D. P. DeWitt, *Fundamentals of Heat and Mass Transfer*, 2nd ed., John Wiley & Sons, New York, 1985.

**Table 3. Properties of air used in natural convection calculations.**

Temperature (°F)	Thermal Conductivity (Btu/h-in.-°F)	Density (lbm/in. <sup>3</sup> )	Specific Heat (Btu/lbm-°F)	Kinematic Viscosity (in. <sup>2</sup> /h)	Thermal Diffusivity (in. <sup>2</sup> /h)	Prandtl Number
-9.67	$1.074 \times 10^{-3}$	$5.039 \times 10^{-5}$	0.240	$6.384 \times 10^1$	$8.872 \times 10^1$	0.720
80.33	$1.266 \times 10^{-3}$	$4.196 \times 10^{-5}$	0.241	$8.867 \times 10^1$	$1.255 \times 10^2$	0.707
170.33	$1.445 \times 10^{-3}$	$3.595 \times 10^{-5}$	0.241	$1.167 \times 10^2$	$1.668 \times 10^2$	0.700
260.33	$1.628 \times 10^{-3}$	$3.147 \times 10^{-5}$	0.242	$1.474 \times 10^2$	$2.137 \times 10^2$	0.690
350.33	$1.796 \times 10^{-3}$	$2.796 \times 10^{-5}$	0.244	$1.807 \times 10^2$	$2.634 \times 10^2$	0.686
440.33	$1.960 \times 10^{-3}$	$2.516 \times 10^{-5}$	0.246	$2.164 \times 10^2$	$3.164 \times 10^2$	0.684
530.33	$2.114 \times 10^{-3}$	$2.286 \times 10^{-5}$	0.248	$2.543 \times 10^2$	$3.722 \times 10^2$	0.683
620.33	$2.258 \times 10^{-3}$	$2.097 \times 10^{-5}$	0.251	$2.940 \times 10^2$	$4.291 \times 10^2$	0.685
710.33	$2.393 \times 10^{-3}$	$1.935 \times 10^{-5}$	0.254	$3.360 \times 10^2$	$4.871 \times 10^2$	0.690
800.33	$2.523 \times 10^{-3}$	$1.797 \times 10^{-5}$	0.257	$3.800 \times 10^2$	$5.468 \times 10^2$	0.695
890.33	$2.644 \times 10^{-3}$	$1.677 \times 10^{-5}$	0.260	$4.261 \times 10^2$	$6.082 \times 10^2$	0.702
980.33	$2.759 \times 10^{-3}$	$1.573 \times 10^{-5}$	0.263	$4.739 \times 10^2$	$6.696 \times 10^2$	0.709
1070.33	$2.870 \times 10^{-3}$	$1.480 \times 10^{-5}$	0.265	$5.234 \times 10^2$	$7.310 \times 10^2$	0.716
1160.33	$2.985 \times 10^{-3}$	$1.397 \times 10^{-5}$	0.268	$5.742 \times 10^2$	$7.979 \times 10^2$	0.720
1250.33	$3.096 \times 10^{-3}$	$1.324 \times 10^{-5}$	0.270	$6.261 \times 10^2$	$8.649 \times 10^2$	0.723
1340.33	$3.212 \times 10^{-3}$	$1.258 \times 10^{-5}$	0.273	$6.802 \times 10^2$	$9.374 \times 10^2$	0.726
1520.33	$3.443 \times 10^{-3}$	$1.144 \times 10^{-5}$	0.277	$7.912 \times 10^2$	$1.088 \times 10^3$	0.728

Source: F. P. Incropera and D. P. DeWitt, *Fundamentals of Heat and Mass Transfer*, 2nd ed., John Wiley & Sons, New York, 1985.

During the NCT transient thermal analyses and the steady-state thermal analyses, the sides of the drum are modeled as a vertical flat plate using the following correlation:<sup>[6]</sup>

$$h = \left( \frac{k}{L} \right) \left[ C_3 + \frac{C_4 Ra^{C_5}}{\left( 1 + \left[ \frac{0.492}{Pr} \right]^{9/16} \right)^{C_6}} \right]^{C_7}, \quad (8)$$

where  $L$  = characteristic length = the drum height,  
 $C_3$  = constant (see Table 2),  
 $C_4$  = constant (see Table 2),  
 $C_5$  = constant (see Table 2),  
 $C_6$  = constant (see Table 2),  
 $C_7$  = constant (see Table 2), and  
 $Pr$  = Prandtl number.

The bottom of the drum is conservatively modeled as adiabatic during the NCT transient analyses and the steady-state analyses.

During the HAC 30-minute fire and the post-fire cool-down, the shipping container is assumed to be in a horizontal orientation (as it is during furnace testing). As such, the top and bottom of the drum are modeled as vertical flat plates using Eq. 8 having a characteristic length,  $L$ , equivalent to the drum diameter, and the sides of the drum are modeled as a horizontal cylinder using the following correlation ( $10^{-5} < Ra < 10^{12}$ ):<sup>[6]</sup>

$$h = \left( \frac{k}{D} \right) \left[ 0.60 + \frac{0.387 Ra^{1/6}}{\left( 1 + \left[ \frac{0.559}{Pr} \right]^{9/16} \right)^{8/27}} \right]^2, \quad (9)$$

where  $D$  = diameter of the package,

The calculated natural convection film coefficients used in the thermal analyses of the ES-3100 are presented graphically in Figure 4 and Figure 5 for NCT and HAC, respectively.

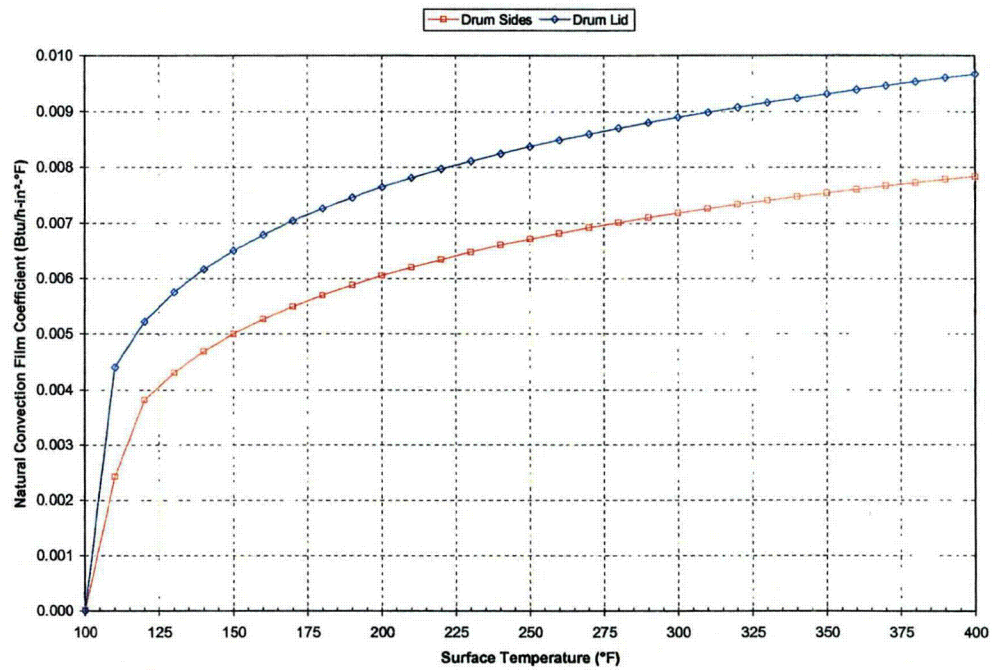


**Figure 4. Natural convection film coefficients applied to the drum surfaces during NCT and steady-state conditions.**

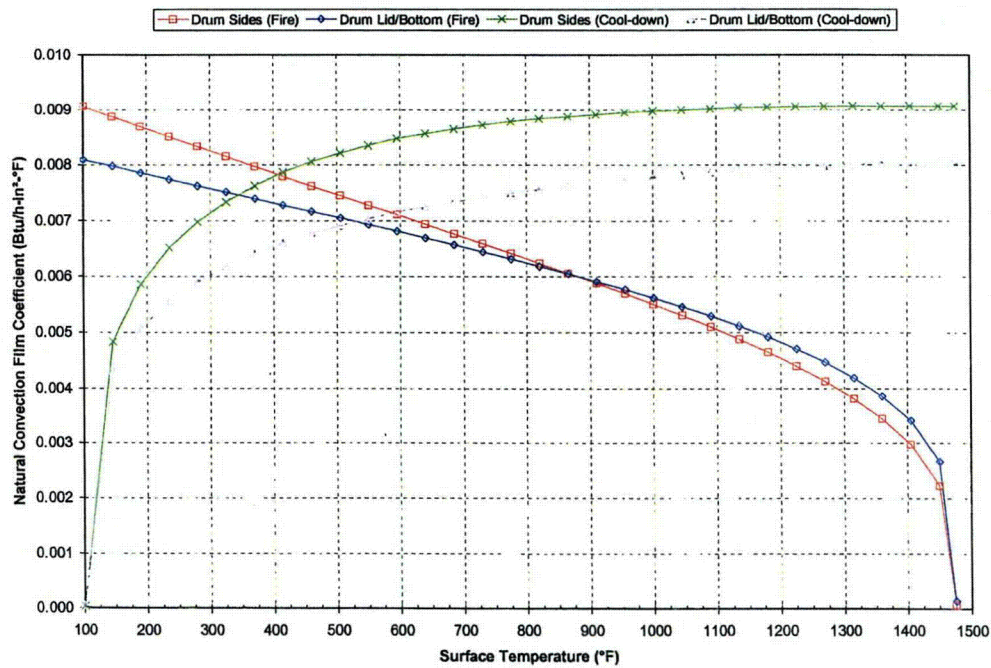


**Figure 5. Natural convection film coefficients applied to the drum surfaces during HAC.**



## Insolation

The following insolation (incident solar radiation) data is required for NCT per 10 CFR 71.71(c)(1):<sup>[1]</sup>

Form and location of surface	Total insolation for a 12-hour period (cal/cm <sup>2</sup> )
Flat surfaces transported horizontally	
Base	None
Other surfaces	800
Flat surfaces not transported horizontally	200
Curved surfaces	400

The total insolation values specified in the previous table are for a 12-hour period. For analytical purposes, these values are “time-averaged” over the entire 12-hour period (i.e., divided by 12). Therefore, the incident solar heat fluxes ( $q''_{\text{solar},i}$ ) used in the analyses for NCT and cool-down following the HAC fire are as follows:

During NCT, the drum is in an upright (vertical) orientation; therefore, the following heat fluxes are applied to the external surfaces of the drum to represent insolation:

$$\text{Top} \quad q''_{\text{solar},i} = 1.7074 \text{ Btu/h} - \text{in.}^2, \quad (10)$$

$$\text{Sides} \quad q''_{\text{solar},i} = 0.8537 \text{ Btu/h} - \text{in.}^2, \quad (11)$$

$$\text{Bottom} \quad q''_{\text{solar},i} = 0. \quad (12)$$

During the cool-down period following the HAC 30-minute fire, the drum is assumed to be in a horizontal orientation; therefore, the following heat fluxes are applied to the external surfaces of the drum to represent insolation:

$$\text{Top} \quad q''_{\text{solar},i} = 0.4269 \text{ Btu/h} - \text{in.}^2, \quad (13)$$

$$\text{Sides} \quad q''_{\text{solar},i} = 0.8537 \text{ Btu/h} - \text{in.}^2, \quad (14)$$

$$\text{Bottom} \quad q''_{\text{solar},i} = 0.4269 \text{ Btu/h} - \text{in.}^2. \quad (15)$$

The insolation is applied as a square-wave function (i.e., alternating on and off in 12-hour periods) in the thermal analysis. The heat flux values presented in Eqs. 10–15 represent the insolation absorbed by the package surface since a drum absorptivity of 1.0 was conservatively assumed. An analytical study has been performed on a similar shipping package that investigated three methods of applying the insolation.<sup>[7]</sup> The three methods consisted of 1) performing a steady-state analysis assuming the insolation is applied continuously by distributing the heat flux evenly throughout a 24-hour period, 2) performing a transient analysis assuming the insolation is represented by a step function (i.e., applied and then not applied in 12-hour cycles, and 3) performing a transient analysis where the incident insolation is represented by a sinusoidal function that varies throughout the day. The results of the study indicate that the method used in applying the insolation has a significant effect on the temperatures of the outermost portions of the package. However, since the total insolation over any 24-hour period is the same for all cases, internal package temperatures are relatively unaffected by the way in which the insolation is applied. Since the containment vessel O-ring temperatures are of primary concern in this evaluation, the step function method for applying the insolation is suitable.

## Heat Transfer Across Gaps in the Package

Heat transfer across all gaps in the package is modeled by a combination of radiant exchange and conduction. Natural convection heat transfer is not included across the gaps in the model. Scoping studies performed for a similar shipping package indicate that the heat transfer due to natural convection in relatively small gaps is approximately a factor of 6 times less than the heat transfer due to radiant exchange.<sup>[7]</sup> These calculations assumed a temperature difference of 9°F across the gap. Based on these previous calculations, the effect of neglecting the natural convection in the gap regions is minimal. The emissivity values used in the analysis for all internal radiating surfaces in the model are presented in Table 1.

Radiant exchange across gaps is modeled using the cavity radiation feature of ABAQUS/Standard.<sup>[8]</sup> For each cavity (or enclosure), radiation surfaces are defined as shown in Figure 6 and Figure 7.

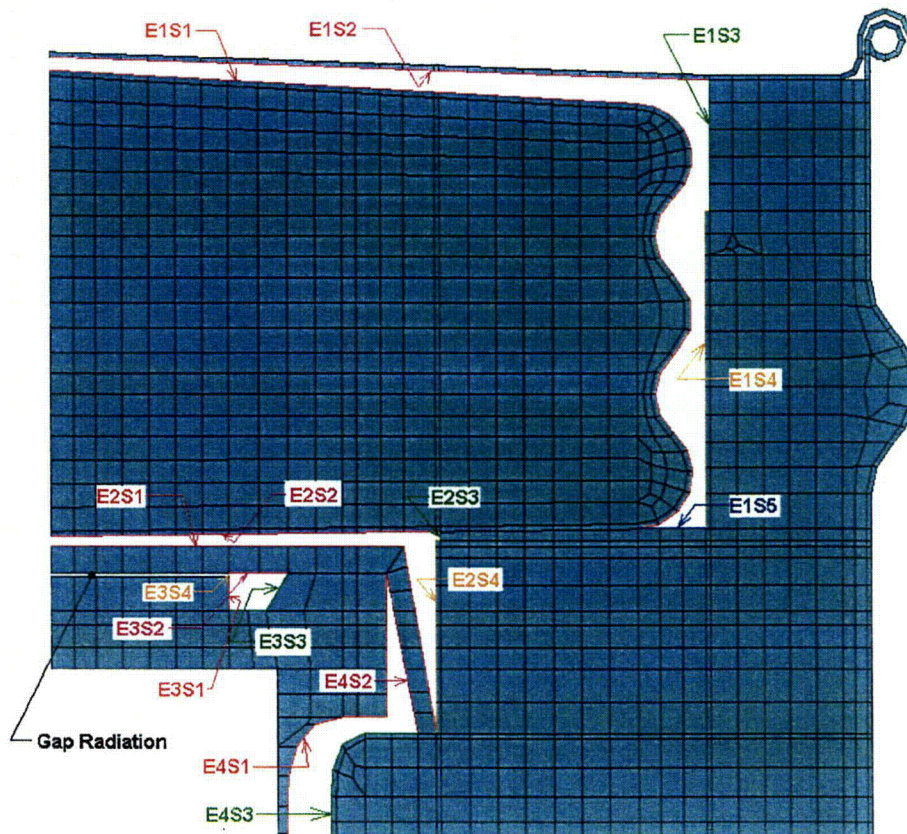
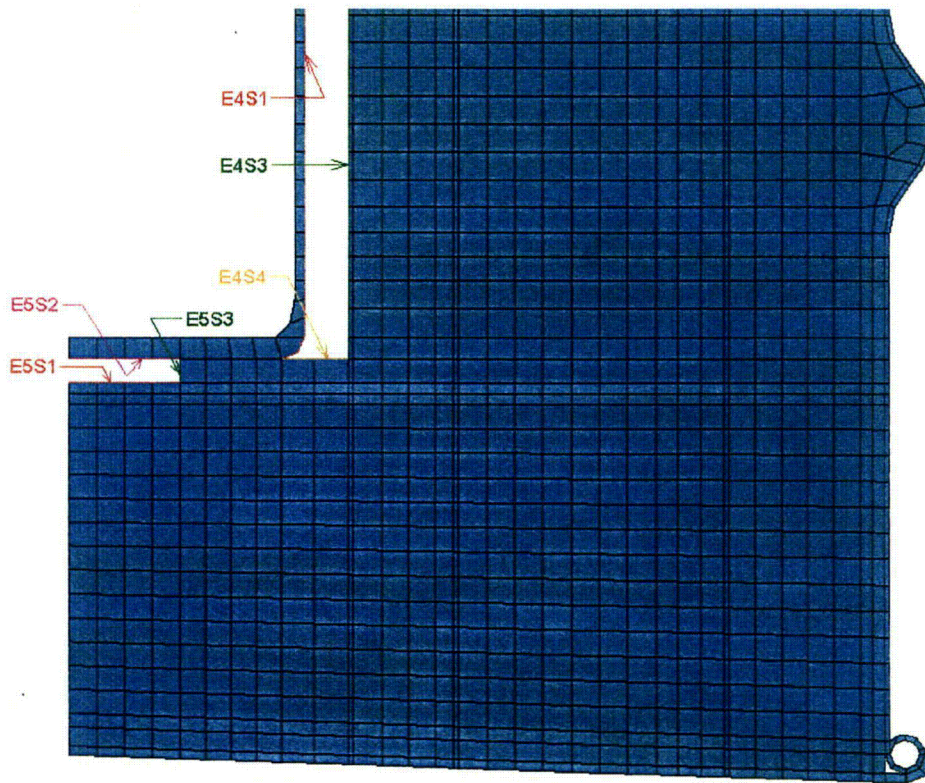


Figure 6. Radiation cavity surface definitions (top portion of the model).





**Figure 7. Radiation cavity surface definitions (bottom portion of the model).**

As shown in Figure 6 and Figure 7, the various gaps in the model are divided into five separate cavities (designated 'E1' through 'E5' in the figures) with between three and five surfaces (designated 'S1' through 'S5' in the figures) in each cavity for radiation calculations. Because the gap between the CV lid and top pad is small in relation to its characteristic length, radiation exchange is modeled using the gap radiation feature in ABAQUS/Standard with a view factor of 1.0 assigned. As a result, a shell element (type DSAX1) is defined in the model with the radiation surface E3S4 (see Figure 6) superimposed to close off cavity 3. The DSAX1 element is assigned the properties of air, and surface E3S4 is assigned a small emissivity value of 0.01 since it is an imaginary surface used to close the cavity.

### **Content Heat Load**

In order to simulate the decay heat generated by the ES-3100 shipping container contents, a uniform heat flux is applied to the element edges representing the inner surface of the containment vessel in the model. Content heat loads of 0, 0.4, 20, and 30 W are investigated in this report. The uniform heat flux ( $q''_{\text{source}}$ ) for a given content heat load is calculated using the following equation:

$$q''_{\text{source}} = \frac{Q \times 3.4123}{2 \left( \frac{\pi D_i^2}{4} \right) + \pi(D_i)(H)}, \quad (16)$$

where,  $Q$  = content heat load (W),  
 $D_i$  = inside diameter of the containment vessel (5.06 in.),  
 $H$  = height of the containment vessel cavity (31.00 in.).

Using Eq. 16, a content heat load of 0.4 W results in a uniform heat flux of  $2.5608 \times 10^{-3}$  Btu/h-in.<sup>2</sup>, a content heat load of 20 W results in a uniform heat flux of 0.12804 Btu/h-in.<sup>2</sup>, and a content heat load of 30 W results in a uniform heat flux of 0.19206 Btu/h-in.<sup>2</sup>.

## DISCUSSION OF ANALYTICAL RESULTS

All thermal analyses discussed in this report were performed using ABAQUS/Standard<sup>[8]</sup> on an Intel Pentium 4-based Microsoft Windows 2000 computer. Temperatures are monitored at selected locations in the model as shown in Figure 8 through Figure 11.

### Steady-state Conditions Analyses Results

Steady-state thermal analyses are performed on the finite element model of the ES-3100 shipping container for three cases having content heat loads of 0.4, 20, and 30 W. The temperature distribution results from these analyses are used as the starting temperature distributions within the model when performing the transient thermal analyses for NCT and the HAC 30-minute fire. The boundary conditions for these steady-state analyses include a combination of thermal radiation exchange and natural convection applied to the top and sides of the drum using an ambient temperature of 100°F. The bottom of the drum is modeled as an adiabatic surface (i.e., no heat transfer). Additionally, the content heat load is simulated by applying a uniform heat flux to the surfaces of the elements representing the inner surface of the containment vessel. The calculated steady-state temperature distribution within the model of the ES-3100 shipping container for content heat loads of 0.4, 20, and 30 W is presented in Table 4.

As presented in Table 4, the maximum accessible surface temperature of the package when exposed to an ambient temperature of 100°F in the shade is 100.43°F (38.02°C), 114.39°F (45.77°C), and 120.08°F (48.93°C) for content heat loads of 0.4, 20, and 30 W, respectively.

### Normal Conditions of Transport Analyses Results

Transient thermal analyses are performed on the finite element model of the ES-3100 shipping container to simulate NCT with content heat loads of 0, 0.4, 20, and 30 W. The insolation required for NCT per 10 CFR 71.71(c)(1)<sup>[1]</sup> is applied to the top and sides of the drum in alternating 12-hour periods (i.e., 12 hours on and 12 hours off) with the drum bottom remaining adiabatic during the transient thermal analysis. An ambient temperature of 100°F as stipulated in 10 CFR 71 is used in the NCT analysis. The initial temperature distribution within the package for the NCT transients was determined from steady-state analyses (with radiation and natural convection boundary conditions applied to the top and sides of the drum) for each internal heat load. For the case with no internal heat source (0 W), the initial temperature distribution within the package was assumed to be at a uniform 100°F. As with the steady-state analyses discussed previously, applying a uniform heat flux to the internal surfaces of the elements representing the containment vessel simulates the content heat load.

The transient thermal analyses simulate a five-day period of cyclic solar loading with 12 hours of insolation being applied at the beginning of each day (i.e., sunrise) followed by 12 hours in which there is no insolation to end the day (i.e., sunset). This five-day period allows for "quasi steady-state" conditions

to be reached. While the temperature of a particular node within the model changes with respect to time in the transient analyses, the maximum temperature that node reaches from day-to-day does not change once a "quasi steady-state" condition is reached. In particular, the maximum temperature of the key location on the containment vessel (i.e., at the O-ring) on day 5 is within 0.004°F of the maximum temperature of the same location on day 4.

The maximum temperatures of several locations within the model are summarized in Table 5 for content heat loads of 0, 0.4, 20, and 30 W. The maximum temperatures reported in Table 5 represent "quasi steady-state" conditions. Temperature-history plots of several locations within the model are also depicted graphically in Figure 12 through Figure 15 for various content heat loads. Additionally, temperature contours of the model at sunrise (0 hours), sunset (12 hours), and 68 to 70 minutes after sunset for a typical day (after the package temperatures reach "quasi steady-state") of the transient are presented in Figure 16 through Figure 19 for various content heat loads. The temperature contours at 68 to 70 minutes after sunset are presented because the temperature of the CV flange (i.e., O-ring location) peaks at this time. The elements representing the air between the drum liner and containment vessel and between the drum liner and top plug liner are not shown in the temperature contours presented in these figures so that the containment vessel temperature contours can be more easily viewed.

The maximum temperature in the model occurs at the top center of the drum lid in most instances. The drum lid maximum temperature is 243.86°F (117.70°C), 243.89°F (117.72°C), 245.32°F (118.51°C), and 246.03°F (118.91°C) for content heat loads of 0, 0.4, 20, and 30 W, respectively, and occurs at sunset in each case (see Table 5). For the case with a content heat load of 30 W, the maximum temperature in the model occurs in the sidewall of the CV approximately 80 minutes after sunset and is 252.87°F (122.71°C). The maximum temperature at the containment vessel O-ring is 189.28°F (87.38°C), 189.90°F (87.72°C), 217.07°F (102.82°C), and 230.51°F (110.28°C) for content heat loads of 0, 0.4, 20, and 30 W, respectively, and occurs at approximately 68 to 70 minutes after sunset in each case (see Table 5).

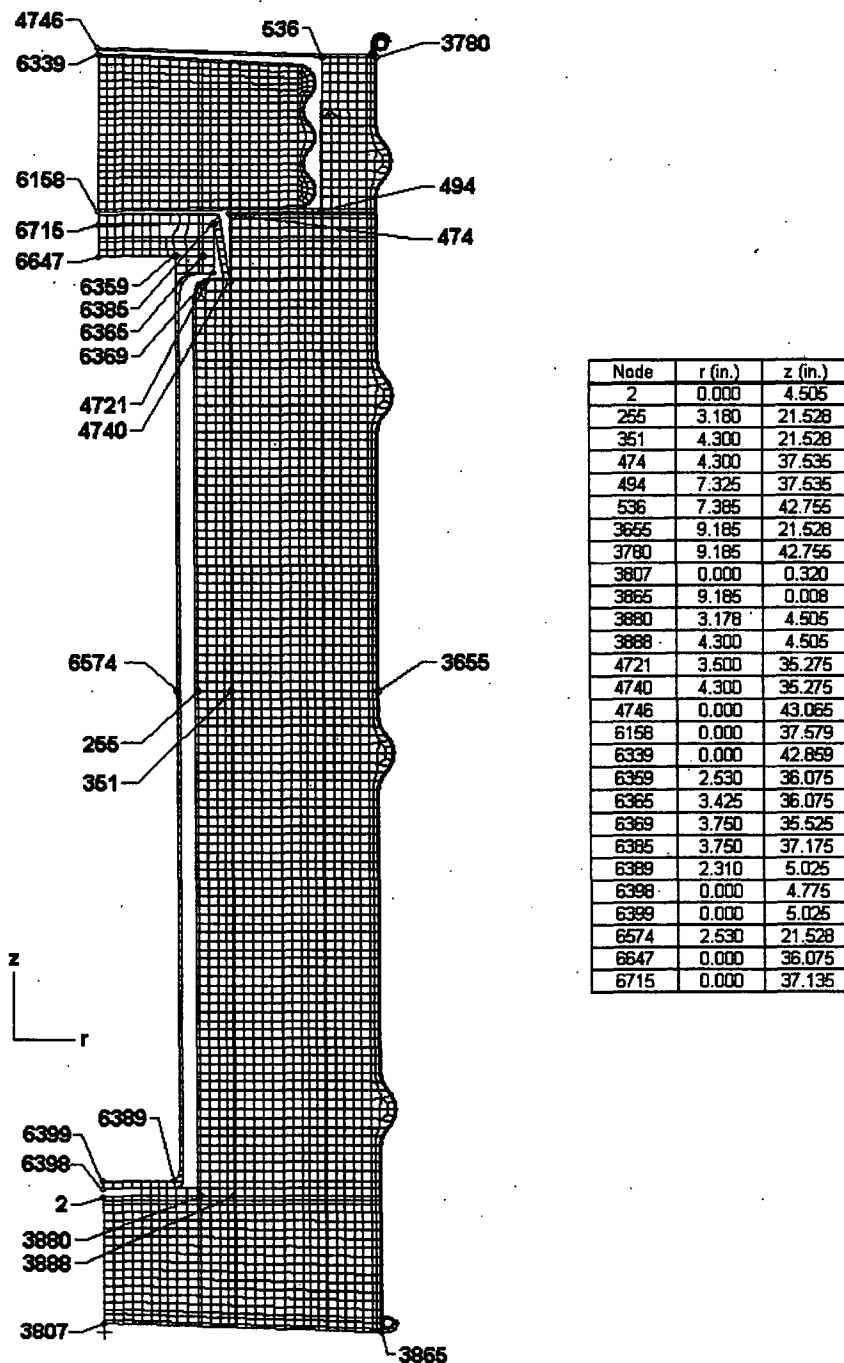
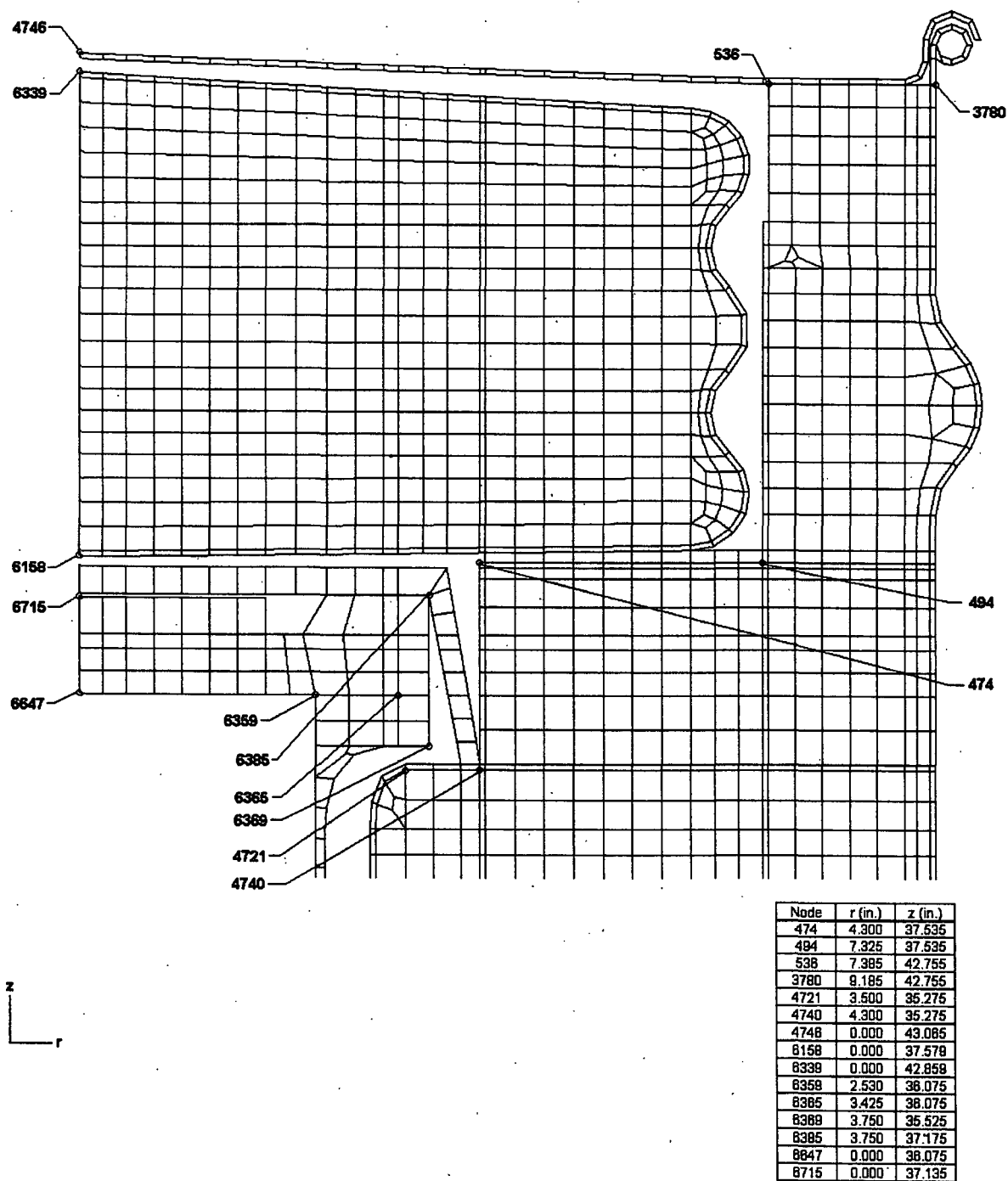
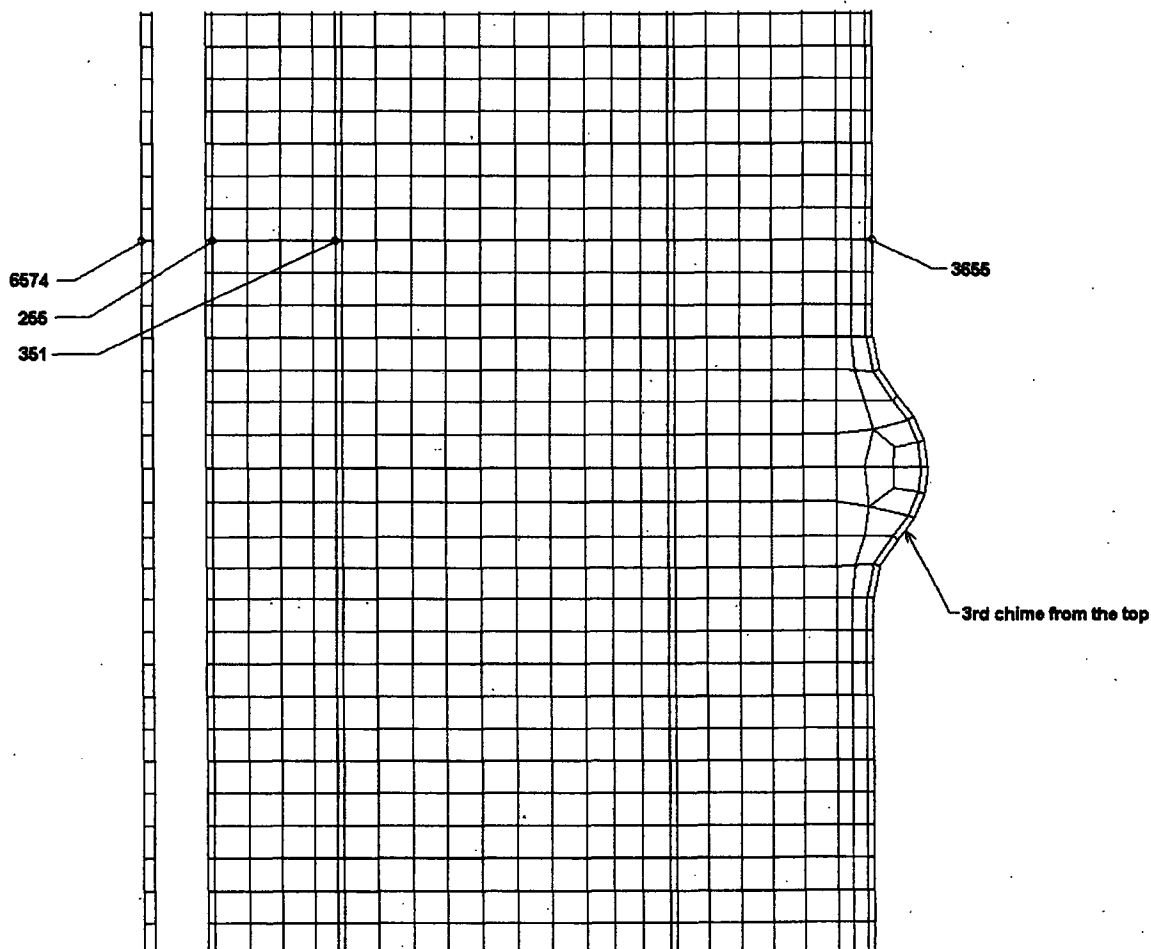


Figure 8. ABAQUS axisymmetric finite element model of the ES-3100 shipping container—nodal locations of interest (elements representing air not shown for clarity).



**Figure 9. ABAQUS axisymmetric finite element model of the ES-3100 shipping container—nodal locations of interest (elements representing air not shown for clarity), upper portion detail.**



Node	r (in.)	z (in.)
265	3.180	21.528
351	4.300	21.528
3655	9.185	21.528
6574	2.530	21.528



**Figure 10. ABAQUS axisymmetric finite element model of the ES-3100 shipping container—nodal locations of interest (elements representing air not shown for clarity), middle portion detail.**



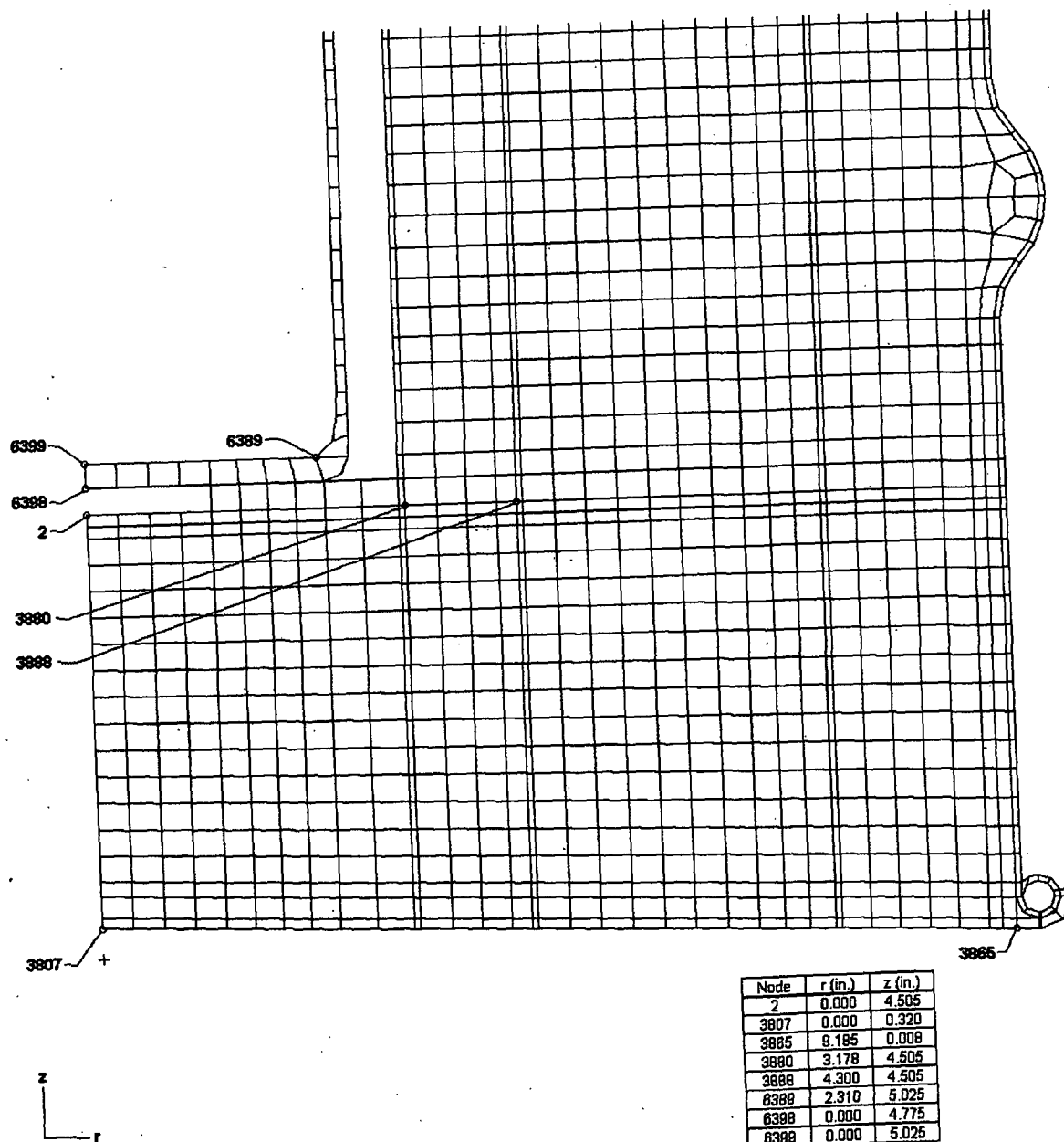


**Figure 11. ABAQUS axisymmetric finite element model of the ES-3100 shipping container—nodal locations of interest (elements representing air not shown for clarity), lower portion detail.**

**Table 4. ES-3100 shipping container steady-state temperatures (100°F ambient temperature, no insolation).**

Node map <sup>(a)</sup>	Node coordinates (in.)			Maximum steady-state temperature (°F)		
	No.	r	z	0.4 W	20 W	30 W
	2	0.000	4.505	100.83	134.54	150.15
	255	3.180	21.528	100.75	131.57	146.21
	351	4.300	21.528	100.71	129.45	142.87
	474	4.300	37.535	100.46	117.90	125.67
	494	7.325	37.535	100.32	110.87	115.19
	536	7.385	42.755	100.21	105.50	107.19
	3655 <sup>(b)</sup>	9.185	21.528	100.28	107.58	109.92
	3780 <sup>(b)</sup>	9.185	42.755	100.21	105.29	106.89
	3807 <sup>(b)</sup>	0.000	0.320	100.43	114.39	120.08
	3865 <sup>(b)</sup>	9.185	0.008	100.32	108.97	111.97
	3880	3.178	4.505	100.74	130.48	144.23
	3888	4.300	4.505	100.71	128.60	141.42
	4721	3.500	35.275	100.59	124.08	134.90
	4740	4.300	35.275	100.57	122.92	133.15
	4746 <sup>(b)</sup>	0.000	43.065	100.20	104.99	106.43
	6158	0.000	37.579	100.57	123.14	133.42
	6339	0.000	42.859	100.25	107.42	110.04
	6359 <sup>(c)</sup>	2.530	36.075	100.80	133.51	148.56
	6365 <sup>(c)</sup>	3.425	36.075	100.79	133.33	148.28
	6369	3.750	35.525	100.79	133.27	148.20
	6385	3.750	37.175	100.78	132.85	147.58
	6389	2.310	5.025	100.97	141.27	160.06
	6398	0.000	4.775	100.96	140.91	159.55
	6399	0.000	5.025	100.96	140.94	159.60
	6574	2.530	21.528	101.33	157.70	183.56
	6647	0.000	36.075	100.80	133.56	148.63
	6715	0.000	37.135	100.79	133.40	148.40

Notes: (a) See Figure 8 through Figure 11 for details of node locations.  
 (b) These are nodes at the accessible surfaces of the package (i.e., the drum, drum lid, and drum bottom plate).  
 (c) Approximate location of the CV O-ring.

**Table 5. ES-3100 shipping container maximum “quasi steady-state” temperatures during NCT with various content heat loads.**

Node map <sup>(a)</sup>	Node coordinates (in.)			Maximum “quasi steady-state” temperature (°F)			
	No.	r	z	0 W	0.4 W	20 W	30 W
	2	0.000	4.505	180.59	181.23	210.15	224.69
	255	3.180	21.528	179.33	179.93	207.32	221.43
	351	4.300	21.528	179.59	180.14	204.73	217.27
	474	4.300	37.535	198.88	199.20	212.72	219.58
	494	7.325	37.535	207.40	207.56	214.40	217.87
	536	7.385	42.755	226.44	226.49	228.31	229.24
	3655	9.185	21.528	198.09	198.15	200.81	202.16
	3780	9.185	42.755	223.47	223.51	225.13	225.95
	3807	0.000	0.320	190.48	190.70	199.84	204.43
	3865	9.185	0.008	195.87	195.97	199.91	201.90
	3880	3.178	4.505	180.72	181.28	206.65	219.52
	3888	4.300	4.505	181.03	181.55	205.08	217.01
	4721	3.500	35.275	189.45	189.90	209.53	219.47
	4740	4.300	35.275	190.56	190.98	209.37	218.68
	4746	0.000	43.065	243.86	243.89	245.32	246.03
	6158	0.000	37.579	198.42	198.84	217.12	226.32
	6339	0.000	42.859	233.98	234.06	237.32	238.95
	6359 <sup>(b)</sup>	2.530	36.075	189.28	189.90	217.07	230.51
	6365 <sup>(b)</sup>	3.425	36.075	189.27	189.88	216.88	230.23
	6369	3.750	35.525	189.23	189.85	216.79	230.12
	6385	3.750	37.175	189.39	190.00	216.57	229.72
	6389	2.310	5.025	179.94	180.70	215.75	233.27
	6398	0.000	4.775	179.99	180.76	215.52	232.92
	6399	0.000	5.025	179.99	180.76	215.55	232.96
	6574	2.530	21.528	179.27	180.35	229.19	252.87
	6647	0.000	36.075	189.40	190.02	217.24	230.72
	6715	0.000	37.135	189.44	190.06	217.14	230.54

Notes: (a) See Figure 8 through Figure 11 for details of node locations.  
(b) Approximate location of the CV O-ring.

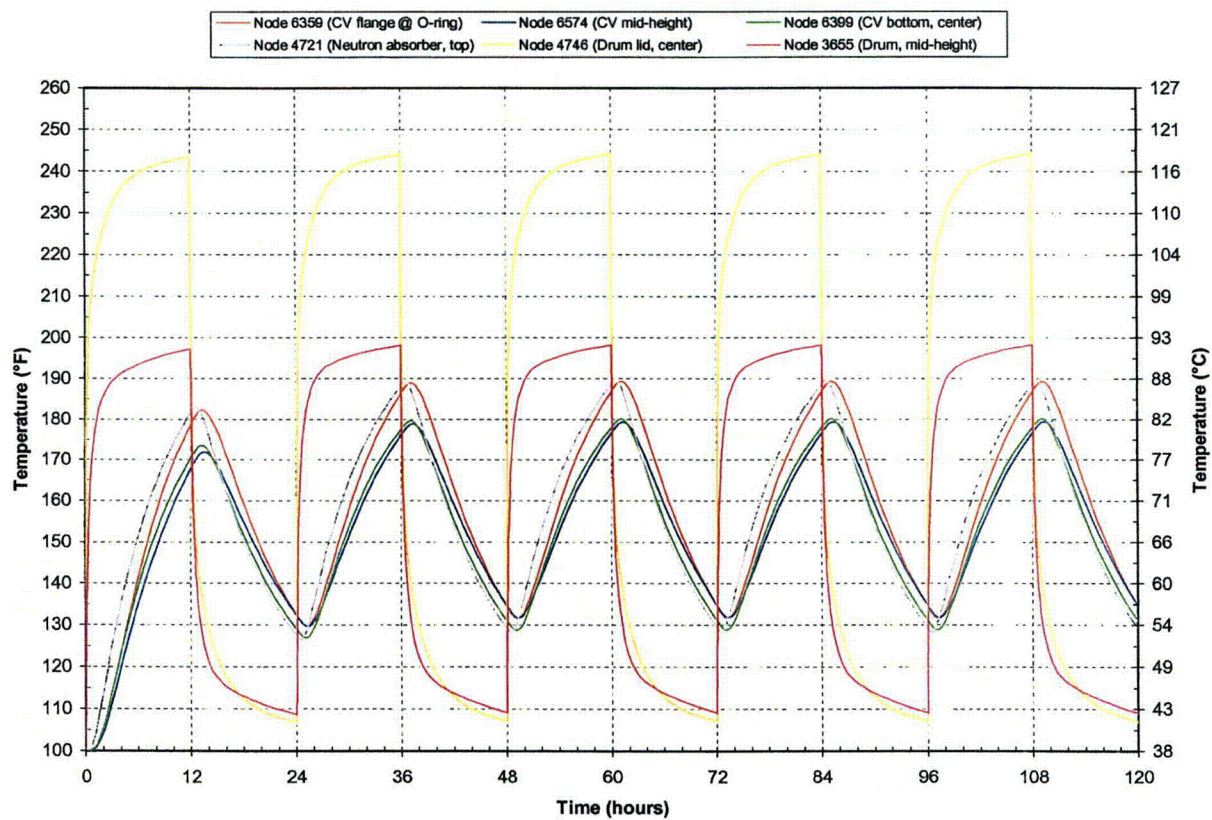


**Figure 12. Transient temperatures of the ES-3100 shipping container for NCT (no content heat load) see Figure 8 through Figure 11 for node locations.**

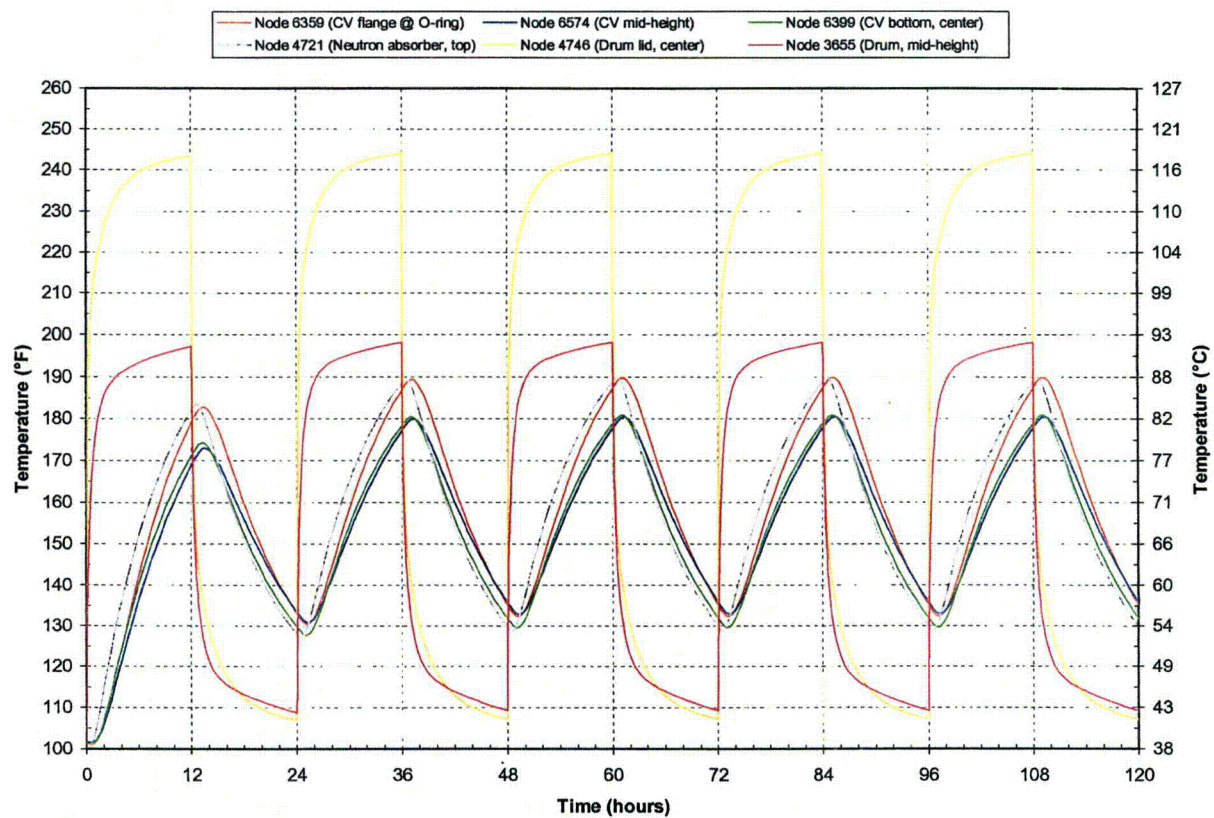
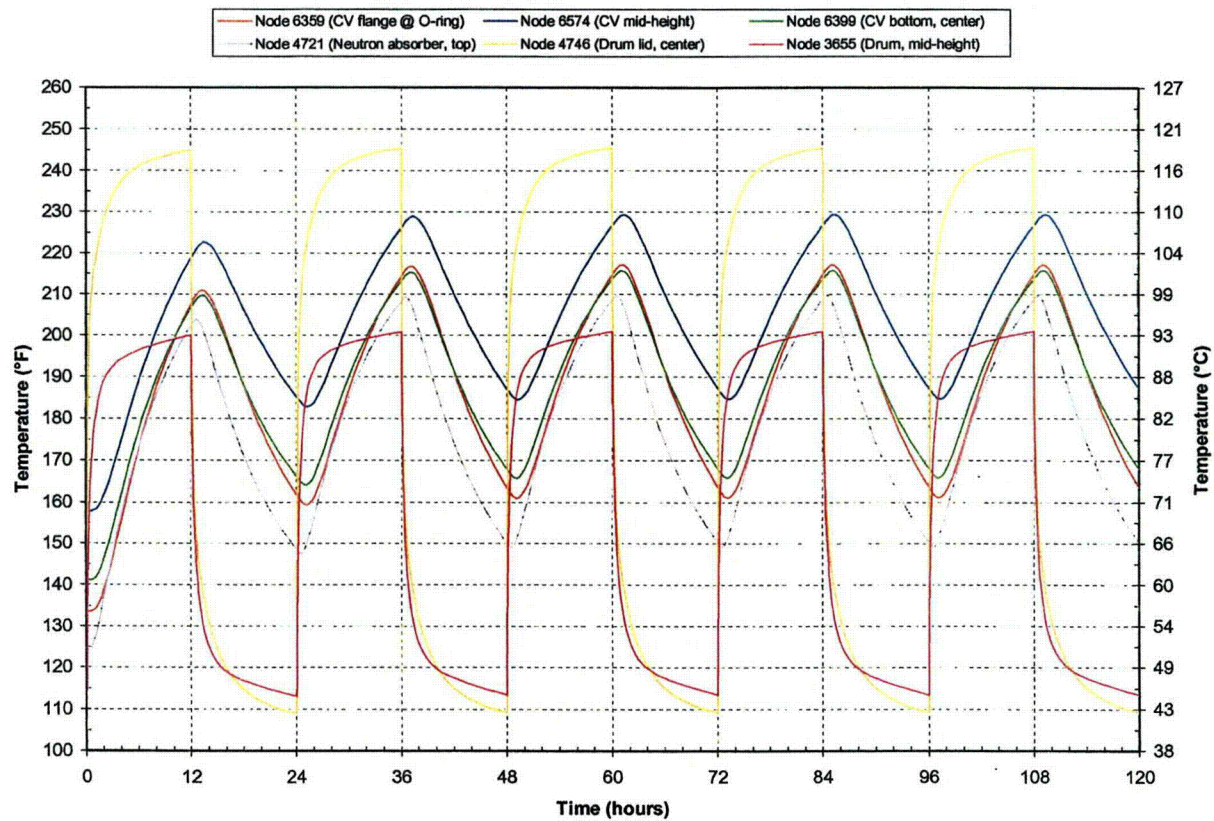


Figure 13. Transient temperatures of the ES-3100 shipping container for NCT (0.4 W content heat load) see Figure 8 through Figure 11 for node locations.



**Figure 14. Transient temperatures of the ES-3100 shipping container for NCT (20 W content heat load) see Figure 8 through Figure 11 for node locations.**



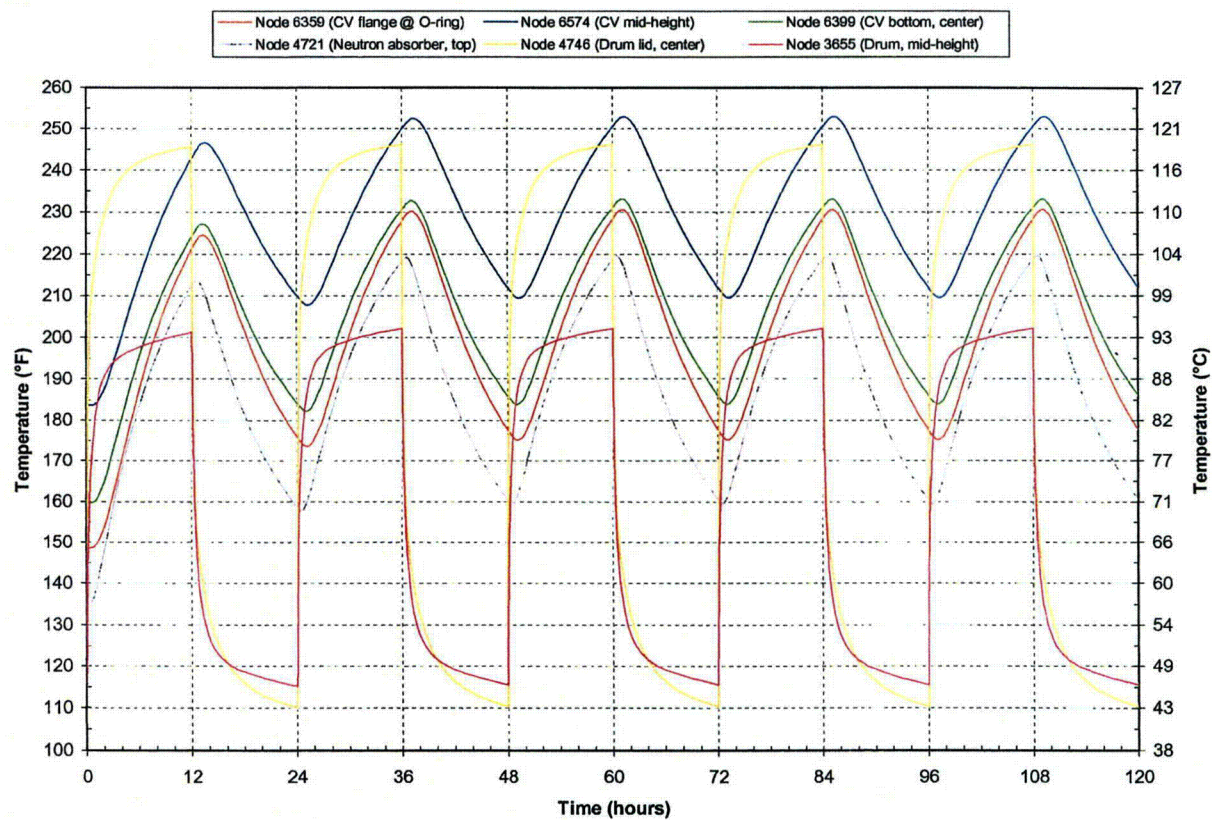


Figure 15. Transient temperatures of the ES-3100 shipping container for NCT (30 W content heat load) see Figure 8 through Figure 11 for node locations.

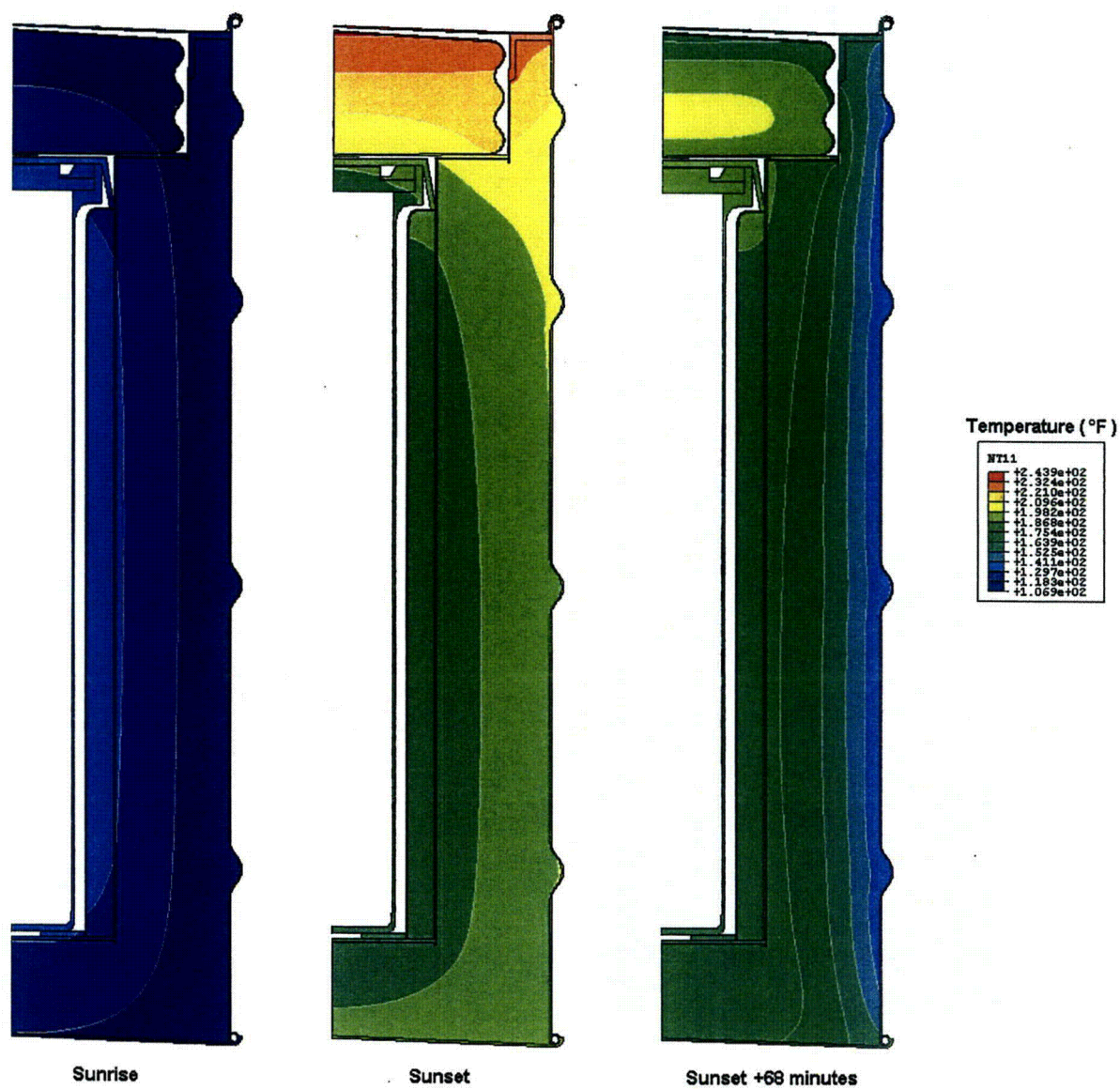


Figure 16. Temperature distribution in the ES-3100 shipping container for NCT (no content heat load) typical day of transient analysis (elements representing air not shown for clarity).



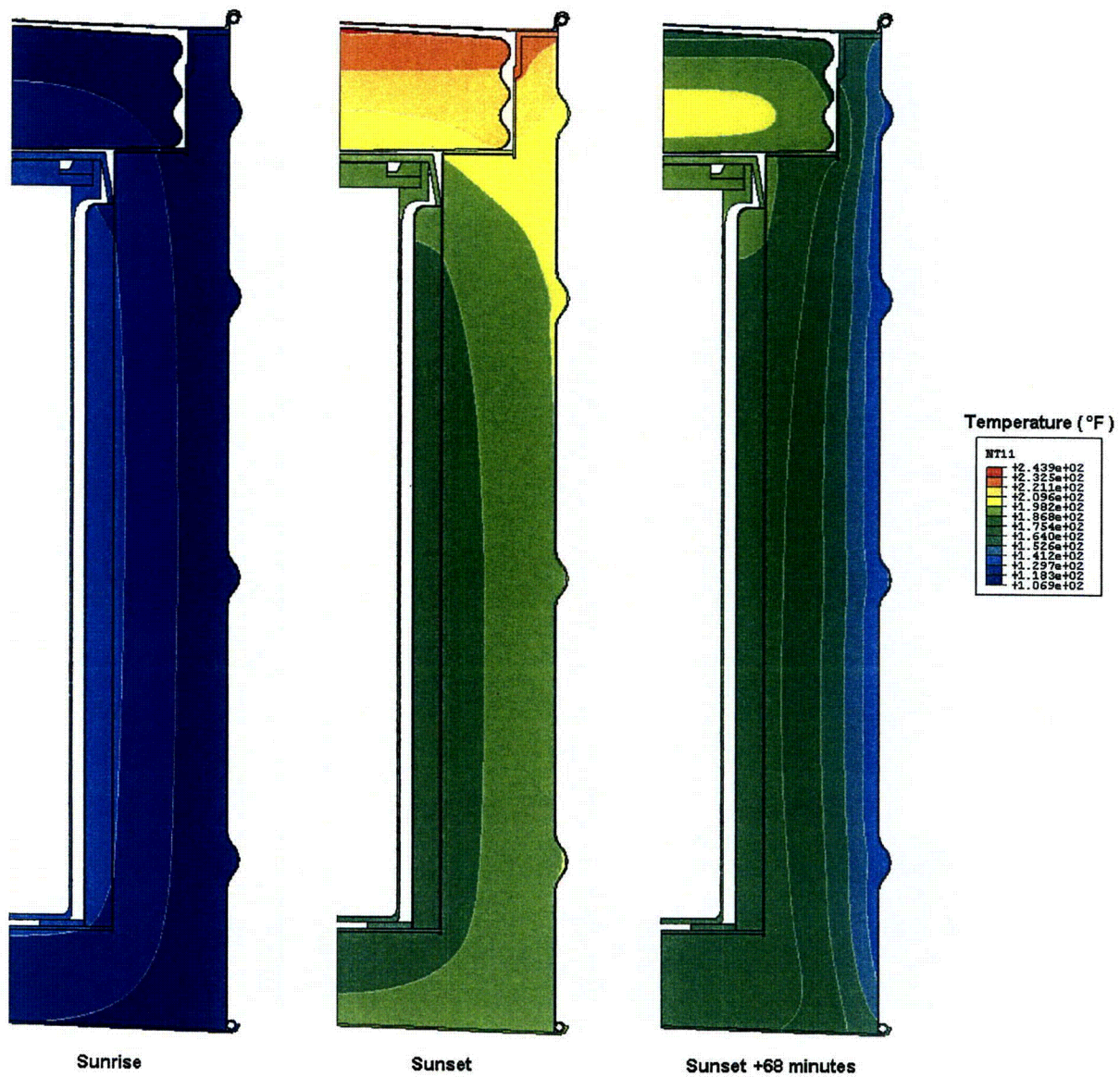


Figure 17. Temperature distribution in the ES-3100 shipping container for NCT (0.4 W content heat load) typical day of transient analysis (elements representing air not shown for clarity).

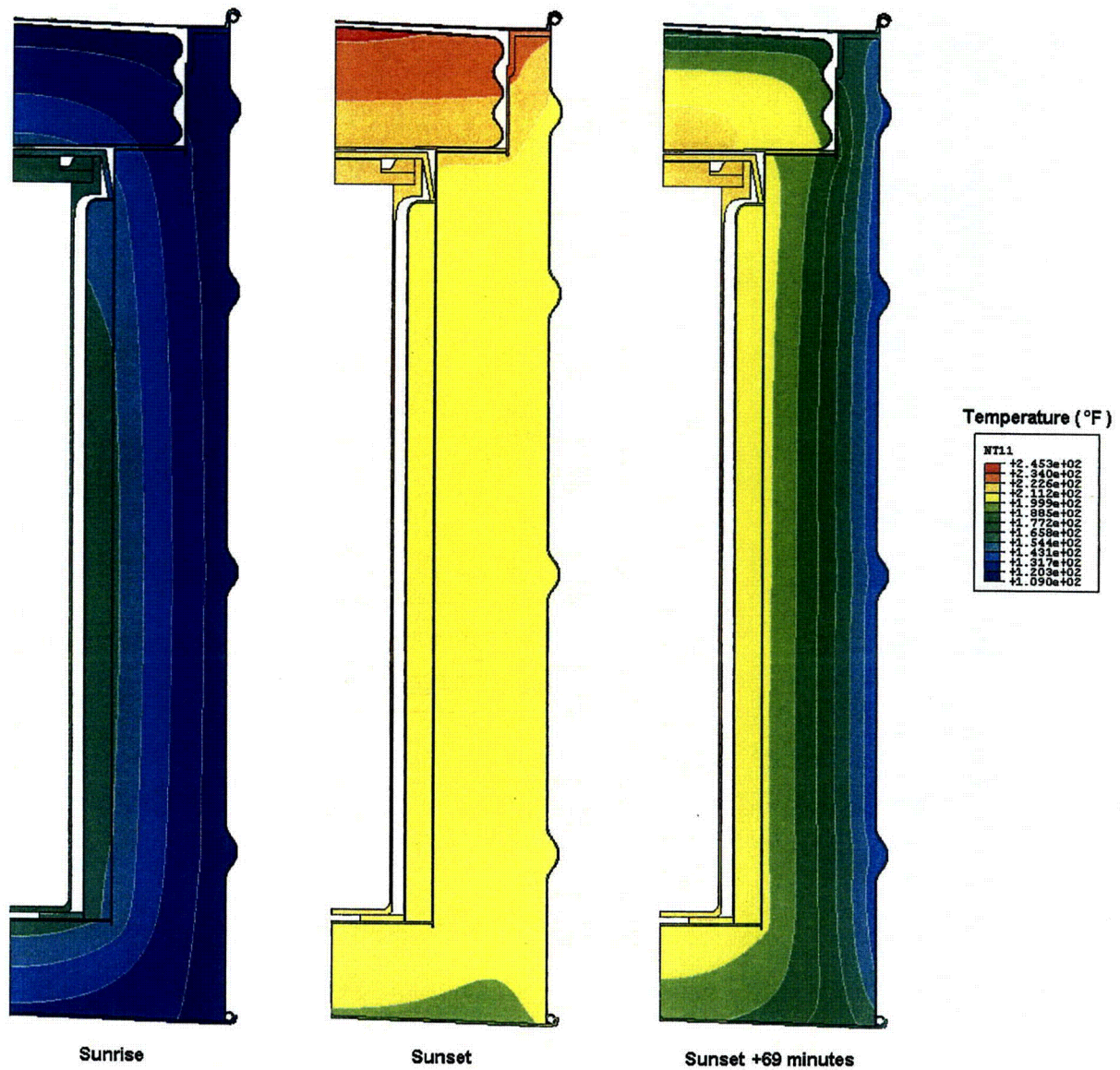


Figure 18. Temperature distribution in the ES-3100 shipping container for NCT (20 W content heat load) typical day of transient analysis (elements representing air not shown for clarity).



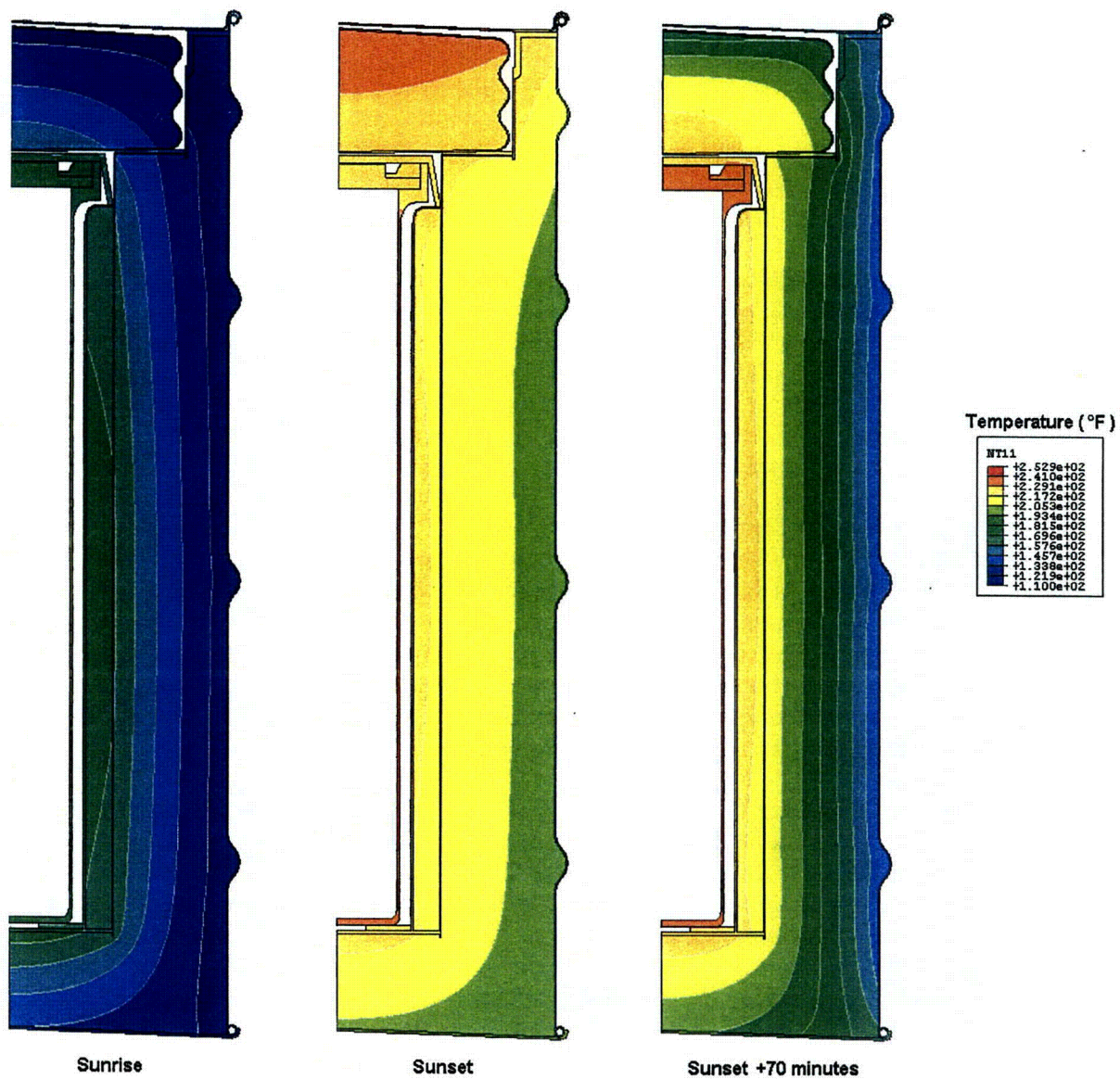


Figure 19. Temperature distribution in the ES-3100 shipping container for NCT (30 W content heat load) typical day of transient analysis (elements representing air not shown for clarity).

## Hypothetical Accident Conditions Analyses Results

Transient thermal analyses are performed on the finite element model of the ES-3100 shipping container (undamaged configuration) to simulate HAC as prescribed by 10 CFR 71.73(c)(4).<sup>[1]</sup> A 30-minute fire of 1475°F (800°C) is simulated by applying natural convection and radiant exchange boundary conditions to all external surfaces of the drum (assuming the drum is in a horizontal orientation) with content heat loads of 0, 0.4, 20, and 30 W. There are no heat flux boundary conditions simulating insolation applied to the model before and during the 30-minute fire. The initial temperature distribution within the package having content heat loads of 0.4, 20, and 30 W is obtained from their respective steady-state analyses. The initial temperature distribution within the package having no content heat load (0 W) is assumed to be at a uniform temperature equal to the ambient temperature of 100°F (37.8°C). As with the steady-state analyses discussed previously, applying a uniform heat flux to the internal surfaces of the elements representing the containment vessel simulates the content heat load.

Following the 30-minute fire transient analyses, 48-hour cool-down transient thermal analyses are performed using the temperature distribution at the end of the fire as the initial temperature distribution. During post-fire cool-down, natural convection and radiant exchange boundary conditions are applied to all external surfaces of the drum (assuming the drum is in a horizontal orientation). Additionally, cases are analyzed in which insolation is included during the post-fire cool-down. For the cases in which insolation is applied to the model during cool-down, insolation is applied during the first 12-hour period following the 30-minute fire, then alternated (off, then on) as was done for NCT.

Based on previous analyses of a similar package<sup>[9]</sup> (see Appendix 3.6.1), it was noted that using the low-end density of Kaolite results in higher containment vessel temperatures than using the high-end density of Kaolite. For this reason, the NCT and HAC thermal analyses were run using a density of 19.4 lbm/ft<sup>3</sup> (see Table 1). Similarly, the low-end density of the neutron absorber (100 lbm/ft<sup>3</sup>) was also used in these analyses. However, while using these low-end densities will result in higher temperatures to the containment vessel, using the high-end densities for these two materials will result in higher temperature differences from the baseline HAC case. Thus, runs are also made for heat loads of 0, 0.4, 20, and 30 W using a Kaolite density of 30 lbm/ft<sup>3</sup> and a neutron absorber density of 110 lbm/ft<sup>3</sup>.

The maximum temperatures calculated for the ES-3100 shipping container for HAC are summarized in Table 6 for the analyses using a Kaolite density of 19.4 lbm/ft<sup>3</sup> and a neutron absorber density of 100 lbm/ft<sup>3</sup>. The maximum temperatures calculated for the ES-3100 shipping container for HAC are summarized in Table 7 for the analyses using a Kaolite density of 30 lbm/ft<sup>3</sup> and a neutron absorber density of 110 lbm/ft<sup>3</sup>. The thermal analyses that use the low-end density values for Kaolite and the neutron absorber achieve the higher package temperatures (see Table 6). Temperature-history plots of several locations within the model are also depicted graphically in Figure 20 through Figure 23 for content heat loads of 0, 0.4, 20, and 30 W for the analyses using a Kaolite density of 19.4 lbm/ft<sup>3</sup> and a neutron absorber density of 100 lbm/ft<sup>3</sup>.

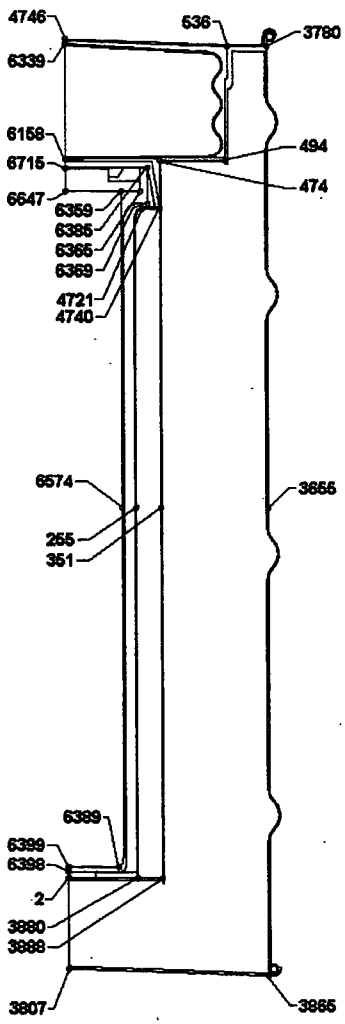
The HAC thermal analyses presented in this report are performed using a finite element model that represents an undamaged ES-3100 shipping container. While the cumulative damage from NCT and HAC drop tests, crush tests, and puncture tests, must be considered when evaluating the performance of the package to HAC, the temperature differences (i.e., adjustments) calculated from the data presented in Table 6 and Table 7 are of value when combined with the physical test data when making this assessment.

Table 6. ES-3100 shipping container HAC maximum temperatures (Kaolite density of 19.4 lbm/ft<sup>3</sup> and neutron absorber density of 100 lbm/ft<sup>3</sup>).

Node map <sup>(a)</sup>	Node coordinates (in.)			HAC maximum temperature (°F)							
	No.	r	z	0 W		0.4 W		20 W		30 W	
				Insolation during cool-down?		Insolation during cool-down?		Insolation during cool-down?		Insolation during cool-down?	
				No <sup>(b)</sup>	Yes	No	Yes	No	Yes	No	Yes
4746	2	0.000	4.505	225.5	232.1	226.2	232.8	255.5	261.7	269.5	275.7
6339	255	3.180	21.528	194.5	212.5	195.2	213.2	223.8	241.3	237.8	255.3
6159	351	4.300	21.528	195.8	211.9	196.4	212.5	222.3	237.8	234.8	250.3
6715	474	4.300	37.535	392.9	395.0	393.2	395.4	407.6	409.7	414.2	416.3
6647	494	7.325	37.535	671.2	672.0	671.4	672.3	679.1	680.0	682.5	683.3
6359	536	7.385	42.755	1380.4	1380.4	1380.4	1380.4	1380.9	1380.9	1381.1	1381.1
6385	3655	9.185	21.528	1457.8	1457.8	1457.8	1457.8	1458.0	1458.0	1458.1	1458.1
6365	3780	9.185	42.755	1427.8	1427.8	1427.9	1427.9	1428.1	1428.1	1428.2	1428.2
6369	3807	0.000	0.320	1454.5	1454.5	1454.5	1454.5	1454.9	1454.9	1455.0	1455.0
4721	3865	9.185	0.008	1470.1	1470.1	1470.1	1470.1	1470.1	1470.1	1470.2	1470.2
4740	3880	3.178	4.505	230.6	236.4	231.2	237.0	257.1	262.5	269.4	274.8
6574	3888	4.300	4.505	236.9	241.7	237.5	242.3	261.5	266.1	272.9	277.5
255	4721	3.500	35.275	245.7	252.8	246.2	253.3	266.8	273.8	276.6	283.6
351	4740	4.300	35.275	258.4	263.5	258.8	264.0	278.1	283.1	287.1	292.1
	4746	0.000	43.065	1448.0	1448.0	1448.0	1448.0	1448.2	1448.2	1448.3	1448.3
	6158	0.000	37.579	308.7	311.6	309.1	312.0	328.3	331.2	337.3	340.2
	6339	0.000	42.859	1335.1	1335.1	1335.2	1335.2	1336.4	1336.4	1336.9	1336.9
	6359 <sup>(c)</sup>	2.530	36.075	236.7	247.6	237.3	248.3	266.2	276.6	279.8	289.9
	6365 <sup>(c)</sup>	3.425	36.075	236.6	247.6	237.3	248.3	266.0	276.4	279.5	289.7
	6369	3.750	35.525	236.5	247.6	237.2	248.2	265.8	276.2	279.3	289.5
	6385	3.750	37.175	237.3	248.2	237.9	248.8	266.1	276.4	279.4	289.5
	6389	2.310	5.025	219.0	227.4	219.9	228.2	255.3	263.1	272.2	279.9
	6398	0.000	4.775	219.7	227.9	220.5	228.7	255.6	263.3	272.5	280.0
	6399	0.000	5.025	219.7	227.9	220.5	228.7	255.6	263.3	272.5	280.0
	6574	2.530	21.528	196.1	214.9	197.3	216.0	246.7	263.8	269.9	286.5
	6647	0.000	36.075	237.2	248.0	237.9	248.6	266.8	277.0	280.4	290.4
	6715	0.000	37.135	237.4	248.1	238.0	248.8	266.8	277.0	280.4	290.4

- Notes: (a) See Figure 8 through Figure 11 for details of node locations.  
(b) Baseline case for  $\Delta T$  comparisons.  
(c) Approximate location of the CV O-ring.

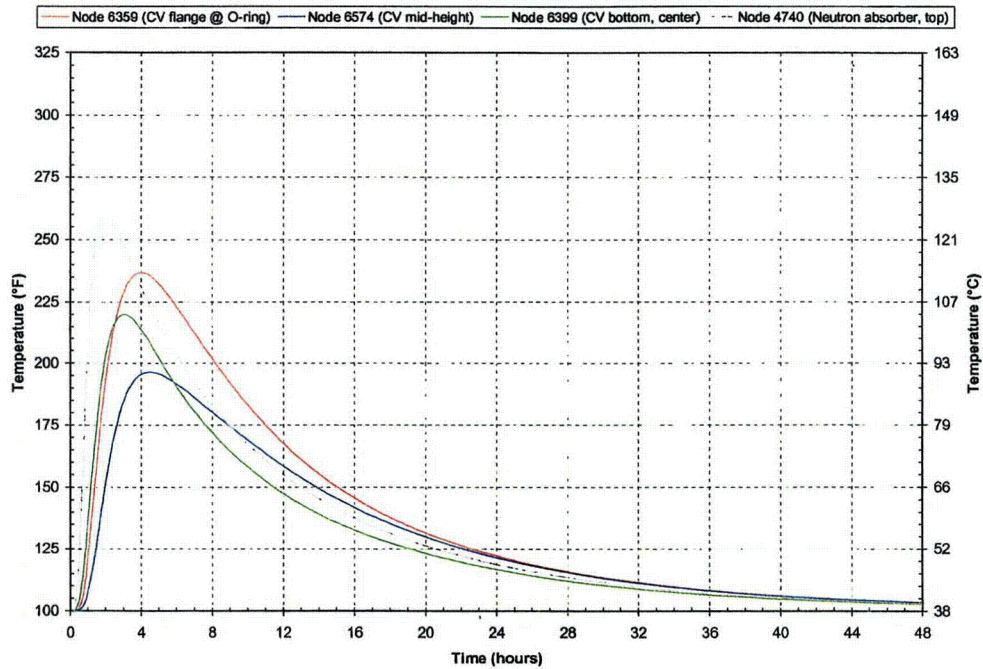
**Table 7. ES-3100 shipping container HAC maximum temperatures (Kaolite density of 30 lbm/ft<sup>3</sup> and neutron absorber density of 110 lbm/ft<sup>3</sup>).**

Node map <sup>(a)</sup>	Node coordinates (in.)			HAC maximum temperature (°F)							
	No.	r	z	0 W		0.4 W		20 W		30 W	
				Insolation during cool-down?		Insolation during cool-down?		Insolation during cool-down?		Insolation during cool-down?	
				No <sup>(b)</sup>	Yes	No	Yes	No	Yes	No	Yes
	2	0.000	4.505	209.9	218.9	210.6	219.6	240.4	248.8	254.6	262.8
	255	3.180	21.528	185.5	207.7	186.1	208.4	215.1	236.6	229.3	250.6
	351	4.300	21.528	185.6	207.4	186.2	208.0	212.3	233.3	225.0	245.9
	474	4.300	37.535	342.9	345.5	343.3	345.9	358.1	360.7	365.0	367.5
	494	7.325	37.535	596.3	597.4	596.5	597.6	604.7	605.8	608.3	609.4
	536	7.385	42.755	1366.8	1366.8	1366.8	1366.8	1367.4	1367.4	1367.6	1367.6
	3655	9.185	21.528	1452.8	1452.8	1452.8	1452.8	1453.0	1453.0	1453.1	1453.1
	3780	9.185	42.755	1420.8	1420.8	1420.8	1420.8	1421.0	1421.0	1421.2	1421.2
	3807	0.000	0.320	1449.4	1449.4	1449.4	1449.4	1449.8	1449.8	1449.9	1449.9
	3865	9.185	0.008	1467.3	1467.3	1467.3	1467.3	1467.4	1467.4	1467.4	1467.4
	3880	3.178	4.505	213.1	221.4	213.7	222.0	240.0	247.9	252.5	260.3
	3888	4.300	4.505	217.0	224.4	217.6	225.0	242.1	249.1	253.8	260.7
	4721	3.500	35.275	228.0	237.5	228.5	238.0	249.7	259.0	259.7	269.0
	4740	4.300	35.275	236.5	243.8	236.9	244.3	256.7	263.9	266.0	273.2
	4746	0.000	43.065	1441.8	1441.8	1441.8	1441.8	1442.0	1442.0	1442.1	1442.1
	6158	0.000	37.579	277.3	281.8	277.8	282.3	297.5	302.0	306.7	311.2
	6339	0.000	42.859	1299.5	1299.5	1299.6	1299.6	1301.1	1301.1	1301.7	1301.7
	6359 <sup>(c)</sup>	2.530	36.075	225.1	237.3	225.8	237.9	254.7	266.1	268.3	279.6
	6365 <sup>(c)</sup>	3.425	36.075	225.0	237.3	225.7	237.9	254.5	266.0	268.1	279.3
	6369	3.750	35.525	224.9	237.2	225.6	237.8	254.3	265.8	267.9	279.2
	6385	3.750	37.175	225.5	237.6	226.2	238.3	254.6	266.1	268.0	279.2
	6389	2.310	5.025	205.3	215.9	206.2	216.8	242.0	251.9	259.2	268.9
	6398	0.000	4.775	205.8	216.3	206.7	217.1	242.2	252.0	259.2	268.8
	6399	0.000	5.025	205.8	216.3	206.7	217.1	242.2	252.0	259.3	268.8
	6574	2.530	21.528	187.8	209.1	189.0	210.2	238.9	258.4	262.4	281.3
	6647	0.000	36.075	225.6	237.7	226.3	238.3	255.2	266.5	268.9	280.0
	6715	0.000	37.135	225.8	237.8	226.4	238.4	255.2	266.5	268.9	280.0

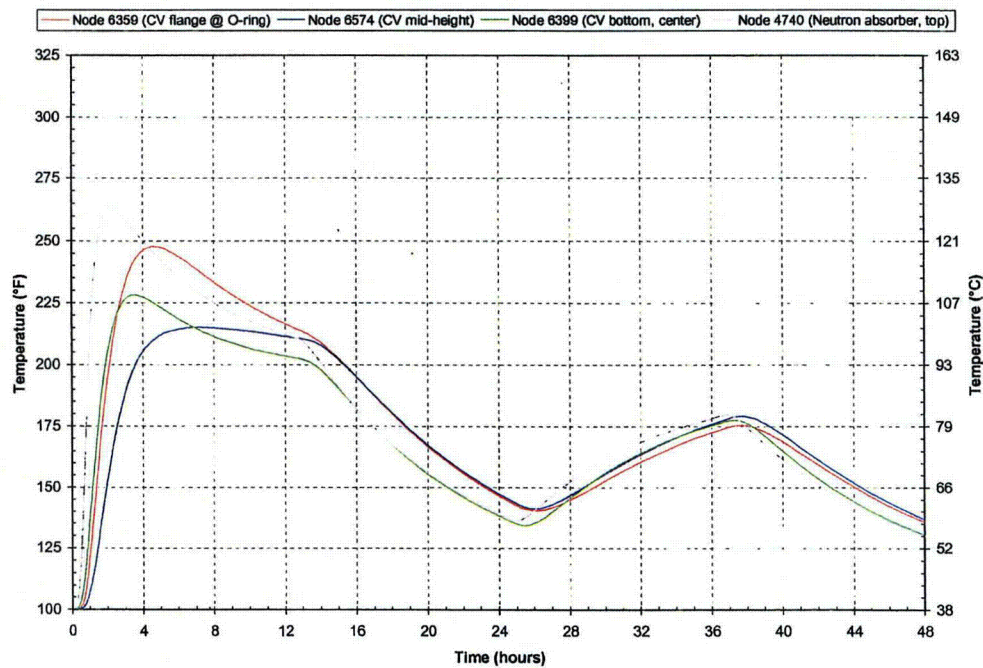
Notes: (a) See Figure 8 through Figure 11 for details of node locations.

(b) Baseline case for  $\Delta T$  comparisons.

(c) Approximate location of the CV O-ring.



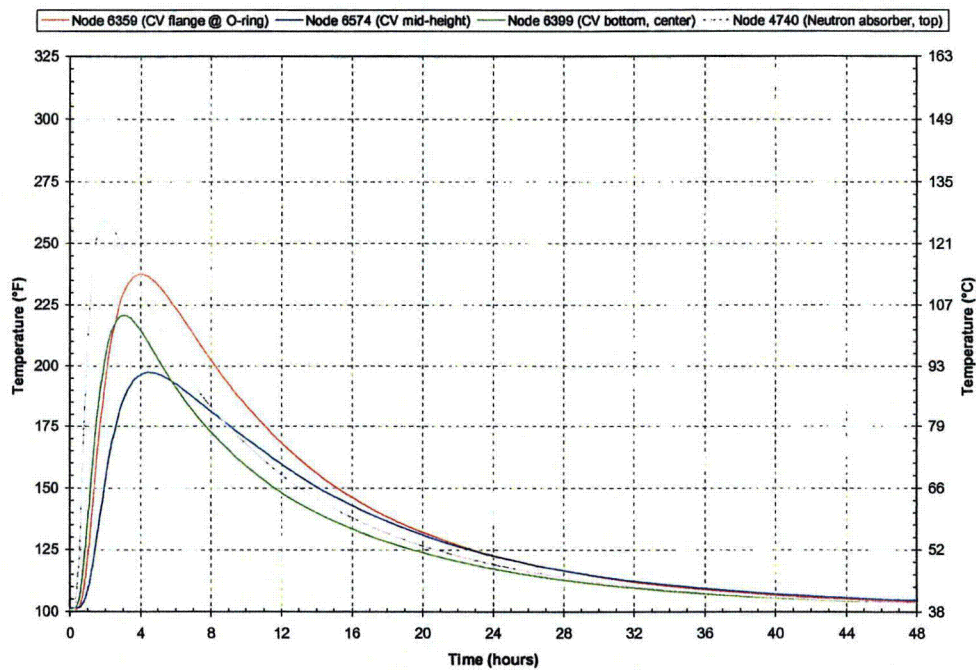
(a) No insolation during post-fire cool-down.



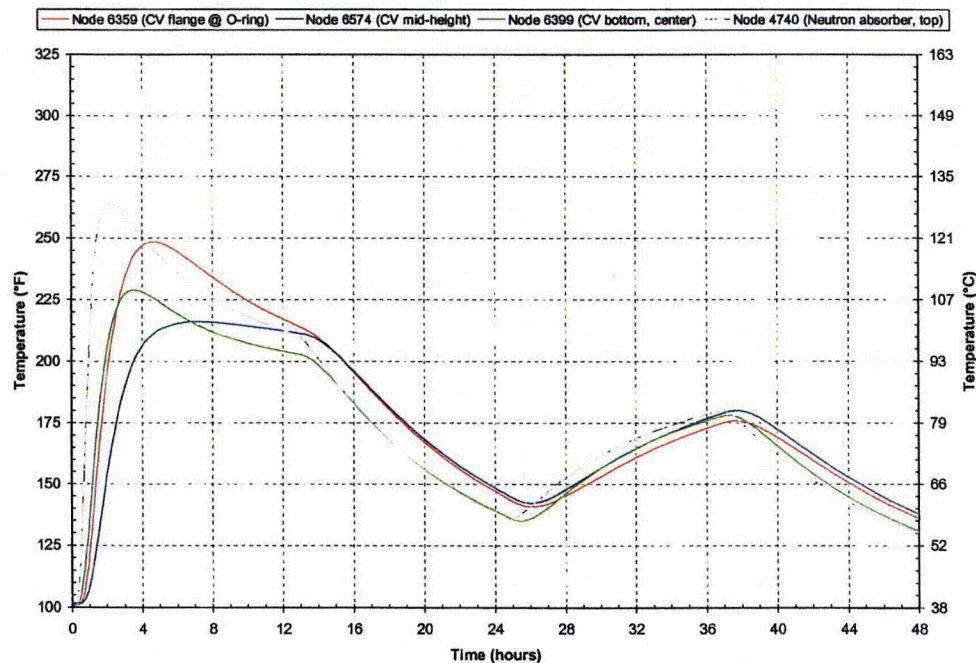
(b) Insolation during post-fire cool-down.

**Figure 20. ES-3100 shipping container transient temperatures for HAC—no content heat load and lower bound Kaolite and neutron absorber densities (see Figure 8 through Figure 11 for node locations).**



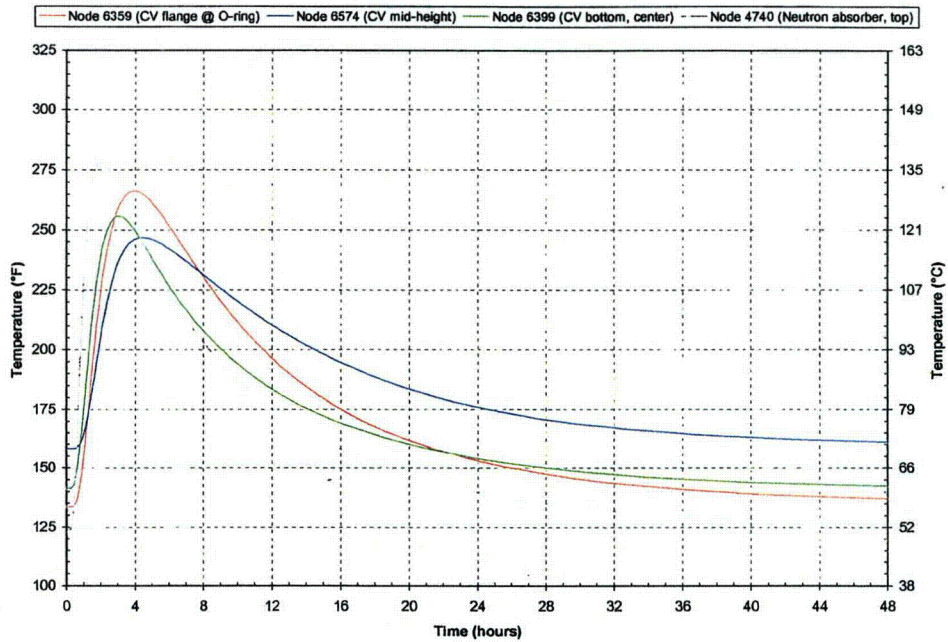


(a) No insolation during post-fire cool-down.

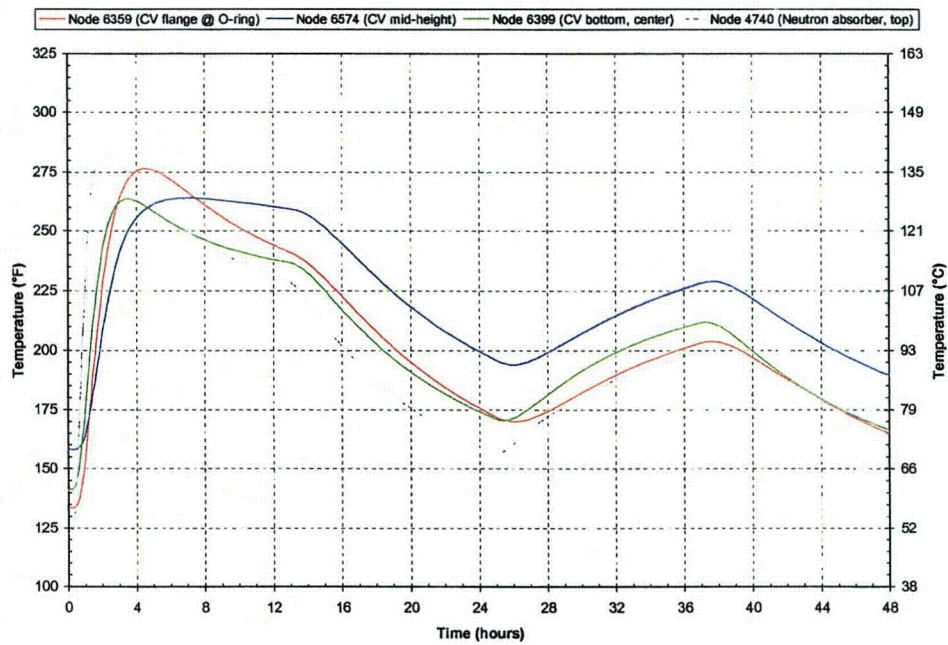


(b) Insolation during post-fire cool-down.

Figure 21. ES-3100 shipping container transient temperatures for HAC, 0.4 W content heat load and lower bound Kaolite and neutron absorber densities (see Figure 8 for through Figure 11 for node locations).

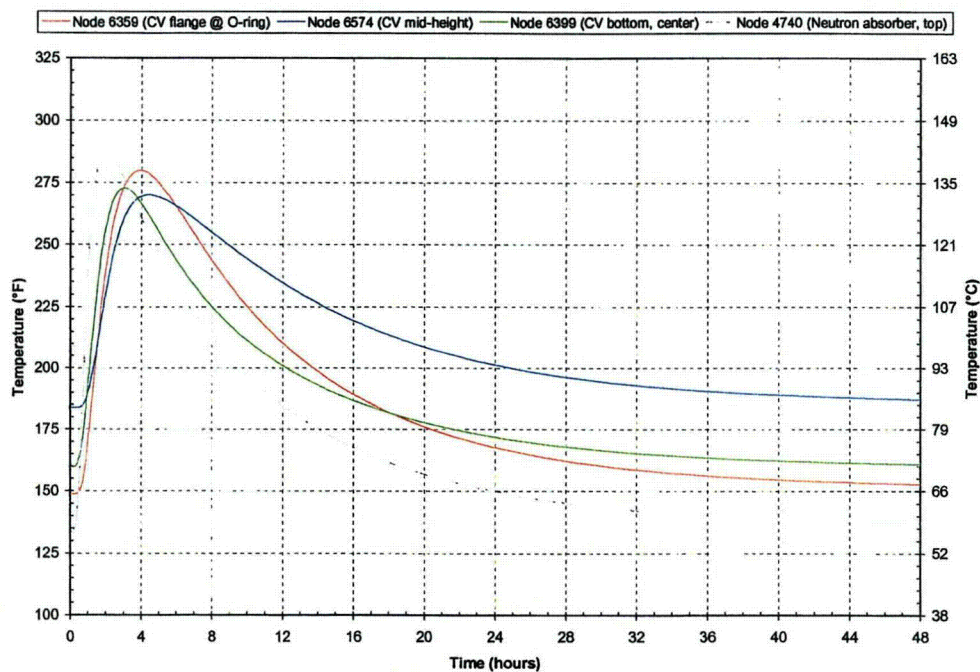


(a) No insolation during post-fire cool-down.

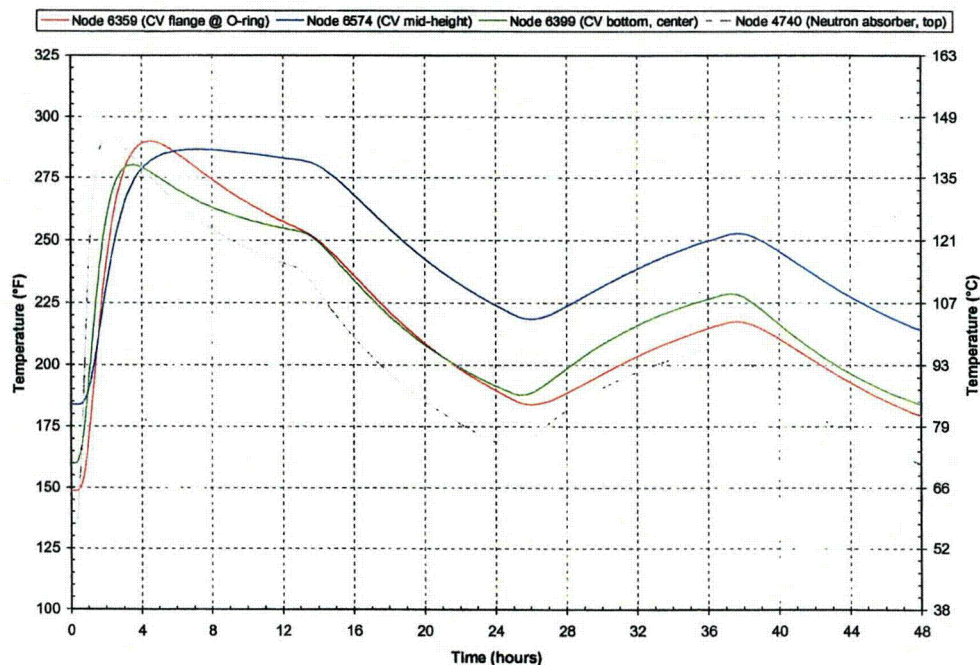


(b) Insolation during post-fire cool-down.

Figure 22. ES-3100 shipping container transient temperatures for HAC, 20 W content heat load and lower bound Kaolite and neutron absorber densities (see Figure 8 through Figure 11 for node locations).



(a) No insolation during post-fire cool-down.



(b) Insolation during post-fire cool-down.

Figure 23. ES-3100 shipping container transient temperatures for HAC, 30 W content heat load and lower bound Kaolite and neutron absorber densities (see Figure 8 through Figure 11 for node locations).

## APPENDIX 3.6.2 REFERENCES

1. *Packaging and Transportation of Radioactive Materials*, U.S. Nuclear Regulatory Commission, Code of Federal Regulations, Title 10 – Energy, Part 71, January 1, 2004.
2. L. S. Dickerson, M. R. Feldman, and R. D. Michaelhaugh, *Test Report of the ES-3100 Package*, Volumes 1–3, ORNL/NTRC-013, Rev. 0, Nuclear Science and Technology Division, Oak Ridge National Laboratory, Oak Ridge, Tennessee, September 10, 2004.
3. MSC. Patran 2004, Version 12.0.044, MacNeal Schwendler Corporation, 2004.
4. ABAQUS/CAE, Version 6.4-1, Build ID: 2003\_09\_29-11.18.28 46457, Abaqus, Inc., 2003.
5. R. Siegel and J. R. Howell, *Thermal Radiation Heat Transfer*, Second Edition, Hemisphere Publishing Corporation, 1981.
6. F. P. Incropera and D. P. DeWitt, *Fundamentals of Heat and Mass Transfer*, Second Edition, John Wiley & Sons, New York, 1985.
7. J. C. Anderson and M. R. Feldman, *Thermal Modeling of Packages for Normal Conditions of Transport with Insolation*, Proceedings of the ASME Heat Transfer Division, HTD-Vol. 317-2, 1995, International Mechanical Engineering Congress and Exposition, November 1995.
8. ABAQUS/Standard, Version 6.4-1, 2003\_09\_29-11.18.28 46457, Abaqus, Inc. , 2003.
9. P. A. Bales, *Thermal Analyses of the ES-3100 Shipping Container for NCT and HAC*, DAC-PKG-801699-A001, Rev. 1, BWXT Y-12, December 30, 2004.



### **APPENDIX 3.6.3**

#### **THERMAL STRESS EVALUATION OF THE ES-3100 SHIPPING CONTAINER DRUM BODY ASSEMBLY FOR NCT (FINAL DESIGN WITH CATALOG 277-4 NEUTRON ABSORBER)**





## APPENDIX 3.6.3

### THERMAL STRESS EVALUATION OF THE ES-3100 SHIPPING CONTAINER DRUM BODY ASSEMBLY FOR NCT (FINAL DESIGN WITH CATALOG 277-4 NEUTRON ABSORBER)

#### INTRODUCTION

Static stress analyses of the ES-3100 shipping container are performed to determine the maximum thermal stresses within the packaging when exposed to Normal Conditions of Transport (NCT) as specified in 10 CFR 71.71(c)(1).<sup>[1]</sup> Transient thermal analyses were previously performed<sup>[2]</sup> (see Appendix 3.6.2) on the ES-3100 shipping container to determine its response to NCT. The thermal analyses treat the problem as a cyclic transient with the incident heat flux due to solar radiation applied and not applied in alternating 12-hour periods. The calculated temperature distributions within the drum body assembly for NCT at various times are then mapped onto the structural model, and static analyses are performed for each time step in the thermal analyses.

#### FINITE ELEMENT MODEL DESCRIPTION

A two-dimensional axisymmetric finite element model of the ES-3100 shipping container is constructed using MSC.Patran<sup>[3]</sup> and imported as an orphaned mesh into ABAQUS/CAE<sup>[4]</sup> for application of boundary conditions, interactions, and loads. The model is constructed of CAX4I (four-node bilinear axisymmetric quadrilateral, incompatible mode) elements for stress evaluation. These elements are chosen because they can accurately capture bending stresses with only one element through the thickness of a structure. A schematic of the finite element model is presented in Figure 1 with details of the upper and lower portions of the model shown in Figure 2 and Figure 3, respectively. The model consists of three materials: stainless steel (drum, drum bottom plate, and drum liner weldment), Kaolite, and neutron absorber. Details of the model are discussed in the following sections.

Surface-to-surface contact interactions are modeled between contacting surfaces in the static stress model. These interactions are shown graphically in Figure 2 and Figure 3. For all interactions, the tangential behavior is modeled as “frictionless” while the normal behavior is modeled as “hard contact.” For the interactions modeled between the bottom of the neutron absorber and the drum liner and between the drum Kaolite bottom and the drum bottom plate, the contacting surfaces are not allowed to separate after contact is made.

The radial degree-of-freedom ( $U_r$ ) of each node along the centerline of the model is fixed to simulate symmetry. Additionally, the axial degree-of-freedom ( $U_z$ ) of one node on the drum bottom plate is fixed.

The temperatures calculated for NCT in Appendix 3.6.2 are stored in the ‘NCT.fil’ file for each of the content head loads analyzed. The temperature distribution for each time of interest is mapped onto the static stress model using the ‘\*Temperature’ keyword. The specific times of interest from the transient thermal analyses are at each increment in the final day/night cycle (after “quasi steady-state” is reached).

The mechanical properties of the materials used in the static stress analyses are presented in Table 1. The modulus of elasticity of Kaolite presented in Table 1 is calculated from the first two points of the compressive stress-strain assuming a Poisson’s ratio of 0.01.<sup>[5]</sup>

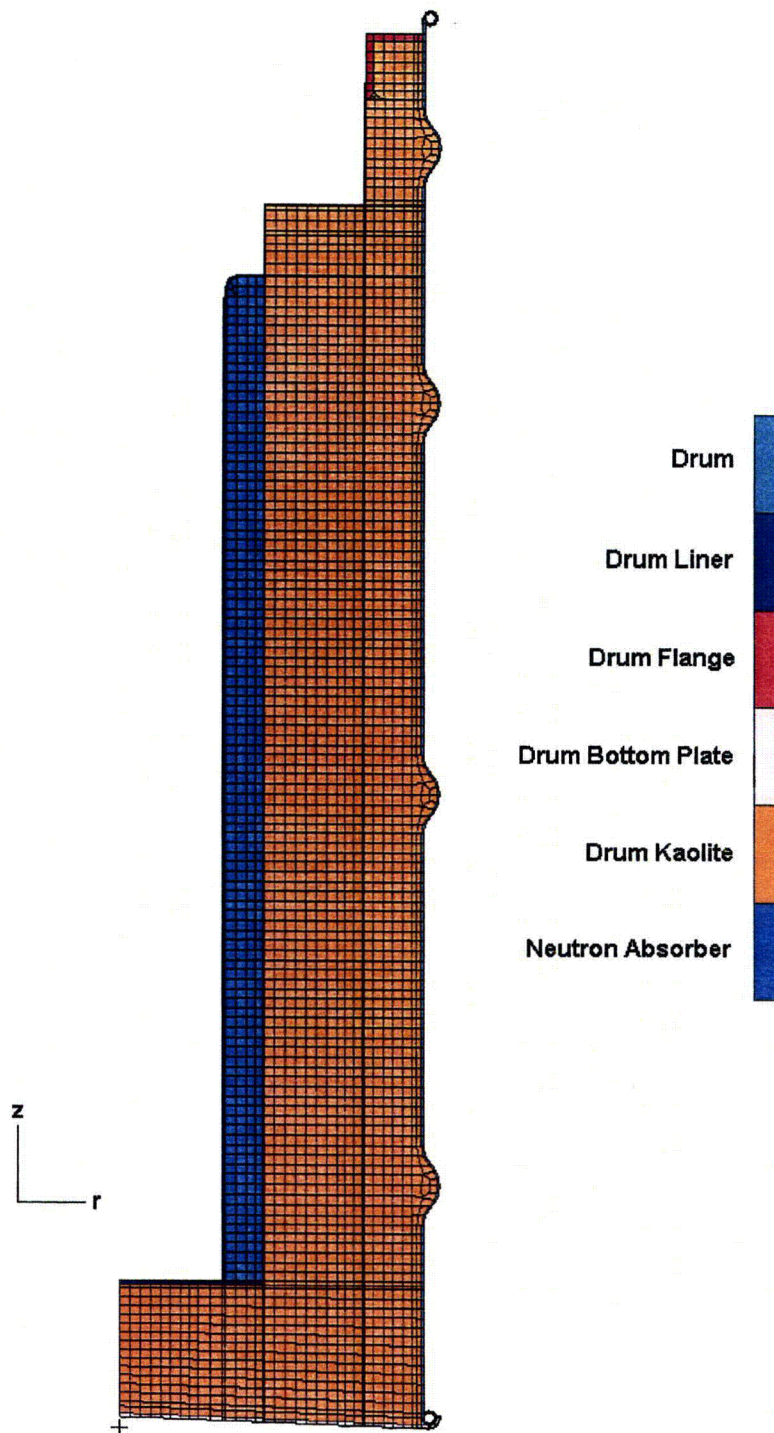


**Figure 1. MSC.Patran axisymmetric finite element model of the ES-3100 shipping container drum body assembly.**

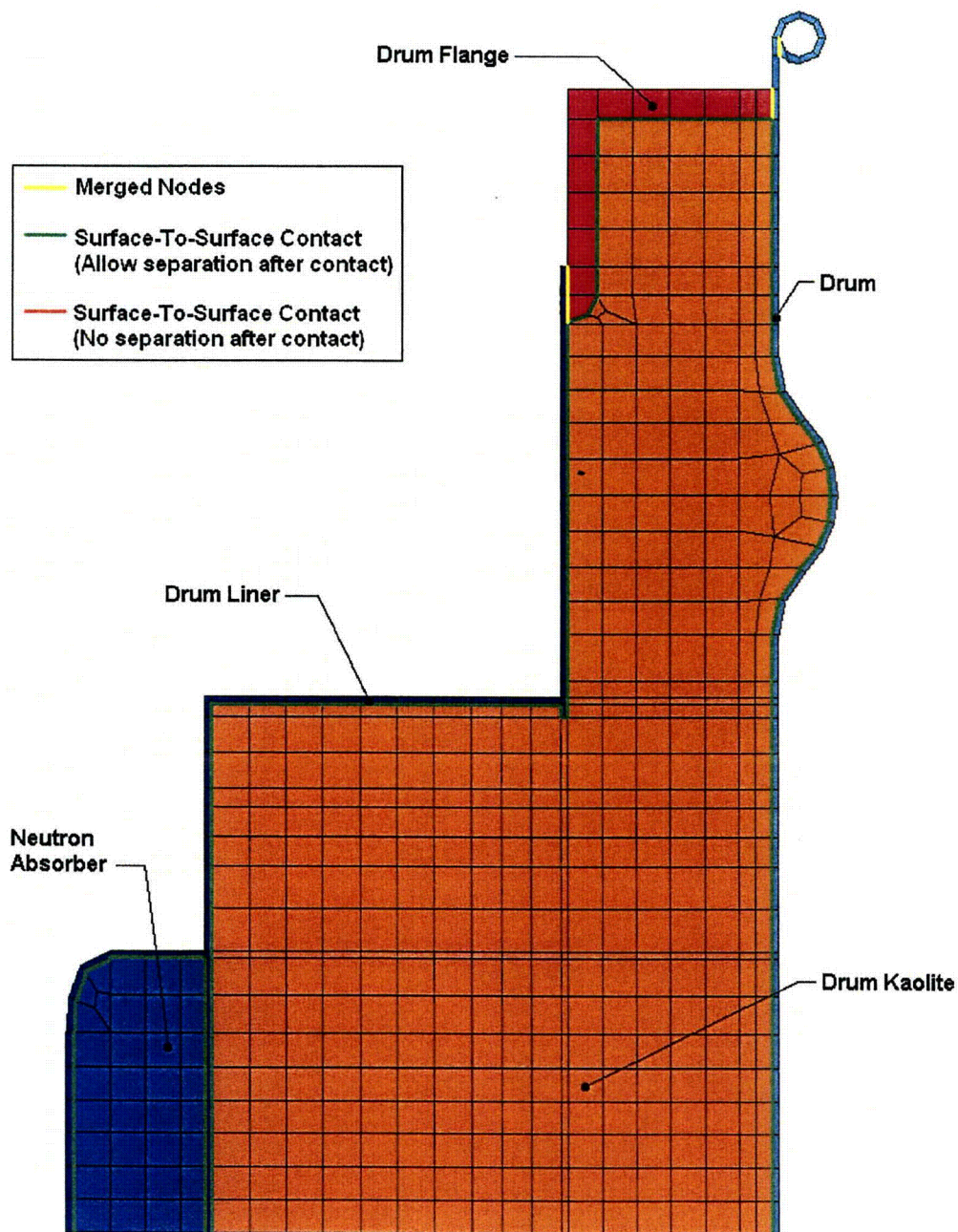
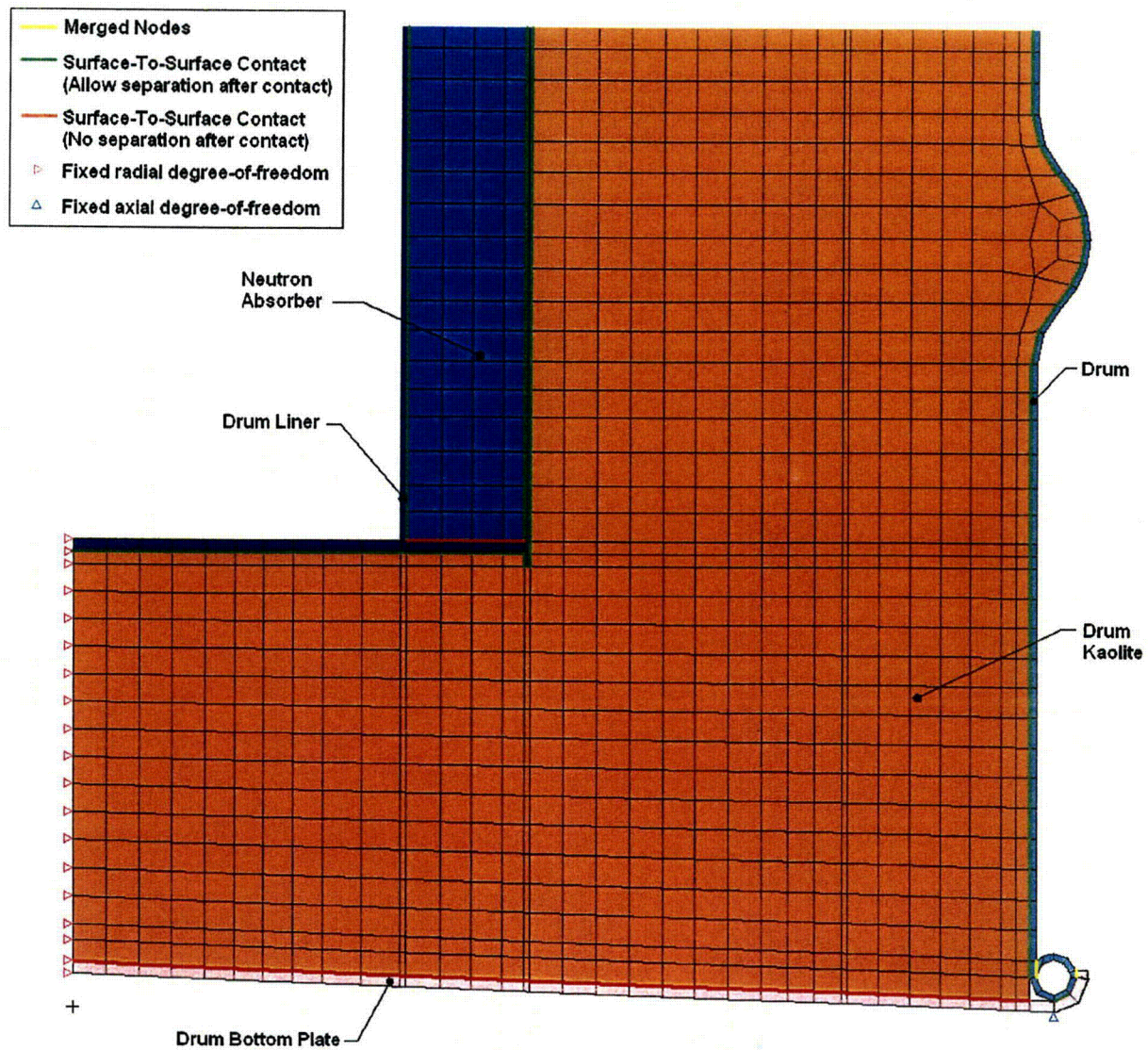


Figure 2. MSC.Patran axisymmetric finite element model of the ES-3100 shipping container drum body assembly (upper portion detail).





**Figure 3. MSC.Patran axisymmetric finite element model of the ES-3100 shipping container drum body assembly (lower portion detail).**

**Table 1. Mechanical properties of the materials used in the static stress analyses.**

Material	Temperature (°F)	Modulus of elasticity (psi)	Poisson's ratio	Density (lbm/in <sup>3</sup> )	Coefficient of thermal expansion (in./in./°F)
Stainless Steel	-40	28.6×10 <sup>6</sup> <sup>(a)</sup>	0.29 <sup>(b)</sup>	0.285 <sup>(c)</sup>	8.2×10 <sup>-6</sup> <sup>(e)</sup>
	100	28.14×10 <sup>6</sup>	—	—	8.6×10 <sup>-6</sup>
	200	27.6×10 <sup>6</sup>	—	—	8.9×10 <sup>-6</sup>
	300	27.0×10 <sup>6</sup>	—	—	9.2×10 <sup>-6</sup>
Kaolite	—	29,210 <sup>(d)</sup>	0.01 <sup>(d)</sup>	0.013 <sup>(f)</sup>	5.04×10 <sup>-6</sup> <sup>(g)</sup>
Neutron Absorber	-40	1.991×10 <sup>6</sup> <sup>(h)</sup>	0.33 <sup>(h)</sup>	0.0608 <sup>(h)</sup>	7.056×10 <sup>-6</sup> <sup>(i)</sup>
	-4	—	—	—	7.222×10 <sup>-6</sup>
	32	—	—	—	7.222×10 <sup>-6</sup>
	70	0.984×10 <sup>6</sup>	0.28	—	—
	100	0.403×10 <sup>6</sup>	0.25	—	—
	104	—	—	—	7.000×10 <sup>-6</sup>
	140	—	—	—	6.444×10 <sup>-6</sup>
	176	—	—	—	5.778×10 <sup>-6</sup>
	212	—	—	—	5.389×10 <sup>-6</sup>
	248	—	—	—	5.056×10 <sup>-6</sup>
	284	—	—	—	4.889×10 <sup>-6</sup>
	302	—	—	—	4.833×10 <sup>-6</sup>

- Notes: (a) ASME Boiler and Pressure Vessel Code, Sect. II, Part D, Subpart 2, Tables TE-1, B column, and TM-1.  
(b) R. A. Bailey, *Strain – A Material Database*, Lawrence Livermore National Laboratory, 1989.  
(c) F. P. Incropera and D. P. DeWitt, *Fundamentals of Heat and Mass Transfer*, 2nd edition, John Wiley & Sons, New York, 1985.  
(d) K. D. Handy, *Impact Analysis of ES3100 Design Concepts Using Borobond*, DAC-EA-801699-A001, BWXT Y-12, Oct. 2004. The Poisson's ratio of Kaolite is assumed to be a small value of 0.1.  
(e) *Metallic Materials and Elements for Aerospace Vehicle Structures*, MIL-HDBK-5E, May 1986.  
(f) Specification JS-YMN3-801580-A003 requires a baked density of 22.4 ± 3 lbm/ft<sup>3</sup>.  
(g) E-mail communication, Ken Moody (Thermal Ceramics, Inc.) to Paul Bales (BWXT Y-12), 12/9/04.  
(h) B. F. Smith and G. A. Byington, *Mechanical Properties of 277-4*, Y/DW-1987, January 19, 2005.  
(i) W. D. Porter and H. Wang, *Thermophysical Properties of Heat Resistant Shielding Material*, ORNL/TM-2004/290, ORNL, Dec. 2004. Coefficient of thermal expansion at each temperature taken as the maximum of values for Runs #2, #3, and #5.

## DISCUSSION OF ANALYTICAL RESULTS

All static stress analyses discussed in this report were performed using ABAQUS/Standard<sup>[6]</sup> on an Intel Pentium 4–based Microsoft Windows 2000 computer. These analyses are sequential-coupled thermal/structural analyses.

As previously stated, the nodal temperature results for the final day/night cycle of the transient thermal analyses of the ES-3100 shipping container were stored in results files (NCT.fil) for each content heat load analyzed. Because automatic time-stepping was used in the transient thermal analyses, the number of increments stored in each 'NCT.fil' file differs for each content heat load analyzed. The static stress analyses of the ES-3100 are performed for each time increment analyzed in the thermal analyses for the final day/night cycle during NCT by copying the 'NCT.fil' and 'NCT.prt' files from the thermal analysis of interest to the directory where the stress analysis is being performed and entering the '\*Temperature' keyword with the proper syntax for the time of interest. For example, for a content heat load of 0.4 W, the thermal stresses for time = 14.127 hours after sunrise (2.127 hours after sunset) on the final day/night

cycle (i.e., step = 11, increment = 29) are analyzed by entering the following keyword syntax via the keyword editor in ABAQUS/CAE:

```
*Temperature, file=NCT, bstep=11, binc=29, estep=11, einc=29
```

A separate static analysis is performed for each time step in the final day/night cycle of each thermal analysis for each content heat load.

The results of the static stress analyses for content heat loads of 0.4, 20, and 30 W are presented in Figure 4 through Figure 6. The stresses presented in these figures are the maximum nodal Mises stresses of each component at each point in time—as such, they don't necessarily occur at the same node location during the duration of the time period analyzed. The x-axes (i.e., time) are scaled in these figures such that the onset of sunrise on the final day/night cycle from the thermal analyses begins at time = 0 hours. Additionally, the stress (Mises) contours of the components of the finite element model are shown at various times in Figure 7 through Figure 11 for the case with a content heat load of 0.4 W. The time chosen for each stress contour plot coincides with the time that particular component reaches its maximum stress during the day/night cycle. The stress contours for the other heat loads investigated are similar to the 0.4 W case.

In addition to the static stress analyses performed for NCT, a static stress analysis is performed for exposure of the package to a -40°F ambient temperature (i.e., cold condition). A transient thermal analysis (24 hours in duration) is performed on the ES-3100 thermal model described in Appendix 3.6.2 to obtain the temperature distribution within the drum body assembly for exposure to cold conditions (see Appendix C for details). The package is assumed to be at an initial uniform temperature of 77°F, and no content heat load is applied. The natural convection coefficients (applied to the top and sides of the drum) are calculated for a -40°F ambient as described in Appendix 3.6.2 and are shown in Figure 12. A schematic of the thermal model showing several node locations for which the temperatures are tracked is presented in Figure 13. The transient temperatures calculated for cold conditions are presented in Figure 14 for several node locations. The maximum thermal stresses are presented in Figure 15 for this cold condition. Additionally, stress contours of the drum liner weldment, drum, and drum bottom plate are presented in Figure 16 through Figure 18 for the cold conditions at various times.

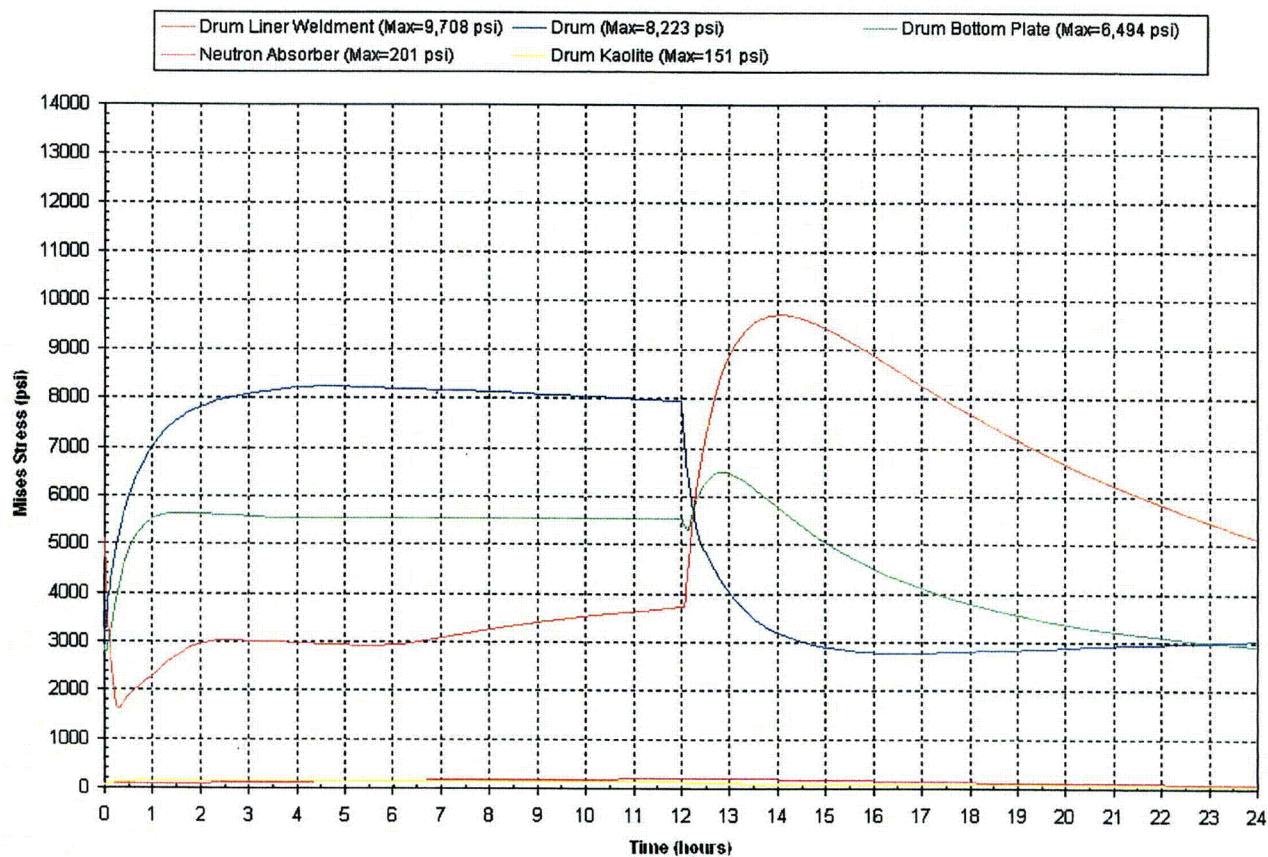


**Figure 4. Thermal stresses (Mises) in the ES-3100 shipping container drum body assembly during a typical NCT day/night cycle—0.4 W content heat load.**



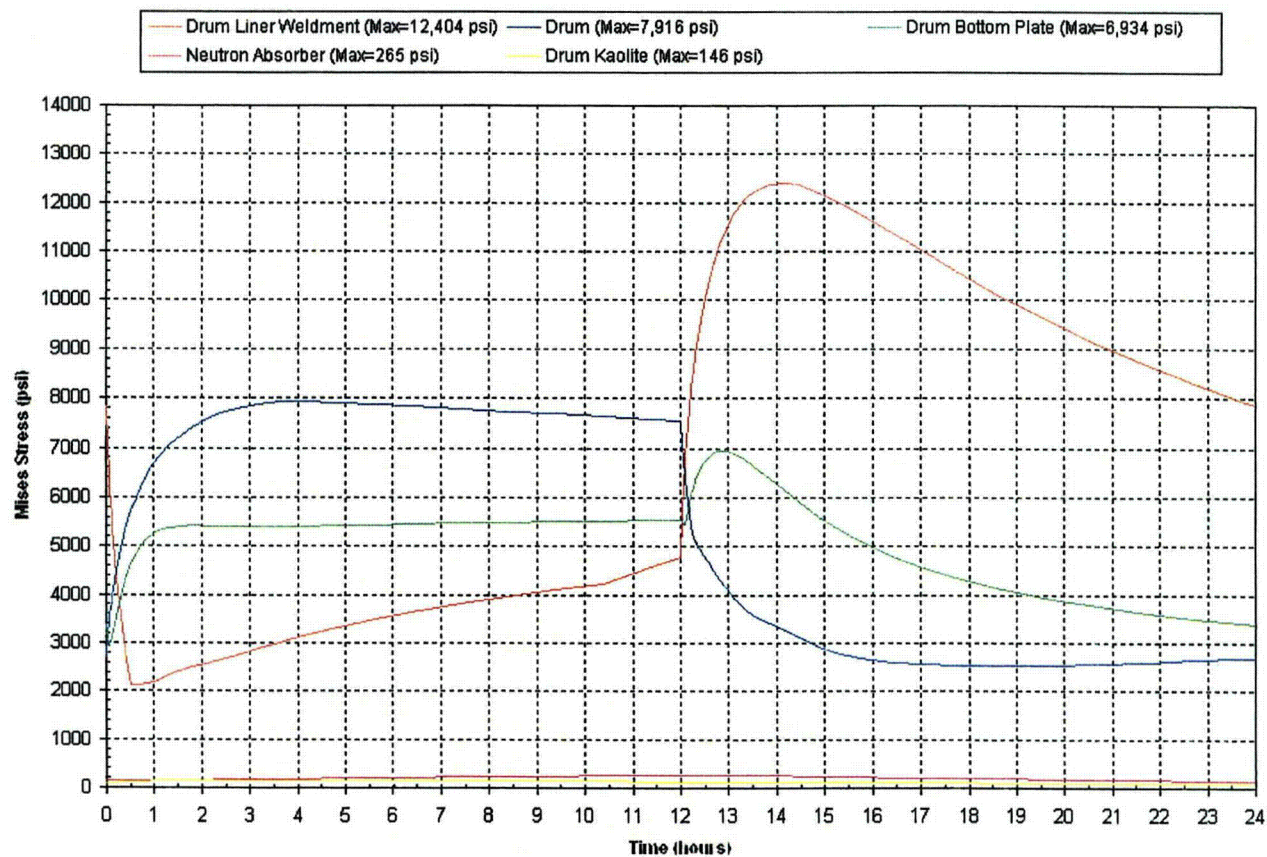


**Figure 5. Thermal stresses (Mises) in the ES-3100 shipping container drum body assembly during a typical NCT day/night cycle—20 W content heat load.**

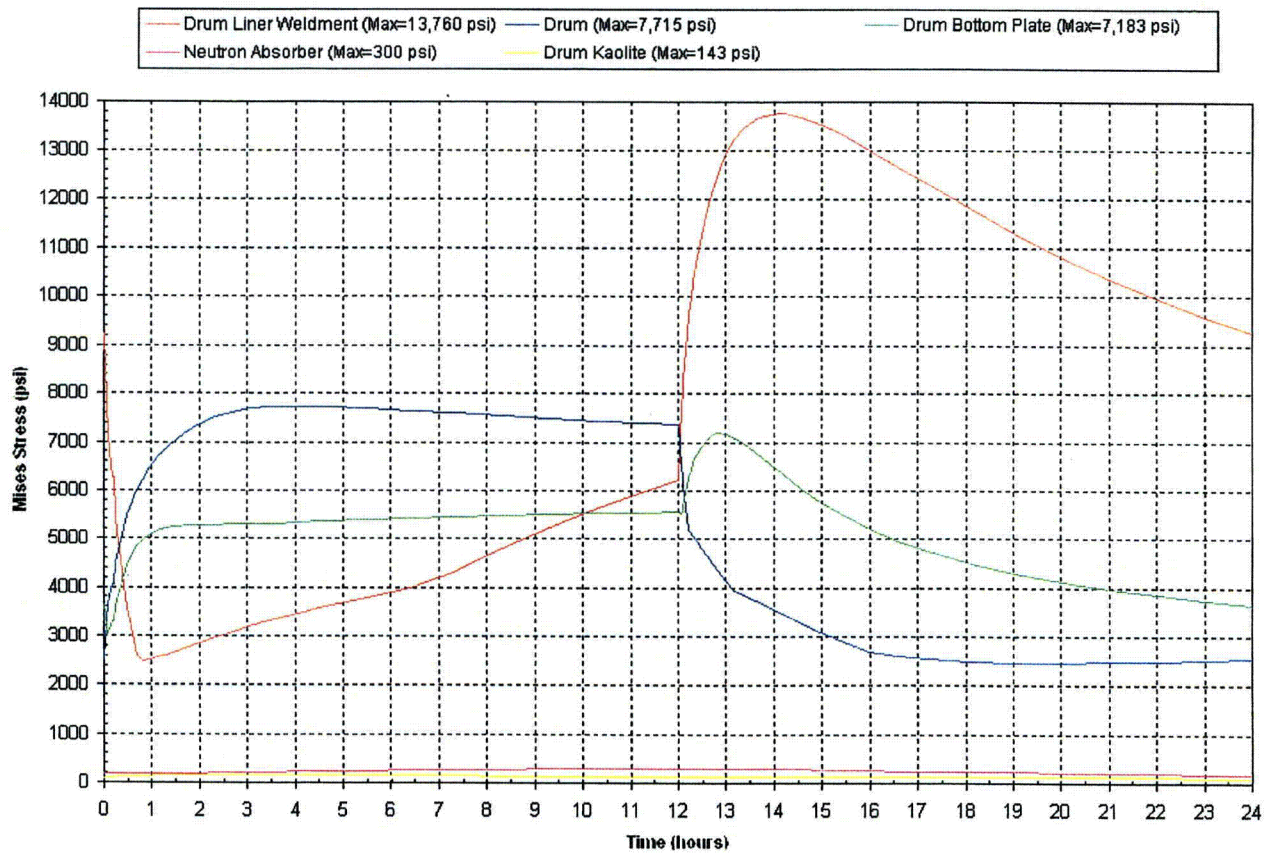
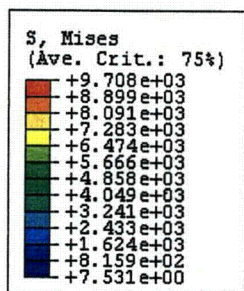
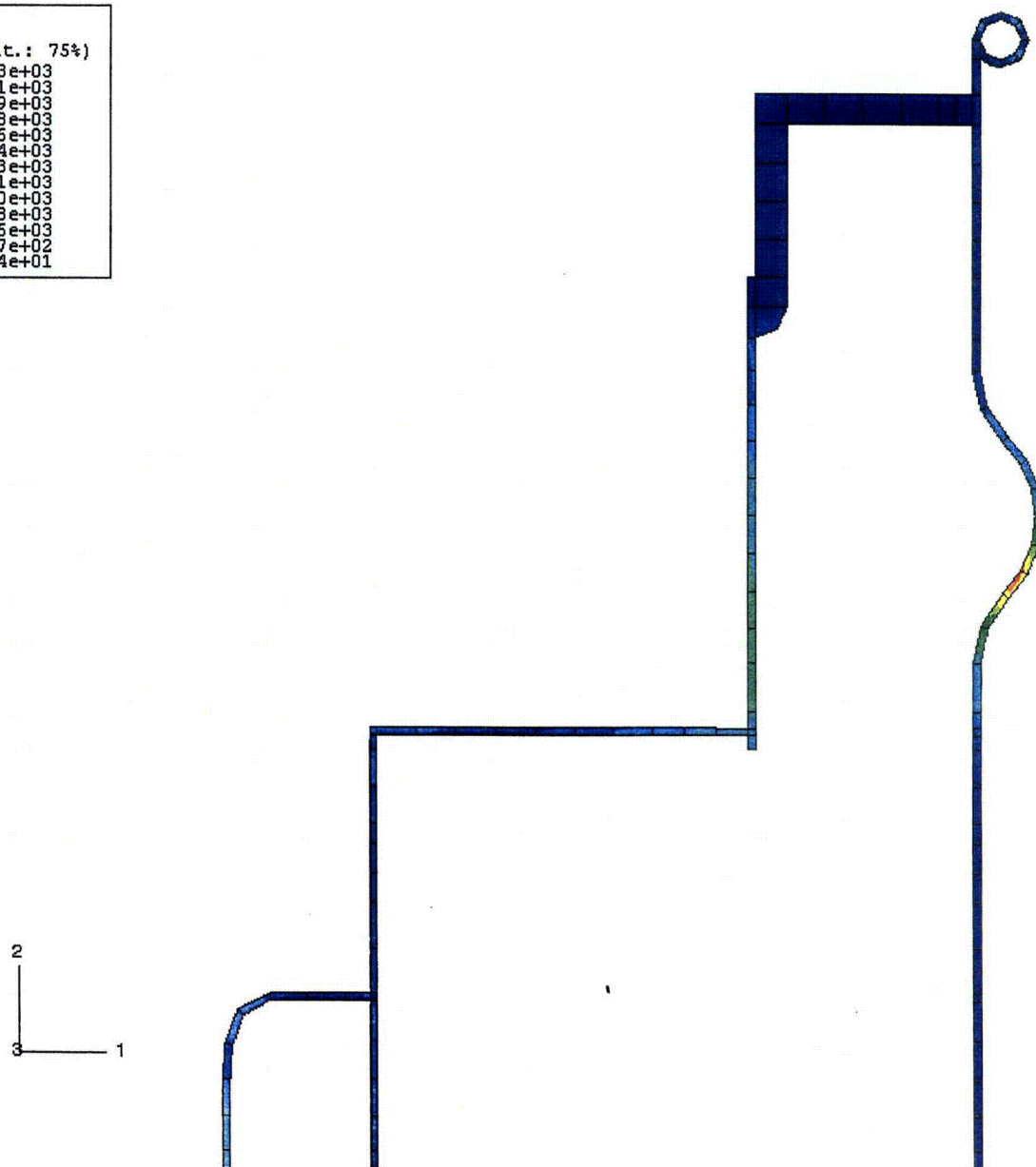
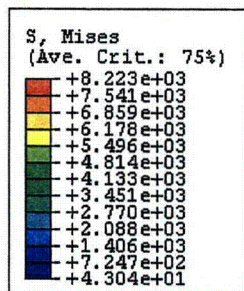


Figure 6. Thermal stresses (Mises) in the ES-3100 shipping container drum body assembly during a typical NCT day/night cycle—30 W content heat load.



**Figure 7. Drum/drum liner weldment Mises stresses (psi) during NCT at  $t = 14.127$  hours (+2.127 hours after sunset)—0.4 W content heat load.**



**Figure 8. Drum/drum liner weldment Mises stresses (psi) during NCT at  $t = 4.724$  hours (+4.724 hours after sunrise)—0.4 W content heat load.**

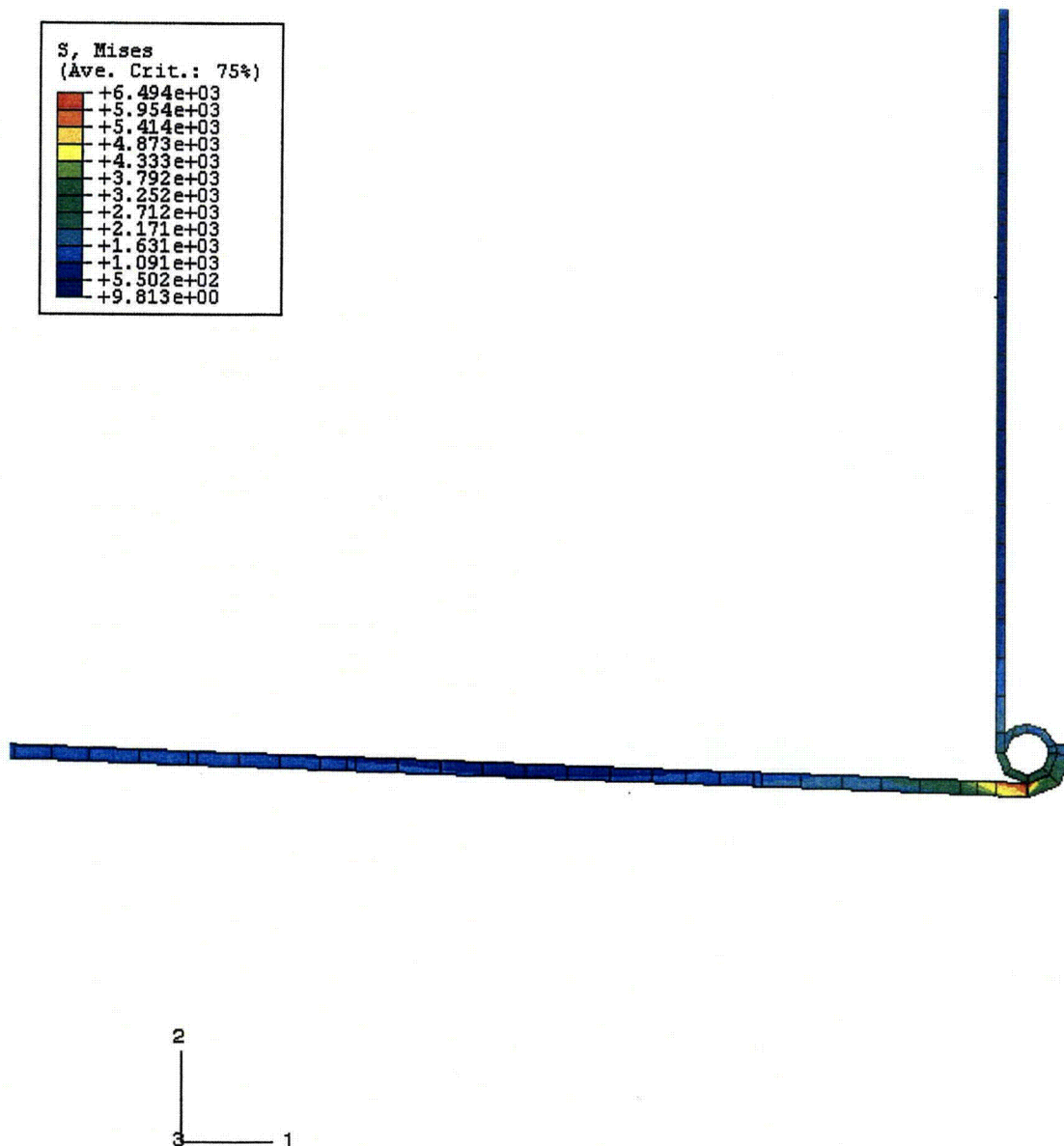


**Figure 9. Drum/drum bottom plate Mises stresses (psi) during NCT at t = 12.814 hours (+0.814 hours after sunset)—0.4 W content heat load.**



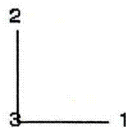
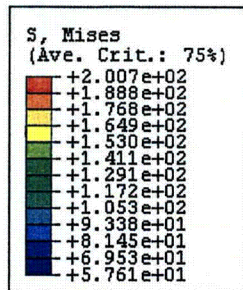


**Figure 10. Neutron absorber Mises stresses (psi) during NCT at  $t = 12.867$  hours (+0.867 hours after sunset)—0.4 W content heat load.**

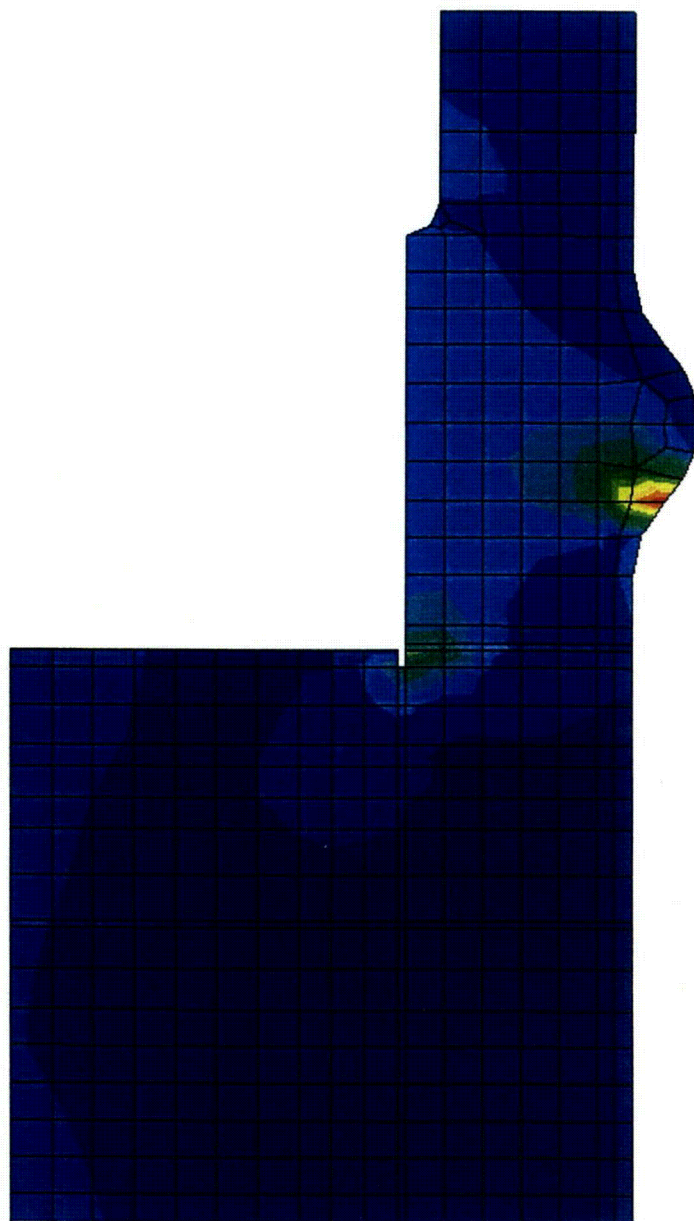
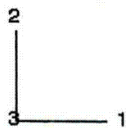
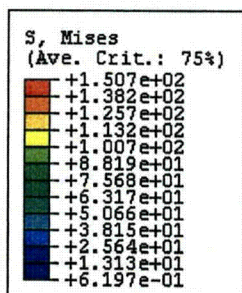


**Figure 11. Drum Kaolite Mises stresses (psi) during NCT at  $t = 3.992$  hours (+3.992 hours after sunrise)—0.4 W content heat load.**



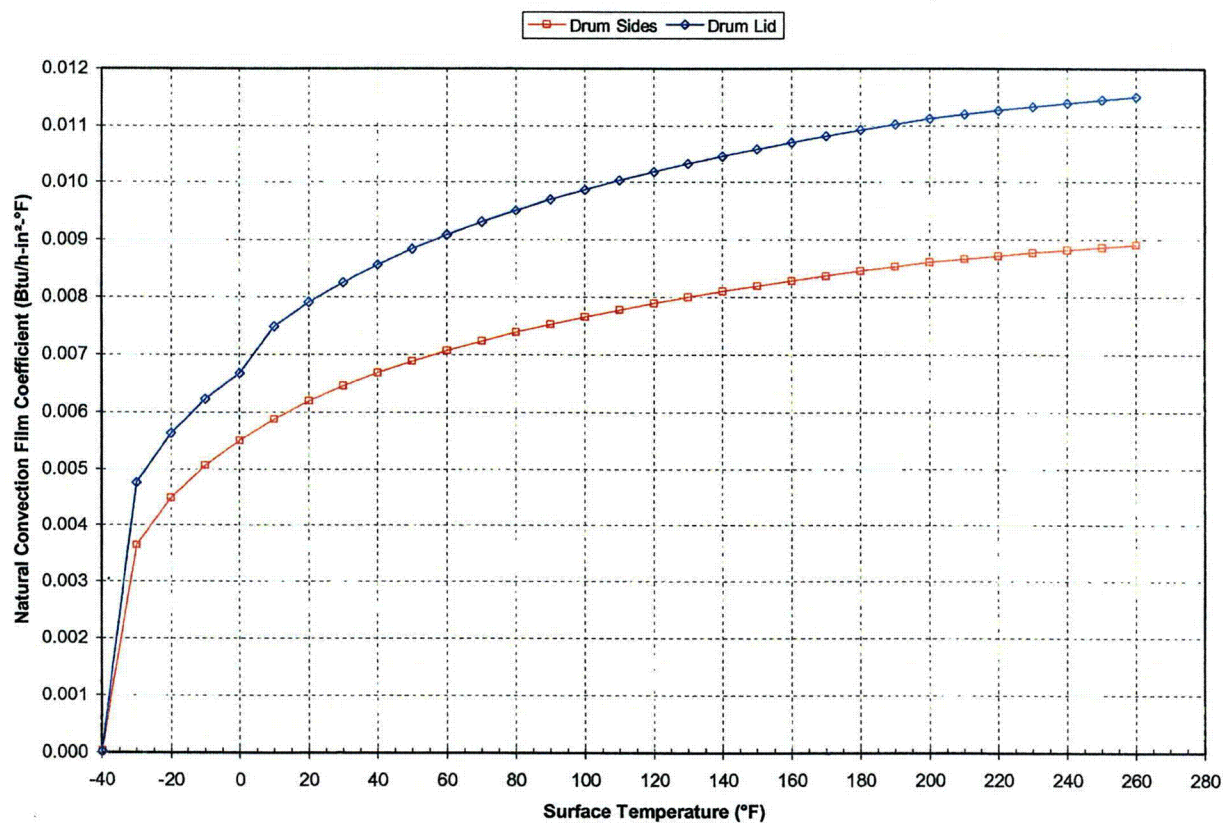


**Figure 12. Natural convection film coefficients applied to the drum surfaces during cold conditions.**

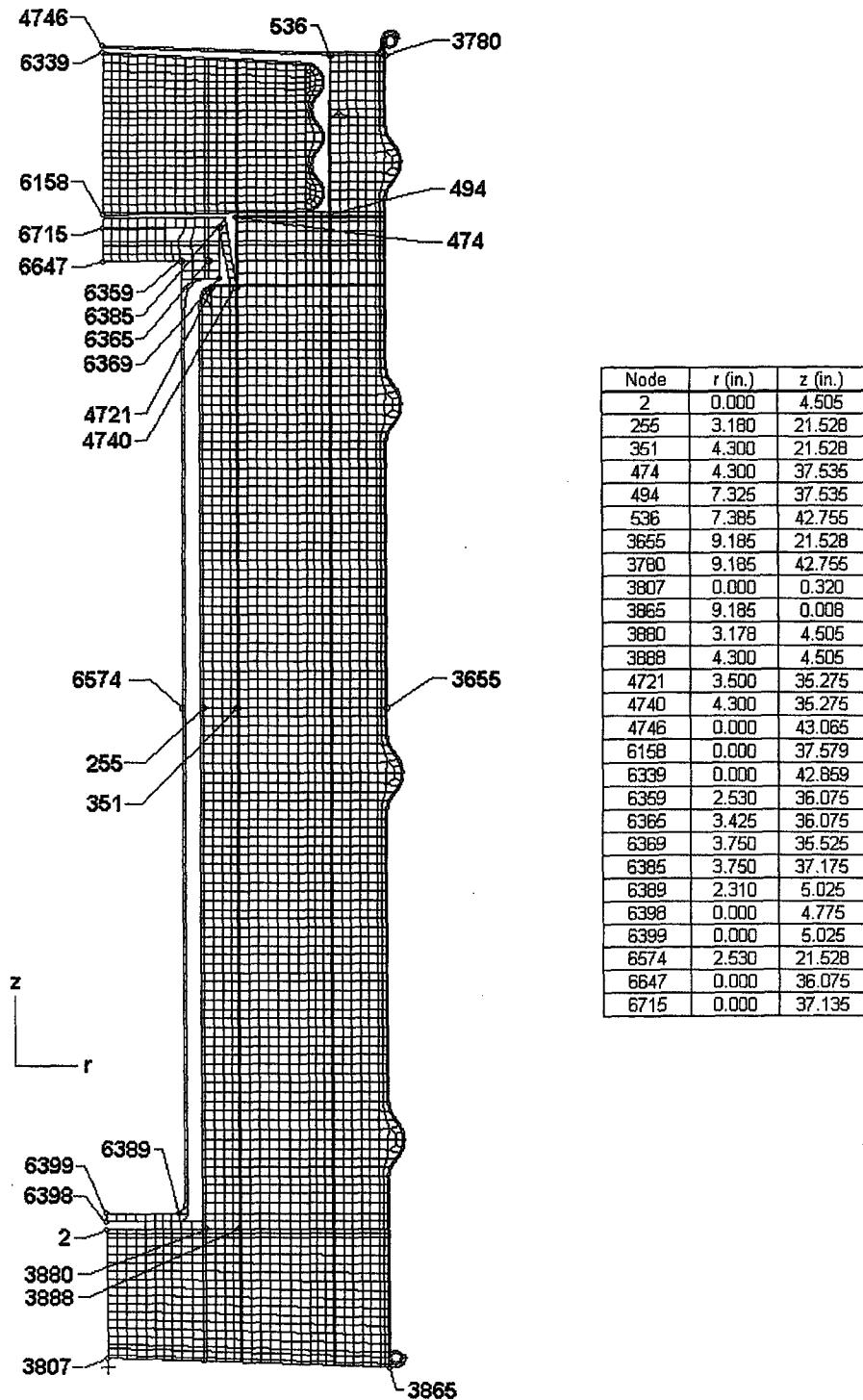
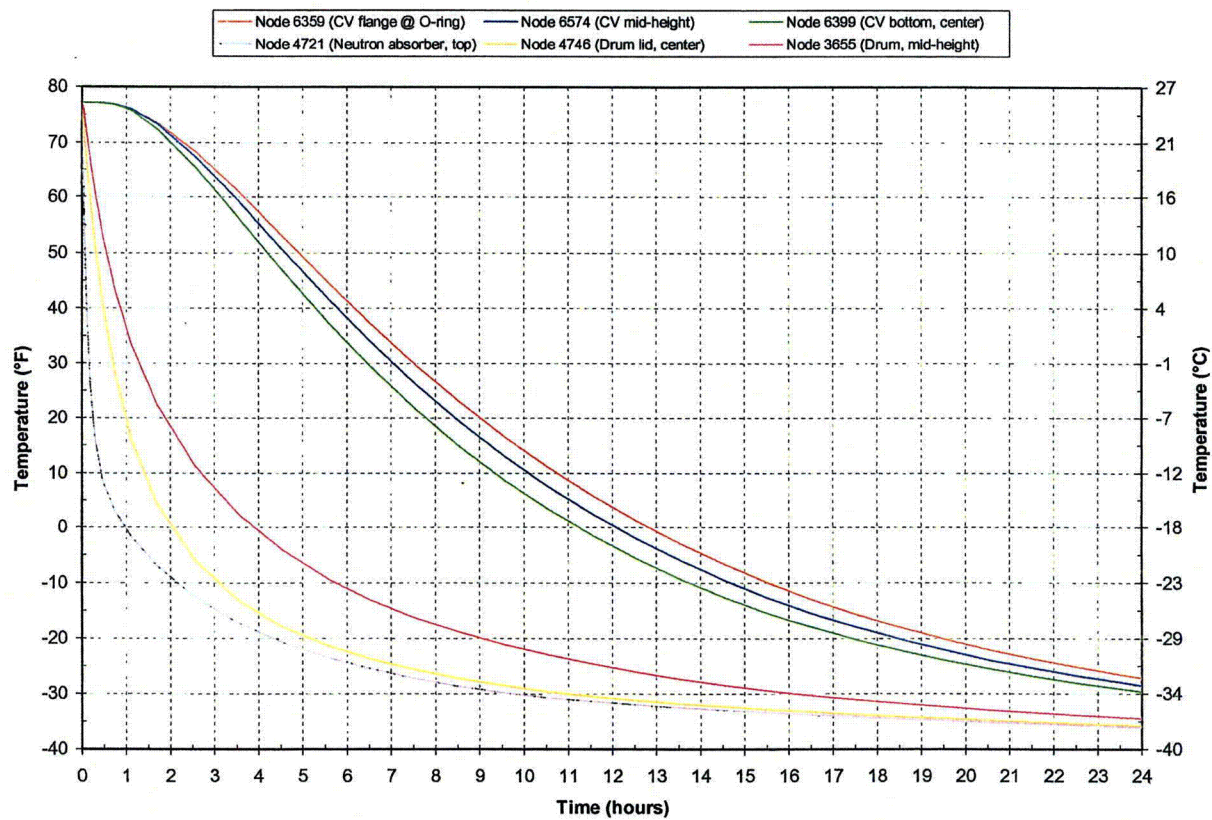


Figure 13. ABAQUS axisymmetric finite element thermal model of the ES-3100 shipping container—nodal locations of interest (elements representing air not shown for clarity).



**Figure 14. Transient temperatures of the ES-3100 shipping container for cold conditions (no content heat load) see Figure 13 for node locations.**

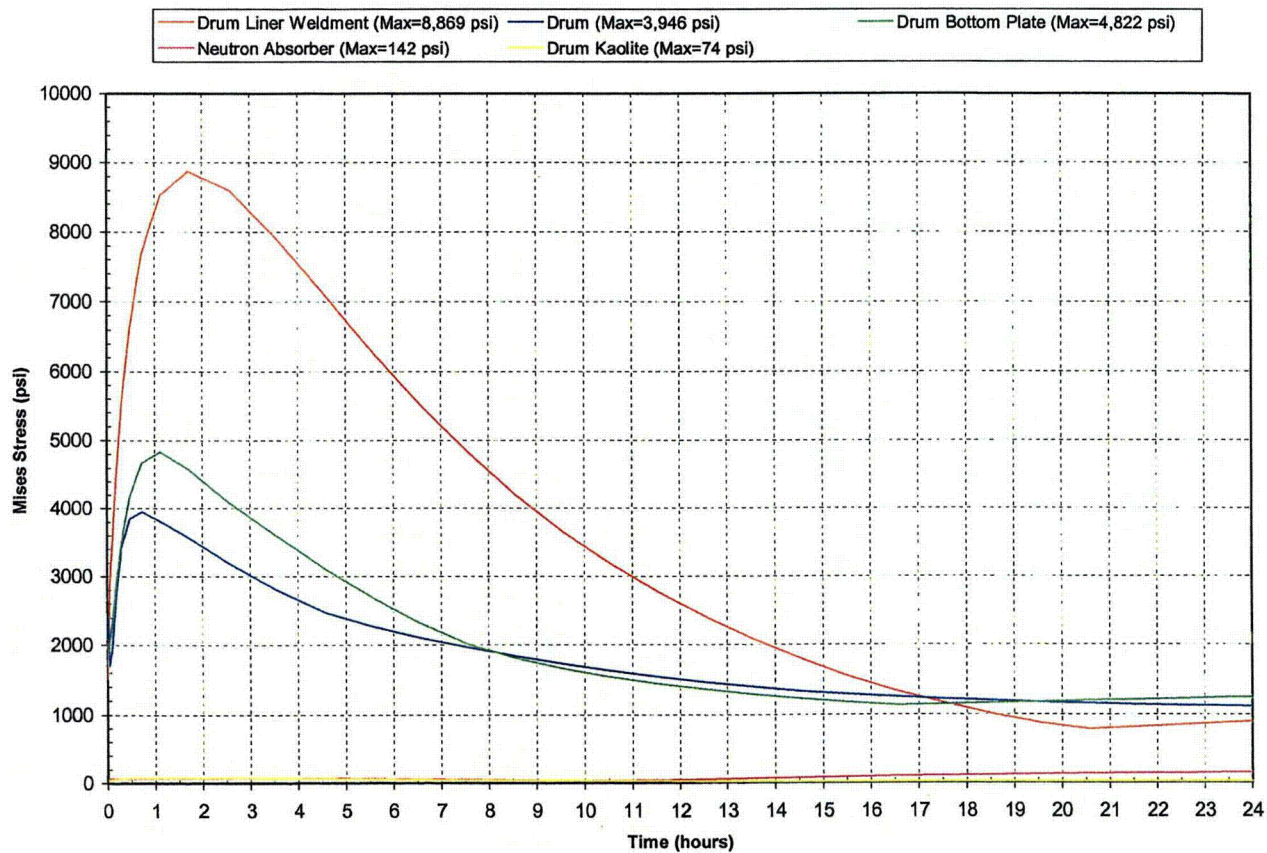
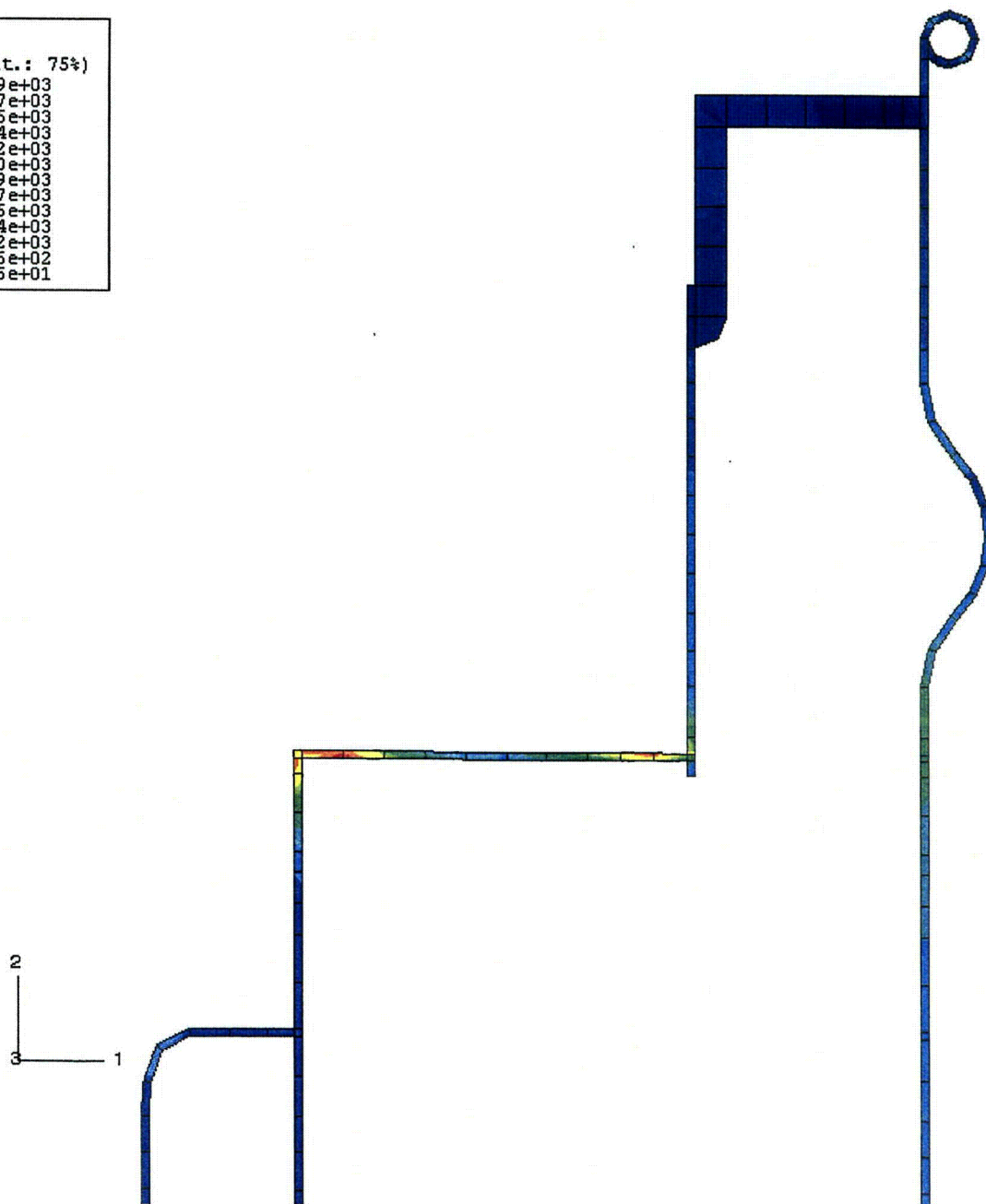
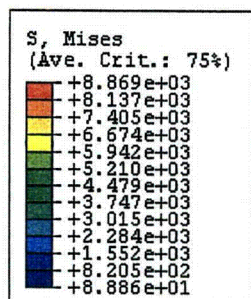
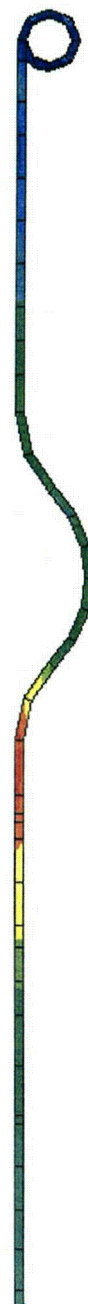
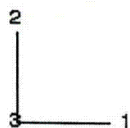
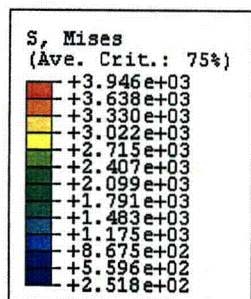


Figure 15. Thermal stresses (Mises) in the ES-3100 shipping container drum body assembly during cold conditions (-40°F ambient temperature)—no content heat load.



**Figure 16. Drum/drum liner weldment Mises stresses (psi) during cold conditions at  $t = 1.698$  hours—no content heat load.**



**Figure 17. Drum Mises stresses (psi) during cold conditions at  $t = 0.726$  hours — no content heat load.**



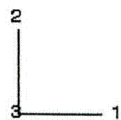
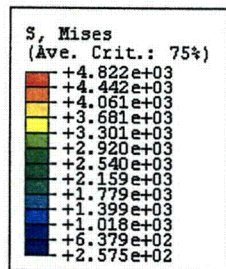


**Figure 18. Drum bottom plate Mises stresses (psi) during cold conditions at  $t = 1.115$  hours—  
no content heat load.**



### APPENDIX 3.6.3 REFERENCES

1. *Packaging and Transportation of Radioactive Materials*, U.S. Nuclear Regulatory Commission, Code of Federal Regulations, Title 10 – Energy, Part 71, January 1, 2004.
2. P. A. Bales, *Thermal Analyses of the ES-3100 Shipping Container for NCT and HAC (Final Design with 277-4 Neutron Absorber)*, DAC-PKG-801699-A002, Rev. 0, BWXT Y-12, January 31, 2005.
3. MSC. Patran 2004, Version 12.0.044, MacNeal Schwendler Corporation, 2004.
4. ABAQUS/CAE, Version 6.4-1, Build ID: 2003\_09\_29-11.18.28 46457, Abaqus, Inc., 2003.
5. K. D. Handy, *Impact Analysis of ES3100 Design Concepts Using Borobond*, DAC-EA-801699-A001, BWXT Y-12, Oct. 2004.
6. ABAQUS/Standard, Version 6.4-1, 2003\_09-11.18.28 46457, Abaqus, Inc.

#### **APPENDIX 3.6.4**

### **CONTAINMENT VESSEL PRESSURE DUE TO NORMAL CONDITIONS OF TRANSPORT FOR THE PROPOSED CONTENTS**

Prepared by: M. L. Goins  
BWXT Y-12  
November 2006

Reviewed by: G. A. Byington  
BWXT Y-12  
November 2006



## APPENDIX 3.6.4

### CONTAINMENT VESSEL PRESSURE DUE TO NORMAL CONDITIONS OF TRANSPORT FOR THE PROPOSED CONTENTS

The following calculations determine the pressure of the containment vessel when subjected to the tests and conditions of Normal Condition of Transport per 10 CFR 71.71 for the most restrictive convenience can arrangements shipped in the ES-3100. The following packaging arrangements are evaluated for shipment:

1. one shipment will contain six cans with external dimensions of 4.25 in. diameter by 4.875 in. high;
2. one shipment will contain five cans with external dimensions of 4.25 in. diameter by 4.875 in. high and three can spacers, top can will be empty;
3. one shipment will contain three cans with external dimension of 4.25 in. diameter by 8.75 in. high and two can spacers;
4. one shipment will contain three cans with external dimension of 4.25 in. diameter by 10 in. high; and
5. one shipment will contain six cans with external dimension of 3.00 in. diameter by 4.75 in. high;
6. one shipment will contain three polyethylene bottles with external dimensions of 4.94 in. diameter by 8.7 in. high; and
7. one shipment will contain three Teflon FEP bottles with external dimensions of 4.69 in. diameter by 9.4 in. high.

To determine this pressure, the following assumptions have been made:

1. The HEU contents are loaded into convenience cans which are placed inside the ES-3100 containment vessel at standard temperature ( $T_{amb}$ ) and pressure (P) [25°C (77°F) and 101.35 kPa (14.7 psia)] with air at a maximum relative humidity of 100%.
2. The convenience cans are assumed to be sealed, which minimizes the void volume inside the containment vessel.
3. Polyethylene bagging of contents and/or convenience cans is limited to 500 g per containment vessel shipping arrangement.

Applying Dalton's law concerning a mixture of gases, the properties of each component are considered as though each component exists separately at the volume and temperature of the mixture. Therefore, the molar quantities of each constituent inside the containment vessel (i.e., dry air, water vapor, polyethylene bagging, and silicone rubber) must be calculated individually.

To calculate these molar properties, the void volume of the containment vessel must be determined. The volume inside an empty ES-3100 containment vessel was determined from Algor finite element software to be 637.18 in.<sup>3</sup> (10,441.51 cm<sup>3</sup>).

## I. Molar quantity determination for dry air and water vapor

According to *Fundamentals of Classical Thermodynamics*,

"Relative humidity ( $\Phi$ ) is defined as the ratio of the mole fraction in the mixture to the mole fraction of vapor in a saturated mixture at the same temperature and total pressure."

Since the vapor is considered an ideal gas, the definition reduces to the ratio of the partial pressure of the vapor ( $P_v$ ) as it exists in the mixture to the saturation pressure of the vapor ( $P_g$ ) at the same temperature.

Therefore,

$$\Phi = P_v / P_g.$$

From the above equation and interpolating the values given in Table A.1.1 of *Fundamentals of Classical Thermodynamics*, the partial pressure of the water vapor at saturation is:

$$\begin{aligned} P_v &= 1.0 (0.464) \text{ psia,} \\ P_v &= 0.464 \text{ psia.} \end{aligned}$$

The partial pressure of the dry air ( $P_a$ ) in the volume:

$$\begin{aligned} P_a &= P_t - P_v \\ &= 14.7 - 0.464 \\ &= 14.236 \text{ psia.} \end{aligned}$$

From the ideal gas law, the number of water vapor moles and dry air moles in the void volume ( $V_v$ ) for each containment vessel arrangement (CVA) is calculated as follows:

$$n_v = \frac{P_v \cdot V_v}{R_u \cdot T_{\text{amb}} \cdot 12}, \quad n_a = \frac{P_a \cdot V_v}{R_u \cdot T_{\text{amb}} \cdot 12}$$

To determine the number of moles, the void volume of the air mixture must be determined. The void volume ( $V_v$ ) in the containment vessel for each CVA is calculated as follows:

$$V_v = V_{\text{ECV}} - V_{\text{SP}} - V_{\text{PB}} - V_{\text{CC}} - V_{\text{CS}} - V_{\text{CH}},$$

where

$$\begin{aligned} V_{\text{ECV}} &= \text{volume inside an empty containment vessel,} \\ V_{\text{SP}} &= \text{silicone pad volume,} \\ V_{\text{PB}} &= \text{polyethylene bagging or lifting sling volume,} \\ V_{\text{CC}} &= \text{external volume of the convenience cans or bottles,} \\ V_{\text{CS}} &= \text{external volume of the can spacers,} \\ V_{\text{CH}} &= \text{external volume of the convenience can handles.} \end{aligned}$$

A summary for each CVA is shown in Table 1.

**Table 1. Containment vessel void volume for each CVA**

CVA		V <sub>ECV</sub> (in. <sup>3</sup> )	V <sub>SP</sub> <sup>a</sup> (in. <sup>3</sup> )	V <sub>FB</sub> (in. <sup>3</sup> )	V <sub>CC</sub> (in. <sup>3</sup> )	V <sub>CS</sub> (in. <sup>3</sup> )	V <sub>CH</sub> (in. <sup>3</sup> )	V <sub>V</sub> (in. <sup>3</sup> )
1	Six 4.875-in.-high cans Seven silicone pads Six can handles	637.18	9.35	30.51	380.47	0.00	1.02	215.83
2	Five 4.875-high cans Nine silicone pads Three Cat 277-4 spacers Eight can handles	637.18	12.03	30.51	317.06	60.60	1.36	215.62
3	Three 8.75-in.- high cans Two Cat 277-4 spacers Six silicone pads Five can handles	637.18	8.02	30.51	345.96	40.40	0.85	211.44
4	Three 10-in.-high cans Four silicone pads Three can handles	637.18	5.35	30.51	396.20	0.00	0.51	204.62
5	Six 4.75 in.-high nickel cans	637.18	0.00	30.51	<del>194.38</del>	0.00	1.02	<del>411.27</del>
6	Three 4.94 in. OD polyethylene bottles	637.18	0.00	<del>30.51</del>	465.33	0.00	0.00	<del>141.34</del>
<del>7</del>	<del>Three 4.69 in. OD Teflon FEP bottles</del>	<del>637.18</del>	<del>0.00</del>	<del>30.51</del>	<del>485.52</del>	<del>0.00</del>	<del>0.00</del>	<del>121.15</del>

Using the above molar equations, the number of moles for water vapor and dry air in the vessel for each CVA is summarized in Table 2.

**Table 2. Water vapor and dry air molar summary for each CVA**

CVA	P <sub>a</sub> (psia)	P <sub>v</sub> (psia)	V <sub>v</sub> (in. <sup>3</sup> )	R <sub>a</sub> (ft-lb/lb-mole-R)	T <sub>amb</sub> (R)	n <sub>v</sub> (lb-mole)	n <sub>a</sub> (lb-mole)
1	14.236	0.464	215.83	1545.32	537	1.0057e-05	3.0855e-04
2	14.236	0.464	215.63	1545.32	537	1.0047e-05	3.0826e-04
3	14.236	0.464	211.44	1545.32	537	9.8522e-06	3.0227e-04
4	14.236	0.464	204.62	1545.32	537	9.5344e-06	2.9252e-04
5	14.236	0.464	<del>411.27</del>	1545.32	537	<del>1.9163e-05</del>	<del>5.8795e-04</del>
6	14.236	0.464	<del>141.34</del>	1545.32	537	<del>6.5858e-06</del>	<del>2.0206e-04</del>
<del>7</del>	<del>14.236</del>	<del>0.464</del>	<del>121.15</del>	<del>1545.32</del>	<del>537</del>	<del>5.6450e-06</del>	<del>1.7320e-04</del>

## II. Molar quantity determination due to off-gassing for each containment vessel arrangement

The maximum temperature calculated for the containment vessel is 87.81°C (190.06°F). This temperature is assumed to be constant throughout the containment vessel and contents. Therefore, the

polyethylene bags, polyethylene bottles, Teflon FEP bottles, and silicone rubber can pads are assumed to be at this temperature.

Using the above calculated results and the specific gas generation of polyethylene bags and silicone rubber pad measurements at temperatures up to 170°C (338°F) conducted by the Y-12 Development Division, the amount of gas ( $V_{bo}$  and  $V_{po}$ ) generated due to off-gassing of the polyethylene bags and bottles, and silicone rubber can pads at any temperature is estimated by first determining the off-gassing volume per unit mass at temperature and multiplying that by the total mass of the bags and can supports inside the containment vessel. Based on testing at a temperature of 93.33°C (200°F), no recordable off-gassing occurred in the polyethylene bags and bottles, or silicone rubber pad material as documented in Y/DZ-2585, Rev. 2 (Appendix 2.10.4). The data showed that the Teflon FEP material off-gassing volume per unit mass ( $V_{ff}$ ) was conservatively assumed to be 0.25 cm<sup>3</sup>/g@STP (Appendix 2.10.9). These values are used to determine the off-gassing volumes as shown below:

$$V_{po} = W_p \times 0.0 / 16.387 \text{ (in.}^3\text{)} \quad \text{(off-gassing volume of silicone rubber pads)}$$

$$V_{bo} = W_b \times 0.0 / 16.387 \text{ (in.}^3\text{)} \quad \text{(off-gassing volume of polyethylene bags and bottles)}$$

$$V_{ff} = W_{ff} \times 0.25 / 16.387 \text{ (in.}^3\text{)} \quad \text{(off-gassing volume of Teflon bottles)}$$

From the ideal gas law, the number of gas moles in the volume at standard temperature and pressure is as follows:

$$n_{io} = \frac{P_v \cdot V_i}{R_u \cdot T_{amb} \cdot 12}$$

A summary of the results obtained using the above equations for each containment vessel arrangement is presented in Tables 3, 4, and 5.

**Table 3. Molar quantity of gas generated due to the silicone rubber pad off-gassing**

CVA	$W_p$ (g)	$V_{po}$ (in. <sup>3</sup> )	$P_v$ (psia)	$R_u$ (ft-lb/lb-mole·R)	$T_{amb}$ (R)	$n_{po}$ (lb-mole)
1	186.74	0.00	14.7	1545.32	537	0.0000e+00
2	240.09	0.00	14.7	1545.32	537	0.0000e+00
3	160.06	0.00	14.7	1545.32	537	0.0000e+00
4	106.71	0.00	14.7	1545.32	537	0.0000e+00
5	0.00	0.00	14.7	1545.32	537	0.0000e+00
6	0.00	0.00	14.7	1545.32	537	0.0000e+00
7	0.00	0.00	14.7	1545.32	537	0.0000e+00



**Table 4. Molar quantity of gas generated due to the polyethylene bag, sling and bottle off-gassing**

CVA	W <sub>b</sub> (g)	V <sub>bo</sub> (in. <sup>3</sup> )	P <sub>v</sub> (psia)	R <sub>u</sub> (ft-lb/lb-mole·R)	T <sub>amb</sub> (R)	n <sub>bo</sub> (lb-mole)
1	500.00	0.00	14.7	1545.32	537	0.0000e+00
2	500.00	0.00	14.7	1545.32	537	0.0000e+00
3	500.00	0.00	14.7	1545.32	537	0.0000e+00
4	500.00	0.00	14.7	1545.32	537	0.0000e+00
5	500.00	0.00	14.7	1545.32	537	0.0000e+00
6	845.00	0.00	14.7	1545.32	537	0.0000e+00
7	500.00	0.00	14.7	1545.32	537	0.0000e+00

**Table 5. Molar quantity of gas generated due to the Teflon bottle off-gassing**

CVA	W <sub>b</sub> (g)	V <sub>bo</sub> (in. <sup>3</sup> )	P <sub>v</sub> (psia)	R <sub>u</sub> (ft-lb/lb-mole·R)	T <sub>amb</sub> (R)	n <sub>bo</sub> (lb-mole)
7	990.00	15.10	14.7	1545.32	537	2.2296e-05

### III. Total pressure due to off-gassing and NCT temperatures inside the containment vessel

The total pressure of the mixture at 87.81°C (190.06°F), P<sub>T</sub>, for each containment vessel arrangement is the sum of each of the previously calculated molar quantities. Table 6 summarizes the molar constituents and total pressure of each containment vessel arrangement. The following equation is used to calculate the final containment vessel pressure:

$$P_{87.81^{\circ}\text{C}} = (\sum n_i \cdot R \cdot T \cdot 12) / V_{\text{GMV}},$$

where

$$\begin{aligned} n_i &= \text{individual molar quantity for each gas,} \\ T &= \text{average gas temperature} = 87.81^{\circ}\text{C} (190.06^{\circ}\text{F}), \\ V_{\text{GMV}} &= V_v = \text{gas mixture volume.} \end{aligned}$$

Table 6. Total pressure inside the containment vessel at 87.81°C (190.06°F) <sup>a</sup>

CVA	$n_a$ (lb-mole)	$n_v$ (lb-mole)	$n_{po}$ (lb-mole)	$n_{bo}$ (lb-mole)	$n_{gr}$ (lb-mole)	$n_T$ (lb-mole)	$P_T$ (psia)
1	3.0855e-04	1.0057e-05	0.0000e+00	0.0000e+00	0.0000e+00	3.1861e-04	17.786
2	3.0826e-04	1.0047e-05	0.0000e+00	0.0000e+00	0.0000e+00	3.1831e-04	17.786
3	3.0227e-04	9.8522e-06	0.0000e+00	0.0000e+00	0.0000e+00	3.1212e-04	17.786
4	2.9252e-04	9.5344e-06	0.0000e+00	0.0000e+00	0.0000e+00	3.0205e-04	17.786
5	1.9163e-05	5.8795e-04	0.0000e+00	0.0000e+00	0.0000e+00	6.0711e-04	17.786
6	2.0206e-04	6.5858e-06	0.0000e+00	0.0000e+00	0.0000e+00	2.0865e-04	17.786
7	5.6450e-06	1.7320e-04	0.0000e+00	0.0000e+00	2.2296e-05	2.0114e-04	20.004

<sup>a</sup> This assumes that the internal convenience cans, polyethylene bottles, Teflon FEP bottles, and Cat 277-4 spacer cans are sealed.

At -40°C (-40°F), the partial pressure of the water vapor is conservatively assumed to be zero. Therefore, the final pressure of the mixture at -40°C (-40°F) is calculated according to the ideal gas law based solely on the partial pressure of the air.

$$\frac{P_1 V_1}{T_1} = \frac{P_2 V_2}{T_2},$$

where

$$\begin{aligned} P_1 &= 14.236 \text{ psi,} \\ T_1 &= 77^\circ\text{F} &= 536.67 \text{ R,} \\ T_2 &= -40^\circ\text{F} &= 419.67 \text{ R,} \\ V_1 &= V_2. \end{aligned}$$

Rearranging and solving for  $P_2$ ,

$$\begin{aligned} P_2 &= P_1 (T_2/T_1), \\ P_2 &= (14.236)(419.67/536.67) = 11.13 \text{ psia.} \end{aligned}$$

## **APPENDIX 3.6.5**

### **CONTAINMENT VESSEL PRESSURE DUE TO HYPOTHETICAL ACCIDENT CONDITIONS FOR THE PROPOSED CONTENTS**

Prepared by: M. L. Goins  
BWXT Y-12  
November 2006

Reviewed by: G. A. Byington  
BWXT Y-12  
November 2006



## APPENDIX 3.6.5

### CONTAINMENT VESSEL PRESSURE DUE TO HYPOTHETICAL ACCIDENT CONDITIONS FOR THE PROPOSED CONTENTS

The following calculations determine the pressure of the containment vessel when subjected to the tests and conditions of Hypothetical Accident Conditions per 10 CFR 71.73 for the most restrictive convenience can arrangements shipped in the ES-3100 package. The following packaging arrangements are evaluated for shipment:

1. one shipment will contain six cans with external dimensions of 4.25 in. diam by 4.875 in. high;
2. one shipment will contain five cans with external dimensions of 4.25 in. diam by 4.875 in. high and three can spacers, the top can is empty;
3. one shipment will contain three cans with external dimensions of 4.25 in. diam by 8.75 in. high and 2 can spacers;
4. one shipment will contain three cans with external dimensions of 4.25 in. diam by 10 in. high;
5. one shipment will contain six nickel cans with external dimensions of 3.00 in. diam by 4.75 in. high;
6. one shipment will contain three polyethylene bottles with external dimensions of 4.94 in. diameter by 8.7 in. high; and
7. one shipment will contain three Teflon FEP bottles with external dimensions of 4.69 in. diameter by 9.4 in. high; and

To determine this pressure, the following assumptions have been made:

1. The highly enriched uranium (HEU) contents are loaded into convenience cans and placed inside the ES-3100 containment vessel at standard temperature [25°C (77°F)] and at the maximum normal operating pressure (see Table 5 of Appendix 3.6.4) with air at a maximum relative humidity of 100%.
2. The convenience cans are assumed to be sealed to minimize the void volume inside the containment vessel.
3. Polyethylene bagging of contents and/or convenience containers is limited to 500 g per containment vessel shipping arrangement.

Applying Dalton's law concerning a mixture of gases, the properties of each component are considered as though each component exists separately at the volume and temperature of the mixture. Therefore, the molar quantities of each constituent inside the containment vessel (i.e., dry air, water vapor, polyethylene bagging and bottles, silicone rubber pads, and ~~teflon bottles~~) must be calculated individually.

To calculate these molar properties, the void volume of the containment vessel must be determined. The volume inside an empty ES-3100 containment vessel was determined from Algor finite element software to be 637.18 in.<sup>3</sup> (10,441.51 cm<sup>3</sup>).

## I. Molar quantity determination based on MNOP

Table 1. Total pressure inside the containment vessel at 87.81°C (190.06°F)<sup>a</sup>

CVA	$n_a$ (lb-mole)	$n_v$ (lb-mole)	$n_{po}$ (lb-mole)	$n_{bo}$ (lb-mole)	$n_{tr}$ (lb-mole)	$n_T$ (lb-mole)	$P_T$ (psia)
1	3.0855e-04	1.0057e-05	0.0000e+00	0.0000e+00	0.0000e+00	3.1861e-04	17.786
2	3.0826e-04	1.0047e-05	0.0000e+00	0.0000e+00	0.0000e+00	3.1831e-04	17.786
3	3.0227e-04	9.8522e-06	0.0000e+00	0.0000e+00	0.0000e+00	3.1212e-04	17.786
4	2.9252e-04	9.5344e-06	0.0000e+00	0.0000e+00	0.0000e+00	3.0205e-04	17.786
5	1.9163e-05	5.8795e-04	0.0000e+00	0.0000e+00	0.0000e+00	6.0711e-04	17.786
6	2.0206e-04	6.5858e-06	0.0000e+00	0.0000e+00	0.0000e+00	2.0865e-04	17.786
7	5.6450e-06	1.7320e-04	0.0000e+00	0.0000e+00	2.2296e-05	2.0114e-04	20.004

<sup>a</sup> This assumes that the internal convenience cans, polyethylene bottles, Teflon FEP bottles, and Cat 277-4 spacer cans are sealed.

To use the maximum normal operating pressure at standard temperature, the number of lb-mole of gas needs to be increased using the following equation:

$$n_{MNOP} = \frac{P_T \cdot V_v}{R_u \cdot T_{amb} \cdot 12}$$

Using the above molar equations, the total number of moles is summarized in Table 2.

Table 2. Molar summary at MNOP and 25°C (77°F)

CVA	$P_T$ (psia)	$V_v$ (in. <sup>3</sup> )	$R_u$ (ft-lb/lb-mole·R)	$T_{amb}$ (R)	$n_{MNOP}$ (lb-mole)
1	17.786	215.83	1545.32	537	3.8549e-04
2	17.786	215.63	1545.32	537	3.8514e-04
3	17.786	211.44	1545.32	537	3.7765e-04
4	17.786	204.62	1545.32	537	3.6547e-04
5	17.786	411.27	1545.32	537	7.3457e-04
6	17.786	141.34	1545.32	537	2.5245e-04
7	20.004	121.15	1545.32	537	2.4337e-04

## II. Molar quantity determination due to off-gassing for each containment vessel arrangement

To determine the maximum pressure inside the containment vessel as a result of thermal testing, the average adjusted gas temperature must be calculated based on the results shown in Sect. 3.5.3. The approach used is to divide the containment vessel volume into three distinct equal regions and then average the three together. The first volume is represented by the gas adjacent to the containment vessel lid and flange region and the top most convenience can. Based on the temperature recorded near the O-rings [116.11°C (241°F)] and the temperature recorded on the external surface of the convenience can [98.89°C (210°F)], the average temperature of the gas in this region is 107.50°C (225.50°F). Using the temperature adjustment of 25.11°C (45.20°F) for this region, the adjusted average temperature in the first region is 132.61°C (270.70°F). The

second volume is represented by the gas adjacent to the second convenience can from the top. Based on the temperature recorded on the containment vessel wall and convenience can [92.78°C (199°F)], the average temperature of gas in this region is 92.78°C (199°F). Using the temperature adjustment of 27.89°C (50.20°F) for this region, the adjusted average temperature in the second region is 120.67°C (249.20°F). The third and final volume is represented by the gas adjacent to the bottom convenience can. Again, based on the convenience can temperature [87.78°C (190°F)] and the containment vessel end cap temperature [98.89°C (210°F)], the average temperature of gas in this region is 93.33°C (200°F). Using the temperature adjustment of 24.94°C (44.90°F) for this region, the adjusted average temperature in the third region is 118.28°C (244.90°F). Averaging these three temperatures, an average adjusted gas temperature of 123.85°C (254.93°F) is determined for the containment vessel.

Using the above calculated results and the specific gas generation of polyethylene bags and silicone rubber pads measurements at temperatures up to 170°C (338°F) conducted by the Y-12 Development Division (Appendix 2.10.4), the amount of gas generated due to off-gassing of the silicone rubber can pads, the polyethylene bags and bottles, and the Teflon FEP bottles at 123.85°C (254.93°F), ( $V_{po}$ ,  $V_{bo}$ , and  $V_{tr}$ ) is estimated by first determining the off-gassing volume per unit mass at temperature and multiplying that by the total mass of the bags, bottles, slings, and silicone rubber can supports inside the containment vessel. Based on testing at an approximate temperature of 141.11°C (286.00°F), values of ~7.0 and ~0.8 cm<sup>3</sup>/g @STP for the polyethylene bagging and bottles, and silicone rubber pads, respectively, were taken from the curves for the off-gassing volume per unit mass as documented in Y/DZ-2585, Rev. 2 (Appendix 2.10.4). The data showed that the Teflon FEP material off-gassing volume per unit mass ( $V_{tr}$ ) was conservatively assumed to be 0.25 cm<sup>3</sup>/g@STP (Appendix 2.10.9). These values are used to determine the off-gassing volume as shown below:

$$V_{po} = W_p \times 0.8 / 16.387 \text{ (in.}^3\text{)} \quad \text{(off-gassing volume of silicone rubber pads)}$$

$$V_{bo} = W_b \times 7.0 / 16.387 \text{ (in.}^3\text{)} \quad \text{(off-gassing volume of polyethylene bags and bottles)}$$

$$V_{tr} = W_{tr} \times 0.25 / 16.387 \text{ (in.}^3\text{)} \quad \text{(off-gassing bottles of Teflon FEP bottles)}$$

From the ideal gas law, the number of gas moles in the volume is as follows:

$$n_i = \frac{P_v \cdot V_i}{R_u \cdot T_{amb} \cdot 12}$$

A summary of the results obtained using the above equations for each containment vessel arrangement is presented in Tables 3, 4, and 5.

**Table 3. Molar quantity of gas generated due to the silicone rubber pad off-gassing**

CVA	$W_p$ (g)	$V_{p3}$ (in. <sup>3</sup> )	$P_v$ (psia)	$R_u$ (ft-lb/lb-mole·R)	$T_{amb}$ (R)	$n_{po}$ (lb-mole)
1	186.74	9.12	14.7	1545.32	537	1.3458e-05
2	240.09	11.72	14.7	1545.32	537	1.7302e-05
3	160.06	7.81	14.7	1545.32	537	1.1535e-05
4	106.71	5.21	14.7	1545.32	537	7.6901e-06
5	0.00	0.00	14.7	1545.32	537	0.0000e+00
6	0.00	0.00	14.7	1545.32	537	0.0000e+00
7	0.00	0.00	14.7	1545.32	537	0.0000e+00



Table 4. Molar quantity of gas generated due to polyethylene bag, sling, and bottle off-gassing

CVA	W <sub>b</sub> (g)	V <sub>bo</sub> (in. <sup>3</sup> )	P <sub>v</sub> (psia)	R <sub>u</sub> (ft-lb/lb-mole·R)	T <sub>amb</sub> (R)	n <sub>bo</sub> (lb-mole)
1	500.00	213.58	14.7	1545.32	537	3.1529e-04
2	500.00	213.58	14.7	1545.32	537	3.1529e-04
3	500.00	213.58	14.7	1545.32	537	3.1529e-04
4	500.00	213.58	14.7	1545.32	537	3.1529e-04
5	500.00	213.58	14.7	1545.32	537	3.1529e-04
6	845.00	360.96	14.7	1545.32	537	5.3284e-04
7	500.00	213.58	14.7	1545.32	537	3.1529e-04

Table 5. Molar quantity of gas generated due to the Teflon FEP bottle off-gassing

CVA	W <sub>b</sub> (g)	V <sub>bo</sub> (in. <sup>3</sup> )	P <sub>v</sub> (psia)	R <sub>u</sub> (ft-lb/lb-mole·R)	T <sub>amb</sub> (R)	n <sub>bo</sub> (lb-mole)
7	990.00	1510	14.7	1545.32	537	2.2296e-05

### III. Total pressure due to off-gassing and HAC temperatures inside the containment vessel

The total pressure of the mixture at 123.85°C (254.93°F), P<sub>T</sub>, for each containment vessel arrangement is the sum of each of the previously calculated molar quantities. Table 6 summarizes the molar constituents and total pressure of each containment vessel arrangement. The following equation is used to calculate the final containment vessel pressure:

$$P_{123.85^{\circ}\text{C}} = (\sum n_i \cdot R \cdot T \cdot 12) / V_{\text{GMV}},$$

where

$$\begin{aligned} n_i &= \text{individual molar quantity for each gas,} \\ T &= \text{average gas temperature} = 123.85^{\circ}\text{C} (254.93^{\circ}\text{F}), \\ V_{\text{GMV}} &= V_v = \text{gas mixture volume.} \end{aligned}$$

Table 6. Total pressure inside the containment vessel at 123.85°C (254.93°F) <sup>a</sup>

CVA	n <sub>MNOP</sub> (lb-mole)	n <sub>po</sub> (lb-mole)	n <sub>bo</sub> (lb-mole)	n <sub>g</sub> (lb-mole)	n <sub>T</sub> (lb-mole)	P <sub>T</sub> (psia)
1	3.8549e-04	1.3458e-05	3.1529e-04	0.0000e+00	7.1424e-04	43.852
2	3.8514e-04	1.7302e-05	3.1529e-04	0.0000e+00	7.1773e-04	44.110
3	3.7765e-04	1.1535e-05	3.1529e-04	0.0000e+00	7.0448e-04	44.151
4	3.6547e-04	7.6901e-06	3.1529e-04	0.0000e+00	6.8845e-04	44.585
5	7.3457e-04	0.0000e+00	3.1529e-04	0.0000e+00	1.0499e-03	33.829
6	2.5245e-04	0.0000e+00	5.3284e-04	0.0000e+00	7.8529e-04	73.625
7	2.4337e-04	0.0000e+00	3.1529e-04	2.2296e-05	5.8096e-04	63.545

<sup>a</sup> This assumes that the internal convenience cans, polyethylene or Teflon FEP bottles, and Cat 277-4 spacer cans are sealed.

## APPENDIX 3.6.6

### SILICONE RUBBER THERMAL PROPERTIES FROM THERM 1.2 DATABASE

The thermal properties for silicone rubber used in the thermal analyses of the ES-3100 shipping container were obtained from the THERM 1.2 Thermal Properties Database by R. A. Bailey. Since THERM 1.2 is not a publicly available program, screen captures from THERM 1.2 of the data for silicone rubber are presented in Figures 1 and 2 in English and SI units, respectively.

silicone rubber, medium k (see ref 5)		
Density	.04696548	lb/in**3
Specific Heat	.3	Btu/lb°F
Conductivity	.01612725	Btu/hr in°F
Maximum Material Temp	545.0	°F
silicone rubber, medium k (see ref 5)		
References:		
fleming p	private collection of plastics data	1968
	materials engr matl selector issue	1967
	metals handbook 8th ed	1961
moyer j	private collection of thermal data	1968
Material properties quality		
Density	-	Good data, or no way of estimating quality.
Specific Heat	-	Poor or conflicting data. Used best or average.
Conductivity	-	Poor or conflicting data. Used best or average.
Transition Temperature	-	Good data, or no way of estimating quality.
Latent Heat	-	No data. Made no estimate.
Specific Heat Tables	-	No data. Made no estimate.
Conductivity Tables	-	No data. Made no estimate.

Figure 1. Silicone rubber thermal properties from Therm 1.2 (English units).

silicone rubber, medium k (see ref 5)		
-----		
Density	1300.0	kg/m**3
Specific Heat	1255.2	J/kgK
Conductivity	.33472	J/sec mK
Maximum Material Temp	558.15	K
silicone rubber, medium k (see ref 5)		
-----		
References:		
fleming p	private collection of plastics data	1968
	materials engr matl selector issue	1967
	metals handbook 8th ed	1961
moyer j	private collection of thermal data	1968
Material properties quality		
Density	- Good data, or no way of estimating quality.	
Specific Heat	- Poor or conflicting data. Used best or average.	
Conductivity	- Poor or conflicting data. Used best or average.	
Transition Temperature	- Good data, or no way of estimating quality.	
Latent Heat	- No data. Made no estimate.	
Specific Heat Tables	- No data. Made no estimate.	
Conductivity Tables	- No data. Made no estimate.	

**Figure 2. Silicone rubber thermal properties from Therm 1.2 (SI units).**

### SECTION 3 REFERENCES

10 CFR 71, *Packaging and Transportation of Radioactive Material*, Jan. 1, 2005.

ABAQUS/Standard, Version 6.4-1, 2003-09-29-11.18.28 46457, Abaqus, Inc., 2003.

*ASME Boiler and Pressure Vessel Code, An American National Standard, Materials*, Sect. II, *Materials*, Part D, American Society of Mechanical Engineers, New York, 2001 ed. with 2002 and 2003 addenda.

*ASME Boiler and Pressure Vessel Code, An American National Standard, Rules for Construction of Nuclear Power Facility Components*, Sect. III, Div. 1, Subsection NB, American Society of Mechanical Engineers, New York, 2001 ed. with 2002 and 2003 addenda.

*ASME Boiler and Pressure Vessel Code, An American National Standard, Welding and Brazing Qualifications*, Sect. IX, American Society of Mechanical Engineers, New York, 2001 ed. with 2002 and 2003 addenda.

ASTM D-2000, *Standard Classification System for Rubber Products in Automotive Applications*, American Society for Testing and Materials, Philadelphia, current revision.

ASTM E-2230-02, *Standard Practice for Thermal Qualification of Type B Packages for Radioactive Materials*, ASTM International, West Conshohocken, Pa., 2002.

Bailey, R. A., *Strain—A Material Database*, Lawrence Livermore Natl. Lab., Nov. 18, 1987.

Bailey, R. A., *THERM 1.2, A Thermal Properties DataBase for the IBM PC*, Lawrence Livermore Natl. Lab., Nov. 18, 1987.

Byington, G. A., *Vibration Test Report of the ES-2M Shipping Package*, GAB1296-2, Lockheed Martin Energy Systems, Inc., Oak Ridge Y-12 Plant, Sept. 3, 1997.

Incropera, F. P., and D. P. DeWitt, *Fundamentals of Heat and Mass Transfer*, 2<sup>nd</sup> ed., John Wiley & Sons, New York, 1985.

MIL-HDBK-5H, *Metallic Materials and Elements for Aerospace Vehicle Structures*, Dec. 1 1998.

MSC.Patran, Version 12.0.044, MacNeal Schwendler Corp., 2004.

OO-PP-986, rev. D, *Procurement Specification for 70A Durometer Preformed Packing (O-rings)*, Lockheed Martin Energy Systems, Inc., Oak Ridge Y-12 Plant, Jan. 26, 1999.

*Parker O-ring Handbook*, Catalog ORD 5700A/US, Parker Hannifin Corp., O-ring Div., Lexington, Ky., 2001.

SG 140.1, *Combination Test Analysis/Method Used to Demonstrate Compliance to DOE Type B Packaging Thermal Test Requirements (30 Minute Fire Test)*, U.S. DOE, Albuquerque Field Office, Nuclear Explosive Safety Division, Feb. 10, 1992.

Van Wylen, G. J., and R. E. Sonntag, *Fundamentals of Classical Thermodynamics*, 2d ed., John Wiley & Sons, Inc., New York, 1973.



#### 4. CONTAINMENT

Design analysis, full-scale testing, and similarity of the ES-3100 prototypes have been used to demonstrate that the ES-3100 package with highly enriched uranium (HEU) is in compliance with the applicable containment requirements of Title 10 Code of Federal Regulations, Part 71 (10 CFR 71). The containment requirements of 10 CFR 71.51 are shown in Table 4.1. A bounding load case has been established for the ES-3100 package, and it assumes that the maximum HEU content is 35.2 kg (Sect. 1.2.3.6) with a decay heat load of 0.4 W (Sect. 1.2.3.7). This decay heat load and the volumes established for the convenience cans, spacers, silicone rubber pads, and the containment vessel void volume are discussed in Sect. 3.1.2 and Appendix 3.6.4. Sections 2 and 3 of this safety analysis report (SAR) also examine the effects of the lightest weight HEU content [2.77 kg (6.11 lb)]. The evaluations in Sects. 2, 3, and 4 have demonstrated that the ES-3100 shipping package with HEU content weight ranging from 2.77 kg (6.11 lb) to 35.2 kg (77.60 lb) meets the containment requirements specified in 10 CFR 71 for all conditions of transport. A summary of the containment boundary design and fabrication acceptance basis is given in Table 4.2. No credit is taken for the various convenience cans' ability to protect the HEU contents from being released.

**Table 4.1. Containment requirements of transport for Type B packages <sup>a</sup>**

Condition	Allowable release rate
Normal Conditions of Transport (NCT)	$R_N = 10^{-6} A_2$ per hour = $2.78 \times 10^{-10} A_2$ per second
Hypothetical Accident Conditions (HAC)	$R_A = A_2$ in 1 week = $1.65 \times 10^{-6} A_2$ per second For $^{85}\text{Kr}$ , a value of $10 A_2$ in 1 week is used

<sup>a</sup> From ANSI N14.5-1997, Sects. 5.4.1 and 5.4.2, and 10 CFR 71.51(a)(1) and (a)(2)

**Table 4.2. Summary of the containment vessel design and fabrication acceptance basis**

Nominal empty weight	15.10 kg (33.29 lb)
Air fill medium temperature at loading	25°C (77°F)
Air fill medium pressure at loading	101.35 kPa (14.70 psia)
Hydrostatic pressure test	1034 ± 34 kPa (150 ± 5) gauge
Helium acceptance leakage rate <sup>a</sup>	$L_T \leq 2.0 \times 10^{-7} \text{ cm}^3/\text{s}$
Air acceptance leakage rate <sup>a</sup>	$L_T \leq 1 \times 10^{-7} \text{ ref-cm}^3/\text{s}$
Air preshipment leakage rate	$L_T \leq 1 \times 10^{-4} \text{ atm-cm}^3/\text{s}$

<sup>a</sup> Acceptance leakage testing includes fabrication, periodic (within 12 months of use), and maintenance testing. According to Sect. 2.1 of ANSI N14.5-1997, *leaktight* is defined as an air leakage rate of  $1 \times 10^{-7} \text{ ref-cm}^3/\text{s}$ ; under the same conditions, this air leakage rate is ~ equal to a helium leakage rate of  $2 \times 10^{-7} \text{ cm}^3/\text{s}$ .

The analysis documented in Appendix 4.6.1 was conducted to establish the upper limit for the total activity and the maximum number of  $A_2$ s proposed for transport in the ES-3100 package. The maximum activity [ $3.2427 \times 10^{-1}$  TBq (8.764 Ci)] of the contents occurs 10 years after initial fabrication. When the maximum activity-to- $A_2$  value (293.99) is reached at ~70 years from material fabrication, the corresponding activity is  $3.2328 \times 10^{-1}$  TBq (8.737 Ci). These values have been determined using a maximum of 35.2 kg of HEU with isotopic weight percents as shown in Table 4.3. By applying the maximum weight percents of isotopes  $^{233}\text{U}$ ,  $^{234}\text{U}$ ,  $^{236}\text{U}$  and by incorporating the traces of  $^{232}\text{U}$  and the transuranic isotopes, the maximum activity, minimum  $A_2$  value, and the minimum leakage requirements were determined for the proposed contents and are summarized in Tables 4.4, 4.5, and 4.6. The mass and isotopic concentrations used for the proposed content do not take into consideration limits based on shielding and subcriticality.

The initial composition of the content contains several isotopes of uranium (Sect. 1.2.3). As a result of radioactive decay, the ingrowth of uranium daughter products occurs, and these concentrations of daughter products will vary with time. The uranium isotopes and daughter products are considered a mixture of radionuclides, and the method for determining the mixture's  $A_2$  value in Section IV, Appendix A, 10 CFR 71 is applied. The  $A_2$  value for the most conservative set of contents defined in Sect. 1.2.3 has been calculated in Appendix 4.6.1. Since the HEU can be in the form of oxides ( $\text{UO}_2$ ,  $\text{UO}_3$ , and  $\text{U}_3\text{O}_8$ ), uranyl nitrate crystals (UNX), or metal and alloy, the calculation of the mixture's  $A_2$  used the various uranium isotopic  $A_2$  values for fast, medium, and slow lung absorption criteria shown in Table A-1 of Appendix A of 10 CFR 71.

## 4.1 DESCRIPTION OF THE CONTAINMENT BOUNDARY

As shown in Table 4.4, the number of  $A_2$ s proposed for shipping exceeds 30 but is less than 3000. In accordance with NUREG 1609, the containment vessel is a Category II vessel. Since this vessel may be used for future contents that exceed 3000  $A_2$ , the containment vessel category has been elevated to a Category I vessel. Therefore, the containment vessel is designed (using nominal dimensions for each component), fabricated, and inspected in accordance with the American Society of Mechanical Engineers (ASME) *Boiler and Pressure Vessel Code*, Sect. III, Division I, Subsection NB and Section IX.

### 4.1.1 Containment Boundary

The containment boundary consists of the vessel's body, lid assembly, and inner O-ring (Sect. 1, Fig. 1.3). Only the inner O-ring is considered part of the boundary. The outer O-ring is provided to allow a post-assembly verification leak check. Two methods of fabrication may be used to fabricate the containment vessel body as shown on Drawing M2E801580A012 (Appendix 1.4.8). The first method uses a standard 5-in., schedule 40 stainless-steel pipe per ASME SA-312 Type TP304L, a machined flat-head bottom forging per ASME SA-182 Type F304L, and a machined top flange forging per ASME SA-182 Type F304L. The nominal outside diameter of the 5-in. schedule 40 pipe is machined to match the nominal wall thickness of 0.254 cm (0.100 in.). Each of these pieces is joined with full-penetration circumferential weld as shown on sheet 2 of Drawing M2E801580A012 (Appendix 1.4.8). The weld filler material conforms to Sect. II, Part C, of the *ASME Boiler and Pressure Vessel Code*. All full-penetration welds are dye penetrant and radiographically inspected in accordance with Sect. III, Div. I, Sect. NB-5000, of the *ASME Boiler and Pressure Vessel Code*. The top flange is machined to match the schedule 40 stainless-steel 5-in. pipe, to provide two concentric half-dove-tailed O-ring grooves in the flat face, to provide locations for two 18-8 stainless-steel dowel pins, and to provide the threaded portion for closure using the lid assembly. The second method of fabrication uses forging, flow forming, or metal spinning to create the complete body (flat bottom, cylindrical body, and flange) from a single forged billet or bar with final material properties in accordance with ASME SA-182 Type F304L. Final machining of the top flange area is identically to that of the welded forging method. The lid assembly, which completes the containment boundary structure,



consists of a sealing lid, closure nut, and external retaining ring (Drawing M2E801580A014, Appendix 1.4.8). The containment vessel sealing lid (Drawing M2E801580A015, Appendix 1.4.8) is machined from Type 304 stainless-steel bar with final material properties in accordance with ASME SA-479. The containment vessel closure nut is machined from a Nitronic 60 stainless-steel bar with material properties in accordance with ASME SA-479. These two components are held together using a WSM-400-S02 external retaining ring made from Type 302 stainless steel. The sealing lid is further machined to accept a  $\frac{3}{8}$ -in.-16 swivel hoist ring bolt, to provide a leak-check port between the elastomeric O-rings, and notched along the perimeter to engage two dowel pins. The lid assembly, with the O-rings in place on the body, are joined together by torquing the closure nut and sealing lid assembly to  $162.7 \pm 6.78 \text{ N}\cdot\text{m}$  ( $120 \pm 5 \text{ ft}\cdot\text{lb}$ ). The sealing lid portion of the assembly is restrained from rotating during this torquing operation by the two dowel pins installed in the body flange. This torquing of the closure nut represents the positive fastening device used to satisfy the requirements of 10 CFR 71.43(c). The effectiveness of this closure system has been demonstrated by the NCT and HAC tests, which show that the complete containment system, including welds and O-ring seals, meet the leaktight criterion as defined in ANSIN14.5-1997 after the conclusion of the test series documented in *Test Report of the ES-3100 Package* (Appendix 2.10.7).

10 CFR 71.73(c) requires that the package containment vessel be immersed in 15 m (50 ft) of water, which is equivalent to an external pressure differential of 150 kPa (21.7 psi). The design analyses (Appendix 2.10.1) show that this vessel is conservatively rated for the 150-kPa (21.7-psi) external pressure differential requirement, as well as for an internal pressure differential of 699.82 kPa (101.5 psig). A summary of the containment boundary design and acceptance basis is given in Table 4.2.

The ES-3100 package has no connections, fittings, or tapped holes that penetrate the containment boundary; therefore, the package does not allow continuous venting during transport.

The containment vessel O-rings (Drawing M2E801580A013, Appendix 1.4.8) are manufactured from an ethylene-propylene elastomer in accordance with specifications for 70A Durometer preformed packing developed at Y-12. These O-rings are rated for continuous service as a static face seal in the temperature range of  $-40$  to  $150^\circ\text{C}$  ( $-40$  to  $302^\circ\text{F}$ ) [*Parker O-ring Handbook*, Fig. 2-24]. Tests conducted by Los Alamos National Laboratory (LANL) on a similar compound, ethylene-propylene rubber (EPDM), used as a static face seal, are documented in *SAFKEG 2863B Tests for Verification of O-ring Performance* (TR 96/12/20). The material compound for the LANL tests was certified to ASTM D-2000 as M3BA610A14B13F17. The ES-3100 package O-rings are also certified to ASTM D-2000 as M3BA712A14B13F17. The class of material in the LANL test is identical except that the durometer and tensile strengths are somewhat less than those of the ES-3100 package. Each material was tested in accordance with ASTM D-2137 for brittleness at  $-40^\circ\text{C}$  ( $-40^\circ\text{F}$ ) without failure. The leak test fixture, as reported in TR 96/12/20, provided a maximum compression of 25.7% in a static face seal configuration. The compression range provided by the flange and lid design of the ES-3100 package is 14.8 to 20.8% or 0.051 to 0.076 cm (0.020 to 0.030 in.) compression due to the half-dovetail design. Furthermore, *Parker O-ring Handbook* states that the minimum squeeze for all seals, regardless of cross-section, should be about 0.018 cm (0.007 in.). Since the minimum compression is 0.051 cm (0.020 in.) and the flange and lid with the closure nut have nearly identical coefficient of thermal expansion, the sealing performance at  $-40^\circ\text{C}$  ( $-40^\circ\text{F}$ ) should not be degraded. Therefore, the performance of the ES-3100 O-rings should be representative of those documented in TR 96/12/20. These tests demonstrated that the O-rings were leaktight over the temperature range of  $-40$  to  $205^\circ\text{C}$  ( $-40$  to  $401^\circ\text{F}$ ), which is greater than the operating temperature range of  $-40$  to  $141.22^\circ\text{C}$  ( $-40$  to  $286.2^\circ\text{F}$ ) of the ES-3100 containment vessel (Table 3.17). In addition to component testing, an ES-3100 full-scale test unit (Test Unit-2) was chilled to  $\leq -40^\circ\text{C}$  and later subjected to an NCT drop test and the entire HAC test battery. The containment vessel was leak tested and achieved

"leaktight" status. Therefore, the continuous service temperature rating of the ethylene-propylene elastomer has been verified by testing.

#### **4.1.2 Special Requirements for Plutonium**

The highly enriched uranium contents have only trace amount of the transuranic isotopes. Therefore, this section is not applicable to the ES-3100 shipping container.

### **4.2 GENERAL CONSIDERATIONS**

#### **4.2.1 Type A Fissile Packages**

The  $A_2$  value of the proposed contents exceed the limits established for Type A packages.

#### **4.2.2 Type B Packages**

##### **Requirements**

- (1) A Type B package, in addition to satisfying the requirements of 10 CFR 71.41–71.47, must be designed, constructed, and prepared for shipment so that under the tests specified in:
  - (a) Section 71.71 ("Normal conditions of transport"): There would be no loss or dispersal of radioactive contents as demonstrated to a sensitivity of  $10^{-6}$   $A_2$ /h, no significant increase in external surface radiation levels, and no substantial reduction in the effectiveness of the packaging; and
  - (b) Section 71.73 ("Hypothetical accident conditions"): There would be no escape of  $^{85}\text{Kr}$  exceeding 10  $A_2$  in one week, no escape of other radioactive material exceeding a total amount  $A_2$  in one week, and no external radiation dose rate exceeding 10 mSv/h (1 rem/h) at 1 m (40 in.) from the external surface of the package.
- (2) Where mixtures of different radionuclides are present, the provisions of Appendix A, paragraph IV of this part shall apply, except that for  $^{85}\text{Kr}$ -85, an effective  $A_2$  value equal to 10  $A_2$  may be used.
- (3) Compliance with the permitted activity release limits of paragraph (a) of this section may not depend on filters or on a mechanical cooling system.

**Analysis.** The  $A_2$  value calculated for the ES-3100 shipping package has been determined in accordance with Appendix A of 10 CFR 71, documented in Appendix 4.6.1, and uses the proposed isotopic distribution shown in Table 4.3. Table 4.4 summarizes the results from Appendix 4.6.1 for the proposed contents from 0 to 70 years after original production.

Table 4.3. Isotopic mass and weight percent for the HEU contents <sup>a</sup>

Nuclide	Weight percent	Mass (g)
U-232	0.000004	0.001408
U-233	0.600000	211.200000
U-234	2.000000	704.000000
U-235	54.895996	19323.390592
U-236	40.000000	14080.000000
U-238	0.000000	0.000000
Transuranic	0.004000	1.408000
Np-237	2.500000	880.000000
Total	100.000000	35200.000000

<sup>a</sup> Weight percent values of individual isotopes are those that generate the largest activity within the allowable ranges presented in Sect. 1.2.3.

Table 4.4. Activity, A<sub>2</sub> value, and number of A<sub>2</sub> proposed for transport

Year	Fast absorption			Medium absorption			Slow absorption		
	Activity (TBq)	A <sub>2</sub> (TBq)	Act / A <sub>2</sub>	Activity (TBq)	A <sub>2</sub> (TBq)	Act / A <sub>2</sub>	Activity (TBq)	A <sub>2</sub> (TBq)	Act / A <sub>2</sub>
0	3.185e-01	1.280e-03	2.489e+02	3.185e-01	1.226e-03	2.599e+02	3.185e-01	1.089e-03	2.926e+02
5	3.238e-01	1.295e-03	2.500e+02	3.238e-01	1.240e-03	2.610e+02	3.238e-01	1.103e-03	2.937e+02
10	3.243e-01	1.296e-03	2.502e+02	3.243e-01	1.241e-03	2.612e+02	3.243e-01	1.104e-03	2.938e+02
20	3.241e-01	1.295e-03	2.503e+02	3.241e-01	1.240e-03	2.613e+02	3.241e-01	1.103e-03	2.938e+02
30	3.239e-01	1.293e-03	2.504e+02	3.239e-01	1.239e-03	2.614e+02	3.239e-01	1.102e-03	2.938e+02
40	3.237e-01	1.292e-03	2.505e+02	3.237e-01	1.238e-03	2.615e+02	3.237e-01	1.101e-03	2.938e+02
50	3.235e-01	1.291e-03	2.506e+02	3.235e-01	1.237e-03	2.616e+02	3.235e-01	1.101e-03	2.939e+02
60	3.234e-01	1.290e-03	2.507e+02	3.234e-01	1.236e-03	2.617e+02	3.234e-01	1.100e-03	2.939e+02
70	3.233e-01	1.289e-03	2.508e+02	3.233e-01	1.235e-03	2.618e+02	3.233e-01	1.100e-03	2.940e+02

### 4.3 CONTAINMENT UNDER NORMAL CONDITIONS OF TRANSPORT (TYPE B PACKAGES)

Title 10 CFR 71.51(a)(1) specifies that there shall be no loss or dispersal of radioactive contents as demonstrated to a sensitivity of  $10^{-6}$  A<sub>2</sub> per hour, no significant increase in external radiation levels, and no substantial reduction in the effectiveness of the packaging. The initial composition of the HEU contains several isotopes of uranium and transuranic contributors (Table 4.3). As a result of radioactive decay, uranium, transuranics, and daughter product isotopes are present in the HEU contents at varying concentrations depending on the length of decay time. The HEU, with its isotopes and daughter isotopes and contributions from unknown transuranic isotopes, qualifies as a mixture for A<sub>2</sub> determination (Appendix A of 10 CFR 71). The A<sub>2</sub> value and the maximum content activity-to-A<sub>2</sub> value ratio for this mixture have been calculated for several different decay times (Table 4.4). As calculated in Appendix 4.6.1, the A<sub>2</sub> value [ $1.0997 \times 10^{-3}$  TBq ( $2.9720 \times 10^{-2}$  Ci)] and the maximum content activity-to-A<sub>2</sub> ratio (293.99) used to qualify this package occurs at about 70 years of decay. As previously stated, these values have been determined using a bounding case maximum of 35.2 kg of HEU with isotopic weight percent values as shown in Table 4.3. The specified composition is a very conservative upper bound achieved by using the maximum weight percent values for the higher specific activity isotopes (<sup>232</sup>U, <sup>233</sup>U, <sup>234</sup>U, and <sup>236</sup>U), including contributions from other transuranics and <sup>237</sup>Np.

The maximum activity, minimum A<sub>2</sub>, and minimum leakage requirements were determined for this worst case scenario and are presented in Tables 4.4 and 4.5. These masses and isotopic concentrations were used for the proposed contents without regard to limits established based on shielding and subcriticality considerations. The actual mass limits affirmed for this shipping package are established in Sect. 1 (Table 1.3). The analyses conducted in Appendix 4.6.2 assumes that the total mass of uranium for each component is available for release as an aerosol (worst case). From experimental tests, the maximum aerosol density containing uranium particulate was reported in *Leakage of Radioactive Powders from Containers* (Curren and Bond 1980) to be  $9.0 \times 10^{-6}$  g/cm<sup>3</sup>. This aerosol density is used to calculate the total activity concentration in ANSI N14.5-1997, Section B.15, examples 13, 27, and 29.

The containment criteria for the ES-3100 package will be leaktight (defined in paragraph 2.1 of ANSI N14.5-1997 as having a leakage rate  $\leq 1 \times 10^{-7}$  ref-cm<sup>3</sup>/s) during the prototype tests. This leaktight criterion satisfies the design verification requirement stipulated in paragraph 7.2.4 of ANSI N14.5-1997. The requirements of ANSI N14.5-1997 are used for all stages of containment verification for the ES-3100 (i.e., design, fabrication, maintenance, periodic and preshipment).

The design, fabrication, maintenance and periodic leakage rate limit is  $1 \times 10^{-7}$  ref-cm<sup>3</sup>/s air. The pass criterion for the preshipment leakage rate test, which demonstrates correct assembly of the containment vessels, is  $1 \times 10^{-4}$  ref-cm<sup>3</sup>/s, which exceeds the requirements given in ANSI N14.5, paragraph 7.6.4. In accordance with the definition of sensitivity of a leakage test procedure provided in Sections 2 and 7.6.4 of ANSI N14.5-1997, the minimum acceptable leakage rate that the procedure needs to be capable of detecting is  $1 \times 10^{-3}$  ref-cm<sup>3</sup>/s. The requirements for the ES-3100 exceed the regulatory criterion by specifying a leakage rate of  $\leq 1 \times 10^{-4}$  ref-cm<sup>3</sup>/s, and equipment used in accordance with Section 7.6.4 of ANSI N14.5-1997 would not detect this leakage. The preshipment, fabrication, maintenance and periodic leakage rate tests are required to be conducted on each containment vessel in accordance with ANSI N14.5 and are specified in Chapters 7 and 8. These leakage rates are not dependent on filters or mechanical cooling.

The complete design verification testing of the ES-3100 package for NCT was conducted on test unit TU-4. Since the containment vessel was assembled at ambient conditions, the pressure was nominally 101.35 kPa (14.70 psia) at 25°C (77°F). In accordance with 10 CFR 71.71(b), the initial pressure inside each containment vessel should be the maximum normal operating pressure (MNOP). As calculated in

Table 4.5. Regulatory leakage criteria for NCT <sup>a</sup>

Verification Activity	Fast Absorption		Medium Absorption		Slow Absorption	
	$L_{RN - air}$ (ref-cm <sup>3</sup> /s)	$L_{RN - He}$ (cm <sup>3</sup> /s)	$L_{RN - air}$ (ref-cm <sup>3</sup> /s)	$L_{RN - He}$ (cm <sup>3</sup> /s)	$L_{RN - air}$ (ref-cm <sup>3</sup> /s)	$L_{RN - He}$ (cm <sup>3</sup> /s)
Design	3.8614e-03	4.1482e-03	3.7003e-03	3.9803e-03	3.2965e-03	3.5587e-03

<sup>a</sup> The procedure used to calculate the above criteria is shown in Appendix 4.6.2. This data has been extracted from Table 1 in Appendix 4.6.2.

Table 4.6. Containment vessel verification tests criteria for NCT

Test Type	Test Values	Leakage test procedure
<i>Design and compliance leakage testing</i>		
Design verification of O-ring seal (air)	$L_T \leq 1.0 \times 10^{-4}$ ref-cm <sup>3</sup> /s	See Appendix 2.10.7
Design verification of containment vessel boundary (helium)	$L_T \leq 2.0 \times 10^{-7}$ cm <sup>3</sup> /s	See Appendix 2.10.7
<i>Verification leakage testing</i>		
Fabrication, periodic, and maintenance (helium)	$L_T \leq 2.0 \times 10^{-7}$ cm <sup>3</sup> /s	Y51-01-B2-R-140, Rev. A.1 (Appendix 8.3.1)
	$L_T \leq 1.0 \times 10^{-4}$ ref-cm <sup>3</sup> /s	Y51-01-B2-R-074, Rev. A.1 (Appendix 7.5.1)

Appendix 3.6.4, the bounding case MNOP is 137.92 kPa (20.004 psia). The stresses at the maximum normal operating pressure [36.57 kPa (5.304 psig)] are insignificant compared to the allowable stresses (Table 2.21). O-ring grooves are designed and fabricated in accordance with guidance from the *Parker O-ring Handbook*. In accordance with Fig. 3-2 of the *Parker O-ring Handbook*, the durometer of the O-ring, and the tolerance gap from the production drawings, the O-ring should be able to withstand ~800 psig before anti-extrusion devices are required. Therefore, conducting a compliance test with the MNOP in the containment vessel will have little, if any, effect on the results.

Following the design verification testing of paragraphs 10 CFR 71.71(c)(5) through 71.71(c)(10) excluding 71.71(c)(8), Test Unit-4 was subjected to the sequential testing of paragraphs 10 CFR 71.73(c)(1) through (c)(4). Upon removal of the containment vessel from the drum assembly, the cavity between the O-rings was leak checked. This unit recorded a leak rate between the O-rings of  $2.4773 \times 10^{-5}$  ref-cm<sup>3</sup>/s.

Following the O-ring leak test, the entire containment boundary of TU-4 was helium leak tested to a value  $\leq 2 \times 10^{-7}$  cm<sup>3</sup>/s, thereby verifying a leak-tight boundary. The leak-test procedure followed to verify this criteria is documented in the ES-3100 test plan (Appendix 2.10.7). The maximum recorded helium leakage rate for this containment vessel was  $2.0 \times 10^{-7}$  cm<sup>3</sup>/s after 20 min of testing. Visual inspection following the testing indicated that neither the vessel body, the O-rings, the seal areas, nor the vessel lid assembly were damaged during the tests. Pictures taken of the containment vessel top following testing showed that the closure nut had rotated a maximum of 0.15 cm (0.060 in.) from its original radial position obtained during assembly. Based on the pitch of the closure nut, this rotation translates into only

0.0013 cm (0.0005 in.) decompression of the O-rings. This compares to the original nominal compression of 0.064 cm (0.025 in.). Therefore, O-ring compression was maintained during compliance testing. Based on these results, the ES-3100 package meets and exceeds the containment criteria specified in 10 CFR 71.51 for NCT when used to ship the contents described in the introductory section of this chapter.

Following fabrication, the containment vessel undergoes hydrostatic pressure testing to 1034 kPa (150 psi) gauge. The hydrostatic test is conducted before the final leakage test. Following the hydrostatic pressure test, and prior to conducting the leakage test, the containment vessel and O-ring cavity must be thoroughly dried. Each vessel is then leak tested with either air or helium to  $\leq 1 \times 10^{-7}$  ref-cm<sup>3</sup>/s or  $2 \times 10^{-7}$  cm<sup>3</sup>/s, respectively. This test ensures the containment vessel's integrity (walls, welds, inner O-ring seal) as delivered for use in accordance with paragraph 6.3.2 of ANSI N14.5-1997.

Following placement of the HEU content inside the containment vessel and joining the body and lid assembly, the volume between the containment vessel's O-ring seals is evacuated and checked to leak  $\leq 1 \times 10^{-4}$  ref-cm<sup>3</sup>/s. This leak-test procedure is a pressure rise air leak test prescribed in Section 7.1.2. This ensures that each containment vessel has been properly assembled in accordance with paragraph 7.6.4 of ANSI N14.5-1997.

The design verification tests were conducted following compliance tests in accordance with 10 CFR 71.71 and 71.73. The effectiveness of this closure system has been demonstrated by the NCT and HAC tests, which show that the complete containment system, including welds and O-ring seals, meet the leaktight criterion as defined in ANSI N14.5-1997 after the conclusion of the test series documented in *Test Report of the ES-3100 Package* (Appendix 2.10.7).

#### 4.4 CONTAINMENT UNDER HYPOTHETICAL ACCIDENT CONDITIONS (TYPE B PACKAGES)

**Requirements.** A Type B package, in addition to satisfying the requirements of paragraphs 10 CFR 71.41 through 71.47, must be designed, constructed, and prepared for shipment so that under the tests specified in Sect. 71.73 ("Hypothetical Accident Conditions"), there would be no escape of <sup>85</sup>Kr exceeding 10 A<sub>2</sub> in one week, no escape of other radioactive material exceeding a total amount A<sub>2</sub> in one week, and no external radiation dose rate exceeding 10 mSv/h (1 rem/h) at 1 m (40 in.) from the external surface of the package.

**Analysis.** Calculations have been conducted in Appendix 4.6.2 to determine the regulatory leakage criteria to satisfy the above requirements. The results are shown in Table 4.7. These analyses assume that the total mass of uranium for each component is available for release as an aerosol (worst case). From experimental tests, the maximum aerosol density containing uranium particulate was reported by Curren and Bond to be  $9.0 \times 10^{-6}$  g/cm<sup>3</sup>. This aerosol density is used to calculate the total activity concentration in ANSI N14.5-1997, Section B.15 examples 13, 27, and 29. Design leakage rate verification testing of the containment boundary (Table 4.8) was conducted on Test Units-1 through -6 and documented in test report (Appendix 2.10.7). Since each containment vessel was assembled at ambient conditions, the pressure was nominally 101.35 kPa (14.70 psi) at 25°C (77°F). In accordance with 10 CFR 71.73(b), for these tests, the initial pressure inside each containment vessel should be the maximum normal operating pressure. As shown in Table 2.21, the stresses at the maximum normal operating pressure are insignificant compared to the allowable stresses. Therefore, conducting compliance testing with nominal pressure in the containment vessel would have little, if any, effect on the results. During the structural and thermal tests conducted on the ES-3100 for HAC, the drum experienced plastic deformation, and the insulation and impact limiter material experienced some deterioration, as anticipated (Sect. 2.7). The containment vessels did not exhibit any signs of damage and passed post-test leak tests and the subsequent 10 CFR 71.73(c)(5)-specified 0.9-m

Table 4.7. Regulatory leakage criteria for HAC <sup>a</sup>

Verification activity	Fast absorption		Medium absorption		Slow absorption	
	$L_{RA - air}$ (ref-cm <sup>3</sup> /s)	$L_{RA - He}$ (cm <sup>3</sup> /s)	$L_{RA - air}$ (ref-cm <sup>3</sup> /s)	$L_{RA - He}$ (cm <sup>3</sup> /s)	$L_{RA - air}$ (ref-cm <sup>3</sup> /s)	$L_{RA - He}$ (cm <sup>3</sup> /s)
Design	6.7061e+00	6.4189e+00	6.4258e+00	6.1523e+00	5.7237e+00	5.4839e+00

<sup>a</sup> The procedure used to calculate the above criteria is shown in Appendix 4.6.2.

Table 4.8. Containment vessel design verification tests for HAC

Test Type	Test Values	Leakage test procedure
<i>Design and compliance leakage testing</i>		
Design verification of O-ring seal (air)	$L_T \leq 1.0 \times 10^{-4}$ ref-cm <sup>3</sup> /s	See Appendix 2.10.7
Design verification of containment vessel boundary (helium)	$L_T \leq 2.0 \times 10^{-7}$ cm <sup>3</sup> /s	See Appendix 2.10.7

(3-ft) water immersion tests except for Test Unit-6. Test Unit-6 was subjected to the test specified by paragraph 10 CFR 71.73(c)(6). After completion of this test, the containment vessel was removed and the lid was drilled and tapped for a helium leak-check port. The entire containment boundary was then helium leak checked and passed the leaktight criteria. Also, no visible water was seen inside the inner O-ring groove of Test Unit-6 and no water was observed inside any of the other test units.

To verify the entire containment boundary to the leaktight criteria, the containment vessels of Test Units-1 through -5 were helium leak tested using the procedure shown in the test report (Appendix 2.10.7). These test units had previously been subjected to the drop test stipulated in 10 CFR 71.71 (c)(6) and the sequential tests stipulated in 10 CFR 71.73 except for Test Unit-4, which had been first subjected to the testing in accordance with 10 CFR 71.71. The maximum recorded helium leak rate for any of these containment vessels was  $2.0 \times 10^{-7}$  cm<sup>3</sup>/s after 20 min of testing on Test Unit-4 as documented in Section 5.2 of the test report (Appendix 2.10.7). Test Units-2 and -5 displayed some unusual pulsing action during leak testing. The peak amplitude changed after adding helium in a manner expected for diffusion through the O-rings rather than a rise immediately following the addition of helium that would indicate a leak to the outside of the containment vessel. This is further discussed and graphically presented on pages 88 through 91 of the ES-3100 test report (Appendix 2.10.7). These measured leakage rates verify that the containment vessels are leaktight in accordance with ANSI N14.5-1997. Therefore, the containment boundary of the ES-3100 package was maintained during the HAC testing.

The 35.2 kg of HEU content is unirradiated; therefore, only very small quantities of fission gas products will be produced from spontaneous fission and subcritical neutron induced fission. Fission gas products are produced in such small quantities that they have no measurable effect on the releasable content source term or containment vessel pressurization. Fission gas products will not be considered further in this SAR.



#### 4.5 LEAKAGE RATE TESTS FOR TYPE B PACKAGES

The maximum allowable release of radioactive material allowed by 10 CFR 71.51(a)(2) under HAC is  $A_2$  in one week. Title 10 CFR 71.51(a)(2) also specifies that there be no escape of  $^{85}\text{Kr}$  exceeding  $10 A_2$  in one week. ANSI N14.5-1997 specifies the leakage test methods and leakage rates that are accepted in Nuclear Regulatory Commission (NRC) Regulatory Guide 7.4 as demonstrating that a package meets the 10 CFR 71.51(a)(2) requirements for containment. The containment criteria for the ES-3100 package will be leaktight, defined in ANSI N14.5 paragraph 2.1 as having a leakage rate  $\leq 1 \times 10^{-7}$  ref-cm<sup>3</sup>/s, during the prototype tests. This leaktight criterion satisfies the design verification requirement stipulated in paragraph 7.2.4 of ANSI N14.5-1997. The requirements of ANSI N14.5-1997 are used for all stages of containment verification for the ES-3100 (i.e., design, fabrication, maintenance, periodic and preshipment). The design, fabrication, maintenance and periodic leakage rate limit is  $1 \times 10^{-7}$  ref-cm<sup>3</sup>/s air (or  $2.0 \times 10^{-7}$  cm<sup>3</sup>/s helium). The pass criterion for the preshipment leakage rate test, which demonstrates correct assembly of the containment vessels, is  $1 \times 10^{-4}$  ref-cm<sup>3</sup>/s, which exceeds the requirements given in ANSI N14.5-1997, paragraph 7.6.4. In accordance with the definition of sensitivity of a leakage test procedure provided in Sections 2 and 7.6.4 of ANSI N14.5-1997, the minimum acceptable leakage rate that the procedure needs to be capable of detecting is  $1 \times 10^{-3}$  ref-cm<sup>3</sup>/s. The requirements for the ES-3100 exceed the regulatory criterion by specifying a leakage rate of  $\leq 1 \times 10^{-4}$  ref-cm<sup>3</sup>/s, and equipment used in accordance with Section 7.6.4 of ANSI N14.5-1997 would not detect this leakage. The preshipment, fabrication, maintenance, and periodic leakage rate tests are required to be conducted on each containment vessel in accordance with ANSI N14.5-1997 and are specified in Chapters 7 and 8. These leakage rates are not dependent on filters or mechanical cooling.

The requirements of ANSI N14.5-1997 are used for all stages of containment verification for the ES-3100; the design (HAC test) leakage rate limit is  $1 \times 10^{-7}$  ref-cm<sup>3</sup>/s (which is defined as leaktight in ANSI N14.5-1997). The packaging has been shown to maintain containment before and after prototype testing by leakage tests performed for containment verification to the requirements of ANSI N14.5-1997. Test Unit-4's containment vessel was subjected to both the NCT and HAC tests. Test Units-1 through -5 were subjected to the free drop stipulated in 10 CFR 71.71(c)(7) and to the sequential HAC test stipulated in 10 CFR 71.73. Following these tests, each containment vessel was helium leak tested in accordance with the test plan. Again, the test results verified that the containment vessels were leaktight. Thus, there could be no release of radioactive materials from the containment vessels. These leakage rates are not dependent on filters or mechanical cooling. These measured leakage rates verify that the containment vessels are leaktight in accordance with ANSI N14.5-1997.

Therefore, the ES-3100 package meets the containment criteria as specified in 10 CFR 71.73 for HAC when shipping the proposed 35.2 kg of HEU in the containment vessel.

## 4.6 APPENDICES

<b>Appendix</b>	<b>Description</b>
4.6.1	DETERMINATION OF $A_2$ FOR THE ES-3100 PACKAGE WITH HEU CONTENTS
4.6.2	CALCULATION OF THE ES-3100 CONTAINMENT VESSEL'S REGULATORY REFERENCE AIR LEAKAGE RATES



**APPENDIX 4.6.1**

**DETERMINATION OF A<sub>2</sub> FOR THE ES-3100 PACKAGE  
WITH HEU CONTENTS**

Prepared by: Monty L. Goins  
BWXT Y-12  
November 2006

Reviewed by: G. A Byington  
BWXT Y-12  
November 2006



## APPENDIX 4.6.1

### DETERMINATION OF $A_2$ FOR THE ES-3100 PACKAGE WITH HEU CONTENTS

#### Introduction

The containment criteria for radioactive, fissile material packages are given in 10 CFR 71.51(a)(1) for Normal Conditions of Transport (NCT) ( $\leq 10^{-6}$   $A_2$ /h) and in 71.51(a)(2) for Hypothetical Accident Conditions (HAC) ( $\leq A_2$  in a week). The  $A_2$  value for this mixture of radioisotopes must be determined to establish the content containment criteria and to determine the maximum release quantity that is allowed by the regulations. These values for a mixture of isotopes are determined by the methodology given in 10 CFR 71, Appendix A, "Determination of  $A_1$  and  $A_2$ ," Sect. IV. The results of these analyses are used to demonstrate compliance of the ES-3100 package with the containment requirements of 10 CFR 71.

#### Scope

The  $A_2$  value of the highly enriched uranium (HEU) content to be shipped is evaluated based on the mass and weight percents of HEU shown in Table 1 and defined in Sect. 1.2.3. The weight percents shown in Table 1 are the ones that generate the largest activity within the known weight percent ranges. Incorporating the new 10 CFR 71  $A_2$  values for the uranium isotopes, three different categories have been established based on the absorption rate of the uranium isotopes. The fast lung absorption, medium lung absorption and slow lung absorption categories are addressed in subsequent sections. By applying the maximum weight percents of isotopes  $^{232}\text{U}$ ,  $^{233}\text{U}$ ,  $^{234}\text{U}$ ,  $^{236}\text{U}$  and by incorporating the traces of  $^{237}\text{Np}$  and the transuranic isotopes, the maximum activity, minimum  $A_2$  value, and the minimum leakage requirements were determined for each category of absorption for the HEU oxides, compounds, and metal pieces. The mass and isotopic concentrations used for the proposed content do not take into consideration limits based on shielding and subcriticality.

Table 1. Isotopic mass and weight percent for the HEU contents <sup>a</sup>

Nuclide	Weight percent	Mass (g)
U-232	0.000004	0.001408
U-233	0.600000	211.200000
U-234	2.000000	704.000000
U-235	54.895996	19323.390592
U-236	40.000000	14080.000000
U-238	0.000000	0.000000
Transuranic	0.004000	1.408000
Np-237	2.500000	880.000000
Total	100.000000	35200.000000

<sup>a</sup> Weight percents values of individual isotopes are those that generate the largest activity within the allowable ranges presented in Sect. 1.2.3.

According to 10 CFR 71, Appendix A, parent and daughter nuclides are considered to be a mixture of different nuclides than those of the parent nuclide. The radioactive decay of uranium (refer to the decay chains presented by Dr. David C. Kocher, *Radioactive Decay Data Tables* [Kocher 1981]) creates isotopes that will accumulate enough activity to exceed their respective criteria for limited quantities (*Shippers—General Requirements for Shipments and Packagings* [49 CFR 173.423], Table A-7, "Activity Limits for Limited Quantities, Instruments, and Articles") and for Type A quantities of radionuclides (10 CFR 71, Table A-1, "A<sub>1</sub> and A<sub>2</sub> Values for Radionuclides"). Furthermore, the A<sub>2</sub> value for the mixture will change over time as a result of radioactive decay. The analysis below shows that the A<sub>2</sub> value for this mixture reaches a minimum at initial fabrication, increases to the 10<sup>th</sup> year, and declines through the 70<sup>th</sup> year.

## Analysis

**Mass Tables.** The mass and weight fractions for HEU isotopes used in the containment calculations are presented in Table 1. For conservatism, a small quantity of <sup>232</sup>U is assumed in this material at fabrication.

**ORIGEN-S Results.** The source terms of the isotopes in the mixtures were evaluated using the ORIGEN-S computer program (Parks 1984). The mass values for the parent and daughter products are presented in Table 2 for the time interval of 0–70 years. Contributions from the transuranics and <sup>237</sup>Np are held constant at each time interval during the 70-year evaluation.

The A<sub>2</sub> value of each mixture was calculated using the procedure shown in Tables 3, 4, and 5 for the above time intervals. The 70<sup>th</sup> year of decay represents the smallest value of A<sub>2</sub> and the maximum activity-to-A<sub>2</sub> value ratio (the smallest maximum allowable leakage rate within the time interval examined). A summary of the content activity and the A<sub>2</sub> value of the various configurations for the above time interval is given in Table 6.

From Section 1.2.3, the activity and mass concentrations for the transuranics are  $6 \times 10^5$  Bq/gU and 40 µg/gU, respectively. Using a maximum uranium mass of 35.2 kg, the mass of transuranics is calculated to be 1.408 g and the activity is calculated to be  $2.112 \times 10^2$  TBq. Dividing this activity by the mass results in a specific activity of  $1.5 \times 10^2$  TBq/g. In accordance with 10 CFR 71, Appendix A, Table A-3 for "contents with no relevant data," an A<sub>2</sub> value of  $9.0 \times 10^5$  TBq is obtained.

Section 1.2.3 gives a maximum concentration for Np-237 of 0.025 g/gU. Using a maximum uranium mass of 35.2 kg, the mass of Np-237 is calculated to be 880 g. This value is used in Tables 3, 4, and 5 of Appendix 4.6.1 for the Np-237 contents.

## Results

The containment criteria analysis indicates that the HEU contents must be shipped in a Type B material package since their activities are greater than the A<sub>2</sub> value. The smallest A<sub>2</sub> value of  $1.0997 \times 10^3$  TBq ( $2.9720 \times 10^2$  Ci) in conjunction with the maximum activity-to-A<sub>2</sub> value ratio of 293.99 occurs after about 70 years of decay for the assumed maximum 35.2 kg of HEU.



Table 2. Mass values of parent and daughter products for 35.2 kg of HEU

Isotope	0 years	5 years	10 years	20 years	30 years	40 years	50 years	60 years	70 years
Pb-210	0.0000e+00	1.4150e-10	1.0912e-09	8.1664e-09	2.5555e-08	5.6672e-08	1.0349e-07	1.6896e-07	2.5274e-07
Pb-212	0.0000e+00	1.8163e-08	2.0275e-08	1.8867e-08	1.7037e-08	1.5488e-08	1.3996e-08	1.2672e-08	1.1475e-08
Bi-210	0.0000e+00	8.7296e-14	6.7302e-13	5.0054e-12	1.5770e-11	3.4918e-11	6.3923e-11	1.0419e-10	1.5558e-10
Bi-212	0.0000e+00	1.7178e-09	1.9149e-09	1.7882e-09	1.6192e-09	1.4643e-09	1.3277e-09	1.2024e-09	1.0884e-09
Po-210	0.0000e+00	2.4077e-12	1.8586e-11	1.3798e-10	4.3507e-10	9.6448e-10	1.7670e-09	2.8653e-09	4.2944e-09
Rn-222	0.0000e+00	1.4150e-12	5.6602e-12	2.2598e-11	5.0829e-11	9.0112e-11	1.4080e-10	2.0205e-10	2.7526e-10
Ra-223	0.0000e+00	6.5313e-12	2.4734e-11	9.0047e-11	1.8454e-10	2.9951e-10	4.3091e-10	5.7390e-10	7.2463e-10
Ra-224	0.0000e+00	1.5770e-07	1.7600e-07	1.6474e-07	1.4925e-07	1.3489e-07	1.2207e-07	1.1053e-07	1.0011e-07
Ra-225	0.0000e+00	2.1120e-08	4.5619e-08	9.1238e-08	1.3686e-07	1.8227e-07	2.2810e-07	2.7245e-07	3.1891e-07
Ra-226	0.0000e+00	2.2035e-07	8.8000e-07	3.5200e-06	7.8848e-06	1.4010e-05	2.1894e-05	3.1469e-05	4.2803e-05
Ra-228	0.0000e+00	2.0557e-13	6.8992e-13	2.0557e-12	3.6186e-12	5.2378e-12	6.8710e-12	8.5184e-12	1.0166e-11
Ac-225	0.0000e+00	1.6896e-08	3.0835e-08	6.1670e-08	9.2506e-08	1.2313e-07	1.5396e-07	1.8459e-07	2.1542e-07
Ac-227	0.0000e+00	4.6183e-09	1.7565e-08	6.3574e-08	1.3043e-07	2.1256e-07	3.0531e-07	4.0579e-07	5.1207e-07
Ac-228	0.0000e+00	2.5062e-17	8.4198e-17	2.5062e-16	4.4070e-16	6.3923e-16	8.3917e-16	1.0391e-15	1.2484e-15
Th-227	0.0000e+00	1.0724e-11	4.0772e-11	1.4782e-10	3.0338e-10	4.9275e-10	7.0917e-10	9.4298e-10	1.1923e-09
Th-228	0.0000e+00	3.0694e-05	3.4214e-05	3.1962e-05	2.9005e-05	2.6189e-05	2.3795e-05	2.1542e-05	1.9430e-05
Th-229	0.0000e+00	6.3360e-03	9.0394e-03	1.8058e-02	2.7034e-02	3.6115e-02	4.4986e-02	5.4067e-02	6.3149e-02
Th-230	0.0000e+00	9.7856e-03	1.9501e-02	3.9072e-02	5.8573e-02	7.8144e-02	9.7856e-02	1.1686e-01	1.3658e-01
Th-231	0.0000e+00	7.8646e-08	7.8646e-08	7.8646e-08	7.8646e-08	7.8646e-08	7.8646e-08	7.8646e-08	7.8646e-08
Th-232	0.0000e+00	2.0416e-03	4.0973e-03	8.1946e-03	1.2292e-02	1.6333e-02	2.0416e-02	2.4640e-02	2.8723e-02
Th-234	0.0000e+00	0.0000e+00	0.0000e+00	0.0000e+00	0.0000e+00	0.0000e+00	0.0000e+00	0.0000e+00	0.0000e+00
Pa-231	0.0000e+00	9.3525e-05	1.8724e-04	3.7487e-04	5.6231e-04	7.4782e-04	9.3525e-04	1.1227e-03	1.3082e-03
Pa-233	0.0000e+00	0.0000e+00	0.0000e+00	0.0000e+00	0.0000e+00	0.0000e+00	0.0000e+00	0.0000e+00	0.0000e+00
U-232	1.4080e-03	1.3376e-03	1.2742e-03	1.1546e-03	1.0447e-03	9.4618e-04	8.5747e-04	7.7581e-04	7.0259e-04
U-233	2.1120e+02	2.1119e+02	2.1119e+02	2.1118e+02	2.1117e+02	2.1116e+02	2.1116e+02	2.1115e+02	2.1114e+02
U-234	7.0400e+02	7.0399e+02	7.0398e+02	7.0396e+02	7.0394e+02	7.0392e+02	7.0390e+02	7.0388e+02	7.0386e+02
U-235	1.9323e+04	1.9323e+04	1.9323e+04	1.9323e+04	1.9323e+04	1.9323e+04	1.9323e+04	1.9323e+04	1.9323e+04
U-236	1.4080e+04	1.4080e+04	1.4080e+04	1.4080e+04	1.4080e+04	1.4080e+04	1.4080e+04	1.4080e+04	1.4080e+04
U-238	0.0000e+00	0.0000e+00	0.0000e+00	0.0000e+00	0.0000e+00	0.0000e+00	0.0000e+00	0.0000e+00	0.0000e+00
Trans.	1.4080e+00	1.4080e+00	1.4080e+00	1.4080e+00	1.4080e+00	1.4080e+00	1.4080e+00	1.4080e+00	1.4080e+00
Np-237	8.8000e+02	8.8000e+02	8.8000e+02	8.8000e+02	8.8000e+02	8.8000e+02	8.8000e+02	8.8000e+02	8.8000e+02
Total	3.5200e+04	3.5200e+04	3.5200e+04	3.5200e+04	3.5200e+04	3.5200e+04	3.5200e+04	3.5200e+04	3.5200e+04

Table 3.  $A_2$  value calculation for 35.2 kg HEU for fast absorption uranium at 70 years

Isotope	Mass at 70 years (g)	Specific activity (TBq/g)	Activity (TBq)	$A_2$ (TBq)	$f(i)$ (TBq/TBq)	$f(i) / A_2$ (1/TBq)
Pb-210	2.5274e-07	2.8000e+00	7.0766e-07	5.0000e-02	2.1890e-06	4.3780e-05
Pb-212	1.1475e-08	5.1000e+04	5.8524e-04	2.0000e-01	1.8103e-03	9.0515e-03
Bi-210	1.5558e-10	4.6000e+03	7.1569e-07	6.0000e-01	2.2138e-06	3.6897e-06
Bi-212	1.0884e-09	5.4000e+05	5.8773e-04	6.0000e-01	1.8180e-03	3.0300e-03
Po-210	4.2944e-09	1.7000e+02	7.3005e-07	2.0000e-02	2.2583e-06	1.1291e-04
Rn-222	2.7526e-10	5.7000e+03	1.5690e-06	4.0000e-03	4.8534e-06	1.2133e-03
Ra-223	7.2463e-10	1.9000e+03	1.3768e-06	7.0000e-03	4.2588e-06	6.0840e-04
Ra-224	1.0011e-07	5.9000e+03	5.9064e-04	2.0000e-02	1.8270e-03	9.1351e-02
Ra-225	3.1891e-07	1.5000e+03	4.7837e-04	4.0000e-03	1.4797e-03	3.6993e-01
Ra-226	4.2803e-05	3.7000e-02	1.5837e-06	3.0000e-03	4.8989e-06	1.6330e-03
Ra-228	1.0166e-11	1.0000e+01	1.0166e-10	2.0000e-02	3.1446e-10	1.5723e-08
Ac-225	2.1542e-07	2.1000e+03	4.5239e-04	6.0000e-03	1.3994e-03	2.3323e-01
Ac-227	5.1207e-07	2.7000e+00	1.3826e-06	9.0000e-05	4.2768e-06	4.7519e-02
Ac-228	1.2404e-15	8.4000e+04	1.0420e-10	5.0000e-01	3.2231e-10	6.4463e-10
Th-227	1.1923e-09	1.1000e+03	1.3115e-06	5.0000e-03	4.0568e-06	8.1136e-04
Th-228	1.9430e-05	3.0000e+01	5.8291e-04	1.0000e-03	1.8031e-03	1.8031e+00
Th-229	6.3149e-02	7.9000e-03	4.9888e-04	5.0000e-04	1.5432e-03	3.0863e+00
Th-230	1.3658e-01	7.6000e-04	1.0380e-04	1.0000e-03	3.2108e-04	3.2108e-01
Th-231	7.8646e-08	2.0000e+04	1.5729e-03	2.0000e-02	4.8655e-03	2.4328e-01
Th-232	2.8723e-02	4.0000e-09	1.1489e-10	1.0000e+75	3.5540e-10	3.5540e-85
Pa-231	1.3082e-03	1.7000e-03	2.2239e-06	4.0000e-04	6.8793e-06	1.7198e-02
U-232	7.0259e-04	8.3000e-01	5.8315e-04	1.0000e-02	1.8039e-03	1.8039e-01
U-233	2.1114e+02	3.6000e-04	7.6010e-02	9.0000e-02	2.3512e-01	2.6125e+00
U-234	7.0386e+02	2.3000e-04	1.6189e-01	9.0000e-02	5.0077e-01	5.5641e+00
U-235	1.9323e+04	8.0000e-08	1.5458e-03	1.0000e+75	4.7817e-03	4.7817e-78
U-236	1.4080e+04	2.4000e-06	3.3792e-02	1.0000e+75	1.0453e-01	1.0453e-76
Transuranic	1.4080e+00	1.5000e-02	2.1120e-02	9.0000e-05	6.5330e-02	7.2588e+02
Np-237	8.8000e+02	2.6000e-05	2.2820e-02	2.0000e-03	7.0775e-02	3.5387e+01
Total Mass =	3.5200e+04	$\Sigma$ Act. =	3.2328e-01		$\Sigma f(i) / A_2 =$	7.7585e+02

$$A_2(\text{mixture}) = \frac{1}{\Sigma f(i) / A_2} = \frac{1}{7.7586 \times 10^2 (1/\text{TBq})} = 1.2889 \times 10^{-3} \text{ TBq}$$

Table 4.  $A_2$  value calculation for 35.2 kg HEU for medium absorption uranium at 70 years

Isotope	Mass at 70 years (g)	Specific activity (TBq/g)	Activity (TBq)	$A_2$ (TBq)	$f(i)$ (TBq/TBq)	$f(i) / A_2$ (1/TBq)
Pb-210	2.5274e-07	2.8000e+00	7.0766e-07	5.0000e-02	2.1890e-06	4.3780e-05
Pb-212	1.1475e-08	5.1000e+04	5.8524e-04	2.0000e-01	1.8103e-03	9.0515e-03
Bi-210	1.5558e-10	4.6000e+03	7.1569e-07	6.0000e-01	2.2138e-06	3.6897e-06
Bi-212	1.0884e-09	5.4000e+05	5.8773e-04	6.0000e-01	1.8180e-03	3.0300e-03
Po-210	4.2944e-09	1.7000e+02	7.3005e-07	2.0000e-02	2.2583e-06	1.1291e-04
Rn-222	2.7526e-10	5.7000e+03	1.5690e-06	4.0000e-03	4.8534e-06	1.2133e-03
Ra-223	7.2463e-10	1.9000e+03	1.3768e-06	7.0000e-03	4.2588e-06	6.0840e-04
Ra-224	1.0011e-07	5.9000e+03	5.9064e-04	2.0000e-02	1.8270e-03	9.1351e-02
Ra-225	3.1891e-07	1.5000e+03	4.7837e-04	4.0000e-03	1.4797e-03	3.6993e-01
Ra-226	4.2803e-05	3.7000e-02	1.5837e-06	3.0000e-03	4.8989e-06	1.6330e-03
Ra-228	1.0166e-11	1.0000e+01	1.0166e-10	2.0000e-02	3.1446e-10	1.5723e-08
Ac-225	2.1542e-07	2.1000e+03	4.5239e-04	6.0000e-03	1.3994e-03	2.3323e-01
Ac-227	5.1207e-07	2.7000e+00	1.3826e-06	9.0000e-05	4.2768e-06	4.7519e-02
Ac-228	1.2404e-15	8.4000e+04	1.0420e-10	5.0000e-01	3.2231e-10	6.4463e-10
Th-227	1.1923e-09	1.1000e+03	1.3115e-06	5.0000e-03	4.0568e-06	8.1136e-04
Th-228	1.9430e-05	3.0000e+01	5.8291e-04	1.0000e-03	1.8031e-03	1.8031e+00
Th-229	6.3149e-02	7.9000e-03	4.9888e-04	5.0000e-04	1.5432e-03	3.0863e+00
Th-230	1.3658e-01	7.6000e-04	1.0380e-04	1.0000e-03	3.2108e-04	3.2108e-01
Th-231	7.8646e-08	2.0000e+04	1.5729e-03	2.0000e-02	4.8655e-03	2.4328e-01
Th-232	2.8723e-02	4.0000e-09	1.1489e-10	1.0000e+75	3.5540e-10	3.5540e-85
Pa-231	1.3082e-03	1.7000e-03	2.2239e-06	4.0000e-04	6.8793e-06	1.7198e-02
U-232	7.0259e-04	8.3000e-01	5.8315e-04	7.0000e-03	1.8039e-03	2.5769e-01
U-233	2.1114e+02	3.6000e-04	7.6010e-02	2.0000e-02	2.3512e-01	1.1756e+01
U-234	7.0386e+02	2.3000e-04	1.6189e-01	2.0000e-02	5.0077e-01	2.5038e+01
U-235	1.9323e+04	8.0000e-08	1.5458e-03	1.0000e+75	4.7817e-03	4.7817e-78
U-236	1.4080e+04	2.4000e-06	3.3792e-02	2.0000e-02	1.0453e-01	5.2264e+00
Transuranic	1.4080e+00	1.5000e-02	2.1120e-02	9.0000e-05	6.5330e-02	7.2589e+02
Np-237	8.8000e+02	2.6000e-05	2.2880e-02	2.0000e-03	0.070774561	3.5387e+01
Total Mass =	3.5200e+04	$\Sigma$ Act. =	3.2328e-01		$\Sigma f(i) / A_2 =$	8.0978e+02

$$A_2(\text{mixture}) = \frac{1}{\Sigma f(i) / A_2} = \frac{1}{8.0978 \times 10^2 (1/\text{TBq})} = 1.2349 \times 10^{-3} \text{ TBq}$$

Table 5.  $A_2$  value calculation for 35.2 kg HEU for slow absorption uranium at 70 years

Isotope	Mass at 70 years (g)	Specific activity (TBq/g)	Activity (TBq)	$A_2$ (TBq)	$f(i)$ (TBq/TBq)	$f(i) / A_2$ (1/TBq)
Pb-210	2.5274e-07	2.8000e+00	7.0766e-07	5.0000e-02	2.1890e-06	4.3780e-05
Pb-212	1.1475e-08	5.1000e+04	5.8524e-04	2.0000e-01	1.8103e-03	9.0515e-03
Bi-210	1.5558e-10	4.6000e+03	7.1569e-07	6.0000e-01	2.2138e-06	3.6897e-06
Bi-212	1.0884e-09	5.4000e+05	5.8773e-04	6.0000e-01	1.8180e-03	3.0300e-03
Po-210	4.2944e-09	1.7000e+02	7.3005e-07	2.0000e-02	2.2583e-06	1.1291e-04
Rn-222	2.7526e-10	5.7000e+03	1.5690e-06	4.0000e-03	4.8534e-06	1.2133e-03
Ra-223	7.2463e-10	1.9000e+03	1.3768e-06	7.0000e-03	4.2588e-06	6.0840e-04
Ra-224	1.0011e-07	5.9000e+03	5.9064e-04	2.0000e-02	1.8270e-03	9.1351e-02
Ra-225	3.1891e-07	1.5000e+03	4.7837e-04	4.0000e-03	1.4797e-03	3.6993e-01
Ra-226	4.2803e-05	3.7000e-02	1.5837e-06	3.0000e-03	4.8989e-06	1.6330e-03
Ra-228	1.0166e-11	1.0000e+01	1.0166e-10	2.0000e-02	3.1446e-10	1.5723e-08
Ac-225	2.1542e-07	2.1000e+03	4.5239e-04	6.0000e-03	1.3994e-03	2.3323e-01
Ac-227	5.1207e-07	2.7000e+00	1.3826e-06	9.0000e-05	4.2768e-06	4.7519e-02
Ac-228	1.2404e-15	8.4000e+04	1.0420e-10	5.0000e-01	3.2231e-10	6.4463e-10
Th-227	1.1923e-09	1.1000e+03	1.3115e-06	5.0000e-03	4.0568e-06	8.1136e-04
Th-228	1.9430e-05	3.0000e+01	5.8291e-04	1.0000e-03	1.8031e-03	1.8031e+00
Th-229	6.3149e-02	7.9000e-03	4.9888e-04	5.0000e-04	1.5432e-03	3.0863e+00
Th-230	1.3658e-01	7.6000e-04	1.0380e-04	1.0000e-03	3.2108e-04	5.2108e-01
Th-231	7.8646e-08	2.0000e+04	1.5729e-03	2.0000e-02	4.8655e-03	2.4328e-01
Th-232	2.8723e-02	4.0000e-09	1.1489e-10	1.0000e+75	3.5540e-10	3.5540e-85
Pa-231	1.3082e-03	1.7000e-03	2.2239e-06	4.0000e-04	6.8793e-06	1.7198e-02
U-232	7.0259e-04	8.3000e-01	5.8315e-04	1.0000e-03	1.8039e-03	1.8039e+00
U-233	2.1114e+02	3.6000e-04	7.6010e-02	6.0000e-03	2.3512e-01	3.9187e+01
U-234	7.0386e+02	2.3000e-04	1.6189e-01	6.0000e-03	5.0077e-01	8.3461e+01
U-235	1.9323e+04	8.0000e-08	1.5458e-03	1.0000e+75	4.7817e-03	4.7817e-78
U-236	1.4080e+04	2.4000e-06	3.3792e-02	6.0000e-03	1.0453e-01	1.7421e+01
Transuranic	1.4080e+00	1.5000e-02	2.1120e-02	9.0000e-05	6.5330e-02	7.2589e+02
Np-237	8.8000e+02	2.6000e-05	2.2880e-02	2.0000e-03	0.070774361	3.5387e+01
Total Mass	3.5200e+04	$\Sigma$ Act. =	3.2328e-01		$\Sigma f(i) / A_2 =$	9.0938e+02

$$A_2(\text{mixture}) = \frac{1}{\Sigma f(i) / A_2} = \frac{1}{9.0937 \times 10^2 (1/\text{TBq})} = 1.0997 \times 10^{-3} \text{ TBq}$$

Table 6. Activity,  $A_2$  value, and activity-to- $A_2$  ratio for the enriched uranium contents

Year	Activity (TBq)	$A_2$ -Mixture (TBq)			Activity/ $A_2$		
		Fast	Medium	Slow	Fast	Medium	Slow
0	3.1846e-01	1.2796e-03	1.2255e-03	1.0885e-03	248.87	259.86	292.57
5	3.2380e-01	1.2950e-03	1.2405e-03	1.1026e-03	250.04	261.03	293.68
10	3.2427e-01	1.2960e-03	1.2415e-03	1.1037e-03	250.21	261.20	293.81
20	3.2410e-01	1.2948e-03	1.2404e-03	1.1031e-03	250.31	261.29	293.82
30	3.2386e-01	1.2934e-03	1.2391e-03	1.1022e-03	250.40	261.38	293.82
40	3.2366e-01	1.2921e-03	1.2379e-03	1.1015e-03	250.49	261.47	293.84
50	3.2350e-01	1.2909e-03	1.2368e-03	1.1008e-03	250.59	261.56	293.87
60	3.2338e-01	1.2899e-03	1.2358e-03	1.1002e-03	250.71	261.68	293.93
70	3.2328e-01 <sup>a</sup>	1.2889e-03	1.2349e-03	1.0997e-03 <sup>a</sup>	250.82	261.79	293.99 <sup>a</sup>

<sup>a</sup> The  $A_2$ , total activity, and activity-to- $A_2$  ratio values used in Appendix 4.6.2.



## **APPENDIX 4.6.2**

### **CALCULATION OF THE ES-3100 CONTAINMENT VESSEL'S REGULATORY REFERENCE AIR LEAKAGE RATES**

Prepared by:

Monty L. Goins  
BWXT Y-12  
November 2006

Reviewed by:

G. A. Byington  
BWXT Y-12  
November 2006





## APPENDIX 4.6.2

### CALCULATION OF THE ES-3100 CONTAINMENT VESSEL'S REGULATORY REFERENCE AIR LEAKAGE RATES

#### Introduction

The ES-3100 leak-testing requirements of the containment boundary are based on the smallest maximum allowable leakage rate generated from the maximum uranium content defined in Table 4.3. Section 5 of ANSI N14.5-1997 defines the maximum allowable leakage rate based on the maximum allowable release rate. These leakage rates,  $L_N$  and  $L_A$ , are the maximum allowable O-ring seal leakage rates for Normal Conditions of Transport (NCT) and Hypothetical Accident Conditions (HAC). The worst-case maximum allowable leakage rates are used to calculate an equivalent leakage hole diameter following ANSI N14.5-1997, Appendix B, for each condition of transport. This leakage hole diameter is used to calculate a reference air and a helium leakage rate for leak testing. A bounding mass for the highly enriched uranium (HEU) content of **35.2 kg** is used in this calculation to certify the ES-3100 package for shipment. The maximum allowable leakage rates are calculated using this maximum content mass in a much more dispersive form (oxide powder) at the highest calculated pressures and temperatures. This appendix shows the procedure used to calculate the leak criteria for the uranium constituents in the "slow lung absorption" group. Table 1 shows the results of using this procedure for fast, medium, and slow absorption uranium constituents as a function of decay time.

#### HEU Content

Calculate  $R_N$  and  $R_A$ :

Table 4.1

The maximum allowable release rate is based on using  $A_2$ .

$$A_2 = 1.0997 \times 10^{-3} \text{ TBq}, (2.9720 \times 10^{-2} \text{ Ci}).$$

Table 6 (Appendix 4.6.1)

The containment requirements for NCT and HAC are:

$$\begin{aligned} R_N &= A_2 \times 10^{-6} \text{ TBq/h} = A_2 \times 2.78 \times 10^{-10} \text{ TBq/s}, & \text{ANSI N14.5-1997 (Eq. 1)} \\ &= 1.0997 \times 10^{-3} \times 2.78 \times 10^{-10} \text{ TBq/s}, \\ R_N &= 3.0570 \times 10^{-13} \text{ TBq/s}, (8.2623 \times 10^{-12} \text{ Ci/s}). \end{aligned}$$

$$\begin{aligned} R_A &= A_2 \text{ (TBq/week)}, \\ &= A_2 \times 1.65 \times 10^{-6} \text{ (TBq/s)}, & \text{ANSI N14.5-1997 (Eq. 2)} \\ &= 1.0997 \times 10^{-3} \times 1.65 \times 10^{-6} \text{ TBq/s}, \\ &= 1.8144 \times 10^{-9} \text{ TBq/s}, (4.9038 \times 10^{-8} \text{ Ci/s}). \end{aligned}$$

or limited to  $10 A_2$ /week of  $^{85}\text{Kr}$

Following ANSI N14.5-1997, the medium aerosol activity must be calculated to determine the leakage rates.

$$\begin{aligned} m &= \text{total nuclide mass in the package available for release (g)}, \\ \text{TotA} &= \text{total activity in the package available for release (TBq)}, \\ \text{TSA} &= \text{total specific activity in the package available for release (TBq/g)}. \end{aligned}$$

For HEU content:

$$\begin{aligned} \text{TSA} &= \text{TotA} / m, \\ \text{TSA} &= 3.2328 \times 10^{-1} \text{ (TBq)} / 35,200 \text{ (g)}, \\ \text{TSA} &= 9.1842 \times 10^{-6} \text{ TBq/g.} \end{aligned} \quad \text{Table 6 (Appendix 4.6.1)}$$

$$\rho_p = 9 \times 10^{-6} \text{ g/cm}^3. \quad \text{The maximum density of powder aerosols in the fill gas}$$

For any packaging arrangement:

$$\begin{aligned} C_N &= \text{activity per unit volume of medium that could escape from the containment system (TBq/cm}^3\text{).} \\ C_N &= \text{TSA} \times \rho_p, \\ C_N &= 9.1842 \times 10^{-6} \text{ (TBq/g)} \times 9 \times 10^{-6} \text{ (g/cm}^3\text{),} \\ C_N &= 8.2658 \times 10^{-11} \text{ TBq/cm}^3. \end{aligned}$$

Using Curren's maximum aerosol density,  $C_A = C_N$ :

$$\begin{aligned} C_A &= \text{activity per unit volume of exiting gas (TBq/cm}^3\text{),} \\ C_A &= 8.2658 \times 10^{-11} \text{ TBq/cm}^3. \end{aligned} \quad \text{HAC}$$

Section 6.1 of ANSI N14.5-1997 calculates  $L_N$  with (Eq. 3) and  $L_A$  with (Eq. 4).  $L_N$  and  $L_A$  are the maximum allowable leakage rates for the containment vessel fill gas aerosol during NCT and HAC, respectively.

$$\begin{aligned} L_N &= \text{maximum allowable leakage rate for the medium for NCT (TBq/cm}^3\text{),} \\ L_N &= R_N / C_N, \\ L_N &= 3.0570 \times 10^{-13} \text{ (TBq/s)} / 8.2658 \times 10^{-11} \text{ (TBq/cm}^3\text{),} \\ L_N &= 3.6984 \times 10^{-3} \text{ cm}^3\text{/s.} \end{aligned} \quad \text{ANSI N14.5-1997 (Eq. 3)}$$

$$\begin{aligned} L_A &= \text{maximum allowable leakage rate for the medium for HAC (TBq/cm}^3\text{),} \\ L_A &= R_A / C_A, \\ L_A &= 1.8144 \times 10^{-9} \text{ (TBq/s)} / 8.2658 \times 10^{-11} \text{ (TBq/cm}^3\text{),} \\ L_A &= 2.1951 \times 10^1 \text{ cm}^3\text{/s.} \end{aligned}$$

$L_N$  and  $L_A$  correspond to the upstream volumetric leakage rate ( $L_u$ ) at the upstream pressure ( $P_u$ ) in the ANSI N14.5-1997 formulas for use later in this appendix. The reference air leakage rates  $L_{R,N}$  and  $L_{R,A}$  for NCT and HAC, based on the  $L_N$  and  $L_A$ , are then calculated using maximum temperatures and pressure combinations from Table 3.16 and Table 5 in Appendix 3.6.5.

### Determination of the Leakage Test Procedure Requirements for the HEU Content

This calculation will examine the most conservative effects of a fully loaded containment vessel with an HEU mass of 35.2 kg. The smallest allowable leakage values are shown in Tables 4.5 and 4.7. The  $A_2$  value and the maximum content activity-to- $A_2$  value ratio for this mixture were calculated for several different decay times (Table 6, Appendix 4.6.1). As calculated in Appendix 4.6.1, the  $A_2$  value and the maximum content activity-to- $A_2$  ratio used to qualify this package occur at about 70 years of decay and are  $1.0997 \times 10^{-3} \text{ TBq}$  ( $2.9720 \times 10^{-2} \text{ Ci}$ ) and 293.99, respectively. These values are used to determine the leakage test procedural requirements when packaging any convenience cans/contents arrangements in the ES-3100 package. The convenience cans are sealed inside the containment vessel in an environmentally controlled area. The ES-3100 package has been analyzed thermally in Sect. 3; it was evaluated at a

maximum NCT gas temperature of 87.81°C (190.06°F) [100°F with solar insolation] and a maximum adjusted HAC gas temperature of 123.85°C (254.93°F).

The following analysis determines the maximum allowable O-ring seal air reference leakage rate for both NCT and HAC. The ANSI N14.5-1997 recommended method using a straight circular tube to model the leakage path is applied. Using this "standard" leakage hole model permits the calculation of equivalent reference leakage rates from which leak-test requirements can be established. Viscosity data for air and helium used in the following analyses were obtained from curve fitting routines at specific temperatures based on viscosity data for air (Handbook of Chemistry and Physics, 55th ed.) and helium (NBS Technical Note 631).

$L_N$  and  $L_A$  correspond to the upstream volumetric leakage rate ( $L_u$ ) at the upstream pressure ( $P_u$ ).

$$\begin{aligned} L_N &= 3.6984 \times 10^{-3} \text{ cm}^3/\text{s}, \\ L_A &= 2.1951 \times 10^1 \text{ cm}^3/\text{s}. \end{aligned}$$

Find the maximum pressure and temperature in the containment vessel:

Converting the temperature to degrees Kelvin:

$$\begin{aligned} T &= 273.15 + T(^{\circ}\text{C}), \\ T &= 273.15 + 5/9 (^{\circ}\text{F} - 32) (\text{K}). \\ T_N &= 273.15 + 5/9 (190.06^{\circ}\text{F} - 32) (\text{K}), & (\text{Sect. 3.4.1, for } T = 190.06^{\circ}\text{F}) \\ T_N &= 360.961 \text{ K}. & \text{NCT} \\ T_A &= 273.15 + 5/9 (254.93^{\circ}\text{F} - 32) (\text{K}), & (\text{Sect. 3.5.3, for } T = 254.93^{\circ}\text{F}) \\ T_A &= 397.000 \text{ K}. & \text{HAC} \end{aligned}$$

Converting the pressures from psia to atmospheres:

$$\begin{aligned} P_N &= P (\text{psia}) / 14.696 (\text{psia/atm}), & \text{where } P \text{ is the pressure in Sect. 3.4.2} \\ P_N &= 20.004 (\text{psia}) / 14.696 (\text{psia/atm}), & \text{NCT} \\ P_N &= 1.3612 \text{ atm}. \\ P_A &= P (\text{psia}) / 14.696 (\text{psia/atm}), & \text{where } P \text{ is the pressure in Sect. 3.5.3} \\ P_A &= 73.625 (\text{psia}) / 14.696 (\text{psia/atm}), & \text{HAC} \\ P_A &= 5.0099 \text{ atm}. \end{aligned}$$

### NCT Leakage Hole Diameter for the HEU Content

The following calculations determine the leakage hole diameter that generates the maximum allowable leakage rate during NCT. To keep these calculations conservative, the maximum values for temperature and pressure were used as steady-state conditions for NCT.

Input data for NCT with air fill gas:

$$\begin{aligned} L_N &= 3.6984 \times 10^{-3} \text{ cm}^3/\text{s}, & \text{Maximum upstream leakage} \\ P_u &= 1.3612 \text{ atm}, & \text{Upstream pressure} = 20.004 \text{ psia} \\ P_d &= 0.2382 \text{ atm}, & \text{Downstream pressure} = 3.5 \text{ psia, per 10 CFR 71.71(3)} \\ a &= 0.3531 \text{ cm}, & \text{Leak path length, 0.139-in. O-ring section diameter} \end{aligned}$$

$$\begin{aligned} T &= 360.96 \text{ K,} \\ \mu &= 0.02141 \text{ cP,} \\ M &= 29 \text{ g/g-mole.} \end{aligned}$$

Fill gas temperature = 190.06°F  
Viscosity at temperature  
Molecular weight of fill gas

The average pressure is:

$$\begin{aligned} P_a &= (P_u + P_d)/2, \\ &= (1.3612 + 0.2382) / 2, \\ P_a &= 0.7997 \text{ atm.} \end{aligned}$$

Average pressure during NCT

According to ANSI N14.5-1997, the flow leakage hole diameter is unknown. Therefore, the mass-like leakage flow rate must be calculated to calculate the average leakage flow rate.

Q is the mass-like leakage for flow using the upstream leakage,  $L_u$ , and pressure,  $P_u$ :

$$\begin{aligned} Q &= P_u L_u, & (\text{Eq. B1}) \\ L_u &= L_N. & \text{NCT leakage} \end{aligned}$$

$$\begin{aligned} Q &= (1.3612)(\text{atm})(3.6984 \times 10^{-3})(\text{cm}^3/\text{s}), \\ Q &= 5.0343 \times 10^{-3} \text{ atm-cm}^3/\text{s}. & \text{NCT mass-like leakage rate} \end{aligned}$$

$$\begin{aligned} Q &= P_a L_a, & (\text{Eq. B1}) \\ L_a &= Q / P_a = 5.0353 \times 10^{-3} (\text{atm-cm}^3/\text{s}) / (0.7997)(\text{atm}), \\ L_a &= 6.2954 \times 10^{-3} \text{ cm}^3/\text{s}. & \text{NCT average leakage rate} \end{aligned}$$

Solve equations B2–B4 from ANSI N14.5-1997:

$$\begin{aligned} L_a &= (F_c + F_m) (P_u - P_d) \text{ cm}^3/\text{s}, & (\text{Eq. B2}) \\ L_a &= (F_c + F_m)(1.3612 - 0.2382), \\ L_a &= (1.1230) (F_c + F_m) \text{ cm}^3/\text{s}. \end{aligned}$$

$$\begin{aligned} F_c &= (2.49 \times 10^6) D^4 / (a \mu) (\text{cm}^3/\text{atm-s}), & (\text{Eq. B3}) \\ F_c &= (2.49 \times 10^6) D^4 / ((0.3531)(0.02141)), \\ F_c &= (3.2943 \times 10^8) D^4 \text{ cm}^3/\text{atm-s}. \end{aligned}$$

$$\begin{aligned} F_m &= (3.81 \times 10^3) D^3 (T / M)^5 / (a P_a) (\text{cm}^3/\text{atm-s}), & (\text{Eq. B4}) \\ F_m &= (3.81 \times 10^3) D^3 (360.96 / 29)^5 / ((0.3531)(0.7997)), \\ F_m &= (4.7610 \times 10^4) D^3 \text{ cm}^3/\text{atm-s}. \end{aligned}$$

From the mass-like leakage calculation:

$$L_a = 6.2954 \times 10^{-3} \text{ cm}^3/\text{s}. \quad \text{NCT average leakage rate}$$

Find the leakage hole diameter that sets:

$$L_2 = L_a.$$

Using the equations:

$$\begin{aligned} L_2 &= (1.1230) (F_c + F_m) \text{ cm}^3/\text{s}, \\ F_c &= (3.2943 \times 10^8) D^4 \text{ cm}^3/\text{atm-s}, \\ F_m &= (4.7610 \times 10^4) D^3 \text{ cm}^3/\text{atm-s}. \end{aligned}$$

To get a better guess on a new D use:

$$D = D_2 (L_a / L_2)^{0.252}$$

Now a guess must be made for  $D_2$  to solve Eq. B2 for NCT:

$$D_2 = 0.001 \text{ cm, and solve for } L_a = 6.2954 \times 10^{-3} \text{ cm}^3/\text{s.} \quad \text{NCT average leakage rate}$$

Diameter	$F_c$	$F_m$	$L_2$	$L_a / L_2$
1.00000e-03	3.29434e-04	4.76097e-05	4.23431e-04	1.48676e+01
1.97426e-03	5.00481e-03	3.66361e-04	6.03197e-03	1.04367e+00
1.99564e-03	5.22516e-03	3.78393e-04	6.29294e-03	1.00039e+00
1.99584e-03	5.22721e-03	3.78504e-04	6.29537e-03	1.00001e+00
1.99584e-03	5.22727e-03	3.78507e-04	6.29543e-03	9.99997e-01

The NCT leakage hole diameter for the HEU oxide content:

$$D = 1.9958 \times 10^{-3} \text{ cm.} \quad \text{NCT diameter}$$

#### NCT Reference Air Leakage Rate for HEU Content

The leakage hole diameter found for the maximum allowable leakage rate for NCT will be used to determine the reference air leakage rate. O-ring seal leakage testing must ensure that no leakage is greater than the leakage generated by the hole diameter  $D = 1.9958 \times 10^{-3} \text{ cm}$ . Therefore, the NCT reference leakage flow rate ( $L_{R,N}$ ) must be calculated to determine the allowable test leakage rate.

Input data for NCT reference air leakage rate:

D	=	$1.9958 \times 10^{-3} \text{ cm,}$	From NCT
a	=	0.3531 cm,	Leak path length, 0.139-in. O-ring section diameter
$P_u$	=	1.0 atm,	Upstream pressure
$P_d$	=	0.01 atm,	Downstream pressure
T	=	298 K,	Fill gas temperature, 77°F
M	=	29 g/g-mole,	Molecular weight of air
$\mu$	=	0.0185 cP,	Viscosity of air at reference temperature

Calculate  $P_a$ :

$$\begin{aligned} P_a &= (P_u + P_d) / 2, \\ &= (1.0 + 0.01) / 2, \\ P_a &= 0.505 \text{ atm.} \end{aligned} \quad \text{NCT average pressure}$$

$$\begin{aligned}
 F_c &= (2.49 \times 10^6) D^4 / (a \mu) (\text{cm}^3/\text{atm-s}), \\
 F_c &= (2.49 \times 10^6) (1.9958 \times 10^{-3})^4 / ((0.3531) (0.0185)), \\
 F_c &= (3.8122 \times 10^8) (1.9958 \times 10^{-3})^4, \\
 F_c &= 6.04790 \times 10^{-3} \text{ cm}^3/\text{atm-s}.
 \end{aligned}
 \tag{Eq. B3}$$

$$\begin{aligned}
 F_m &= (3.81 \times 10^3) D^3 (T/M)^5 / (a P_a) (\text{cm}^3/\text{atm-s}), \\
 F_m &= (3.81 \times 10^3) (1.9958 \times 10^{-3})^3 (298/29)^5 / ((0.3531) (0.505)), \\
 F_m &= (6.8501 \times 10^4) (1.9958 \times 10^{-3})^3, \\
 F_m &= 5.4459 \times 10^{-4} \text{ cm}^3/\text{atm-s}.
 \end{aligned}
 \tag{Eq. B4}$$

$$\begin{aligned}
 L_u &= (F_c + F_m) (P_u - P_d) (P_a / P_u) (\text{cm}^3/\text{s}), \\
 L_u &= (6.0490 \times 10^{-3} + 5.4459 \times 10^{-4}) (\text{cm}^3/\text{atm-s}) (1.0 - 0.01) (\text{atm}) (0.505 / 1.0), \\
 L_u &= (6.5937 \times 10^{-3}) (\text{cm}^3/\text{atm-s}) (0.49995) (\text{atm}), \\
 L_u &= 3.2965 \times 10^{-3} \text{ cm}^3/\text{s}.
 \end{aligned}
 \tag{Eq. B5}$$

The reference air leakage rate as defined in ANSI N14.5-1997, Sect. B.3, is the upstream leakage in air.

$$L_{RN,Air} = 3.2965 \times 10^{-3} \text{ ref-cm}^3/\text{s}. \quad \text{For HEU oxide content}$$

The same equations can be used to calculate an allowable leakage rate using helium for leak testing.

$$\begin{aligned}
 M &= 4 \text{ g/g-mole}, & \text{Molecular weight of helium} \\
 \mu &= 0.0198 \text{ cP}. & \text{Viscosity of helium at temperature}
 \end{aligned}$$

$$\begin{aligned}
 F_c &= (2.49 \times 10^6) D^4 / (a \mu) (\text{cm}^3/\text{atm-s}), \\
 F_c &= (2.49 \times 10^6) (1.9958 \times 10^{-3})^4 / ((0.3531) (0.0198)), \\
 F_c &= (3.5619 \times 10^8) (1.9958 \times 10^{-3})^4, \\
 F_c &= 5.6518 \times 10^{-3} \text{ cm}^3/\text{atm-s}.
 \end{aligned}
 \tag{Eq. B3}$$

$$\begin{aligned}
 F_m &= (3.81 \times 10^3) D^3 (T/M)^5 / (a P_a) (\text{cm}^3/\text{atm-s}), \\
 F_m &= (3.81 \times 10^3) (1.9958 \times 10^{-3})^3 (298/4)^5 / ((0.3531) (0.505)), \\
 F_m &= (1.8444 \times 10^5) (1.9958 \times 10^{-3})^3, \\
 F_m &= 1.4664 \times 10^{-3} \text{ cm}^3/\text{atm-s}.
 \end{aligned}
 \tag{Eq. B4}$$

$$\begin{aligned}
 L_u &= (F_c + F_m) (P_u - P_d) (P_a / P_u) (\text{cm}^3/\text{s}), \\
 L_u &= (5.6518 \times 10^{-3} + 1.4664 \times 10^{-3}) (\text{cm}^3/\text{atm-s}) (1.0 - 0.01) (\text{atm}) (0.505 / 1.0), \\
 L_u &= (7.1182 \times 10^{-3}) (\text{cm}^3/\text{atm-s}) (0.49995) (\text{atm}), \\
 L_u &= 3.5587 \times 10^{-3} \text{ cm}^3/\text{s}.
 \end{aligned}
 \tag{Eq. B5}$$

The allowable leakage rate using helium for leak testing is:

$$L_{RN,He} = 3.5587 \times 10^{-3} \text{ cm}^3/\text{s}. \quad \text{NCT helium test value}$$

### HAC Leakage Hole Diameter for HEU Content

The calculation of a maximum allowable leakage rate hole diameter is based on the temperature and pressure of the fill gas aerosol for HAC, assuming the content is in an oxide powder form. Keeping this calculation conservative, the maximum values for temperature and pressure were used as steady-state conditions for a week. The maximum values were generated during the 30-min burn test for HAC.



# Input data for HAC:

$$\begin{aligned} L_A &= 21.951 \text{ cm}^3/\text{s}, \\ P_u &= 5.0099 \text{ atm}, \\ P_d &= 1.0 \text{ atm}, \\ T &= 397.000 \text{ K}, \\ \mu &= 0.02297 \text{ cP}, \\ M &= 29 \text{ g/g-mole}, \\ a &= 0.3531 \text{ cm}. \end{aligned}$$

Maximum exit leakage  
Upstream pressure = 73.625 psia  
Downstream pressure  
Fill gas temperature = 254.93°F  
Viscosity of air at temperature  
Molecular weight of air  
Leak path length, 0.139-in. O-ring section diameter

$$\begin{aligned} P_a &= (P_u + P_d) / 2 \\ &= (5.0099 + 1.0) / 2, \\ P_a &= 3.0049 \text{ atm}. \end{aligned}$$

HAC average pressure

Q is the mass-like leakage for flow using the upstream leakage,  $L_u$ , and pressure,  $P_u$ :

$$\begin{aligned} Q &= P_u L_u, & \text{(Eq. B1)} \\ L_u &= L_A. & \text{HAC leakage} \end{aligned}$$

$$\begin{aligned} Q &= (5.0099)(\text{atm})(21.951)(\text{cm}^3/\text{s}), \\ Q &= 109.973 \text{ atm-cm}^3/\text{s}. & \text{HAC mass-like leakage rate} \end{aligned}$$

$$\begin{aligned} Q &= P_a L_a, & \text{(Eq. B1)} \\ L_a &= Q / P_a \\ &= 109.973 (\text{atm-cm}^3/\text{s}) / (3.0049)(\text{atm}), \\ L_a &= 36.597 \text{ cm}^3/\text{s}. & \text{HAC average leakage rate} \end{aligned}$$

Solve equations B2–B4 from ANSI N14.5-1997:

$$\begin{aligned} L_a &= (F_c + F_m) (P_u - P_d) (\text{cm}^3/\text{s}), & \text{(Eq. B2)} \\ L_a &= (F_c + F_m) (5.0099 - 1.0), \\ L_a &= 4.0099 (F_c + F_m) \text{ cm}^3/\text{s}. \end{aligned}$$

$$\begin{aligned} F_c &= (2.49 \times 10^6) D^4 / (a \mu) (\text{cm}^3/\text{atm-s}), & \text{(Eq. B3)} \\ F_c &= (2.49 \times 10^6) D^4 / ((0.3531) (0.02297)), \\ F_c &= (3.0706 \times 10^8) D^4 \text{ cm}^3/\text{atm-s}. \end{aligned}$$

$$\begin{aligned} F_m &= (3.81 \times 10^3) D^3 (T / M)^5 / (a P_a) (\text{cm}^3/\text{atm-s}), & \text{(Eq. B4)} \\ F_m &= (3.81 \times 10^3) D^3 (397.00 / 29)^5 / ((0.3531) (3.0049)), \\ F_m &= (1.5287 \times 10^4) D^3 \text{ cm}^3/\text{atm-s}. \end{aligned}$$

From the mass-like leakage calculation:

$$L_a = 36.597 \text{ cm}^3/\text{s}. \quad \text{HAC average leakage rate}$$

Find the leakage hole diameter that sets:

$$L_2 = L_a.$$

Using the equations:

$$\begin{aligned} L_2 &= 4.0099 (F_c + F_m) \text{ cm}^3/\text{s}, \\ F_c &= (3.0706 \times 10^8) D^4 \text{ cm}^3/\text{atm-s}, \\ F_m &= (1.3287 \times 10^4) D^3 \text{ cm}^3/\text{atm-s}. \end{aligned}$$

To get a better guess on a new D use:

$$D = D_2 (L_a / L_2)^{0.252}.$$

Now a guess must be made for  $D_2$  to solve Eq. B2 for HAC:

$$D_2 = 0.01 \text{ (cm)}, \text{ and solve for } L_a = 36.597 \text{ (cm}^3/\text{s}). \quad \text{HAC average leakage rate}$$

Diameter	$F_c$	$F_m$	$L_2$	$L_a / L_2$
1.0000e-02	3.0706e+00	1.3287e-02	1.2366e+01	2.9595e+00
1.3145e-02	9.1678e+00	3.0179e-02	3.6883e+01	9.9225e-01
1.3119e-02	9.0955e+00	3.0001e-02	3.6592e+01	1.0001e+00
1.3119e-02	9.0955e+00	3.0001e-02	3.6592e+01	1.0001e+00

The HAC leakage hole diameter for the HEU oxide content is:

$$D = 1.3119 \times 10^{-2} \text{ cm.} \quad \text{HAC diameter}$$

### HAC Reference Air Leakage Rate for HEU Content

The leakage hole diameter found for the maximum allowable leakage rate for HAC will be used to determine the reference air leakage rate. O-ring seal leakage testing must assure that no leakage is greater than the leakage generated by the hole diameter  $D = 1.3119 \times 10^{-2} \text{ cm}$ . Therefore, the HAC reference air leakage rate ( $L_{R,A}$ ) must be calculated to determine the acceptable test leakage rate for post-HAC leakage testing.

Input data for HAC reference air leakage rate:

$$\begin{aligned} D &= 1.3119 \times 10^{-2} \text{ cm,} \\ a &= 0.3531 \text{ cm,} \\ P_u &= 1.0 \text{ atm,} \\ P_d &= 0.01 \text{ atm,} \\ T &= 298 \text{ K,} \\ M &= 29 \text{ g/g-mole,} \\ \mu &= 0.0185 \text{ cP.} \end{aligned}$$

From the HAC of transport  
Leak path length, 0.139-in. O-ring section diameter  
Upstream pressure  
Downstream pressure  
Fill gas temperature, 77°F  
Molecular weight of air  
Viscosity at temperature

Calculate  $P_a$ :

$$\begin{aligned} P_a &= (P_u + P_d) / 2 \\ &= 0.505 \text{ atm.} \end{aligned} \quad \text{HAC average pressure}$$

$$\begin{aligned} F_c &= (2.49 \times 10^6) D^4 / (a \mu) (\text{cm}^3/\text{atm-s}), \\ F_c &= (2.49 \times 10^6) (1.3119 \times 10^{-2})^4 / ((0.3531) (0.0185)), \\ F_c &= (3.8122 \times 10^8) (1.3119 \times 10^{-2})^4, \\ F_c &= 1.1294 \times 10^1 \text{ cm}^3/\text{atm-s}. \end{aligned} \quad (\text{Eq. B3})$$

$$\begin{aligned} F_m &= (3.81 \times 10^3) D^3 (T / M)^{0.5} / (a P_a) (\text{cm}^3/\text{atm-s}), \\ F_m &= (3.81 \times 10^3) (1.3119 \times 10^{-2})^3 (298 / 29)^{0.5} / ((0.3531) (0.505)), \\ F_m &= (6.8501 \times 10^4) (1.3119 \times 10^{-2})^3, \\ F_m &= 1.5468 \times 10^{-1} \text{ cm}^3/\text{atm-s}. \end{aligned} \quad (\text{Eq. B4})$$

$$\begin{aligned} L_u &= (F_c + F_m) (P_u - P_d) (P_a / P_u) (\text{cm}^3/\text{s}), \\ L_u &= (1.1294 \times 10^1 + 1.5468 \times 10^{-1}) (\text{cm}^3/\text{atm-s}) (1.0 - 0.01) (\text{atm}) (0.505 / 1.0), \\ L_u &= (11.4485 \times 10^1) (\text{cm}^3/\text{atm-s}) (0.49995) (\text{atm}), \\ L_u &= 5.7237 \text{ cm}^3/\text{s}. \end{aligned} \quad (\text{Eq. B5})$$

The HAC reference air leakage rate as defined in ANSI N14.5-1997, Sect. B.3, is the upstream leakage in air.

$$L_{RA, \text{Air}} = 5.7237 \text{ ref-cm}^3/\text{s.} \quad \text{for HEU oxide content}$$

The same equations can be used to calculate an allowable leakage rate using helium for leak testing.

$$\begin{aligned} M &= 4 \text{ g/g-mole,} \\ \mu &= 0.0198 \text{ cP.} \end{aligned} \quad \begin{array}{l} \text{Molecular weight of helium} \\ \text{Viscosity of helium at temperature} \end{array}$$

$$\begin{aligned} F_c &= (2.49 \times 10^6) D^4 / (a \mu) (\text{cm}^3/\text{atm-s}), \\ F_c &= (2.49 \times 10^6) (1.3119 \times 10^{-2})^4 / ((0.3531) (0.0198)), \\ F_c &= (3.5619 \times 10^8) (1.3119 \times 10^{-2})^4, \\ F_c &= 1.0552 \times 10^1 \text{ cm}^3/\text{atm-s}. \end{aligned} \quad (\text{Eq. B3})$$

$$\begin{aligned} F_m &= (3.81 \times 10^3) D^3 (T / M)^{0.5} / (a P_a) (\text{cm}^3/\text{atm-s}), \\ F_m &= (3.81 \times 10^3) (1.3119 \times 10^{-2})^3 (298 / 4)^{0.5} / ((0.3531) (0.505)), \\ F_m &= (1.8444 \times 10^5) (1.3119 \times 10^{-2})^3, \\ F_m &= 4.1650 \times 10^{-1} \text{ cm}^3/\text{atm-s}. \end{aligned} \quad (\text{Eq. B4})$$

$$\begin{aligned} L_u &= (F_c + F_m) (P_u - P_d) (P_a / P_u) (\text{cm}^3/\text{s}), \\ L_u &= (1.0052 \times 10^1 + 4.1650 \times 10^{-1}) (\text{cm}^3/\text{atm-s}) (1.0 - 0.01) (\text{atm}) (0.505 / 1.0), \\ L_u &= (1.0969 \times 10^1) (\text{cm}^3/\text{atm-s}) (0.49995) (\text{atm}), \\ L_u &= 5.4839 \text{ cm}^3/\text{s}. \end{aligned} \quad (\text{Eq. B5})$$

The allowable leakage rate using helium for leak testing for HAC is:

$$L_{RA, \text{He}} = 5.4839 \text{ cm}^3/\text{s.} \quad \text{HAC helium test value}$$

Table 1. Regulatory leakage criteria for 35.2 kg of HEU

Years from fabrication	NCT		HAC		
	$L_{RN-air}$ (ref-cm <sup>3</sup> /s)	$L_{RN-He}$ (cm <sup>3</sup> /s)	$L_{RA-air}$ (ref-cm <sup>3</sup> /s)	$L_{RA-He}$ (cm <sup>3</sup> /s)	
Fast absorption	0	3.8917e-03	4.1797e-03	6.7586e+00	6.4689e+00
	5	3.8735e-03	4.1608e-03	6.7271e+00	6.4390e+00
	10	3.8709e-03	4.1581e-03	6.7225e+00	6.4346e+00
	20	3.8693e-03	4.1564e-03	6.7197e+00	6.4319e+00
	30	3.8680e-03	4.1550e-03	6.7174e+00	6.4297e+00
	40	3.8665e-03	4.1536e-03	6.7149e+00	6.4274e+00
	50	3.8650e-03	4.1519e-03	6.7122e+00	6.4248e+00
	60	3.8632e-03	4.1501e-03	6.7092e+00	6.4219e+00
	70	3.8614e-03	4.1482e-03	6.7061e+00	6.4189e+00
Medium absorption	0	3.7276e-03	4.0088e-03	6.4734e+00	6.1975e+00
	5	3.7110e-03	3.9915e-03	6.4445e+00	6.1701e+00
	10	3.7086e-03	3.9890e-03	6.4404e+00	6.1661e+00
	20	3.7072e-03	3.9875e-03	6.4379e+00	6.1637e+00
	30	3.7061e-03	3.9864e-03	6.4359e+00	6.1619e+00
	40	3.7048e-03	3.9851e-03	6.4337e+00	6.1598e+00
	50	3.7034e-03	3.9836e-03	6.4313e+00	6.1575e+00
	60	3.7019e-03	3.9820e-03	6.4286e+00	6.1549e+00
	70	3.7003e-03	3.9803e-03	6.4258e+00	6.1523e+00
Slow absorption	0	3.3124e-03	3.5754e-03	5.7514e+00	5.5103e+00
	5	3.2999e-03	3.5623e-03	5.7297e+00	5.4896e+00
	10	3.2985e-03	3.5609e-03	5.7273e+00	5.4873e+00
	20	3.2983e-03	3.5607e-03	5.7270e+00	5.4870e+00
	30	3.2983e-03	3.5607e-03	5.7269e+00	5.4870e+00
	40	3.2981e-03	3.5605e-03	5.7266e+00	5.4866e+00
	50	3.2977e-03	3.5600e-03	5.7259e+00	5.4860e+00
	60	3.2972e-03	3.5595e-03	5.7250e+00	5.4851e+00
	70	3.2965e-03	3.5587e-03	5.7237e+00	5.4839e+00

## SECTION 4 REFERENCES

10 CFR 71, *Packaging and Transportation of Radioactive Material*, Jan. 1, 2005.

49 CFR 173, *Shippers—General Requirements for Shipments and Packagings*, Oct. 1, 2004.

*ASME Boiler and Pressure Vessel Code, An American National Standard, Sect. II, Materials, Part C, Specifications for Welding, Rods, Electrodes, and Filler Metals*, American Society of Mechanical Engineers, New York, 2001 ed. with 2002 and 2003 addenda.

*ASME Boiler and Pressure Vessel Code, An American National Standard, Rules for Construction of Nuclear Facility Components*, Sect. III, Div. 1, Subsection NB, American Society of Mechanical Engineers, New York, 2001 ed. with 2002 and 2003 addenda.

*ASME Boiler and Pressure Vessel Code, An American National Standard, Welding and Brazing Qualifications*, Sect. IX, American Society of Mechanical Engineers, New York, 2001 ed. with 2002 and 2003 addenda.

ANSI N 14.5-1997, *Radioactive Materials—Leakage Tests on Packages for Shipment*, American Natl. Standards Institute, Feb. 5, 1998.

Curren, W. D. and R. D. Bond, *Leakage of Radioactive Powders from Containers*, Proceedings of the Sixth International Symposium on Packaging and Transportation of Radioactive Material: PATRAM '80, West Berlin, F.R.G., November 10–14, 1980, pp. 463–471.

Kocher, D. C., *Radioactive Decay Data Tables, A Handbook of Decay Data for Application to Radiation Dosimetry and Radiological Assessments*, DOE/TIC-11026, U.S. DOE, Office of Scientific and Technical Information, 1981.

NUREG-1609, *Standard Review Plan for Transportation Packages for Radioactive Material*, U.S. NRC, Mar. 31, 1999.

*Parker O-ring Handbook*, Catalog ORD 5700/US, Parker Hannifin Corp., Lexington, Ky., 2001.

R.D. McCarty Cryogenics Division, National Bureau of Standards Technical Note 631, *Thermophysical Properties of Helium-43 from 2 to 1500 K with Pressures to 100 Atmospheres*, pg 49, Nov. 1972.

Regulatory Guide 7.4, *Leakage Tests on Packages for Shipment of Radioactive Materials*, U.S. NRC, June 1975.

Robert C. Weast, Ph. D., *Handbook of Chemistry and Physics*, 55th ed., pg. F-13, 1974.

*SCALE 4.1—System Module to Calculate Fuel Depletion, Actinide Transmutation Fission Product Buildup and Decay, and Associated Radiation Source Terms*, Vol. 2, Sect. F, NUREG/CR-2000, C. V. Parks, ed., Radiation Shielding Information Center, Oak Ridge Natl. Lab., Dec. 1984.

TR 96/12/20, Issue A, *SAFKEG 2863B Tests for Verification of O-ring Performance*, Los Alamos Natl. Lab., Albuquerque, N.M., December 1996.



## 5. SHIELDING EVALUATION

This section describes the shielding evaluation performed for the shipment of up to 36 kg of highly enriched uranium (HEU) in the ES-3100 shipping package. The objective of this evaluation is to demonstrate, for both Normal Conditions of Transport (NCT) and Hypothetical Accident Conditions (HAC), compliance of this package with the performance requirements specified in Title 10 Code of Federal Regulations (CFR) 71 and 49 CFR 173.

## 5.1 DESCRIPTION OF SHIELDING DESIGN

### 5.1.1 Design Features

The ES-3100 package for NCT consists of stainless-steel convenience cans loaded with HEU material, spacer assemblies to support and position the convenience cans, the ES-3100 containment vessel, and an insulation-filled drum as shown in Appendix 1.4.1. None of the package materials are specifically designed for shielding gamma rays (photons), the primary contributor to external package dose rates. For HAC, it is assumed that the containment vessel and content remain intact, but all exterior packaging materials are removed. The geometry of the shielding analysis model is a conservative, cylindrical representation of the package. Two sets of contents have been investigated for the shielding analysis. These are 36 kg of HEU metal and 24 kg of HEU oxide powder. The analyses of these models have been performed such that the results and conclusions cover other proposed contents, in an equivalent or conservative manner. For the source calculation, the uranium is enriched at 92%  $^{235}\text{U}$  and is assumed to contain 0.6%  $^{233}\text{U}$ , 2.5%  $^{237}\text{Np}$ , 40 ppb (parts per billion)  $^{232}\text{U}$ , and 40 ppm (parts per million) plutonium.

### 5.1.2 Summary Table of Maximum Radiation Levels

The results of these shielding model evaluations, summarized in Tables 5.1 and 5.2, are the calculated dose rates at the locations indicated. The uncertainty associated with the results is one standard deviation of the mean (expressed as a percentage of the mean) of the Monte Carlo calculated results. As shown from the dose rates in the tables and the discussion in Sect. 5.3, the shielding evaluation demonstrates that the package meets all dose-rate limits for both NCT and HAC for all proposed contents.

## 5.2 SOURCE SPECIFICATION

The source for the calculated dose rates is from the decay and fission of the radioactive isotope contents. The isotopic content used in the shielding calculations is shown in Table 5.3. This composition was chosen to represent all proposed package contents. The primary contribution to the dose rates in Tables 5.1 and 5.2 is from decay of the  $^{232}\text{U}$  isotope (this applies to any mix of the other uranium isotopes in Table 5.3). The photon and neutron source spectra are given in Tables 5.4 and 5.5. In Table 5.4, the group 6 photons are from the decay chain of  $^{232}\text{U}$ . Group 18 photons were omitted from the source for the dose rate calculation due to negligible contribution from photons at these energies. Oxygen was not included in the uranium oxide source calculation, but the neutron source includes ( $\alpha$ , n) neutrons from the  $\text{UO}_2$  default option in the ORIGEN-S code (NUREG/CR-0200, rev. 6). The uranium metal source is assumed to be the same as that for the oxides, per unit HEU mass. Spontaneous fission neutrons are



**Table 5.1. Calculated external dose rates for the ES-3100 package with 36 kg of HEU metal contents (mrem/h)<sup>a</sup>**

	Drum surface			One meter from surface <sup>b</sup>		
	Side	Top	Bottom	Side	Top	Bottom
<i>NCT</i>						
Photon	92.264 ± 0.5%	38.746 ± 4.2%	77.410 ± 3.8%	6.441 ± 0.2%	1.419 ± 1.0%	1.450 ± 0.9%
Neutron <sup>c</sup>	1.767 ± 3.4%	0.144 ± 3.3%	3.690 ± 3.1%	0.062 ± 3.0%	0.028 ± 3.3%	0.084 ± 3.2%
Total	94.031 ± 0.5%	38.890 ± 4.2%	81.100 ± 3.8%	6.503 ± 0.2% <sup>d</sup>	1.447 ± 1.0%	1.534 ± 0.9%
Limit <sup>e</sup>	200	200	200	10	10	10
<i>HAC</i>						
Photon	NA <sup>f</sup>	NA	NA	11.183 ± 0.2%	1.644 ± 0.9%	1.895 ± 0.9%
Neutron <sup>c</sup>	NA	NA	NA	0.029 ± 3.0%	0.007 ± 3.3%	0.018 ± 3.3%
Total	NA	NA	NA	11.212 ± 0.2%	1.651 ± 0.9%	1.913 ± 0.9%
Limit <sup>g</sup>	NA	NA	NA	1000	1000	1000

<sup>a</sup> MORSE-CGA Monte Carlo code results (ORNL-6174).

<sup>b</sup> Drum for NCT and containment vessel for HAC.

<sup>c</sup> Includes secondary photon dose rate (<1% of neutron dose rates).

<sup>d</sup> The radiation shielding transport index is 6.6.

<sup>e</sup> 10 CFR 71.47 and 49 CFR 173.441.

<sup>f</sup> Not applicable.

<sup>g</sup> 10 CFR 71.51.

**Table 5.2. Calculated external dose rates for the ES-3100 package with 24 kg of HEU oxide contents (mrem/h)<sup>a</sup>**

	Drum surface			One meter from surface <sup>b</sup>		
	Side	Top	Bottom	Side	Top	Bottom
<i>NCT</i>						
Photon	82.201 ± 0.4%	14.315 ± 2.1%	62.208 ± 1.4%	4.975 ± 0.3%	1.249 ± 0.6%	1.519 ± 0.6%
Neutron <sup>c</sup>	1.035 ± 1.2%	0.084 ± 2.7%	2.181 ± 3.0%	0.038 ± 1.3%	0.016 ± 1.6%	0.047 ± 1.6%
Total	83.236 ± 0.4%	14.399 ± 2.1%	64.389 ± 1.4%	5.013 ± 0.3% <sup>d</sup>	1.265 ± 0.6%	1.566 ± 0.6%
Limit <sup>e</sup>	200	200	200	10	10	10
<i>HAC</i>						
Photon	NA <sup>f</sup>	NA	NA	8.363 ± 0.4%	1.471 ± 1.2%	1.686 ± 1.2%
Neutron <sup>c</sup>	NA	NA	NA	0.027 ± 0.7%	0.010 ± 0.8%	0.018 ± 0.8%
Total	NA	NA	NA	8.390 ± 0.4%	1.481 ± 1.2%	1.704 ± 1.2%
Limit <sup>g</sup>	NA	NA	NA	1000	1000	1000

<sup>a</sup> MORSE-CGA Monte Carlo code results (ORNL-6174).

<sup>b</sup> Drum for NCT and containment vessel for HAC.

<sup>c</sup> Includes secondary photon dose rate (<1% of neutron dose rates).

<sup>d</sup> The radiation shielding transport index is 5.1.

<sup>e</sup> 10 CFR 71.47 and 49 CFR 173.441.

<sup>f</sup> Not applicable.

<sup>g</sup> 10 CFR 71.51.

included in Table 5.5 spectrum. Induced fission neutrons and secondary photons are included in the dose rate calculations. Details of the source specifications and use in the dose rate calculations are given in the Sect. 5 appendices.

### 5.3 DOSE RATE ANALYSIS MODELS

The photon and neutron sources from the radioactive content as described in the previous section, and listed in Tables 5.4 and 5.5, are input into the MORSE Monte Carlo radiation code to calculate the ES-3100 external package dose rates given in Tables 5.1 and 5.2. The packaging component drawings are shown in Appendix 1.4.1. A cylindrical model of this packaging and proposed HEU material content is shown in Fig. 5.1 and Table 5.6. The dose rate detector locations relative to the package model exterior are listed in Table 5.7. The materials and densities used in the calculational model are given in Table 5.8. These models are described in more detail in the input data and other information given in the Sect. 5 appendices. Kaolite is an insulation material, and Cat 277-4 is a criticality control material. Additional information on these two materials can be found in Sects. 1, 2, and 6.

Two proposed package contents have been analyzed: (1) 36 kg of HEU metal and (2) 24 kg of HEU oxide. The analyses of these models have been performed in a manner that covers other proposed contents, not analyzed, in an equivalent or conservative manner. Due to the simple source and packaging geometry, there are no radiation streaming paths from the source toward the package exterior. Each of the two models is analyzed for both photon and neutron sources, and for both NCT and HAC.

In addition to the analyses for the dose rates shown in Tables 5.1 and 5.2, many preliminary and auxiliary calculations were made for each model to ensure that all proposed content loadings in the ES-3100 vessel were covered. These extra analyses are necessary since only a content mass limit is specified for each shipment, and various geometric configurations must be investigated to determine if the maximum external package dose rates have been found. In some cases it is not possible, or practical, to find an exact maximum dose rate geometric configuration due to the statistical uncertainty of the calculation method, variations in model radius vs. height, variable densities, etc. The dose rate values shown in Tables 5.1 and 5.2 are all at or near possible maximum values for the package specifications given in Sect. 1. All package models investigated, including the preliminary and auxiliary models, are conservative.

**Table 5.3. Radioisotope specification for all ES-3100 package analysis source calculations with HEU content and other nuclides per HEU unit weight**

Isotope	wt %
<sup>232</sup> U	0.000004
<sup>233</sup> U	0.600000
<sup>234</sup> U	2.000000
<sup>235</sup> U	92.000000
<sup>236</sup> U	1.000000
<sup>238</sup> U	4.399996
<sup>237</sup> Np	2.500000
Pu <sup>a</sup>	0.004000

<sup>a</sup> Nominal weapons-grade at 40 ppm uranium by weight—see Appendix 5.5.1.

Table 5.4. Photon source for one gram of HEU for all contents<sup>a</sup>

Group number	Energy range (MeV)	Source (photons/s)
1	10.00–8.00	$4.409 \times 10^{-6}$
2	8.00–6.50	$2.552 \times 10^{-3}$
3	6.50–5.00	$1.654 \times 10^{-3}$
4	5.00–4.00	$5.106 \times 10^{-4}$
5	4.00–3.00	$2.182 \times 10^{-3}$
6	3.00–2.50	$1.011 \times 10^{-4}$
7	2.50–2.00	$1.011 \times 10^{-1}$
8	2.00–1.66	$9.761 \times 10^{-1}$
9	1.66–1.33	$1.101 \times 10^{-3}$
10	1.33–1.00	$3.426 \times 10^{-2}$
11	1.00–0.80	$1.595 \times 10^{-3}$
12	0.80–0.60	$4.620 \times 10^{-3}$
13	0.60–0.40	$2.347 \times 10^{-4}$
14	0.40–0.30	$1.977 \times 10^{-3}$
15	0.30–0.20	$4.550 \times 10^{-4}$
16	0.20–0.10	$1.150 \times 10^{-3}$
17	0.10–0.05	$3.534 \times 10^{-3}$
18 <sup>b</sup>	0.05–0.01	-
Total		$7.530 \times 10^{-3}$

<sup>a</sup> ORIGEN-S code results at 10½ years decay.

<sup>b</sup> Omitted in the dose rate calculations.

Table 5.5. Neutron source for one gram of HEU for all contents<sup>a</sup>

Group number	Energy range (MeV)	Source in uranium metal and oxide (neutrons/s)
1	$2.00 \times 10^{-1} - 6.43 \times 10^{-2}$	$5.614 \times 10^{-3}$
2	$6.43 \times 10^{-2} - 3.00 \times 10^{-2}$	$2.250 \times 10^{-2}$
3	$3.00 \times 10^{-2} - 1.85 \times 10^{-2}$	$6.246 \times 10^{-3}$
4	$1.85 \times 10^{-2} - 1.40 \times 10^{-2}$	$1.702 \times 10^{-3}$
5	$1.40 \times 10^{-2} - 9.00 \times 10^{-3}$	$9.946 \times 10^{-3}$
6	$9.00 \times 10^{-3} - 4.00 \times 10^{-3}$	$3.397 \times 10^{-3}$
7	$4.00 \times 10^{-3} - 1.00 \times 10^{-3}$	$5.582 \times 10^{-3}$
8 <sup>b</sup>	$1.00 \times 10^{-3} - 1.70 \times 10^{-2}$	0
Total		$1.160 \times 10^{-1}$

<sup>a</sup> ORIGEN-S results at 15 years decay.

<sup>b</sup> Source is zero for Groups 9–27.

**Table 5.6. Geometric data for the shielding analysis models of the ES-3100 shipping package as shown in Fig. 5.1 for NCT.** Each item is modeled as a cylinder or cylindrical shell. The content volume not identified (HEU metal photon shell model interior) is modeled as void. All materials interior to the containment vessel except the HEU material content are omitted. Each of the four content models is placed in the packaging to create four separate calculational models. All dimensions are in centimeters. For HAC, all material external to the containment vessel is omitted.

	Material	Outer radius	Base reference height <sup>a</sup>	Height <sup>b</sup> (h)	Side wall thickness	Top thickness	Bottom thickness
<b>Content</b>							
HEU metal shell photon model	HEU	6.35	11.195	76.2	0.6639	-	-
HEU metal neutron model	HEU	6.35	11.195	15.1003	-	-	-
Oxide photon model	UO <sub>2</sub>	6.35	11.195	63.5	-	-	-
Oxide neutron model	UO <sub>2</sub>	6.35	11.195	17.2864	-	-	-
<b>Packaging (identical for all models)</b>							
Inner vessel gap	void	6.4008	11.195	76.2	0.0508	-	-
ES-3100 containment vessel <sup>c</sup>	SS304 <sup>e</sup>	6.6548	10.56	77.47	0.254	0.635	0.635
Outer vessel gap	void	7.9248	10.56	77.47	1.27	-	-
Inner Cat 277-4 liner	SS304	8.0748	10.56	77.47	0.15	-	-
Criticality control material	Cat 277-4	10.9196	10.56	77.47	2.8448	-	-
Outer Cat 277-4 liner	SS304	11.0696	10.26	77.92	0.15	0.15	0.3
Upper insulation	Kaolite <sup>d</sup>	23.0275	88.18	19.385	-	-	-
Base and radial insulation	Kaolite	23.0275	0.26	87.92	11.9579	-	10
Drum	SS304	23.1775	0	107.715	0.15	0.15	0.26

<sup>a</sup> Measured from the lower drum base.

<sup>b</sup> Vessel interior content (and gap) height varies with density to preserve content mass.

<sup>c</sup> Upper flange and lid detail omitted.

<sup>d</sup> Modeled as void.

<sup>e</sup> 304 stainless steel

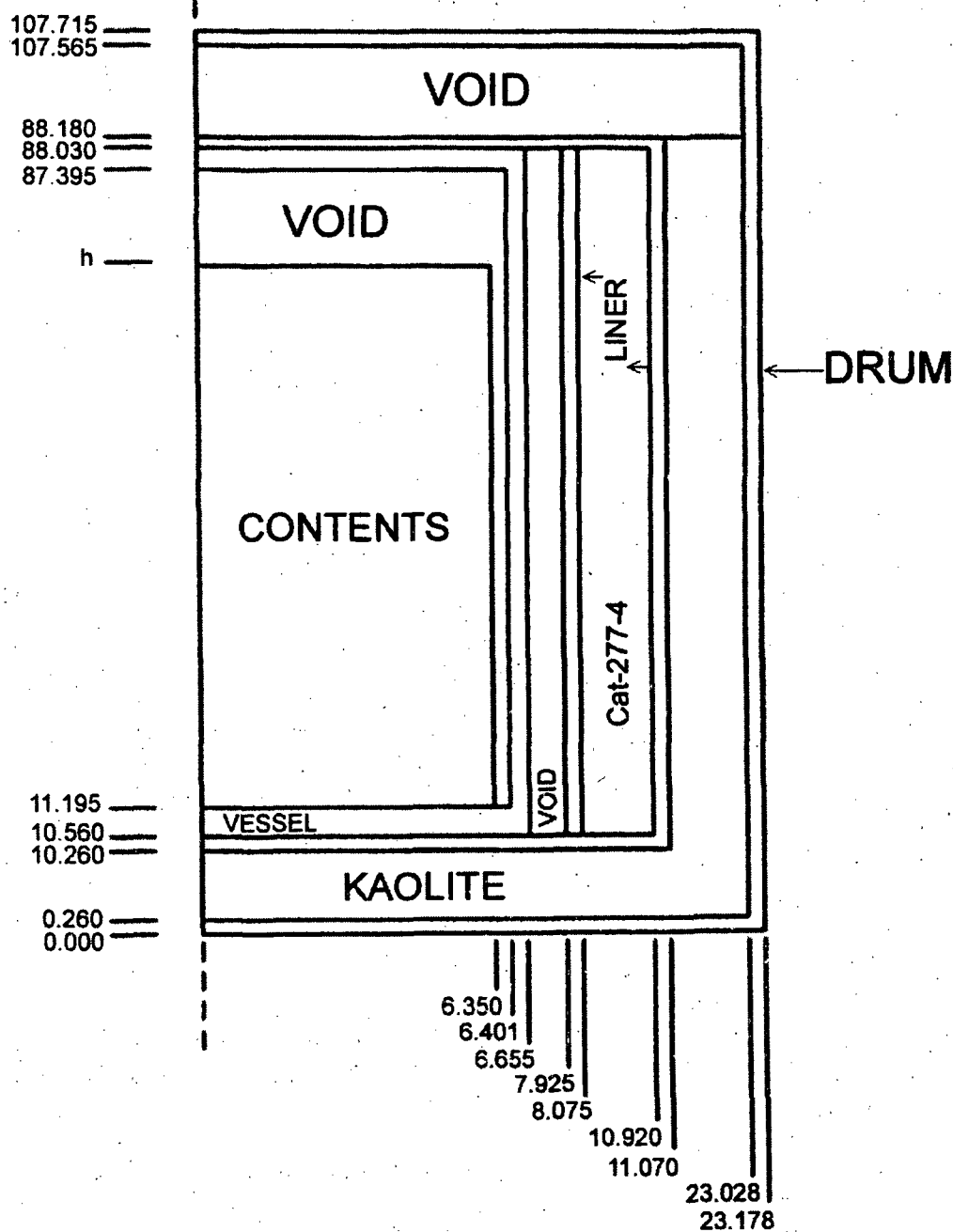


**Fig. 5.1. Cylindrical calculational model of the ES-3100 shipping package for NCT.** See Tables 5.6–5.8 for data on the contents, materials, and detector locations (not to scale; all dimensions are in centimeters). For HAC, all material external to the containment vessel is omitted.

**Table 5.7. Detector locations relative to the drum for NCT and to the containment vessel for HAC**

	Radius (cm)	H <sup>a</sup> (cm)
NCT detectors		
Side surface <sup>b</sup>	24.1775	49.2950
Top surface	0.0000	108.7150
Bottom surface	0.0000	-1.0000
Side 1 meter <sup>b</sup>	123.1775	49.2950
Top 1 meter	0.0000	207.7150
Bottom 1 meter	0.0000	-100.0000
HAC detectors		
Side 1 meter <sup>b</sup>	106.6548	49.2950
Top 1 meter	0.0000	188.0300
Bottom 1 meter	0.0000	-89.4400

<sup>a</sup> Height above drum base.

<sup>b</sup> Surface side location is at the axial mid-point of the content; values shown are for the first content in Table 5.6.

### 5.3.1 Packaging Model Conservative Features

Several conservative features applying to all content models are included in the packaging model. All material dimensions, thicknesses, and densities for the packaging are modeled at or less than specified or nominal values. All non-cylindrical detail has been omitted from the shielding models (see packaging drawings in Appendix 1.4.1). All minor items, such as the silicone rubber pads supporting the ES-3100 containment vessel, have been omitted. It was determined from preliminary analysis that the maximum axial external dose rates would occur relative to the package lower surface. All contents were modeled to contact the containment vessel lower surface, and the upper containment vessel geometry, containment vessel lid, and upper packaging, insulation, lids, covers, etc., were conservatively simplified and/or modeled as void (see Fig. 5.1).

All models of the vessel interior contain HEU material content only. All convenience cans, spacers, content wrappings, covers, supports, etc., are omitted. All contents are modeled as cylinders or cylindrical shells with the base resting on the lower vessel surface, with a maximum specified radius of 6.35 cm (the maximum allowable convenience can diameter is 5 in.), and with a height, inner radius (if any), and density adjusted for each specific model to preserve the content mass. In this conservative manner, it is possible to cover all specified combinations of can loadings and can and spacer placements with a minimum number of calculations. The geometric configuration of some of the cases investigated represents a situation where the maximum possible mass loading for a convenience can would be exceeded if the cans had been included in the model. However, the calculated dose rates from the models used will always exceed those from a model where the geometry is expanded so the can mass loadings are not exceeded and the internal vessel hardware is included. All the general, conservative items relative to the ES-3100 package shielding model are applied to each individual content model.

**Table 5.8. Shielding model material specifications for the ES-3100 package with HEU content.** Only the two principal uranium isotopes are used in the dose rate calculations. The uranium oxide density varies with the geometric model volume to preserve the 24-kg mass.

Material	Density (g/cm <sup>3</sup> )	Constitute	Weight percent	Atomic density (atoms/barn-cm)
Uranium metal	18.82	<sup>235</sup> U	95.00	$4.582 \times 10^{-2}$
		<sup>238</sup> U	5.00	$2.381 \times 10^{-3}$
UO <sub>2</sub>	10.960 <sup>a</sup>	O	11.98	$4.941 \times 10^{-2}$
		<sup>235</sup> U	83.62	$2.349 \times 10^{-2}$
		<sup>238</sup> U	4.40	$1.221 \times 10^{-3}$
Stainless steel	7.92	Cr	19.00	$1.743 \times 10^{-2}$
		Ni	9.50	$7.721 \times 10^{-3}$
		Fe	69.50	$5.936 \times 10^{-2}$
		Mn	2.00	$1.736 \times 10^{-3}$
Cat 277-4	1.682	H	4.62	$4.642 \times 10^{-2}$
		<sup>10</sup> B	0.79	$8.002 \times 10^{-4}$
		<sup>11</sup> B	3.44	$3.168 \times 10^{-3}$
		C	1.51	$1.274 \times 10^{-3}$
		O	60.00	$3.798 \times 10^{-2}$
		Mg	0.38	$1.584 \times 10^{-4}$
		Al	21.16	$7.944 \times 10^{-3}$
		Si	1.32	$4.760 \times 10^{-4}$
		S	0.15	$4.739 \times 10^{-5}$
		Na	0.13	$5.728 \times 10^{-5}$
		Ca	6.18	$1.562 \times 10^{-3}$
		Fe	0.32	$5.804 \times 10^{-5}$
Kaolite	0.321	O	40.43	$4.888 \times 10^{-3}$
		Na	1.45	$1.219 \times 10^{-4}$
		Mg	7.86	$6.251 \times 10^{-4}$
		Al	5.58	$3.998 \times 10^{-4}$
		Si	16.12	$1.110 \times 10^{-3}$
		Ca	23.40	$1.129 \times 10^{-3}$
		Fe	5.16	$1.786 \times 10^{-4}$

<sup>a</sup> Theoretical density—a density of 2.984 g/cm<sup>3</sup> is used in the Table 5.6 geometric model for photons.



### 5.3.2 Photon model for 36-kg HEU metal content

The HEU metal content in the ES-3100 may be many small, irregularly shaped pieces, each placed at some arbitrary orientation inside the convenience cans. Several conservative, regular geometry models have been devised to cover these and other proposed loadings. Some of these models violate, in a conservative manner, the volume capacity of a convenience can. The cans and spacers are omitted from the models.

The photon model for the dose rates shown in Table 5.1 is that given for the first content item in Table 5.6 (the HEU metal shell). Here, the content is a cylindrical shell the same height as the containment vessel model (76.2 cm). The inner radius of the shell, 5.6861 cm, was used to preserve the 36 kg HEU metal at 18.82 g/cm<sup>3</sup> for an outer radius of 6.35 cm. This case corresponds to a three-can loading configuration with a maximum of 12 kg in each 25.4-cm (10-in.) tall can.

Several 36-kg HEU metal cylindrical shell photon dose rate models were evaluated at lesser heights than the containment vessel inside height (in each case the shell wall thickness was adjusted to preserve the mass). The 1-m side photon dose rate in Table 5.1 is the calculated value for the entire analysis that gave the largest overall fraction of the regulatory limit, 65% of the 10-mrem/h limit. There was some increase in the side surface (not 1-m) photon dose at lesser shell heights. At ~50 cm content height, the maximum side surface dose rate for the shell model was calculated to be 98 mrem/h, 49% of the regulatory limit. This geometry would approximate a 12-kg loading in each of the 8.75-in. cans. The maximum calculated axial surface dose rate of 101 mrem/h was at the bottom drum surface for a shell height of 25 cm and inner radius of 4.0 cm, a gross conservative violation of an actual can loading.

The cylindrical shell representation of the HEU metal content is a convenient, conservative model for multiple possible loading configurations inside the vessel. Some other, more complicated, geometric radial models were also analyzed. The radial geometric cross-sections of these models are shown schematically in Fig. 5.2:

- a. The cylindrical shell as described above.
- b. A vertical flat plate across the center of the vessel. The maximum calculated photon package surface dose rate for a plate of dimensions 1.9766 cm × 12.7 cm × 76.2 cm was 63 mrem/h.
- c. A cylindrical hemi-shell. The maximum calculated package surface photon dose rate was 69 mrem/h for an outer radius of 6.35 cm, an inner radius of 4.0436 cm, and a height of 50.8 cm.
- d. A single solid rod placed against the side wall of the vessel. The maximum calculated package surface dose rate for a rod of radius 3.0966 cm and a height of 63.5 cm was 48 mrem/h.
- e. A cylindrical segment (the shape a liquid would assume in a horizontal vessel). The maximum calculated package surface dose rate was calculated to be 71 mrem/h for a radius of 6.35 cm, an inner flat surface 11.495 cm across, and a height of 63.5 cm.

The variations in dose rates described here are due to the variations in source-detector point geometry and the self-absorption of photons in the source material. It may be possible to devise other geometric configurations that could produce slightly higher dose rates. However, it can be said with

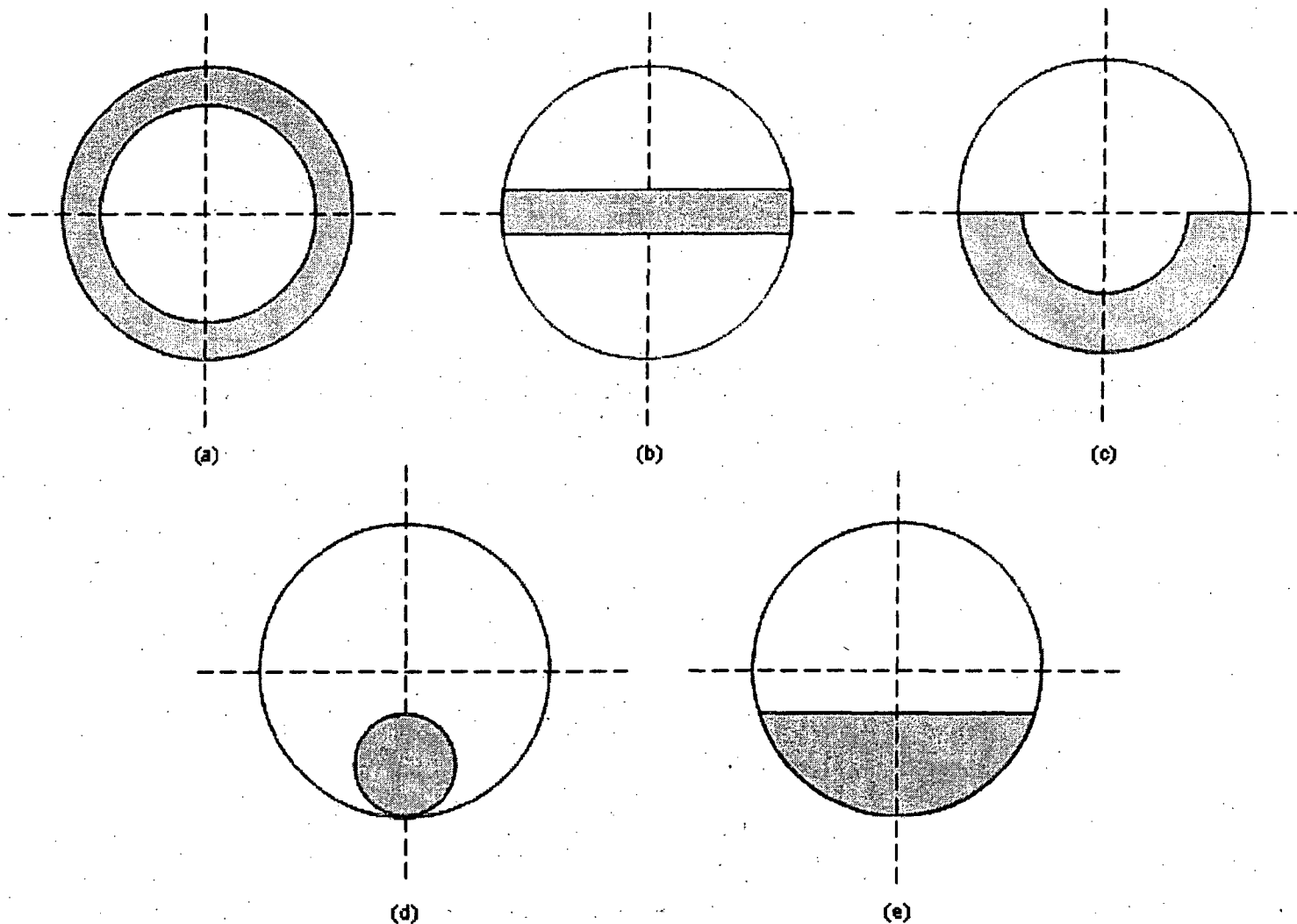


**Fig. 5.2. ES-3100 HEU metal content radial (top view) geometric models.** The 36-kg mass is conserved for each case. Detector locations were adjusted both vertically and radially from those given in Table 5.7 in the search for maximum external package dose rates for each case.

some certainty that the calculated photon dose rates for 36-kg HEU metal content defined in Table 5.3 should never exceed 110 mrem/h on the package surface, 7.6 mrem/h at one meter, and 16 mrem/h for HAC.

### 5.3.3 Neutron model for 36-kg HEU metal content

In the model for the neutron dose rates for the 36-kg HEU contents, it was assumed that all the uranium was a solid cylinder at the bottom of the vessel. The neutron results in Table 5.1 are from this configuration. This is a gross, conservative violation of a convenience can capacity, and no further investigation was made due to the low neutron dose rates obtained from this conservative model relative to the photon results.

### 5.3.4 Photon model for 24-kg HEU oxide content

A package photon dose rate calculation model was created to apply to 24 kg HEU oxide for all three common uranium oxides— $\text{UO}_2$ ,  $\text{UO}_3$ , and  $\text{U}_3\text{O}_8$ . The theoretical densities for these oxides are 10.96 g/cm<sup>3</sup>, 7.29 g/cm<sup>3</sup>, and 8.30 g/cm<sup>3</sup>, respectively. In the package loading models, the convenience can locations are completely filled with oxide powder, and the actual densities, always less than theoretical values, will be the oxide mass divided by the model can volume.

The dose rate model excludes the convenience cans and spacers and it is represented by a solid cylinder of oxide resting on the vessel interior base. The cylinder radius is 6.35 cm, and the height is variable. The density is adjusted for each calculation to preserve the 24-kg oxide mass. The HEU mass is 21.126 kg for  $\text{UO}_2$ , the largest uranium mass of the three oxides for 24 kg of HEU oxide. In the dose rate calculations, the partial density of oxygen was set to zero, so that the analysis conservatively applies to all three oxides without regard to variations in the oxygen density. The photon dose rates in Table 5.2 are for a cylinder height of 63.5 cm. The 1-m dose rates are slightly higher for 76.2 cm height, and the surface values are slightly higher for a 50.8 cm height. The bottom dose rates approach the side values in Table 5.2 when the cylinder is compressed to the  $\text{UO}_2$  theoretical density at the vessel bottom. From the various analyses, it can be stated that no calculated HEU oxide photon dose rates should exceed 90 mrem/h on the package surface, 6 mrem/h at one meter, and 12 mrem/h for HAC.

### 5.3.5 Neutron model for 24-kg HEU oxide content

The neutron model for the calculated values shown in Table 5.2 was for a solid cylinder of  $\text{UO}_2$  at the containment vessel bottom. The density was 10.96 g/cm<sup>3</sup> and the height was 17.286 cm.

## 5.4 SHIELDING EVALUATION

Several computer programs were used in the shielding evaluation. These included the ORIGEN-S computer code, the CSASN analysis module, the ICE-S computer code, and the MORSE-CGA computer code. ORIGEN-S, CSASN, and ICE-S are parts of the SCALE code. MORSE-CGA is a stand-alone code. Brief descriptions of the programs are presented below.

1. ORIGEN-S is a general depletion and decay code. Given an initial isotopic distribution, materials are decayed to provide time-dependent, energy-grouped photon and neutron sources.
2. CSASN is a sequence of codes for performing resonance processing of neutron cross sections using the SCALE modules BONAMI-S and NITAWL-S.

3. ICE-S is a SCALE module used to format a cross-section library for MORSE-CGA.
4. MORSE-CGA is a general-purpose Monte Carlo code that treats multidimensional neutron, photon, and coupled problems in either a forward or an adjoint mode. Sources and detectors may be defined through user-supplied subroutines. Model definition is facilitated by combinatorial array geometry. Dose rates are calculated by the SAMBO analysis module.

Dose rates were calculated at the detector locations in Table 5.7 by converting the calculated photon and neutron fluxes using the American National Standards Institute (ANSI) conversion factors (ANSI/ANS-6.1.1). These factors for the energy groups used in the shielding evaluation are shown in Tables 5.9 and 5.10.

The results of these shielding model evaluations, summarized in Tables 5.1 and 5.2, are the calculated dose rates at the locations indicated. As shown from the dose rates in the tables and the discussion in Sect. 5.3, the shielding evaluation demonstrates that the package meets all dose-rate limits for both NCT and HAC. The shielding analyses were done in a conservative manner applicable to all proposed ES-3100 package contents listed in Sect. 1.2.3.

**Table 5.9. ANSI standard photon flux-to-dose-rate conversion factors**

Group number	Energy (MeV)	Factor (mrem/h)/(photons/s/cm <sup>2</sup> )
1	10.00–8.00	$8.771 \times 10^{-3}$
2	8.00–6.50	$7.478 \times 10^{-3}$
3	6.50–5.00	$6.374 \times 10^{-3}$
4	5.00–4.00	$5.413 \times 10^{-3}$
5	4.00–3.00	$4.622 \times 10^{-3}$
6	3.00–2.50	$3.959 \times 10^{-3}$
7	2.50–2.00	$3.468 \times 10^{-3}$
8	2.00–1.66	$3.019 \times 10^{-3}$
9	1.66–1.33	$2.627 \times 10^{-3}$
10	1.33–1.00	$2.205 \times 10^{-3}$
11	1.00–0.80	$1.832 \times 10^{-3}$
12	0.80–0.60	$1.522 \times 10^{-3}$
13	0.60–0.40	$1.172 \times 10^{-3}$
14	0.40–0.30	$8.759 \times 10^{-4}$
15	0.30–0.20	$6.306 \times 10^{-4}$
16	0.20–0.10	$3.833 \times 10^{-4}$
17	0.10–0.05	$2.669 \times 10^{-4}$
18	0.05–0.01	$9.347 \times 10^{-4}$

**Table 5.10. ANSI standard neutron flux-to-dose-rate conversion factors**

Group number	Energy (MeV)	Factor (mrem/h)/(neutrons/s/cm <sup>2</sup> )
1	$2.00 \times 10^{+1} - 6.43 \times 10^{+0}$	$1.4916 \times 10^{-1}$
2	$6.43 \times 10^{+0} - 3.00 \times 10^{+0}$	$1.4464 \times 10^{-1}$
3	$3.00 \times 10^{+0} - 1.85 \times 10^{+0}$	$1.2701 \times 10^{-1}$
4	$1.85 \times 10^{+0} - 1.40 \times 10^{+0}$	$1.2811 \times 10^{-1}$
5	$1.40 \times 10^{+0} - 9.00 \times 10^{-1}$	$1.2977 \times 10^{-1}$
6	$9.00 \times 10^{-1} - 4.00 \times 10^{-1}$	$1.0281 \times 10^{-1}$
7	$4.00 \times 10^{-1} - 1.00 \times 10^{-1}$	$5.1183 \times 10^{-2}$
8	$1.00 \times 10^{-1} - 1.70 \times 10^{-2}$	$1.2319 \times 10^{-2}$
9	$1.70 \times 10^{-2} - 3.00 \times 10^{-3}$	$3.8365 \times 10^{-3}$
10	$3.00 \times 10^{-3} - 5.50 \times 10^{-4}$	$3.7247 \times 10^{-3}$
11	$5.50 \times 10^{-4} - 1.00 \times 10^{-4}$	$4.0150 \times 10^{-3}$
12	$1.00 \times 10^{-4} - 3.00 \times 10^{-5}$	$4.2926 \times 10^{-3}$
13	$3.00 \times 10^{-5} - 1.00 \times 10^{-5}$	$4.4744 \times 10^{-3}$
14	$1.00 \times 10^{-5} - 3.05 \times 10^{-6}$	$4.5676 \times 10^{-3}$
15	$3.05 \times 10^{-6} - 1.77 \times 10^{-6}$	$4.5581 \times 10^{-3}$
16	$1.77 \times 10^{-6} - 1.30 \times 10^{-6}$	$4.5185 \times 10^{-3}$
17	$1.30 \times 10^{-6} - 1.13 \times 10^{-6}$	$4.4879 \times 10^{-3}$
18	$1.13 \times 10^{-6} - 1.00 \times 10^{-6}$	$4.4665 \times 10^{-3}$
19	$1.00 \times 10^{-6} - 8.00 \times 10^{-7}$	$4.4345 \times 10^{-3}$
20	$8.00 \times 10^{-7} - 4.00 \times 10^{-7}$	$4.3271 \times 10^{-3}$
21	$4.00 \times 10^{-7} - 3.25 \times 10^{-7}$	$4.1975 \times 10^{-3}$
22	$3.25 \times 10^{-7} - 2.25 \times 10^{-7}$	$4.0976 \times 10^{-3}$
23	$2.25 \times 10^{-7} - 1.00 \times 10^{-7}$	$3.8390 \times 10^{-3}$
24	$1.00 \times 10^{-7} - 5.00 \times 10^{-8}$	$3.6748 \times 10^{-3}$
25	$5.00 \times 10^{-8} - 3.00 \times 10^{-8}$	$3.6748 \times 10^{-3}$
26	$3.00 \times 10^{-8} - 1.00 \times 10^{-8}$	$3.6748 \times 10^{-3}$
27	$1.00 \times 10^{-8} - 1.00 \times 10^{-11}$	$3.6748 \times 10^{-3}$



## 5.5 APPENDICES

<b>Appendix</b>	<b>Descriptions</b>
5.5.1	ORIGEN INPUT DATA FROM TABLE 5.3
5.5.2	CSASN AND ICE INPUT FROM TABLE 5.8
5.5.3	MORSE ROUTINES AND INPUT DATA





## **APPENDIX 5.5.1**

### **ORIGEN INPUT DATA FROM TABLE 5.3**

This file is for generation of the photon spectra in Table 5.4 and the metal and oxide neutron data in Table 5.5. The concentration for each isotope is given based on 1 g of HEU.

```

#origen
0$$ 6 13 a8 26 e
1$$ 1 t
master photon
3$$ 21 0 1 -88 6 a16 2 a33 18
4** a4 1-70 t
35$$ 0 t
56$$ 0 10 a13 13 5 3 a17 2 e
57** 0 e t
es3100 uranium metal and oxides
one gram HEU
60** 8 9 10 10.5 11 12 15 20 40 50
65$$ a7 1 a25 1 a28 1 a31 1 a49 1 e
73$$ 922320 922340 922350 922360 922380
      922330 942380 942390 932370
      942400 942410 942420 952410
74** 0.4000-07 .020000 0.92000 .010000 0.04399996
      6.00-03 8.00-09 3.7032-05 0.025
      2.60-06 2.24-07 1.60-08 1.20-07
75$$ 2 2 2 2 2 2 2 2 2 2 2 2 2
81$$ 2 0 26 1 e
82$$ 2 2 2 2 2 2 2 2 0 0
83** 10+6 8+6 6.5+6 5+6 4+6 3+6 2.5+6 2+6 1.66+6 1.33+6 1+6 .8+6
      .6+6 .4+6 .3+6 .2+6 .1+6 .05+6 .01+6 t
      8
      9
      10
      10.5
      11
      12
      15
      20
56$$ f0 t
end

```

## APPENDIX 5.5.2

### CSASN AND ICE INPUT FROM TABLE 5.8

This file is the input data for the generation and preparation (format) of the cross-section data used in the MORSE code. The data generated from this input file can be used for all MORSE media input cases. Oxygen is omitted from the oxide models, and HEU is assumed to be all U-235 in the neutron models in the MORSE data. The atomic densities for all dose rate calculations in Appendix 5.5.3 cases are given, or indicated, in Table 5.8.

```

=csasn
es3100: morse-cg cross section library
27n-18couple
multiregion
  arbm02      10.9600  3  0  0  0   8016  11.9800
              92235  83.6200
              92238   4.4000   1 1.0000 293.0 end
  arbmssst    7.9200  4  0  0  0   26304 69.5000
              24304  19.0000
              28304   9.5000
              25055   2.0000   2 1.0000 293.0 end
  arbmcat     1.6820 12  0  0  0   1001   4.6200
              5010   0.7900
              5011   3.4400
              6012   1.5100
              8016  60.0000
              12000  0.3800
              13027 21.1600
              14000   1.3200
              16000   0.1500
              11023   0.1300
              20000   6.1800
              26304   0.3200   3 1.0000 293.0 end
  arbmkoa     0.3210  7  0  0  0   8016  40.4300
              11023   1.4500
              12000   7.8600
              13027   5.5800
              14000  16.1200
              20000  23.4000
              26304   5.1600   4 1.0000 293.0 end

end comp
spherical end
  1 1.0      noextermod
end zone
end
=ice
es31 ice : morse cross section library
-1$$ a3 2200 e
1$$ 26 26 0 10 0 0 1 1t
2$$ 1 2 3 4 5 6 7 8 9 10 11 12 13 14 15 16 17 18 19 20 21 22 23 24
    25 26
3$$ 1008016 1092235 1092238
    2024304 2025055 2026304 2028304
    3001001 3005010 3005011 3006012 3008016 3012000 3013027
    3014000 3016000 3011023 3020000 3026304
    4008016 4011023 4012000 4013027 4014000 4020000 4026304
4** 26r1.0
5$$ 26r10
7$$ 3 16 60 0 0 0 e 2t
9$$ 258I1 260
10$$ 1 1452 27 3t
end

```

### **APPENDIX 5.5.3**

#### **MORSE ROUTINES AND INPUT DATA**

Included here are the routines and input files used for the dose rate calculations for the results in Tables 5.1 and 5.2. For each case, there are two routines, INSCOR and SOURCE, followed by the NCT and the HAC input. The normalization is given in INSCOR, which is the appropriate Total value in Tables 5.4 or 5.5 times the content mass. The spatial and energy distributions for the photon and neutron sources from Tables 5.4 and 5.5 are in the data statements in the SOURCE routine. Induced fission and secondary photons are included in the MORSE calculation. It is assumed that the energy group distribution of induced fissions is the same as for the spectra in Table 5.5. The photon source is biased, and weight corrected, so that half of all primary photons are selected in group 6 from Table 5.4.

For each case, the input data for NCT and HAC follow the two routines. For the HAC cases, all material external to the containment vessel is set to void and the detectors (now three) are set one meter from the external vessel surface. The 24-kg oxide neutron case, similar to the 36-kg metal neutron case, is not shown.

```

subroutine inscor
common /pdet/ nd, nne, ne, nt, na, nresp,
1 nex, nexnd, nend, ndnr, ntnr, ntne,
2 nane, ntndnr, ntnend, naniend, locrsp, locxd,
3 locib, locco, loct, locud, locsd, locqe,
4 locqt, locqte, locqae, lmax, efirst, egtop
common bc(1)
do 100 i = 1,nd
  bc(locxd + 5*nd + i) = 2.711e+10
100 continue
return
end
subroutine source( ig,u,v,w,x,y,z,
1 wate,med,ag,isour,itstr,ngpqt3,ddf,
2 isbias,nmtg )
dimension spect(1,18)
data xst,yst,zst /0.000,0.0,11.195/
data cyl_ht/76.200/
c40ppb u232
data (spect(1,k),k=1,18) /
1 4.409e-6,2.552e-5,1.654e-4,5.106e-4,2.182e-3,7.429e+5,
2 1.011e-1,9.761e+1,1.101e+3,
3 3.426e+2,1.595e+3, 4.620e+03,
4 2.347e+04,1.977e+5,4.550e+4,1.150e+5,3.534e+5,0.000e-00/
data icall / 1 /
if (icall) 10,10,5
5 icall = 0
r02 = 5.6861**2
r12 = 6.3500**2
i=1
sum=0.0
do 92 j = 1,nmtg
  sum = sum + spect(i,j)
92 spect(i,1) = spect(i,1) / sum
do 93 j = 2,nmtg
  spect(i,j) = spect(i,j-1) + spect(i,j) / sum
93 continue
r1 = fltrnf( 0 )
call azirn( sinang,cosang )
rad = sqrt( r1 * r12 + ( 1.0 - r1 ) * r02 )
x = rad * sinang + xst
y = rad * cosang + yst
z = zst + fltrnf( 0 ) * cyl_ht
i=1
rn = fltrnf( 0 )
do 94 j = 1,nmtg
  if ( rn .le. spect(i,j) ) goto 95
94 continue
j = nmtg
95 ig = j
c40ppb u232
if(ig.ne.6)wate=wate*1.97315
if(ig.eq.6)wate=wate*0.026853
return
end

```

```

es3100 package nct 36kg u metal 40 ppb u232
$$ 500 850 500 1 0 17 18 18 0 0 99. 4 0
$$ 0 0 0 0 ** 1.0 1.0000e-5 1.0000e+4 1.0 2.2000e+5
** 0.0 0.0 0.0 0.0 0.0 0.0 0.0 0.0
**
10.000e+6 8.0000e+6 6.5000e+6 5.0000e+6 4.0000e+6 3.0000e+6 2.5000e+6
2.0000e+6 1.6600e+6 1.3300e+6 1.0000e+6 0.8000e+6 0.6000e+6 0.4000e+6
0.3000e+6 0.2000e+6 0.1000e+6 0.0500e+6
bla303a31a34
$$ 1 1 0 0 0 1 18
$$ 1 1 10 1 1 1 ** 0.1 .001 .010 5.000e-01
$$ 11 1 14 1 1 1 ** 1.0 .010 .100 5.000e-01
$$ 15 1 18 1 1 1 ** 10. .100 1.00 5.000e-01
$$ -1 9r0
0 0 0 0
0 0
0 0 1 0
rcc 1 0.000 0.0 11.1950 0.00 0.0 76.2000 5.6861
rcc 2 0.000 0.0 11.1950 0.00 0.0 76.2000 6.3500
rcc 3 0.000 0.0 11.1950 0.00 0.0 76.2000 6.4008
rcc 4 0.000 0.0 10.5600 0.00 0.0 77.4700 6.6548
rcc 5 0.000 0.0 10.5600 0.00 0.0 77.4700 7.9248
rcc 6 0.000 0.0 10.5600 0.00 0.0 77.4700 8.0748
rcc 7 0.000 0.0 10.5600 0.00 0.0 77.4700 10.9196
rcc 8 0.000 0.0 10.2600 0.00 0.0 77.9200 11.0696
rcc 9 0.000 0.0 0.2600 0.00 0.0 87.9200 23.0275
rcc 10 0.000 0.0 0.2600 0.00 0.0 107.3050 23.0275
rcc 11 0.000 0.0 0.0000 0.00 0.0 107.7150 23.1775
sph 12 0.0 0.0 0.0 1000.
sph 13 0.0 0.0 0.0 2000.
end
vid 1
con 2 -1
vid 3 -2
sst 4 -3
vid 5 -4
sst 6 -5
bor 7 -6
sst 8 -7
kao 9 -8
vid 10 -9
sst 11 -10
vid 12 -11
vix 13 -12
end
1 1 1 1 1 1 1 1 1 1 1 1
13z
1000 1 1000 2 1000 2 3 2 4 1000 2 1000 0
0
27N18P LIBRARY (P5)
$$ 0 0 18 18 45 60 16 4 26 26 6 3 1 3
0 0 0 0 0 0 0 20 0 0 0
1 2 3 4 5 6 11 12 13 14 15 16 21 22
23 24 25 26 31 32 33 34 35 36 41 42 43 44
45 46 51 52 53 54 55 56 61 62 63 64 65 66
71 72 73 74 75 76 81 82 83 84 85 86 91 92
93 94 95 96 101 102 103 104 105 106 111 112 113 114
115 116 121 122 123 124 125 126 131 132 133 134 135 136
141 142 143 144 145 146 151 152 153 154 155 156 161 162
163 164 165 166 171 172 173 174 175 176 181 182 183 184
185 186 191 192 193 194 195 196 201 202 203 204 205 206
211 212 213 214 215 216 221 222 223 224 225 226 231 232
233 234 235 236 241 242 243 244 245 246 251 252 253 254
255 256
$$ 1 12 ** 1.0000e-9
$$ 1 2 ** 4.5820e-2

```

\$\$ 1 -3 \*\* 2.3810e-3  
 \$\$ 2 5 \*\* 1.7360e-3  
 \$\$ 2 6 \*\* 5.9360e-2  
 \$\$ 2 7 \*\* 7.7210e-3  
 \$\$ 2 -4 \*\* 1.7430e-2  
 \$\$ 3 8 \*\* 4.6420e-2  
 \$\$ 3 9 \*\* 8.0020e-4  
 \$\$ 3 10 \*\* 3.1680e-3  
 \$\$ 3 11 \*\* 1.2740e-3  
 \$\$ 3 12 \*\* 3.7980e-2  
 \$\$ 3 13 \*\* 1.5840e-4  
 \$\$ 3 14 \*\* 7.9440e-3  
 \$\$ 3 15 \*\* 4.7600e-4  
 \$\$ 3 16 \*\* 4.7390e-5  
 \$\$ 3 17 \*\* 5.7280e-5  
 \$\$ 3 18 \*\* 1.5620e-3  
 \$\$ 3 -19 \*\* 5.8040e-5  
 \$\$ 4 20 \*\* 4.8880e-3  
 \$\$ 4 21 \*\* 1.2190e-4  
 \$\$ 4 22 \*\* 6.2510e-4  
 \$\$ 4 23 \*\* 3.9980e-4  
 \$\$ 4 24 \*\* 1.1100e-3  
 \$\$ 4 25 \*\* 1.1290e-3  
 \$\$ 4 -26 \*\* 1.7860e-4

SAMBO ANALYSIS INPUT DATA

\$\$ 6 0 0 0 0 1 1 2  
 \*\*

24.1775 0.0 49.295  
 0.0 0.0 -1.00  
 0.0 0.0 108.715  
 123.1775 0.0 49.295  
 0.0 0.0 -100.00  
 0.0 0.0 207.7150

UNCOLLIDED AND TOTAL PHOTON DOSE RATES

ANSI STANDARD GAMMA DOSE RATES

\*\*

8.7716e-3 7.4785e-3 6.3748e-3 5.4136e-3 4.6221e-3 3.9596e-3 3.4686e-3  
 3.0192e-3 2.6276e-3 2.2051e-3 1.8326e-3 1.5228e-3 1.1725e-3 8.7594e-4  
 6.3061e-4 3.8338e-4 2.6693e-4 9.3472e-4



es3100 package hac 36kg u metal 40 ppb u232

```
$$ 500 850 500 1 0 17 18 18 0 0 99. 4 0
$$ 0 0 0 0 0 ** 1.0 1.0000e-5 1.0000e+4 1.0 2.2000e+5
** 0.0 0.0 0.0 0.0 0.0 0.0 0.0 0.0 0.0
**
```

```
10.000e+6 8.0000e+6 6.5000e+6 5.0000e+6 4.0000e+6 3.0000e+6 2.5000e+6
2.0000e+6 1.6600e+6 1.3300e+6 1.0000e+6 0.8000e+6 0.6000e+6 0.4000e+6
0.3000e+6 0.2000e+6 0.1000e+6 0.0500e+6
```

bla303a31a34

```
$$ 1 1 0 0 0 1 18
$$ 1 1 10 1 1 1 ** 0.1 .001 .010 5.000e-01
$$ 11 1 14 1 1 1 ** 1.0 .010 .100 5.000e-01
$$ 15 1 18 1 1 1 ** 10. .100 1.00 5.000e-01
$$ -1 9r0
```

```
0 0 0 0
```

```
0 0
```

heu in es-3100 36kg cylinder model

```
0 0 1 0
```

```
rcc 1 0.000 0.0 11.1950 0.00 0.0 76.2000 5.6861
rcc 2 0.000 0.0 11.1950 0.00 0.0 76.2000 6.3500
rcc 3 0.000 0.0 11.1950 0.00 0.0 76.2000 6.4008
rcc 4 0.000 0.0 10.5600 0.00 0.0 77.4700 6.6548
rcc 5 0.000 0.0 10.5600 0.00 0.0 77.4700 7.9248
rcc 6 0.000 0.0 10.5600 0.00 0.0 77.4700 8.0748
rcc 7 0.000 0.0 10.5600 0.00 0.0 77.4700 10.9196
rcc 8 0.000 0.0 10.2600 0.00 0.0 77.9200 11.0696
rcc 9 0.000 0.0 0.2600 0.00 0.0 87.9200 23.0275
rcc 10 0.000 0.0 0.2600 0.00 0.0 107.3050 23.0275
rcc 11 0.000 0.0 0.0000 0.00 0.0 107.7150 23.1775
```

```
sph 12 0.0 0.0 0.0 1000.
```

```
sph 13 0.0 0.0 0.0 2000.
```

end

```
vid 1
```

```
con 2 -1
```

```
vid 3 -2
```

```
sst 4 -3
```

```
vid 5 -4
```

```
sst 6 -5
```

```
bor 7 -6
```

```
sst 8 -7
```

```
kao 9 -8
```

```
vid 10 -9
```

```
sst 11 -10
```

```
vid 12 -11
```

```
vix 13 -12
```

end

```
1 1 1 1 1 1 1 1 1 1 1 1 1
```

```
13z 1000 1 1000 2 1000 1000 1000 1000 1000 1000 1000 1000 0
```

0

27N18P LIBRARY (P5)

```
$$ 0 0 18 18 45 60 16 4 26 26 6 3 1 3
0 0 0 0 0 0 0 20 0 0 0
1 2 3 4 5 6 11 12 13 14 15 16 21 22
23 24 25 26 31 32 33 34 35 36 41 42 43 44
45 46 51 52 53 54 55 56 61 62 63 64 65 66
71 72 73 74 75 76 81 82 83 84 85 86 91 92
93 94 95 96 101 102 103 104 105 106 111 112 113 114
115 116 121 122 123 124 125 126 131 132 133 134 135 136
141 142 143 144 145 146 151 152 153 154 155 156 161 162
163 164 165 166 171 172 173 174 175 176 181 182 183 184
185 186 191 192 193 194 195 196 201 202 203 204 205 206
211 212 213 214 215 216 221 222 223 224 225 226 231 232
233 234 235 236 241 242 243 244 245 246 251 252 253 254
255 256
```

```
$$ 1 12 ** 1.0000e-9
```

```
$$ 1 2 ** 4.5820e-2
```

```

$$ 1  -3 ** 2.3810e-3
$$ 2   5 ** 1.7360e-3
$$ 2   6 ** 5.9360e-2
$$ 2   7 ** 7.7210e-3
$$ 2  -4 ** 1.7430e-2
$$ 3   8 ** 4.6420e-2
$$ 3   9 ** 8.0020e-4
$$ 3  10 ** 3.1680e-3
$$ 3  11 ** 1.2740e-3
$$ 3  12 ** 3.7980e-2
$$ 3  13 ** 1.5840e-4
$$ 3  14 ** 7.9440e-3
$$ 3  15 ** 4.7600e-4
$$ 3  16 ** 4.7390e-5
$$ 3  17 ** 5.7280e-5
$$ 3  18 ** 1.5620e-3
$$ 3 -19 ** 5.8040e-5
$$ 4  20 ** 4.8880e-3
$$ 4  21 ** 1.2190e-4
$$ 4  22 ** 6.2510e-4
$$ 4  23 ** 3.9980e-4
$$ 4  24 ** 1.1100e-3
$$ 4  25 ** 1.1290e-3
$$ 4 -26 ** 1.7860e-4

```

SAMBO ANALYSIS INPUT DATA

```

$$ 3  0  0  0  0  1  1  2
**
106.6548 0.0 49.295
0.0 0.0 -89.440
0.0 0.0 188.03

```

UNCOLLIDED AND TOTAL PHOTON DOSE RATES

ANSI STANDARD GAMMA DOSE RATES

```

**
8.7716e-3 7.4785e-3 6.3748e-3 5.4136e-3 4.6221e-3 3.9596e-3 3.4686e-3
3.0192e-3 2.6276e-3 2.2051e-3 1.8326e-3 1.5228e-3 1.1725e-3 8.7594e-4
6.3061e-4 3.8338e-4 2.6693e-4 9.3472e-4

```

```

subroutine inscor
common /pdet/ nd, nne, ne, nt, na, nresp,
1 nex, nexnd, nend, ndnr, ntnr, ntne,
2 nane, ntndnr, ntnend, nanend, locrsp, locxd,
3 locib, locco, loci, locud, locsd, locqe,
4 locqt, locqte, locqae, lmax, efirst, egtop
common bc(1)
do 100 i = 1,nd
  bc(locxd + 5*nd + i) = 4.1800e+03
100 continue
return
end
subroutine source( ig,u,v,w,x,y,z,
1 wate,med,ag,isour,itstr,ngpqt3,ddf,
2 isbias, nmtg )
dimension spect(1,8)
data xst,yst,zst /0.000,0.0, 11.1950/
data cyl_ht/15.1003/
data (spect(1,k),k=1,8) /
1 6.614e-5,2.250e-2,6.246e-2,1.702e-2,9.946e-3,3.397e-3,
2 5.582e-4,0.000e+0/
data icall / 1 /
if (icall) 10,10,5
5 icall = 0
r11 = 6.3500
i=1
sum=0.0
do 92 j = 1,8
92 sum = sum + spect(i,j)
  spect(i,1) = spect(i,1) / sum
  do 93 j = 2,8
93 spect(i,j) = spect(i,j-1) + spect(i,j) / sum
10 continue
r1 = fltrnf( 0 )
call azirn( sinang,cosang )
rad = sqrt( r1)* r11
x = rad * sinang + xst
y = rad * cosang + yst
z = zst + fltrnf( 0 ) * cyl_ht
i=1
rn = fltrnf( 0 )
do 94 j = 1,8
  if ( rn .le. spect(i,j) ) goto 95
94 continue
  j = 8
95 ig = j
return
end

```

es3100 package nct 36kg u metal neutrons

```

$$ 200 850 200 1 27 18 27 45 0 0 60. 4 0
$$ 0 0 0 0 ** 1.0 1.0000e-5 1.0000e+4 1.0 2.2000e+5
$$ 0.0 0.0 0.0 0.0 0.0 0.0 0.0 0.0
**

```

```

2.0000e+7 6.4300e+6 3.0000e+6 1.8500e+6 1.4000e+6 9.0000e+5 4.0000e+5
1.0000e+5 1.7000e+4 3.0000e+3 5.5000e+2 1.0000e+2 3.0000e+1 1.0000e+1
3.0500e+0 1.7700e+0 1.3000e+0 1.1300e+0 1.0000e+0 8.0000e-1 4.0000e-1
3.2500e-1 2.2500e-1 9.9999e-2 5.0000e-2 3.0000e-2 1.0000e-2 1.0000e-7
8.0000e+6 6.5000e+6 5.0000e+6 4.0000e+6 3.0000e+6 2.5000e+6 2.0000e+6
1.6600e+6 1.3300e+6 1.0000e+6 0.8000e+6 0.6000e+6 0.4000e+6 0.3000e+6
0.2000e+6 0.1000e+6 0.0500e+6

```

b3a343b203a1

```

$$ 1 1 0 0 0 1 45
$$ 1 1 9 1 1 1 ** 50. .050 .500 5.000e-01
$$ 10 1 27 1 1 1 ** 50. 1.00 10.0 5.000e-01
$$ 28 1 45 1 1 1 ** 20. .500 2.00 5.000e-01
$$ -1 9r0
$$ 0 1 0 0
** 1.0
**

```

6.6140e-5 2.250e-2 6.246e-2 1.702e-2 9.946e-3 3.397e-3 5.582e-4

0.0000e-0 19z

\*\* 27z

\*\* 27z

\*\* 27z

\*\* 27r.01

```

0 0 heu in es-3100 36kg cylinder model
0 0 1 0
rcc 1 0.000 0.0 11.1950 0.00 0.0 15.1003 0.0001
rcc 2 0.000 0.0 11.1950 0.00 0.0 15.1003 6.3500
rcc 3 0.000 0.0 11.1950 0.00 0.0 76.2000 6.4008
rcc 4 0.000 0.0 10.5600 0.00 0.0 77.4700 6.6548
rcc 5 0.000 0.0 10.5600 0.00 0.0 77.4700 7.9248
rcc 6 0.000 0.0 10.5600 0.00 0.0 77.4700 8.0748
rcc 7 0.000 0.0 10.5600 0.00 0.0 77.4700 10.9196
rcc 8 0.000 0.0 10.2600 0.00 0.0 77.9200 11.0696
rcc 9 0.000 0.0 0.2600 0.00 0.0 87.9200 23.0275
rcc 10 0.000 0.0 0.2600 0.00 0.0 107.3050 23.0275
rcc 11 0.000 0.0 0.0000 0.00 0.0 107.7150 23.1775
sph 12 0.0 0.0 0.0 1000.
sph 13 0.0 0.0 0.0 2000.
end

```

```

vid 1
con 2 -1
vid 3 -2
sst 4 -3
vid 5 -4
sst 6 -5
bor 7 -6
sst 8 -7
kao 9 -8
vid 10 -9
sst 11 -10
vid 12 -11
vix 13 -12
end

```

```

1 1 1 1 1 1 1 1 1 1 1 1 1

```

```

13z
1000 1 1000 2 1000 2 3 2 4 1000 2 1000 0

```

27N18P LIBRARY (P5)

```

$$ 27 27 18 18 45 60 16 4 26 26 6 3 1 3
0 0 0 0 0 0 0 20 0 0 0
1 2 3 4 5 6 11 12 13 14 15 16 21 22
23 24 25 26 31 32 33 34 35 36 41 42 43 44

```



3.0192e-3 2.6276e-3 2.2051e-3 1.8326e-3 1.5228e-3 1.1725e-3 8.7594e-4  
 6.3061e-4 3.8338e-4 2.6693e-4 9.3472e-4

es3100 package hac 36kg u metal neutrons

\$\$ 200 850 200 1 27 18 27 45 0 0 60. 4 0  
 \$\$ 0 0 0 0 \*\* 1.0 1.0000e-5 1.0000e+4 1.0 2.2000e+5  
 \$\$ 0.0 0.0 0.0 0.0 0.0 0.0 0.0 0.0  
 \*\*

2.0000e+7 6.4300e+6 3.0000e+6 1.8500e+6 1.4000e+6 9.0000e+5 4.0000e+5  
 1.0000e+5 1.7000e+4 3.0000e+3 5.5000e+2 1.0000e+2 3.0000e+1 1.0000e+1  
 3.0500e+0 1.7700e+0 1.3000e+0 1.1300e+0 1.0000e+0 8.0000e-1 4.0000e-1  
 3.2500e-1 2.2500e-1 9.9999e-2 5.0000e-2 3.0000e-2 1.0000e-2 1.0000e-2  
 8.0000e+6 6.5000e+6 5.0000e+6 4.0000e+6 3.0000e+6 2.5000e+6 2.0000e+6  
 1.6600e+6 1.3300e+6 1.0000e+6 0.8000e+6 0.6000e+6 0.4000e+6 0.3000e+6  
 0.2000e+6 0.1000e+6 0.0500e+6

b3a343b203a1

\$\$ 1 1 0 0 0 1 45  
 \$\$ 1 1 9 1 1 1 \*\* 50. .050 .500 5.000e-01  
 \$\$ 10 1 27 1 1 1 \*\* 50. 1.00 10.0 5.000e-01  
 \$\$ 28 1 45 1 1 1 \*\* 20. .500 2.00 5.000e-01  
 \$\$ -1 9r0  
 \$\$ 0 1 0 0  
 \*\* 1.0  
 \*\*

6.6140e-5 2.107e-2 5.841e-2 1.593e-2 9.334e-3 3.219e-3 5.304e-4

0.0000e-0 19z

\*\* 27z

\*\* 27z

\*\* 27z

\*\* 27r.01

0 0 heu in es-3100 36kg cylinder model  
 0 0 1 0  
 rcc 1 0.000 0.0 11.1950 0.00 0.0 15.1003 0.0001  
 rcc 2 0.000 0.0 11.1950 0.00 0.0 15.1003 6.3500  
 rcc 3 0.000 0.0 11.1950 0.00 0.0 76.2000 6.4008  
 rcc 4 0.000 0.0 10.5600 0.00 0.0 77.4700 6.6548  
 rcc 5 0.000 0.0 10.5600 0.00 0.0 77.4700 7.9248  
 rcc 6 0.000 0.0 10.5600 0.00 0.0 77.4700 8.0748  
 rcc 7 0.000 0.0 10.5600 0.00 0.0 77.4700 10.9196  
 rcc 8 0.000 0.0 10.2600 0.00 0.0 77.9200 11.0696  
 rcc 9 0.000 0.0 0.2600 0.00 0.0 87.9200 23.0275  
 rcc 10 0.000 0.0 0.2600 0.00 0.0 107.3050 23.0275  
 rcc 11 0.000 0.0 0.0000 0.00 0.0 107.7150 23.1775  
 sph 12 0.0 0.0 0.0 1000.  
 sph 13 0.0 0.0 0.0 2000.  
 end  
 vid 1  
 con 2 -1  
 vid 3 -2  
 sst 4 -3  
 vid 5 -4  
 sst 6 -5  
 bor 7 -6  
 sst 8 -7  
 kao 9 -8  
 vid 10 -9  
 sst 11 -10  
 vid 12 -11  
 vix 13 -12  
 end

1 1 1 1 1 1 1 1 1 1 1 1  
 13z  
 1000 1 1000 2 1000 1000 1000 1000 1000 1000 1000 1000 0  
 0

# 27N18P LIBRARY (P5)

27	27	18	18	45	60	16	4	26	26	6	3	1	3
0	0	0	0	0	0	0	20	0	0	0			
1	2	3	4	5	6	11	12	13	14	15	16	21	22
23	24	25	26	31	32	33	34	35	36	41	42	43	44
45	46	51	52	53	54	55	56	61	62	63	64	65	66
71	72	73	74	75	76	81	82	83	84	85	86	91	92
93	94	95	96	101	102	103	104	105	106	111	112	113	114
115	116	121	122	123	124	125	126	131	132	133	134	135	136
141	142	143	144	145	146	151	152	153	154	155	156	161	162
163	164	165	166	171	172	173	174	175	176	181	182	183	184
185	186	191	192	193	194	195	196	201	202	203	204	205	206
211	212	213	214	215	216	221	222	223	224	225	226	231	232
233	234	235	236	241	242	243	244	245	246	251	252	253	254
255	256												

\$\$ 1 12 \*\* 1.0000e-9  
 \$\$ 1 2 \*\* 4.8240e-2  
 \$\$ 1 -3 \*\* 1.2210e-9  
 \$\$ 2 5 \*\* 1.7360e-3  
 \$\$ 2 6 \*\* 5.9360e-2  
 \$\$ 2 7 \*\* 7.7210e-3  
 \$\$ 2 -4 \*\* 1.7430e-2  
 \$\$ 3 8 \*\* 4.6420e-2  
 \$\$ 3 9 \*\* 8.0020e-4  
 \$\$ 3 10 \*\* 3.1680e-3  
 \$\$ 3 11 \*\* 1.2740e-3  
 \$\$ 3 12 \*\* 3.7980e-2  
 \$\$ 3 13 \*\* 1.5840e-4  
 \$\$ 3 14 \*\* 7.9440e-3  
 \$\$ 3 15 \*\* 4.7600e-4  
 \$\$ 3 16 \*\* 4.7390e-5  
 \$\$ 3 17 \*\* 5.7280e-5  
 \$\$ 3 18 \*\* 1.5620e-3  
 \$\$ 3 -19 \*\* 5.8040e-5  
 \$\$ 4 20 \*\* 4.8880e-3  
 \$\$ 4 21 \*\* 1.2190e-4  
 \$\$ 4 22 \*\* 6.2510e-4  
 \$\$ 4 23 \*\* 3.9980e-4  
 \$\$ 4 24 \*\* 1.1100e-3  
 \$\$ 4 25 \*\* 1.1290e-3  
 \$\$ 4 -26 \*\* 1.7860e-4

## SAMBO ANALYSIS INPUT DATA

\$\$ 3 0 0 0 0 3 1 2  
 \*\*

106.6548 0.0 18.745  
 0.0 0.0 -89.44  
 0.0 0.0 188.03

uncollided and total photon dose rates  
 ansi standard neutron dose rates :

\*\*  
 1.4916e-1 1.4464e-1 1.2701e-1 1.2811e-1 1.2977e-1 1.0281e-1 5.1183e-2  
 1.2319e-2 3.8365e-3 3.7247e-3 4.0150e-3 4.2926e-3 4.4744e-3 4.5676e-3  
 4.5581e-3 4.5185e-3 4.4879e-3 4.4665e-3 4.4345e-3 4.3271e-3 4.1975e-3  
 4.0976e-3 3.8390e-3 3.6748e-3 3.6748e-3 3.6748e-3 3.6748e-3  
 18r0.0

ansi standard photon dose rates :

\*\*  
 27r0.0  
 8.7716e-3 7.4785e-3 6.3748e-3 5.4136e-3 4.6221e-3 3.9596e-3 3.4686e-3  
 3.0192e-3 2.6276e-3 2.2051e-3 1.8326e-3 1.5228e-3 1.1725e-3 8.7594e-4  
 6.3061e-4 3.8338e-4 2.6693e-4 9.3472e-4

ansi standard total dose rates :

\*\*  
 1.4916e-1 1.4464e-1 1.2701e-1 1.2811e-1 1.2977e-1 1.0281e-1 5.1183e-2  
 1.2319e-2 3.8365e-3 3.7247e-3 4.0150e-3 4.2926e-3 4.4744e-3 4.5676e-3  
 4.5581e-3 4.5185e-3 4.4879e-3 4.4665e-3 4.4345e-3 4.3271e-3 4.1975e-3

4.0976e-3 3.8390e-3 3.6748e-3 3.6748e-3 3.6748e-3 3.6748e-3  
8.7716e-3 7.4785e-3 6.3748e-3 5.4136e-3 4.6221e-3 3.9596e-3 3.4686e-3  
3.0192e-3 2.6276e-3 2.2051e-3 1.8326e-3 1.5228e-3 1.1725e-3 8.7594e-4  
6.3061e-4 3.8338e-4 2.6693e-4 9.3472e-4



```

subroutine inscor
  common /pdet/  nd,      nne,      ne,      nt,      na,      nresp,
1               nex,      nexnd,  nend,      ndnr,      ntnr,      ntne,
2               nane,      ntndnr, ntnend, nanend, locrsp, locxd,
3               locib,      locco,  loct,      locud,      locsd,      locqe,
4               locqt,      locqte, locqae, lmax,      efirst, egtop
  common bc(1)
  do 100 i = 1,nd
    bc(locxd + 5*nd + i) = 2.7110e+10*24./36.*0.88024
100  continue
  return
end
  subroutine source( ig,u,v,w,x,y,z,
1                   wate,med,ag,isour,itstr,ngpqt3,ddf,
2                   isbias,nmtg )
  dimension spect(1,18)
  data xst,yst,zst /0.000,0.0,11.195/
  data cyl_ht/63.500/
c40ppb u232
  data (spect(1,k),k=1,18) /
1  4.409e-6,2.552e-5,1.654e-4,5.106e-4,2.182e-3,7.429e+5,
2  1.011e-1,9.761e+1,1.101e+3,
3  3.426e+2,1.595e+3, 4.620e+03,
4  2.347e+04,1.977e+5,4.550e+4,1.150e+5,3.534e+5,0.000e-00/
  data icall / 1 /
  if (icall) 10,10,5
5  icall = 0
c  r02 = 5.6861**2
  r02 = 0.0001**2
  r12 = 6.3500**2
  i=1
  sum=0.0
  do 92 j = 1,nmtg
92   sum = sum + spect(i,j)
  spect(i,1) = spect(i,1) / sum
  do 93 j = 2,nmtg
93   spect(i,j) = spect(i,j-1) + spect(i,j) / sum
10  continue
  r1 = fltrnf( 0 )
  call azirn( sinang,cosang )
  rad = sqrt( r1 * r12 + ( 1.0 - r1 ) * r02 )
  x = rad * sinang + xst
  y = rad * cosang + yst
  z = zst + fltrnf( 0 ) * cyl_ht
  i=1
  rn = fltrnf( 0 )
  do 94 j = 1,nmtg
    if ( rn .le. spect(i,j) ) goto 95
94  continue
  j = nmtg
95  ig = j
c40ppb u232
  if(ig.ne.6)wate=wate*1.97315
  if(ig.eq.6)wate=wate*0.026853
  return
end

```

```

es3100 package photon nct 24kg u oxide 40 ppb u232
$$ 500 850 500 1 0 17 18 18 0 0 99. 4 0
$$ 0 0 0 0 ** 1.0 1.0000e-5 1.0000e+4 1.0 2.2000e+5
** 0.0 0.0 0.0 0.0 0.0 0.0 0.0 0.0
**
10.000e+6 8.0000e+6 6.5000e+6 5.0000e+6 4.0000e+6 3.0000e+6 2.5000e+6
2.0000e+6 1.6600e+6 1.3300e+6 1.0000e+6 0.8000e+6 0.6000e+6 0.4000e+6
0.3000e+6 0.2000e+6 0.1000e+6 0.0500e+6
bla303a31a34
$$ 1 1 0 0 0 1 18
$$ 1 1 10 1 1 1 ** 0.1 .001 .010 5.000e-01
$$ 11 1 14 1 1 1 ** 1.0 .010 .100 5.000e-01
$$ 15 1 18 1 1 1 ** 10. .100 1.00 5.000e-01
$$ -1 9r0
0 0 0 0
0 0
0 0 1 0
oxide in es-3100 24kg cylinder model
rcc 1 0.000 0.0 11.1950 0.00 0.0 63.5000 0.0001
rcc 2 0.000 0.0 11.1950 0.00 0.0 63.5000 6.3500
rcc 3 0.000 0.0 11.1950 0.00 0.0 76.2000 6.4008
rcc 4 0.000 0.0 10.5600 0.00 0.0 77.4700 6.6548
rcc 5 0.000 0.0 10.5600 0.00 0.0 77.4700 7.9248
rcc 6 0.000 0.0 10.5600 0.00 0.0 77.4700 8.0748
rcc 7 0.000 0.0 10.5600 0.00 0.0 77.4700 10.9196
rcc 8 0.000 0.0 10.2600 0.00 0.0 77.9200 11.0696
rcc 9 0.000 0.0 0.2600 0.00 0.0 87.9200 23.0275
rcc 10 0.000 0.0 0.2600 0.00 0.0 107.3050 23.0275
rcc 11 0.000 0.0 0.0000 0.00 0.0 107.7150 23.1775
sph 12 0.0 0.0 0.0 1000.
sph 13 0.0 0.0 0.0 2000.
end
vid 1
con 2 -1
vid 3 -2
sst 4 -3
vid 5 -4
sst 6 -5
bor 7 -6
sst 8 -7
kao 9 -8
vid 10 -9
sst 11 -10
vid 12 -11
vix 13 -12
end
1 1 1 1 1 1 1 1 1 1 1 1
13z
1000 1 1000 2 1000 2 3 2 4 1000 2 1000 0
0
27N18P LIBRARY (P5)
$$ 0 0 18 18 45 60 16 4 26 26 6 3 1 3
0 0 0 0 0 0 0 20 0 0 0
1 2 3 4 5 6 11 12 13 14 15 16 21 22
23 24 25 26 31 32 33 34 35 36 41 42 43 44
45 46 51 52 53 54 55 56 61 62 63 64 65 66
71 72 73 74 75 76 81 82 83 84 85 86 91 92
93 94 95 96 101 102 103 104 105 106 111 112 113 114
115 116 121 122 123 124 125 126 131 132 133 134 135 136
141 142 143 144 145 146 151 152 153 154 155 156 161 162
163 164 165 166 171 172 173 174 175 176 181 182 183 184
185 186 191 192 193 194 195 196 201 202 203 204 205 206
211 212 213 214 215 216 221 222 223 224 225 226 231 232
233 234 235 236 241 242 243 244 245 246 251 252 253 254
255 256
$$ 1 12 ** 1.0000e-9
$$ 1 2 ** 6.3940e-3

```

```

$$ 1   -3 ** 3.3220e-4
$$ 2    5 ** 1.7360e-3
$$ 2    6 ** 5.9360e-2
$$ 2    7 ** 7.7210e-3
$$ 2   -4 ** 1.7430e-2
$$ 3    8 ** 4.6420e-2
$$ 3    9 ** 8.0020e-4
$$ 3   10 ** 3.1680e-3
$$ 3   11 ** 1.2740e-3
$$ 3   12 ** 3.7980e-2
$$ 3   13 ** 1.5840e-4
$$ 3   14 ** 7.9440e-3
$$ 3   15 ** 4.7600e-4
$$ 3   16 ** 4.7390e-5
$$ 3   17 ** 5.7280e-5
$$ 3   18 ** 1.5620e-3
$$ 3  -19 ** 5.8040e-5
$$ 4   20 ** 4.8880e-3
$$ 4   21 ** 1.2190e-4
$$ 4   22 ** 6.2510e-4
$$ 4   23 ** 3.9980e-4
$$ 4   24 ** 1.1100e-3
$$ 4   25 ** 1.1290e-3
$$ 4  -26 ** 1.7860e-4

```

SAMBO ANALYSIS INPUT DATA

```

$$ 6 0 0 0 0 1 1 2
**

```

```

24.1775 0.0 42.945
0.0 0.0 -1.00
0.0 0.0 108.715
123.1775 0.0 42.945
0.0 0.0 -100.00
0.0 0.0 207.715

```

UNCOLLIDED AND TOTAL PHOTON DOSE RATES

ANSI STANDARD GAMMA DOSE RATES

\*\*

```

8.7716e-3 7.4785e-3 6.3748e-3 5.4136e-3 4.6221e-3 3.9596e-3 3.4686e-3
3.0192e-3 2.6276e-3 2.2051e-3 1.8326e-3 1.5228e-3 1.1725e-3 8.7594e-4
6.3061e-4 3.8338e-4 2.6693e-4 9.3472e-4

```

es3100 package photon hac 24kg u oxide 40 ppb u232

```
$$ 500 850 500 1 0 17 18 18 0 0 99. 4 0
$$ 0 0 0 0 0 ** 1.0 1.0000e-5 1.0000e+4 1.0 2.2000e+5
** 0.0 0.0 0.0 0.0 0.0 0.0 0.0 0.0 0.0
**
```

```
10.000e+6 8.0000e+6 6.5000e+6 5.0000e+6 4.0000e+6 3.0000e+6 2.5000e+6
2.0000e+6 1.6600e+6 1.3300e+6 1.0000e+6 0.8000e+6 0.6000e+6 0.4000e+6
0.3000e+6 0.2000e+6 0.1000e+6 0.0500e+6
```

bla303a31a34

```
$$ 1 1 0 0 0 1 18
$$ 1 1 10 1 1 1 ** 0.1 .001 .010 5.000e-01
$$ 11 1 14 1 1 1 ** 1.0 .010 .100 5.000e-01
$$ 15 1 18 1 1 1 ** 10. .100 1.00 5.000e-01
$$ -1 9r0
```

```
0 0 0 0
0 0
0 0 1 0
oxide in es-3100 24kg cylinder model
```

```
rcc 1 0.000 0.0 11.1950 0.00 0.0 63.5000 0.0001
rcc 2 0.000 0.0 11.1950 0.00 0.0 63.5000 6.3500
rcc 3 0.000 0.0 11.1950 0.00 0.0 76.2000 6.4008
rcc 4 0.000 0.0 10.5600 0.00 0.0 77.4700 6.6548
rcc 5 0.000 0.0 10.5600 0.00 0.0 77.4700 7.9248
rcc 6 0.000 0.0 10.5600 0.00 0.0 77.4700 8.0748
rcc 7 0.000 0.0 10.5600 0.00 0.0 77.4700 10.9196
rcc 8 0.000 0.0 10.2600 0.00 0.0 77.9200 11.0696
rcc 9 0.000 0.0 0.2600 0.00 0.0 87.9200 23.0275
rcc 10 0.000 0.0 0.2600 0.00 0.0 107.3050 23.0275
rcc 11 0.000 0.0 0.0000 0.00 0.0 107.7150 23.1775
sph 12 0.0 0.0 0.0 1000.
sph 13 0.0 0.0 0.0 2000.
```

```
end
vid 1
con 2 -1
vid 3 -2
sst 4 -3
vid 5 -4
sst 6 -5
bor 7 -6
sst 8 -7
kao 9 -8
vid 10 -9
sst 11 -10
vid 12 -11
vix 13 -12
end
```

```
1 1 1 1 1 1 1 1 1 1 1 1 1
13z
1000 1 1000 2 1000 1000 1000 1000 1000 1000 1000 1000 0
0
```

27N18P LIBRARY (P5)

```
$$ 0 0 18 18 45 60 16 4 26 26 6 3 1 3
0 0 0 0 0 0 0 20 0 0 0
1 2 3 4 5 6 11 12 13 14 15 16 21 22
23 24 25 26 31 32 33 34 35 36 41 42 43 44
45 46 51 52 53 54 55 56 61 62 63 64 65 66
71 72 73 74 75 76 81 82 83 84 85 86 91 92
93 94 95 96 101 102 103 104 105 106 111 112 113 114
115 116 121 122 123 124 125 126 131 132 133 134 135 136
141 142 143 144 145 146 151 152 153 154 155 156 161 162
163 164 165 166 171 172 173 174 175 176 181 182 183 184
185 186 191 192 193 194 195 196 201 202 203 204 205 206
211 212 213 214 215 216 221 222 223 224 225 226 231 232
233 234 235 236 241 242 243 244 245 246 251 252 253 254
```

```

255 256
$$ 1 12 ** 1.0000e-9
$$ 1 2 ** 6.3940e-3
$$ 1 -3 ** 3.3220e-4
$$ 2 5 ** 1.7360e-3
$$ 2 6 ** 5.9360e-2
$$ 2 7 ** 7.7210e-3
$$ 2 -4 ** 1.7430e-2
$$ 3 8 ** 4.6420e-2
$$ 3 9 ** 8.0020e-4
$$ 3 10 ** 3.1680e-3
$$ 3 11 ** 1.2740e-3
$$ 3 12 ** 3.7980e-2
$$ 3 13 ** 1.5840e-4
$$ 3 14 ** 7.9440e-3
$$ 3 15 ** 4.7600e-4
$$ 3 16 ** 4.7390e-5
$$ 3 17 ** 5.7280e-5
$$ 3 18 ** 1.5620e-3
$$ 3 -19 ** 5.8040e-5
$$ 4 20 ** 4.8880e-3
$$ 4 21 ** 1.2190e-4
$$ 4 22 ** 6.2510e-4
$$ 4 23 ** 3.9980e-4
$$ 4 24 ** 1.1100e-3
$$ 4 25 ** 1.1290e-3
$$ 4 -26 ** 1.7860e-4
SAMBO ANALYSIS INPUT DATA
$$ 3 0 0 0 0 1 1 2
**
106.6548 0.0 42.945
0.0 0.0 -89.440
0.0 0.0 188.03
UNCOLLIDED AND TOTAL PHOTON DOSE RATES
ANSI STANDARD GAMMA DOSE RATES
**
8.7716e-3 7.4785e-3 6.3748e-3 5.4136e-3 4.6221e-3 3.9596e-3 3.4686e-3
3.0192e-3 2.6276e-3 2.2051e-3 1.8326e-3 1.5228e-3 1.1725e-3 8.7594e-4
6.3061e-4 3.8338e-4 2.6693e-4 9.3472e-4

```



## SECTION 5 REFERENCES

10 CFR 71, *Packaging and Transportation of Radioactive Material*, Jan. 1, 2005.

49 CFR 173, *Transportation*, Oct. 1, 2004.

ANSI/ANS-6.1.1, *Neutron and Gamma Ray Flux-to-Dose-Rate Factors*, American Natl. Standards Institute, American Nuclear Society, La Grange, Ill., 1977.

MORSE-CGA, *Monte Carlo Radiation Transport Code with Array Geometry Capability*, ORNL-6174, M. B. Emmett, Oak Ridge Natl. Lab., April 1985.

*SCALE: A Modular Code System for Performing Standardized Computer Analyses for Licensing Evaluation*, C. V. Parks, ed., NUREG/CR-0200, rev. 6, ORNL/NUREG/CSD-2/R6, May 2000.

